CRANFIELD INSTITUTE OF TECHNOLOGY

SCHOOL OF MECHANICAL ENGINEERING

PhD THESIS

Academic Year 1993

W.BERRY

Reusable Launchers

Supervisor: J.B.Moss

July 1993

This Thesis is submitted for the degree of Doctor of Philosophy

ABSTRACT

This research on Reusable Launchers was motivated by the need to reduce substantially the cost of space transportation. The specific objective was to explore the perception that launcher reusability is the key to achieving these major cost reductions. The exploration was achieved by undertaking a comparative system study on potentially feasible reusable launcher concepts, using a consistent set of design tools, a standard analysis methodology and a standard reference mission.

To set the background for the research, the results of an extensive literature review are presented on the vehicle studies and technology developments that are engaged across the world on reusable launchers. Comprehensive vehicle studies appear to be engaged without justification for the choice of selected concepts in the absence of results from comparative system studies of reusable launchers. Technology developments also appear to be engaged without clear links to needs derived from vehicle system studies.

The challenge of reusability is then addressed. Firstly, to set the performance and cost targets of reusable launchers, the capabilities of current expendable launchers are derived. Secondly, to establish the operational requirements for reusable launchers, the probable space transportation needs for the early 21st century are derived. Thirdly, the concepts and characteristics of reusable launchers are derived, allowing the selection, on a rationale basis, of a short-list of 13 potentially feasible reusable launcher concepts for analysis in the research.

The performance equations of reusable launchers are then derived, leading to the preparation of the comparative analysis tools.

The major work of the research, which comprises the performance analysis, technical feasibility assessment and cost analysis of each candidate vehicle are then presented and compared.

A set of acceptance requirements for performance, technical feasibility and operational costs of reusable launchers is then derived. The results of the comparative analysis for each candidate launcher are then measured against these requirements. The results of the comparative analysis show that only 2 of the 13 candidate reusable launcher concepts are able to meet all the acceptance requirements. These two acceptable vehicles are both rocket-propelled. They are, in order of preference:

- a single-stage-to-orbit, rocket-propelled, vertical launch and vertical landing vehicle;
- a two-stage-to-orbit, rocket-propelled, vertical launch and horizontal landing vehicle.

The operational costs per launch for these two vehicles, based on a utilisation plan of 3 vehicles operating for 20 years at a launch rate of 12 launches per year, was calculated to be about 20 % of the current costs of the European Ariane 44L expendable launcher. This warrants their further evaluation in a thorough feasibility study.

The more complex, air-breathing propelled, horizontal launch and landing vehicles were found to be unable to meet the performance, technical feasibility and cost requirements:

- Several vehicles were found to be unable to deliver a positive payload mass to orbit;
- Several vehicles were found to have technology requirements that were deemed to be infeasible to achieve;
- Several vehicles were found to have operational costs ranging from equal to double that of the European Ariane 44L expendable launcher, which was adopted as a comparative reference vehicle.

The contributions of this research to the advancement of knowledge on reusable launchers are:

- a clear identification of the performance capability limits of 13 plausible reusable launcher concepts;
- an analysis methodology for determining the performance capability limits for any reusable launcher concept;
- a clear identification of the reasons for the poor practical performance of air-breathing propulsion systems for Earth-to-orbit launchers, which results from their installed operational characteristics.

ACKNOWLEDGEMENTS

I was fortunate to be able to undertake this research because of the availability of a Total Engineering PhD Course for external students in the School of Mechanical Engineering at the Cranfield Institute of Technology. The creation of this course has fulfilled a significant need for many mature and experienced engineers like myself, who wish to extend their academic qualifications after many years in industry, but who cannot undertake a full time study because of their employment commitments. I am therefore grateful to and I applaud the Cranfield academic authorities for having created this external PhD course.

I was also fortunate because Professor J.B.Moss, Director of Academic Affairs and Head of the Department of Propulsion, Power and Automotive Engineering in the School of Mechanical Engineering, not only accepted my application to undertake this research as an external student, but also accepted to supervise the research. I am most grateful to Professor Moss for his guidance in my work and for his continuing support and encouragement to me to follow it through to its completion, in the face of difficulties experienced in undertaking the research whilst executing my full time professional duties.

CONTENTS

FIGURES

TABLES

1 INTRODUCTION

1.1 Motivation for the Research

The space age began nearly 36 years ago on 4 October 1957 with the launching by the USSR of the world's first artificial Earth satellite: Sputnik 1. This momentous event in the history of man was made possible by the successful development of the transportation means to space: the expendable, multi-stage, rocket-propelled launcher. Since then, the use of space for scientific research, followed quickly by its commercial exploitation for telecommunications, meteorology and Earth observation, has expanded rapidly and with amazing technical success. Indeed, the technological pace and success have been so great that space science and technology have transformed the world, yielding fundamental new scientific knowledge and bestowing practical benefits for all mankind. All this success has been made possible by the expendable, multi-stage, rocket-propelled launcher, but at a high price: high, not only because the advanced technology of launchers makes them inherently expensive, but also because they are usable once only, that is, they are expendable!

It is now perceived that despite the remarkable successes that have been made possible by the expendable, multi-stage, rocket-propelled launcher, that the high cost of these vehicles is now the principal curb on the further rapid exploration and exploitation of space. It is also perceived, intuitively, that the key to the major reduction of launch costs, is simply, to make launchers reusable!

This then is the challenge for the launcher technologist: is it technically feasible to make launchers reusable and if so, will they reduce space transportation costs? This challenge is not a completely new one. Indeed it was addressed by NASA

as long ago as 1968 and has resulted in the development and operation of the World's first partially reusable launcher system: the National Space Transportation System (NSTS), shown in Figure 1.1 below.

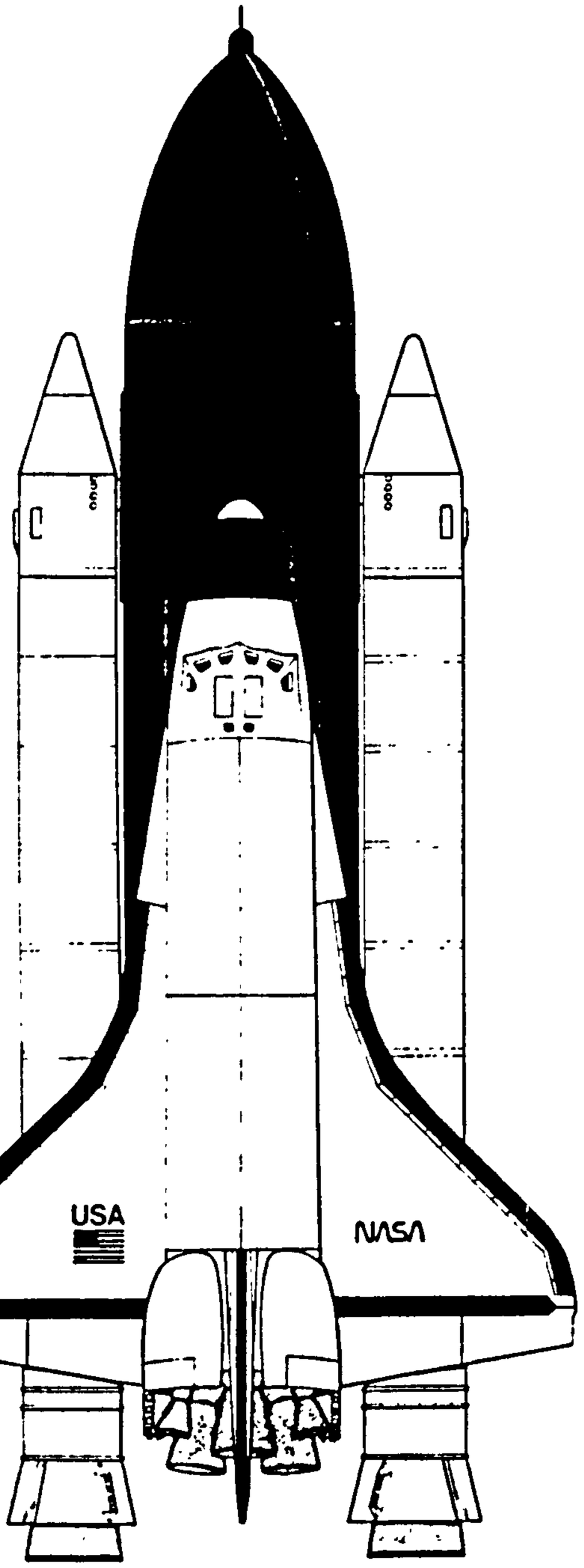

Height: 38.1 m.
Gross Mass: 2040 tonnes
Thrust at Lift-Off: 28200 KN
LEO Payload: 22.8 tonnes

The NSTS comprises a pair of recoverable and reusable solid propellant rocket motors (SRM's), an expendable external liquid hydrogen/liquid oxygen tank (External Tank) and a recoverable and reusable upper stage: the Orbiter spaceplane. The NSTS entered service on 12 April 1981 and despite the major accident on 28 January 1986 in which the "Challenger" vehicle on NSTS Flight 25 exploded catastrophically during its launch ascent, the NSTS system has been progressively developed to its present highly reliable status with 55 completely successful missions to date (26 April 1993). However, despite this technical success and the complex space missions that have been made possible by the STS, unfortunately, this, the world's first, partially reusable launcher, has not resulted in launch cost reductions. On the contrary, the NSTS has emerged to be exorbitantly expensive, with operation costs estimated between 500 and 1000 million dollars per flight, even for satellite delivery missions that are performed routinely by expendable launchers like Ariane 4, at a cost of about 100 million dollars per flight. The high operation costs that have evolved for the NSTS were not expected in 1981, when the USA adopted the NSTS as its primary launch system and simultaneously terminated the use of their fully developed expendable launchers Atlas, Delta and Titan for commercial launch operations. The results of this policy effectively eliminated the USA from the commercial satellite launcher market for a critical period from 1981 to 1989. This decision has directly benefitted Arianespace, the European commercial launch services organisation, which was set up in 1980 to exploit the use of the European Ariane expendable launcher, enabling Arianespace to emerge as the principal commercial launch services organisation in the world. These historical facts are reported here to underline the severe consequences that can result from the simple intuitive assumption that reusability of launchers is the key to reduction of space transportation costs! The brilliant technical success of the NSTS has been

eclipsed by its commercial failure! Following the Challenger accident and the subsequent major efforts made to recover the shuttle system, which was achieved with the successful launch of the STS 26 mission on 29 September 1988, the United States government finally recognised that the high operational cost of the NSTS was severely penalising for commercial satellite delivery missions and authorised the reintroduction of their expendable launchers for commercial use. Substantially improved and larger versions of the Atlas, Delta and Titan launchers were promptly reintroduced into the commercial market in 1989 and these launchers are slowly acquiring a share of the commercial satellite launch services market.

The NSTS experience has made launcher technologists across the world aware of the potential cost implications of partial or full reusability of launchers. Yet, the will and effort persists to develop reusable launchers. This will is driven by the major technical challenge of reusability and the hope that technology advancements that have been made since the development of the NSTS in the 1970's will now make reusable launchers technically feasible, and, even more hopefully, affordable!

It is also perceived that the technical requirements for fully reusable launchers are much more demanding than those of fully expendable and partially reusable ones. It is also perceived that the specific impulse of even the best performing and fully developed rocket propellant combination (liquid hydrogen/liquid oxygen) would be too low to achieve useful payload mass ratios on reusable launchers because of their intrinsically higher net vehicle mass ratios. More advanced rocket propulsion systems then seem to be essential to allow the evolutionary development of reusable launchers from expendable ones. But we seem to be at the very limit of technological developments in rocket propulsion and that major rocket propulsion advances are hardly conceivable.

Clearly then, there is a need to look at alternative propulsion systems, and to meet this need, the launcher community has recently revived a high interest in air-breathing propulsion systems installed in winged launch vehicles, to benefit, at least intuitively, from the propellant mass savings that would be possible from not having to carry all the oxidiser in the vehicle and from the aerodynamic lift that is made possible by a winged vehicle. Thus, air-breathing propelled, winged launcher concepts, represent an alternative, revolutionary approach to the challenge of reusability!

With this background, the motivation for this research can now be summarised:

- there is a clear need to reduce the cost of space transportation to expand further the exploration and exploitation of space;
- it is perceived by launcher technologists that reusable launchers are the key to achieving space transportation cost reductions and that technology advances will make reusable launchers feasible;
- the technical challenge of reusability is the spur for the development of fully reusable launchers.

1.2 Objectives of the Research

Despite the major national efforts that are currently engaged to develop reusable launchers, which are reported in Chapter 2, an extensive survey of the literature by the author at the start of this research on 1 March 1989, revealed a significant omission of studies that compared the various types of reusable launcher concepts at complete vehicle system level. Furthermore, there was also an absence of vehicle system analysis reports for the particular reusable launcher concepts that had been selected for study by individual nations. Therefore, for those interested in the potential of reusable launchers to fulfil future launcher needs at substantially reduced costs, it was not possible to understand the selection of a particular preferred vehicle in the absence of fundamental knowledge of the performance feasibility, operational characteristics, domains of application and life cycle costs of the various reusable launcher concepts. On the other hand, the literature revealed many publications dealing with the various enabling technologies: air-breathing propulsion; advanced rocket propulsion; aerodynamics and aerothermodynamics; advanced materials and structures; thermal control and protection; trajectories and guidance. It was therefore perceived by the author that the various technology studies were being pursued in isolation, as interesting technological entities, but ahead of and without links to requirements derived from complete vehicle system studies.

With this background, it became evident to the author, that there was a clear need for a fundamental, comparative study of reusable launcher concepts at vehicle system level, which could provide a proper technical basis for use in selecting appropriate vehicle concepts to meet any specified set of future launcher requirements. To undertake this comparative study, the tasks of this research were established: to derive

and compare the performance capabilities, technical feasibility, application domains, operational features and life-cycle costs for a range of potentially feasible reusable launcher concepts. The clear intention was that the results of these tasks would then allow to fulfil the primary objective of the research, which is, to provide clear answers to the following three fundamental, but absolutely imperative questions:

- which reusable launcher concepts can actually deliver a positive payload mass to orbit?

- what advanced technologies are needed to enable the practical realisation of each reusable launcher concept and is it feasible to develop these technologies in a reasonable time scale and at affordable costs?

- what are the development, procurement and operation costs of each reusable launcher concept and are these costs substantially less than those of the currently available expendable launchers, thus justifying their development?

1.3 Methodology of the Research and Structure of the Thesis

To meet the objectives of the research, a clear methodology had to be established at the start of the research in March 1989. This methodology, which is described below, was then implemented as planned. The Structure adopted for the Thesis therefore presents the work done in each successive step of the research.

The first step in the research was to review the literature on future launcher concepts, with particular emphasis on reusable launchers: to establish what had already been studied and what activities were currently engaged across the world in the analysis, design and development of reusable launchers and the advanced technologies that are required to enable their realisation into practical vehicles. This review, which was pursued throughout the research period, amassed a great deal of information on reusable launchers, but most of this related either to studies of particular launcher concepts, without justifications for the selection of the concept, or to advanced technologies for future launchers. This review revealed however, that major efforts had been pursued since 1986 in all the space-faring nations, on selected reusable launcher concepts, but again, without justification for their selection. Therefore, to provide the background to the Thesis, the results of this review are briefly presented in Chapter 2 of the Thesis: Current Activities on Reusable Launchers.

The second step in the research was to understand and establish an operational and performance framework for reusable launchers. This comprised the following three activities:

- derivation of the performance, reliability and costs of current expendable launchers, as fundamental pre-requisites, to be able to set the minimum performance targets and expectations for the inherently more technically demanding reusable launchers;

- assessment of the probable space transportation needs for the early 21st century, to see how reusable launchers could fulfil these needs;

- derivation of a range of reusable launcher concepts which were deemed by the author, on an intuitive basis at the start of this research, to be potentially feasible concepts and to define their performance and operational characteristics. These vehicles would then be adopted as candidate vehicles in a comparative performance and cost assessment, which would be the major activity of the research.

These three activities are reported in Chapter 3 of the Thesis: The Challenge of Launcher Reusability.

The third step in the research was the preparation of the performance analysis tools that would be required for the comparative performance of the selected launcher types. The major tool required was a trajectory analysis computer code that could be used for the full range of vehicle types: single and two-stage-to-orbit vehicles; rocket-propelled and/or air-breathing propelled: ballistic and/or lifting ascent and descent. The results of this work are presented in Chapter 4 of the Thesis: Performance Analysis of Reusable Launchers.

The fourth step in the research was the most crucial one and was conceived to give clear answers to the three fundamental, but imperative questions that must be posed for any prospective reusable launcher type:

1) Has the reusable launcher adequate performance to deliver a positive payload mass to orbit?

2) If the answer to Question 1 is Yes, then what are the technology requirements needed to deliver this performance and is it feasible to develop the needed technologies and what would be the development time scale?

3) If the answer to Question 2 is also Yes, then is the launcher cost effective and affordable and how does its costs compare with those of other feasible vehicles?

An effort to find answers to these three fundamental questions for each selected reusable launcher type, has been the major work of this research.

The answers to Question 1 are addressed in Chapter 5 of the Thesis: Calculated Performance of Reusable Launchers.

The answers to Question 2 are addressed in Chapter 6 of the Thesis: Technology Assessment for Reusable Launchers.

The answers to Question 3 are addressed in Chapter 7 of the Thesis: Cost Analysis of Reusable Launchers.

The fifth step in the research was a comparative analysis of the selected reusable launcher concepts, based on the research results of their performance, technical feasibility and cost. This work is reported in Chapter 8 of the Thesis:

Results of the Comparative Analysis of Candidate Reusable Launcher Concepts.

Finally, Chapter 9 of the Thesis presents the Conclusions of the Research and Chapter 10 presents the list of References that have been used.

2 CURRENT ACTIVITIES ON REUSABLE LAUNCHERS

2.1 Background

Since the advent of the space age, fully reusable launchers have been a subject of continuous interest in all the space-faring nations. The major focus of interest in all these studies has been the potential use of air-breathing propulsion as the key to reusability. Despite these efforts, no launch vehicles have emerged, not even expendable ones, that utilise air-breathing propulsion as an enabling technology. What has emerged however, is the continuing use of rocket propulsion in the only two partially reusable launchers to date: the USA NSTS which entered service on 12 April 1981 and the former USSR's Buran/Energia (Figure 2.1) which had its first, and only flight to date, on 15 November 1988. These developments, undertaken by the two most powerful space nations, seemed to signify that fully reusable launchers were somehow not feasible or affordable. In the meantime, world interests in air-breathing propulsion for fully reusable launchers has proceeded with studies by enthusiasts.

Figure 2.1

The World's Second Partially Reusable Launcher:

The CIS Buran/Energia

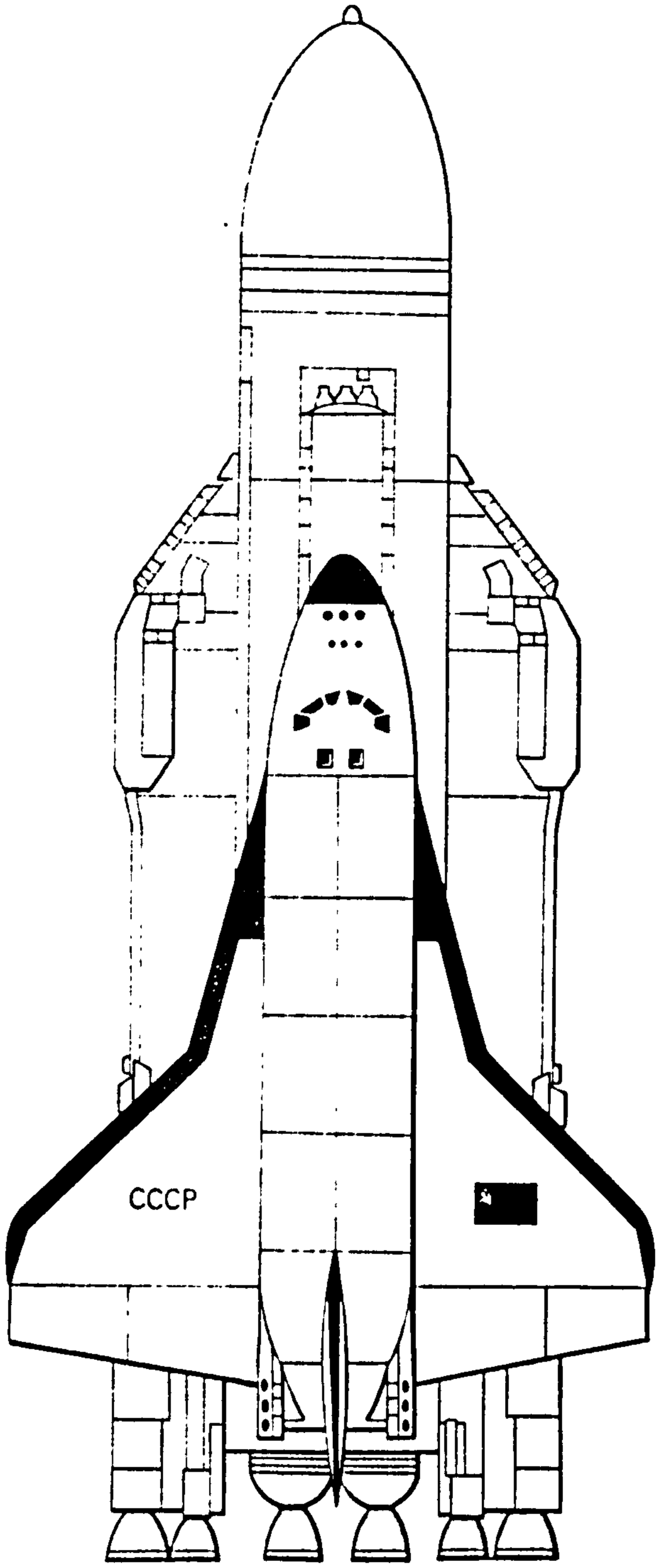

Height: 60.3 m.
Gross Mass: 2505 tonnes
Thrust at Lift-Off: 35000 KN
LEO Payload: 30 tonnes

This situation, however, was changed dramatically in 1984 when the United Kingdom announced HOTOL (Figure 2.2), a single-stage-to-orbit (SSTO), fully reusable launcher, powered by a revolutionary new engine: a combined air-breathing and rocket engine. HOTOL, which is an acronym for 'horizontal take-off and landing launcher' was to be a 275 tonnes unmanned vehicle capable of delivering a 7 tonnes payload into a low earth orbit (LEO). HOTOL was to be launched horizontally from a rocket-propelled rail-guided trolley and would land on a conventional runway using its own landing gear. HOTOL was to reduce the cost of transporting payloads to orbit to 20% of the transportation costs of the expendable launchers. Apparently, the key to the feasibility of HOTOL was its new engine, the patented design of which was immediately classified as secret by the UK Ministry of Defence. Thus, despite the high excitement and interest that the announcement of HOTOL had created in the world's launcher community, it was not possible for this community to independently verify the feasibility of this startling concept because of the complete absence of information on the performance of its new engine: the Rolls-Royce RB 545 (Swallow) engine. This engine concept has now been declassified. It can be described as a cryo-rocket engine, in which the liquid hydrogen propellant is used to deeply cool intake air in a heat exchanger. This cold air is then raised to a high pressure by a turbocompressor before injection into a hydrogen fuelled rocket engine.

The announcement of HOTOL and the mystery surrounding its new engine, resulted immediately in the stimulation and coordination of major new efforts in reusable launchers in the USA, Germany, France, Europe (under the auspices of ESA), Japan, the former USSR and China. These efforts have gained considerable momentum since 1985 and have evolved into major research activities. These current activities are briefly described below:

2.2 Reusable Launcher Activities in the USA

In the USA, research efforts are concentrated on two fully reusable launcher concepts. These are:

- the National Aerospace Plane (NASP);
- the Delta-Clipper.

The NASP is a programme which plans to build and test an experimental research vehicle called the X30 (Figure 2.2), which is a SSTO winged vehicle, propelled by a combined air-breathing and rocket propulsion system comprising: an unspecified and secret low speed propulsion system for take-off, which then transitions to a subsonic combustion ramjet and then to a supersonic combustion ramjet (scramjet) and finally to rocket propulsion for the final ascent to orbit. The X30 will take-off horizontally from a conventional runway, accelerate to low earth orbit, re-enter the earth's atmosphere and descend to land horizontally on a conventional runway. The X30, being an experimental vehicle, has no operational mission requirements. It will serve instead as a flight demonstrator to validate critical technologies and to demonstrate the feasibility of the fully reusable SSTO concept. The NASP/X30 programme is a $5 billion effort co-funded by the US Air Force and NASA. The programme was initiated in 1986 and the first flight of the X30 is planned for 1996. The experience gained from the X30 will form the basis for the development of NASP-derived fully reusable operational launchers.

The Delta-Clipper (Figure 2.2) is a vertical launch and vertical landing (VLVL) rocket-propelled SSTO vehicle. It is being developed by the McDonnell Douglas Company under contract to the Space Defence Initiative Organisation (SDIO). The concept employs advanced rocket propulsion and utilises low weight, advanced structural materials and other advanced technologies that have been developed under the NASP and

Advanced Launch System (ALS) programmes. Phase 1 concept studies were initiated in 1989 under four parallel industrial studies by Rockwell, General Dynamics, Boeing and McDonnell Douglas respectively. A Phase 2 feasibility demonstration contract was awarded to McDonnell Douglas in mid 1991, to design, build and fly in mid 1993, a one-third scale prototype vehicle called the DC-X. This prototype will be used to demonstrate the critical vertical descent manoeuvre and to validate ground preparation and rapid turn-around operations. A suborbital flight demonstration could take place in 1996.

2.3 Reusable Launcher Activities in Germany

In Germany, studies have been performed since 1987 on both reusable rocket-propelled and winged air-breathing launcher concepts. The reusable rocket-propelled launcher, called EARL (European Advanced Reusable Launcher), is a fully reusable TSTO vehicle. The study was performed by Dornier and was completed in 1990.

In 1988, an ambitious hypersonic technology programme was formally initiated by the Federal Ministry for Research and Technology (BMFT) to conduct research and developments leading to a fully reusable European aerospace plane powered by a combined air-breathing and rocket propulsion system. The reference concept for this programme is the Saenger II vehicle (Figure 2.2), which is a TSTO launcher which takes-off and lands horizontally. The first stage vehicle is powered by a turbojet engine for take-off, transitioning to a subsonic combustion ramjet for operation up to the second stage separation altitude of about 34 km at Mach 6.8. The first stage then returns to land like a conventional aircraft. The second stage is rocket propelled for its ascent to orbit. After re-entry, it performs a gliding descent to a horizontal landing. The first stage vehicle is also

envisioned as the basis for a future hypersonic transport aircraft. The hypersonic technology programme also includes studies for a flight demonstration vehicle called Hytex, which is to be used to demonstrate and validate enabling technologies, notably the turboramjet engine.

2.4 Reusable Launcher Activities in France

In France, conceptual studies on fully reusable air-breathing propelled launchers were initiated in 1986. Both SSTO and TSTO concepts have been studied: Aerospatiale studied both SSTO and TSTO vehicles (Figure 2.2) under its STS 2000 study; Dassault Aviation studied a TSTO concept called STAR-H (Figure 2.2) using the ESA Hermes vehicle as the second stage. In September 1991, a French hypersonics technology programme called PREPHA was formally initiated to undertake research and developments in scramjet propulsion, leading to a fully reusable SSTO aerospace plane propelled by a combined air-breathing and rocket propulsion system including scramjet propulsion. This reference concept is analogous to the USA X30 vehicle.

2.5 Reusable Launcher Activities in the United Kingdom

In the United Kingdom, the work on the HOTOL vehicle, which was started in 1983, came to a virtual halt in 1988 because of the withdrawal of financial support from the UK Government. Private funding by the designers, British Aerospace, allowed the project to proceed at a very low level of effort until 1990. At this time, the results of the parallel work in the ESA Winged Launcher Configuration studies, revealed that the SSTO concept based on HOTOL, was not feasible for the ESA-specified mission. This triggered British Aerospace to initiate a joint study with the Soviet Ministry of Aviation Industry in July 1990 to study the feasibility of air-launching an interim version of HOTOL from

the back of the Soviet Union's Antonov AN-225 heavy-lift transport aircraft, at an altitude of 9 km and a speed of Mach 0.8. HOTOL was thus transformed into a TSTO vehicle called Interim HOTOL (Figure 2.2). The combined air-breathing and rocket propulsion system of HOTOL was replaced by a rocket propulsion system for Interim HOTOL.

2.6 Reusable Launcher Activities in ESA

At European level, the European Space Agency (ESA) initiated the development of the Hermes spaceplane in October 1987 The programme was postponed in November 1992. Hermes was to be launched into orbit by the Ariane 5 expendable launcher in 2002. This partially reusable system which was analogous to the NSTS, was considered to be an essential first development for European autonomy in manned space flight. Hermes had a specified launch mass of 22 tonnes and could carry a crew of three plus a payload mass of 3 tonnes.

Looking beyond Hermes and Ariane 5, ESA is studying both reusable rocket-propelled and winged launcher concepts. The reusable launcher studies have been performed since 1988 and are based on the use of Ariane 5 technologies. A study on winged launcher configurations was also initiated in 1988. Both SSTO and TSTO concepts have been studied. To meet the ESA mission specification, and to provide ESA with direct insight into the HOTOL and Saenger studies, the SSTO concept was developed from the UK HOTOL vehicle and the TSTO concept was developed from the German Saenger II vehicle. A key feature of the ESA specification was to limit the air-breathing propulsion to subsonic combustion systems only. This specification was deliberate, to allow the capabilities of subsonic combustion systems, which are well developed in Europe, to be explored independently, before embarking, if the study results warranted it, on supersonic combustion

studies, for which Europe currently has only a limited capability.

2.7 Reusable Launcher Activities in Japan

In Japan, fully reusable launcher studies were initiated in 1986 and these studies have grown into three complementary major projects. These are:

- H2 Orbiting Plane (HOPE), which is an unmanned vehicle to be launched into low earth orbit in 1999 on top of Japan's new heavy-lift launcher, the H2 vehicle. The HOPE/H2 concept is a partially reusable launch system, analogous to the ESA Hermes/Ariane 5 concept, except that HOPE is an unmanned vehicle and is much smaller, with a launch mass of 10 tonnes. After re-entry, HOPE would make a gliding descent to land horizontally on a conventional runway. Study activates on HOPE were suspended in 1992.

- Highly Manoeuvrable Experimental Space Vehicle (HIMES) is a fully reusable, unmanned single-stage-to orbit, ballistic flight test vehicle. HIMES is to be rocket-propelled and to be launched either vertically or on a rocket-propelled sled and would land horizontally on its own undercarriage. HIMES will serve as a test bed for hypersonic flight and air-breathing engines and will thus constitute an interim vehicle and flight demonstrator, leading to the development of a future Japanese air-breathing propelled, fully reusable SSTO launcher. Scale models of HIMES have already been flight tested. Low speed flight was tested in helicopter drop tests in 1986. Re-entry flight was demonstrated in 1987 and 1988 using scale models boosted into orbit from high altitude helium balloons. A prototype version of HIMES is planned to be available in 1998.

- SSTO Aerospace Plane. The Japanese National Aerospace Laboratory (NAL) is studying a horizontal take-off and landing SSTO aerospace plane with a launch mass of 350 tonnes, propelled by combined air-breathing and rocket propulsion systems (Figure 2.2). Three Japanese companies: Fuji, Kawasaki and Mitsubishi have been actively engaged since 1988 in individual conceptual designs of manned hypersonic experimental aircraft of about 50 tonnes launch mass, to be used as flight demonstrators for the SSTO aerospace plane. Japan is making a major effort in the development of advanced propulsion systems for aerospace planes. Efforts are concentrated on: a liquified air cycle engine (LACE) for take-off and low speed propulsion; a supersonic combustion ramjet for high speed propulsion.

2.8 Reusable Launcher Activities in the CIS

In the CIS, efforts are engaged in the study of a partially reusable TSTO concept called MAKS. This comprises the air-launch of a rocket-propelled second stage, which itself comprises an assembly of a large disposal external tank on top of which is mounted either a small, winged, crewed and reusable vehicle, or a larger, ballistic, expendable cargo vehicle (Figure 2.2). Study and experimental activities in advanced rocket and air-breathing propulsion for fully reusable SSTO launchers are also engaged. Research efforts are concentrated on tri-propellant rocket engines, liquid air cycle engines (LACE) and scramjet engines.

Figure 2.2

Photo-Montage of Current Reusable Launcher Concepts

Legend Diagram

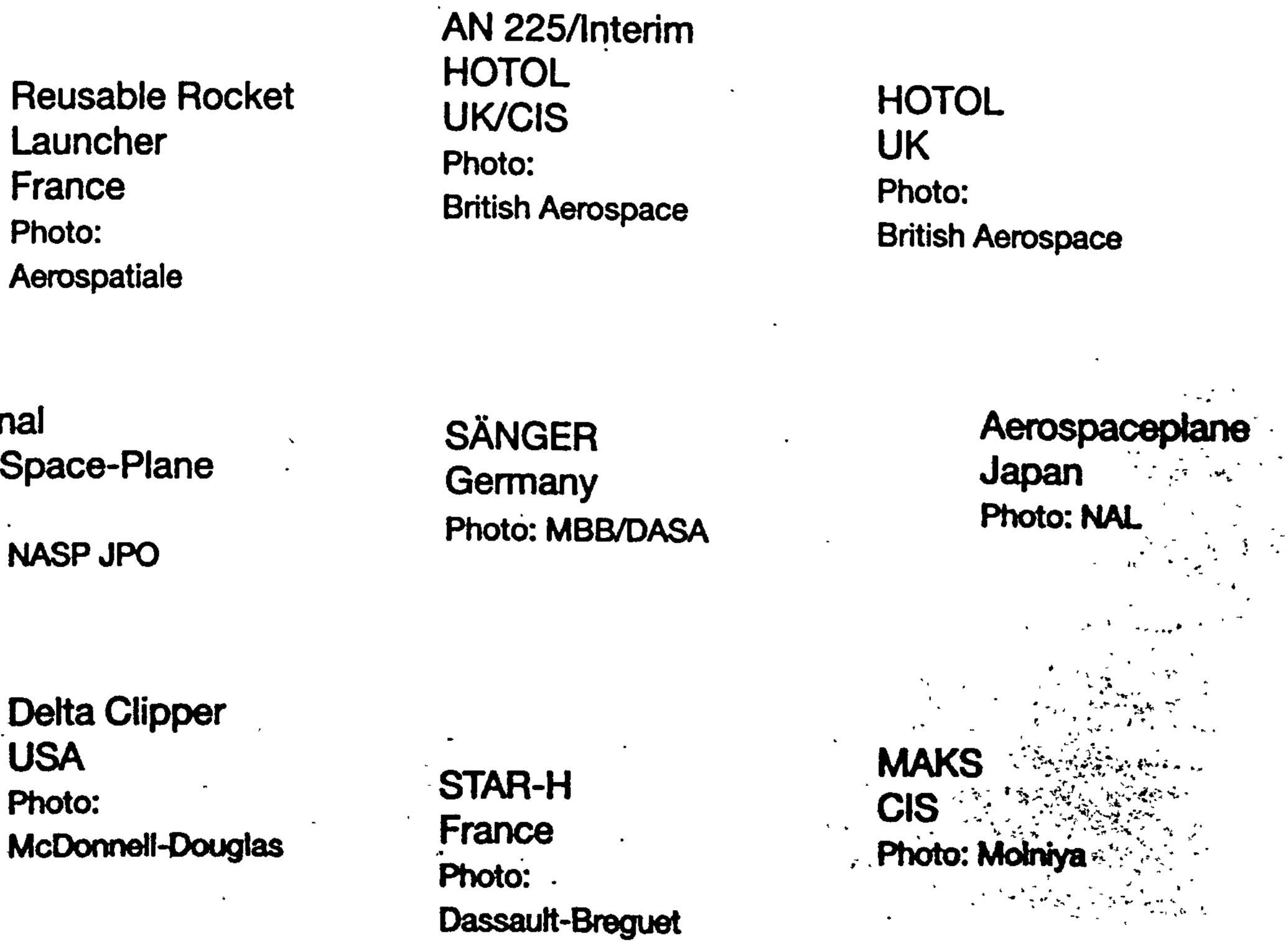

TEXT CUT OFF IN ORIGINAL


SÄNGER
DELTA Clipper
USA

3 THE CHALLENGE OF LAUNCHER REUSABILITY

The design, development, manufacture and operation of the currently available expendable, rocket-propelled launchers has been, and still is, a major technical challenge, requiring the utmost skills and resources in aeronautical engineering. The results of these engineering efforts is that these expendable vehicles are able to deliver small payload mass ratios to orbit (typically 2 %), but the reliability record is poor and catastrophic launch failures still occur, even for the oldest launch vehicles like Atlas, Delta and Titan that have been progressively developed over the last 40 years!. This poor reliability, which is addressed further, later in this Chapter, has resulted in the loss of valuable satellite payloads and the consequent levying of high launch insurance premiums, which are currently running at the level of about 20 % of the launch cost!. These high premiums are a major impediment to the growth of commercial space activities.

With this background, how then can we expect to develop and operate Reusable Launchers when it is obvious that these vehicles will pose more demanding technical requirements to:

- improve payload mass ratio;
- improve reliability;
- improve safety;
- improve versatility;
- improve resiliency

AND achieve these demanding technical requirements whilst succeeding to substantially:

- reduce launch costs

This then is the challenge of Launcher Reusability!

The key to meeting this challenge is the development and application of advanced technology and the use of new innovative design approaches. These key technologies are:

- propulsion;
- aerodynamics and aerothermodynamics;
- materials and structures;
- trajectories and guidance;
- vehicle subsystems.

Advances in any of these technical areas alone will probably be insufficient to meet the challenge of reusability, but the simultaneous major advance in all of them can probably make reusable vehicles possible. The prospects for this are presented in Chapter 6: Technology Assessment for Reusable Launchers.

To establish clearly the specific targets and requirements that would have to be met to achieve launcher reusability, the first step is to know exactly the performance, reliability and costs of the currently available expendable launchers. This is established in Section 3.1 of this Chapter. The second step is to define the likely space transportation needs that reusable launchers would have to fulfil in the first few decades of the 21st century. This is addressed in Section 3.2 of this Chapter. The third step is to derive a set of potentially feasible reusable launcher concepts for analysis in this research. This is addressed in Section 3.3 of this Chapter.

3.1 Performance, Reliability and Costs of Current Expendable Launchers

3.1.1 The Current Expendable Launcher Scenario

Countries with a launch capability are:

- United States of America;
- Commonwealth of Independent States (CIS),
- Western Europe;

- Japan;
- China;
- India;
- Israel.

These countries, between them, currently have eighteen different expendable launcher systems available. The configuration and performance of these launchers are shown in Figures 3.1A to 3.1D. There are fifteen different geographic launch sites. These are shown in Figure 3.2. Sixteen of the eighteen currently available launch systems are expendable vehicles, which therefore, can only deliver payloads to orbit. The remaining two launchers are partially reusable vehicles (NSTS and Buran/Energia), which can deliver and return both cargo and crew payloads to and from orbit. Only five of the launcher systems are available for commercial launch services. These are:

- Atlas, Delta and Titan (from the USA);
- Ariane 4 (from Western Europe);
- Long March (from China).

It is expected that by 1995, that the CIS, with its Proton and Zenit launchers and Japan with its H2 launcher, will also establish themselves in the commercial launch services market. Western Europe, through Arianespace, with its Ariane series of launchers, has captured 50 % of the world's commercial launch services. The current market shares of the five competing launch systems is shown in Figure 3.3.

Figure 3.1A Current Launchers of the USA (Reference 1)

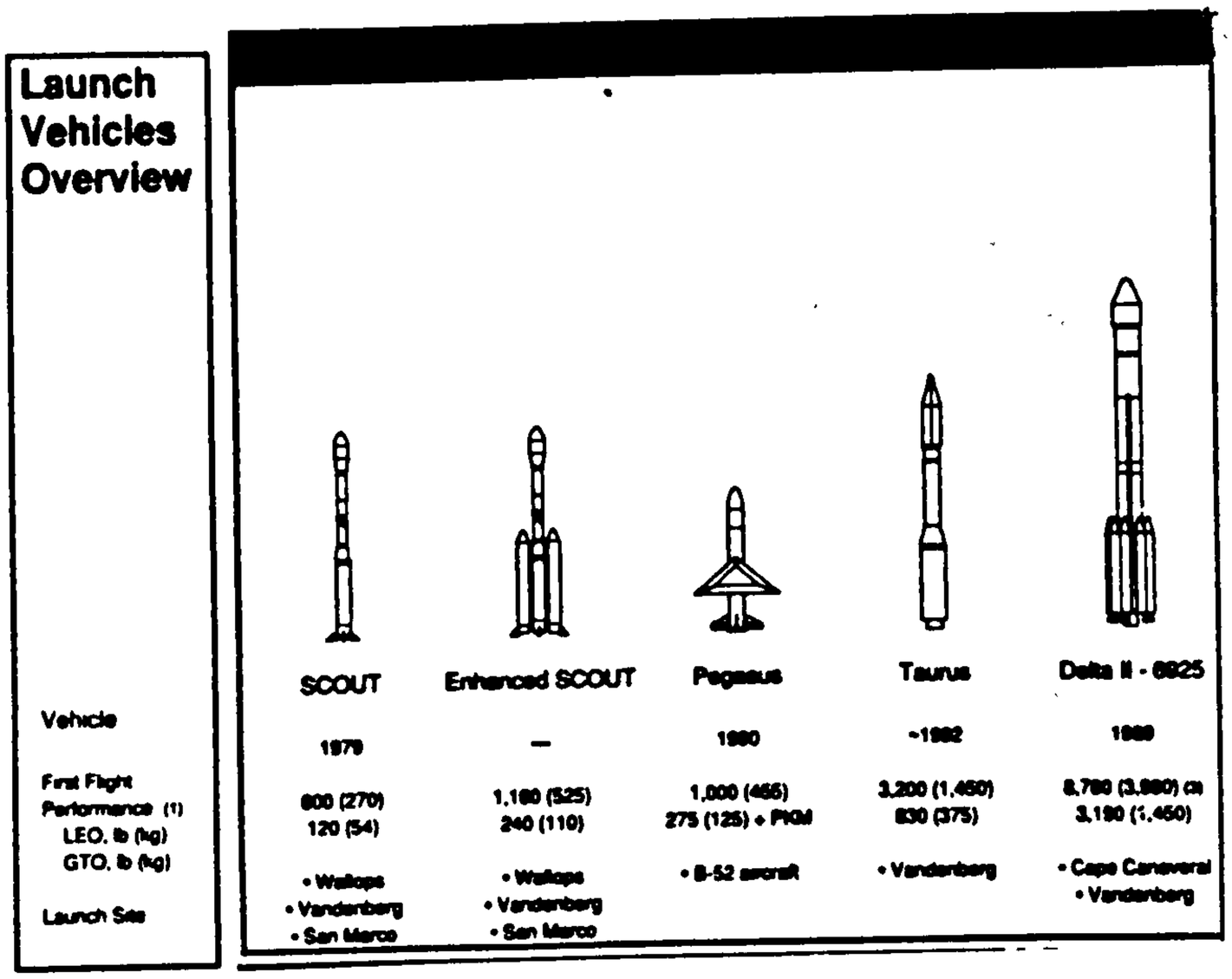

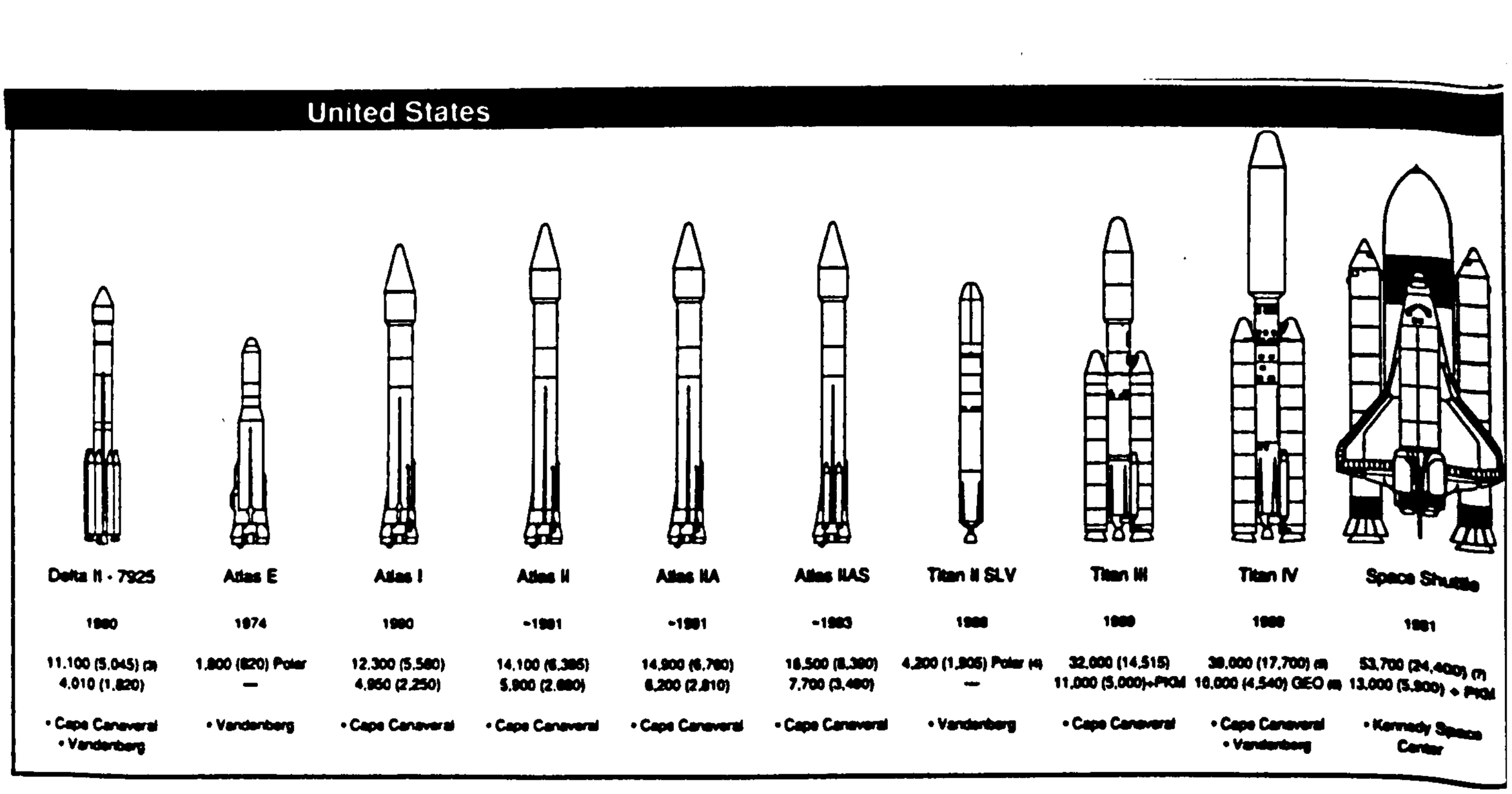

Figure 3.1B Current Launchers of the CIS (Reference 1)

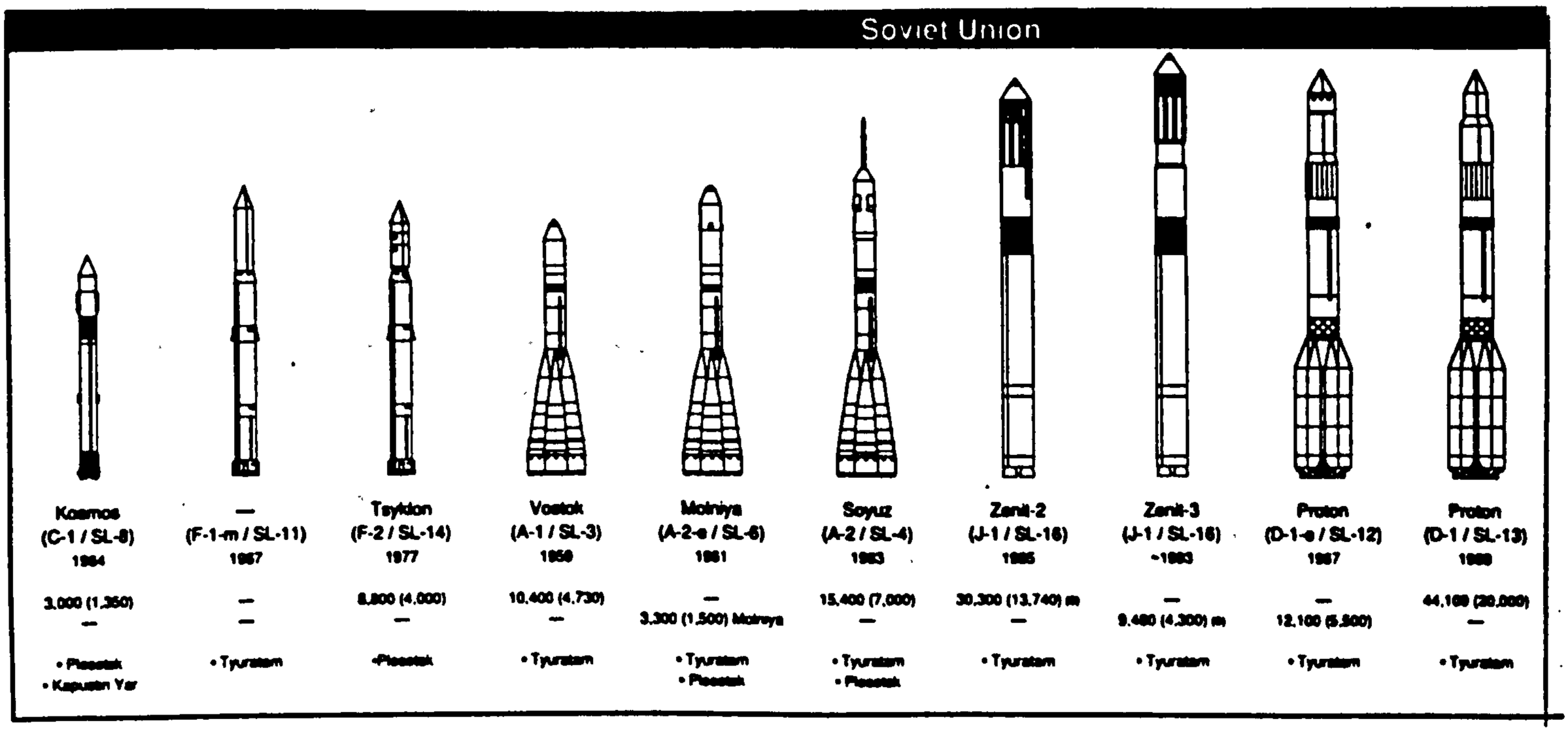

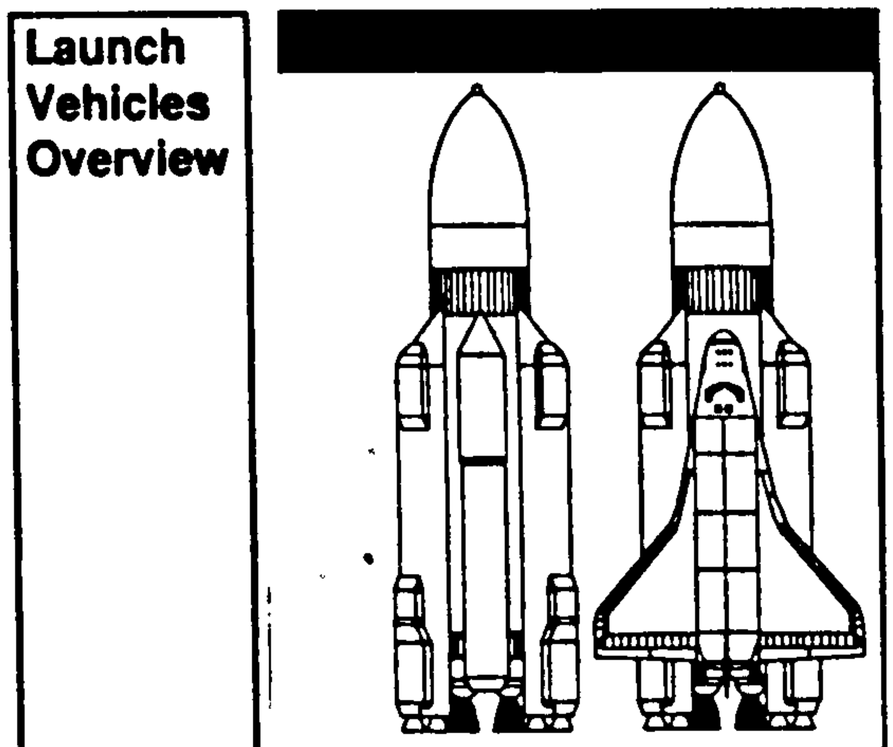

Figure 3.1C Current Launchers of China, Israel, Japan and India (Ref.

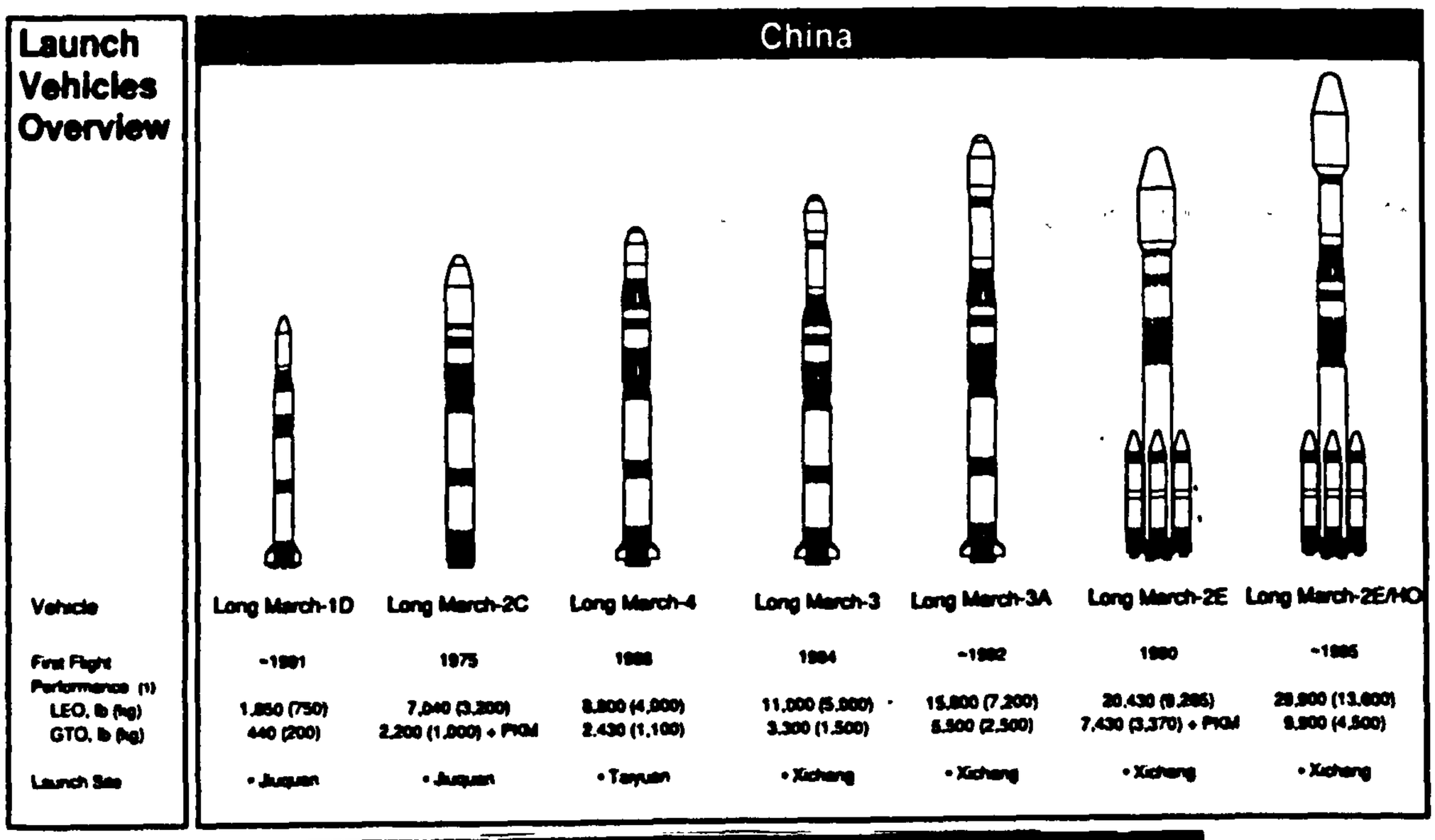

Figure 3.1D Current Launchers of Europe (Reference 1)

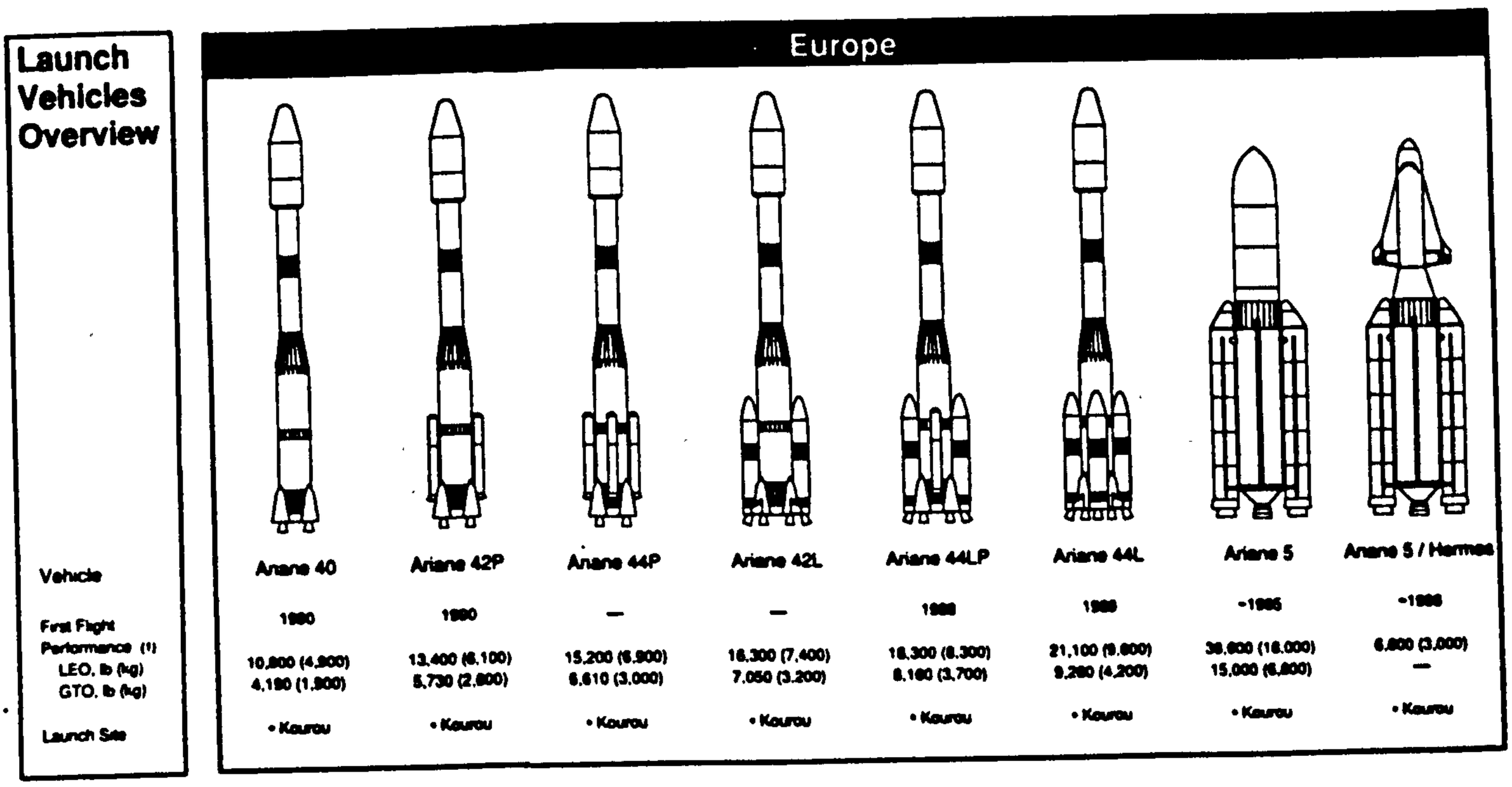

Figure 3.2 Current World Launch Sites

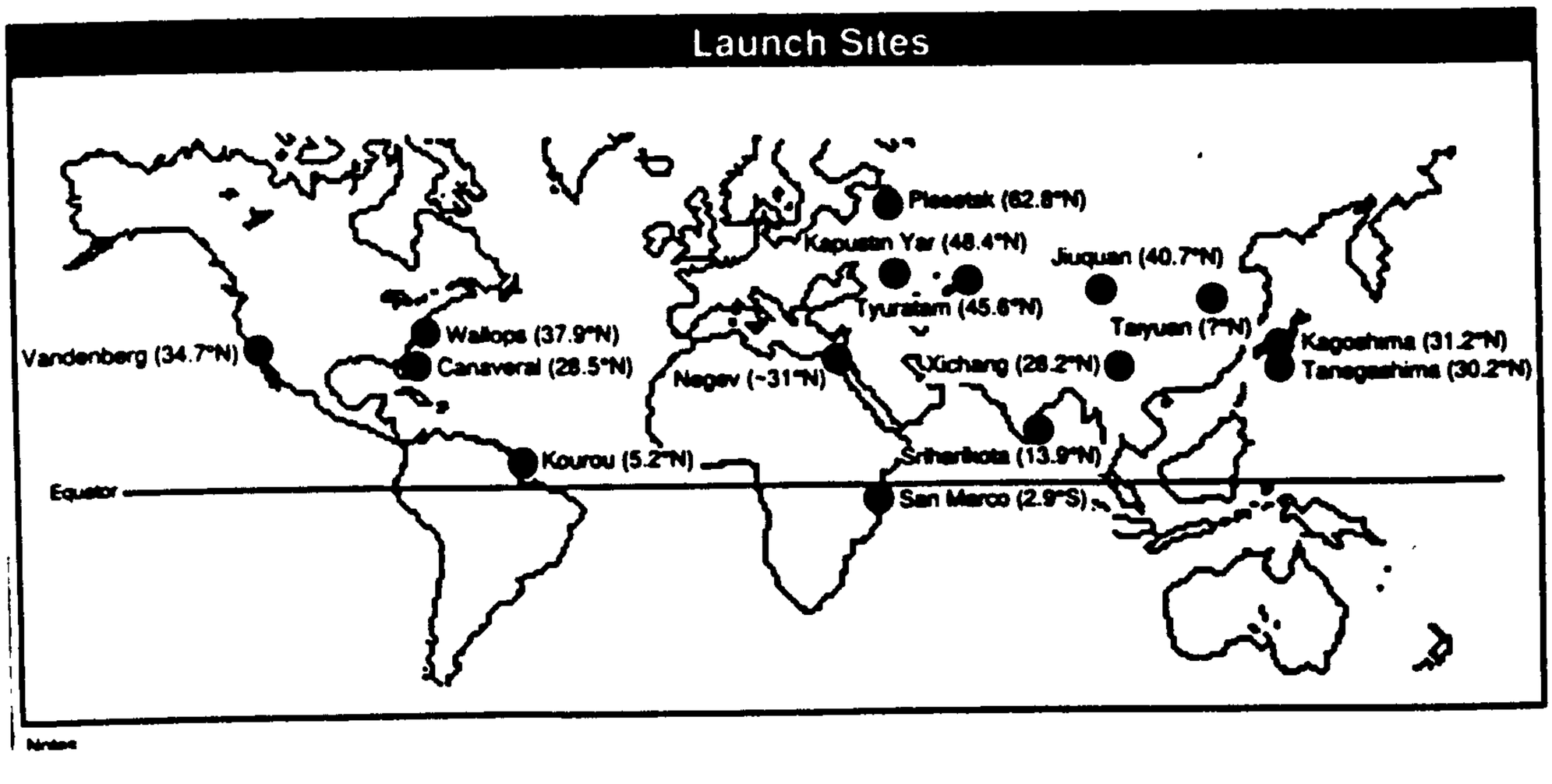

Figure 3.3

Launch Services Market Shares for Commercial Satellites
Period 1986 to 1992 (Percentages)

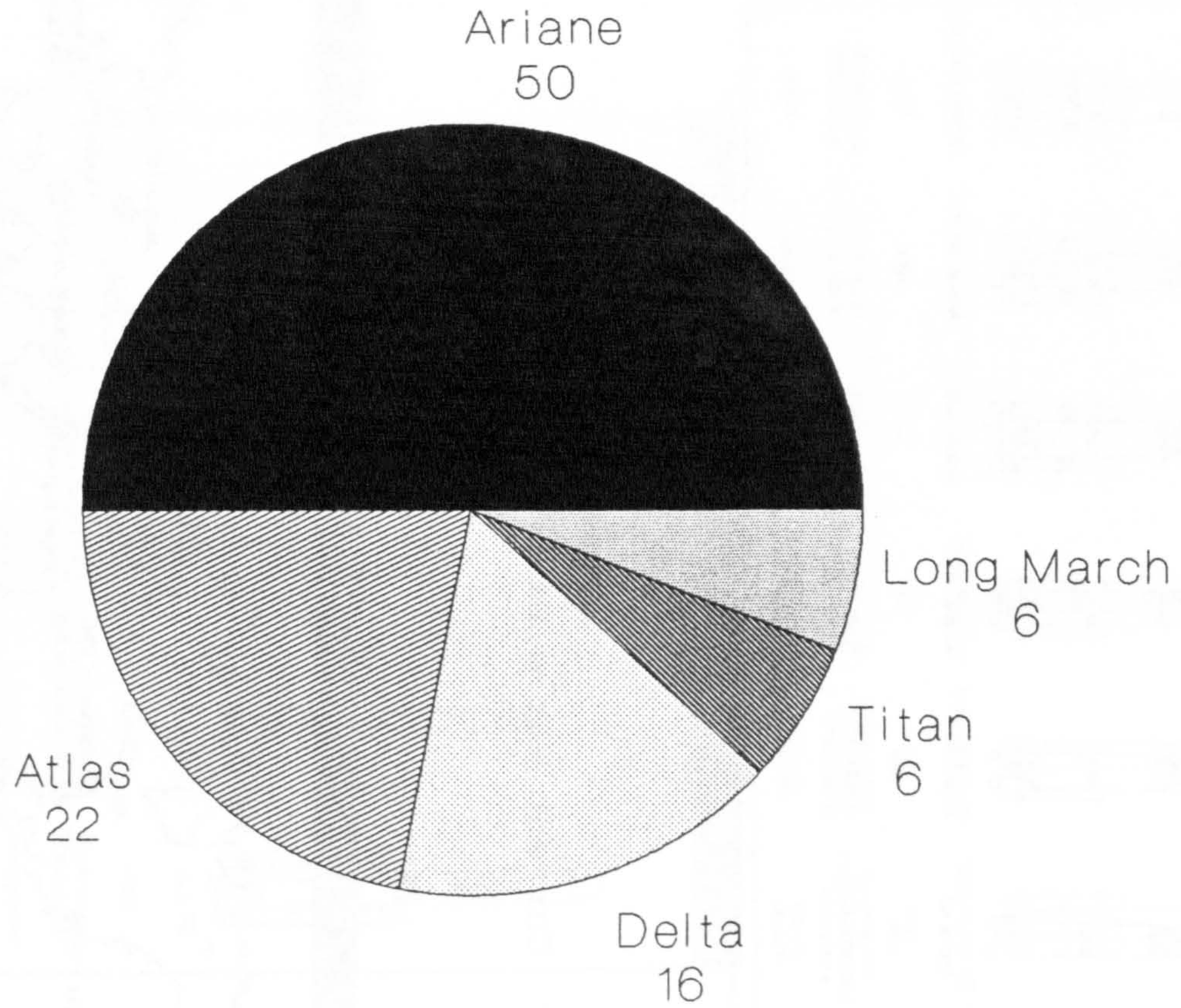

3.1.2 Performance of Current Expendable Launchers

The performance of 14 of the currently available expendable launchers, delivering payloads into standard orbits, compiled from Reference 1 is shown in Table 3.1. The most important performance parameter is the payload mass ratio. It can be seen from Table 3.1 that the payload mass ratio range has a lowest value of 0.39 % for the five-stage all-solid propellant ASLV from India, to a highest value of 3.66 % for the all-liquid propellant Energia launcher from the CIS. It can also be seen that the solid propelled vehicles have the lowest payload mass ratio values and that the liquid propelled vehicles using hydrogen/oxygen propellants have the highest values. The liquid-propelled launchers using storable propellants have intermediate payload mass ratios of about 2 %. It can also be seen that the lift-off thrust/weight ratio range is from a low value of 1.17 for Ariane 44L to a high value of 1.66 for the Titan IV launcher.

Thus, based on the achieved performance of the currently available expendable launchers, we could select a value of 2 % as a payload mass ratio target for reusable vehicles. Larger values will be difficult to achieve because of the inherently higher vehicle net mass of reusable launchers and lower values that 2 % would be commercially unattractive.

It is also interesting and relevant to this research, to know the actually achieved net mass ratios of the individual stages and of the complete launcher for the current expendable launchers. This data, again compiled from Reference 1, is shown in Table 3.2. It can be seen that an average net mass value of a liquid propellant stage is about 10 % and that the overall launcher net mass ratio, defined as the mass ratio of the empty vehicle without its payload mass, is also about 10 %. Thus, unless we can radically improve launcher technology in all areas, it can be seen that it will

be difficult to reduce further the net mass ratios for reusable launchers. The required technology improvements are:

- the development of propulsion systems with higher specific impulse to reduce the propellant mass and hence the structural mass;
- the development of propulsion systems with higher thrust/weight ratios to reduce the dry mass of the engines;
- the development of aerodynamically efficient vehicles to reduce aerodynamic drag losses and hence the propellant mass, resulting again in reductions in the structural mass;
- the development of advanced high specific strength materials to reduce directly the structural mass of the vehicle;
- the design of minimum energy ascent trajectories to reduce the propellant mass and hence the structural mass.

3.1.3 Reliability of Current Expendable Launchers

The launch record of the five commercial launchers and that of the NSTS, compiled from Reference 1, are shown in Table 3.3. It can be seen that the failure rate range is from 5.4 % for Delta to a very high value of 12.5 % for Long March. The NSTS, which is a crewed vehicle, has had only one catastrophic failure in 55 flights to the end of April 1993, giving a failure rate of 1.8 %. It can also be seen that the last failure for most of the launchers was quite recent, which demonstrates clearly the random nature of these failures, which were all caused by unforseen technical failures.

Thus, it can be concluded from these reliability results, that despite the very long production and operational experience of several of these expendable launchers, that the failure rates are still very high. The lesson to be learned from this and applied to future launchers, is that the

failure tolerance, or resiliency, of these future vehicles must be improved by design. For example, a mission must not be lost due to an engine failure.

3.1.4 Costs of Current Expendable Launchers

The costs of launch services for each of the currently available expendable launchers, compiled from Reference 1, are shown in Table 3.4. It can be seen that the delivery cost per kilogram to a geostationary transfer orbit are in the range of 25000 US Dollars per kilogram for the Long March and Ariane Launchers and about 50000 US Dollars per kilogram for the USA vehicles Atlas and Delta.

Thus, for future launchers, the lower value of 25000 US Dollars per kilogram must be substantially reduced to say, by 50 % to 12500 US Dollars per kilogram to make it worthwhile to invest in the development of any new commercial launcher.

We can now set minimum targets for performance, reliability and costs for future commercial launchers, which could of course be expendable or reusable vehicles:

- Performance Target: More than 2 % Payload Mass Ratio into Low Earth Orbit;
- Reliability Target: Less than 1 % Failure Rate
- Cost Target: Less than 12500 US Dollars per kilogram into Low Earth Orbit.

TABLE 3.1 PERFORMANCE OF CURRENT EXPENDABLE LAUNCHERS (STATUS 1 MAY 1993)

COUNTRY	LAUNCHER	NUMBER OF STAGES	PROPULSION SYSTEMS				LIFT-OFF VALUES		PAYLOAD MASS (Kg)	RATIOS	
			BOOSTERS	STAGE 1	STAGE 2	STAGE 3	LAUNCH MASS (TONNES)	THRUST (KN)		THRUST/ WEIGHT	PAYLOAD/ LAUNCH MASS (%)
CHINA	LONG MARCH CZ - 2E	2	4 NTO/UDMH	NTO/UDMH	NTO/UDMH		464	5922	9200 (200 Km circular 28.5 deg)	1.30	1.98
EUROPE	ARIANE 44L	3	4 NTO/UH25	NTO/UH25	NTO/UH25	LOX/LH2	470	5380	9600 (185 Km circular 5.2 deg) 4600 in GTO	1.17	2.04
INDIA	ASLV	4 (ALL SOLID)	2 HTPB	HTPB	HTPB	HEF-20 STAGES 3 & 4	39	880	150 (400 Km circular 43 deg)	2.30	0.39
JAPAN	H - I	2	9 CTPB	LOX/RJ1	LOX/LH2	HTPB	140	1800	3200 (185 Km circular 30 deg)	1.31	2.28
USA	SCOUT GI DELTA II 7925 ATLAS IIA TITAN IV	4 (SOLID) 2 OR 3 2½ 2 OR 3	HTPB 9(HTPB) 4(HTPB) 4(PBAN)	PBAN LOX/RP1 LOX/RP1 NTO/AZ50	CTPB NTO/AZ50 LOX/LH2 NTO/AZ50	HTPB HTPB - -	21.75 230 187.7 860	464.7 2630 2110 14000	270 5045 6760 17700 (all 185Km circular 28.5 deg.	2.18 1.166 1.146 1.66	1.24 2.19 3.60 2.06
CIS	KOSMOS TSYCLON F2 SOYUZ PROTON DI ZENIT 2 ENERGIA	2 3 2½ 3 2 2	- - LOX/RPI - - -	NTO/UDMH NTO/UDMH LOX/RP1 NTO/UDMH LOX/RP1 LOX/RP1	NTO/UDMH NTO/UDMH LOX/RPI NTO/UDMH LOX/RP1 LOX/LH2	- NTO/UDMH - NTO/UDMH - -	120 190 290 705 459 2400	1470 2745 4020 9000 7259 34800	1350 4000 7000 20000 13740 88000 (all 200km circular 51.6 deg)	1.25 1.47 1.41 1.30 1.61 1.48	1.12 2.10 2.41 2.84 3.00 3.66

TABLE 3.2 MASSES OF CURRENT EXPENDABLE LAUNCHERS

COUNTRY AND LAUNCHER	MASSES (TONNES)	BOOSTERS	STAGE 1	STAGE 2	STAGE 3	TOTAL PROPELLANT MASS (Mp) (Tonnes)	GROSS LAUNCH MASS (Ml) (Tonnes)	PAYLOAD MASS (Mpl) (Tonnes)	* VEHICLE NET MASS (Mv) (Tonnes)	Mp / Ml (%)	Mv / Ml (%)
CHINA CZ - 2E	Gross Propellant Net Net/Gross (%)	164 152 12 7.32	196.5 187.0 9.5 4.83	91.5 86 5.5 6.0		425	464	9.2	29.8	91.6	6.42
EUROPE ARIANE 44L	Gross Propellant Net Net/Gross (%)	174.0 156.0 18.0 10.34	251.0 233.0 18.0 7.17	38.5 35.2 3.3 8.57	12.1 10.8 1.3 10.74	435	470	** 4.6 (GTO)	30.4	92.5	6.46
JAPAN H - 1	Gross Propellant Net Net/Gross (%)	40.32 33.57 6.75 16.74	85.8 81.4 4.4 5.13	10.6 8.8 1.8 17.0	2.20 1.86 0.34 15.45	125.63	140	3.2	11.17	89.7	8.0
USA DELTA II - 7925	Gross Propellant Net Net/Gross (%)	117.0 105.3 11.7 10.0	101.9 96.0 5.9 5.8	6.997 6.076 0.921 13.16		207.376	230	5.045	17.579	90.2	7.64
USA TITAN IV	Gross Propellant Net Net/Gross (%)	634.0 546.0 88.0 13.88	163.0 155.0 8.0 4.9	39.60 35.10 4.50 11.36		736.1	860	17.70	106.2	85.6	12.35
CIS PROTON D1	Gross Propellant Net Net/Gross (%)		455.6 410.2 45.4 9.96	165.6 150.0 15.6 9.42	55.6 50.0 5.6 10.07	610.2	705	20	74.8	86.6	10.6
CIS ZENIT 2	Gross Propellant Net Net/Gross (%)		352.7 318.8 33.9 9.61	89.9 80.6 9.3 10.34		399.4	459	13.74	45.86	87	10

* Net Vehicle mass Mv = Ml - Mp - Mpl
** Ariane 44L GTO Payload mass used because LEO payload mass of 9600 kg cannot be achieved due to Structural Strength limits

TABLE 3.3 LAUNCH RECORD OF CURRENT COMMERICAL LAUNCHERS

COUNTRY AND LAUNCHER	LAUNCH PERIOD	NUMBER OF FLIGHTS	NUMBER OF FAILURES	SUCCESS RATE (%)	FAILURE RATE (%)	YEAR AND FLIGHT NUMBER OF LAST FAILURE
CHINA LONG MARCH	1970 - 1992	32	4	87.5	12.5	1992 / No. 31
EUROPE ARIANE	1979 - 1992	56	5	91.1	8.9	1990 / No. 36
USA ATLAS	1958 - 1992	261	32	87.7	12.3	1987 / No. 237
USA DELTA	1960 - 1992	221	12	94.6	5.4	1986 / No. 178
USA TITAN	1964 - 1992	182	12	93.4	6.6	1990 / No. 169
USA NSTS	1981 - 5/1993	55	1	98.2	1.8	1986 / No. 25

TABLE 3.4 COSTS OF COMMERCIAL LAUNCH SERVICES

COUNTRY AND LAUNCHER	LAUNCH PRICE SINGLE CUSTOMER MISSION MILLON USD (1990)	PAYLOAD MASS (Kg)	PRICE PER KILOGRAM USD (1990)
CHINA LONG MARCH CZ - ZE	40	1500 (GTO)	26666
EUROPE ARIANE 44 L	110	4200 (GTO)	26190
USA ATLAS II A	80	1500 (GTO)	53333
USA DELTA II - 6925	45	910 (GTO)	49450
USA TITAN IV / CENTAUR	227	5220 (GTO)	43486

3.2 Space Transportation Needs in the 21st Century

The development of space transportation systems is an expensive undertaking and will only be warranted under one or both of the following conditions:

- if there is a need for new space transportation tasks that are not feasible with the currently available launcher systems;
- if new launcher concepts can offer substantial improvements in cost, performance, operational resilience, reliability and safety compared to currently available launch systems.

In the 35 year history of space, two primary uses of space have emerged and these are certain to remain the primary uses. Indeed, every space mission undertaken to date can be classified into one of the two usage categories. These primary uses are:

- the use of space for fundamental scientific research in the natural and life sciences;
- the use of space for commercial and military applications in telecommunications, meteorology and Earth observation.

For both these primary uses of space, the role of man in space is an important and emotive issue. For undertaking fundamental scientific research, the essential role of man as a researcher in space is indisputable and has already been acknowledged. The new era of laboratories in space: the permanently manned space stations in low Earth orbit, will dominate space activities in the next decade and will serve to gain experience to prepare for the further manned exploration of outer space.

The space station era will pose major new requirements on space transportation systems. The space transportation tasks

will comprise:

- transportation of payloads to orbit and their deployment;
- retrieval of cargo payloads from orbit and return to Earth;
- transportation to orbit of space station crews;
- return transportation to Earth of space station crews;
- emergency crew rescue missions to space stations;

Examination of these space transportation tasks shows that expendable launchers can only perform the first task: the transportation and deployment of payloads. Partially reusable launchers like the NSTS are able to perform all the tasks, but at a very high cost. It can also be seen, that apart from the classical case of transportation to and deployment of payloads into orbit, that all the space station tasks require rendez-vous and docking operations. This will pose additional major capabilities for future launchers.

The future space transportation tasks also show a clear need to transport both cargo and crew to and from space. These functions can of course be combined in the same launch vehicle. This is the approach that has been adopted for the NSTS, which not only carries cargo and crew, but also requires the crew for launcher piloting functions. It is now well known, that the high cost of the NSTS, estimated at 500 to 1000 million dollars per launch (Ref. 2), results from the complexity and servicing requirements of a manned, piloted and partially reusable launcher. Thus, learning from the NSTS experience, if we wish to transport both cargo and crew in the same launcher, substantial cost reductions may result by simply transporting the crew as passive live cargo. Of course, crew accommodation and life-support systems would have to be provided and these would still increase substantially the cost of a manned launcher compared to an unmanned one.

An alternative future launcher approach, which may result in

substantial cost and operational benefits, is to separate the cargo and crew transportation requirements and assign them to two specialised vehicles: a cargo transporter; a crew transporter. For both vehicles, a rendez-vous and docking capability will be required. For the crew transporter, this should be an automatically piloted vehicle and should not require piloting actions by the crew. This two-vehicle or 'mixed fleet' approach also allows to exploit the inherent characteristics of rocket-propelled launchers for the cargo transporter role and of combined air-breathing/rocket-propelled launchers (the aerospace planes) for the crew transporter role.

Because of the need to deliver cargo and crew to and from space stations and for Earth observation missions, low Earth orbits will become the primary target orbits for future space transportation systems. The low Earth orbits of primary interest are:

- a circular orbit at about 450 km altitude and 28.5 degrees inclination, this being the nominal orbit of the International Space Station 'Freedom', which is planned to be operational in 1998;
- a circular orbit at altitudes between 500 and 800 km and 97 degrees inclination, the sun-synchronous orbit, for Earth observation missions.
- an elliptic orbit with a perigee altitude of about 100 km and an apogee altitude of about 200 km with an inclination equal to the latitude of the launch site, allowing a due east launch to minimise launcher propulsive energy. The altitude of this orbit is low enough to minimise launcher propulsive energy whilst being high enough to assure orbital stability and acceptable aerodynamic heating of the satellite. This orbit is required as a parking orbit for the deployment of satellite payloads, which would then be transferred to higher energy orbits using their own

propulsion systems. Such higher energy orbits are:

- the geostationary orbit for telecommunication and meteorology satellites;
- highly elliptic orbits for a variety of space science observatory missions;
- Earth escape trajectories for interplanetary missions.

For future European launchers, the CSG launch site in Kourou, French Guiana (5.23 degrees North, 52.72 degrees West) will remain the primary launch site for the foreseeable future because it is the only launch site available to Europe and is fully developed and operational. Thus, for the 28.5 degree inclined orbit, the Earth's rotation velocity of 464 m/s that benefits a due East launch from Kourou, is reduced to about 409 m/s. For the 97 degree inclined orbit, no benefits are derived from the Earth's rotation. Instead, a small penalty of about 35 m/s must be added to achieve this retrograde orbit. It should be noted however, that the Kourou launch site has been developed only for vertical rocket launchers and that only a small airfield exists on the site for horizontal take-off launchers. The nearest large airport to Kourou is the International Airport at Cayenne, some 40 km south of Kourou. It is unlikely, that Cayenne or any other civilian airport, would be allowed to be used for complex and hazardous space launch operations!

Europe is currently completely dependent on the continuing availability of the Kourou launch site for its access to space. Concern about this dependence has prompted considerations of a truly European launch site based in mainland Europe. The location of such a site in highly populated Europe is difficult to find. Such a site should of course be in a remote area and as far south as is possible to minimise propulsive energy to achieve low inclination orbits.

A potential site is at Istres in southern France (43.5 degrees North, 5 degrees East), which is a French military flight test range, and as such, has potential for further development.

The future space transportation needs for Europe can now be summarised:

- there is a need to transport both cargo and crew to and from low Earth orbit;
- there are three low Earth orbits of primary interest: the Space Station Freedom orbit (450 km circular, 28.5 degree inclination); the sun synchronous orbit (500 to 800 km circular, 97 degree inclination); the LEO parking orbit (100 km x 200 km x 5.2 degree inclination)
- the only available launch site available to Europe is CSG Kourou in French Guiana;
- a European mainland launch site could be developed at Istres in Southern France.

Reusable launchers, if technically feasible and affordable, could fulfil the future space transportation needs of Europe.

3.3 Reusable Launcher Concepts and their Characteristics

This Chapter derives the vehicles that have been selected for study in this research and presents their characteristics.

There are three approaches to the development of fully reusable launchers. These are:

1) the further development of the currently operational, expendable, multi-stage rocket-propelled vehicle into a fully reusable launcher. This is a logical evolutionary approach;

2) the development of the high speed aircraft into a fully reusable space launcher. This is a new, revolutionary approach;

3) combinations of the evolutionary and revolutionary approaches described above.

In the first approach, for which the expendable rocket launcher is the progenitor, the presence of the atmosphere through which the vehicle has to ascend, is regarded as an inconvenience. The vehicle is designed to traverse the atmosphere with minimum impact on its performance: the vehicle shape is designed for minimum drag; the vehicle does not use aerodynamic lift to augment its propulsive performance; the rocket propulsion does not use atmospheric air to minimise the mass of stored oxidiser; the ascent trajectory is designed to allow the vehicle to traverse the atmosphere with minimum aerodynamic drag and gravity losses.

In the second approach, for which the aircraft is the progenitor, the presence of the atmosphere is regarded as an asset and resource. The vehicle is designed to derive maximum aerodynamic and propulsive benefits from the atmosphere as it traverses through it: the vehicle shape is deigned for

maximum lift and minimum drag; the vehicle uses aerodynamic lift to augment its propulsive performance; the vehicle uses atmospheric air to minimise the mass of stored oxidiser; the ascent trajectory is designed to maximise the benefits of aerodynamic lift and air-breathing propulsion, resulting in flying along high dynamic pressure trajectories at low altitudes.

In the third approach, an optimum combination of the advantages of both the expendable rocket launcher and aircraft progenitors is sought.

Based on these three possible approaches to the development of fully reusable vehicles, the complete range of reusable launch vehicle operational modes and design variables can now be defined.

The operational modes are:

1) The Launch Mode: this may be vertical, horizontal or inclined;
2) The Landing Mode: this may be vertical or horizontal;
3) The Ascent Mode: this may be ballistic or lifting or combined ballistic and lifting;
4) The Descent Mode: this may be ballistic or lifting or combined ballistic and lifting;
5) The Staging Mode: this may be single or multi-stage, with two stages having been adopted in this research as a practical limit. A further sub-variable is the vehicle velocity at staging: this may be subsonic or supersonic;
6) The Propulsion Mode: This may be rocket propulsion or air-breathing propulsion with rocket propulsion, either operated sequentially or in parallel. A further sub-variable is the air-breathing combustion mode: this may be subsonic or supersonic.
7) The Utilisation Mode: The vehicle may be designed to transport cargo only, crew only or combinations of cargo

and crew. A sub-variable for crewed vehicles is the piloting mode: the vehicle may be piloted by the crew or piloted automatically.

Thus, from this list, it can be seen that there are a total of 7 operational modes and 18 design variables, the large theoretical combination of which would result in mostly unrealistic cases. The approach adopted therefore, was to identify potentially attractive concepts by combining operational modes and design variables based on engineering judgement and common sense. The results of this exercise yielded a manageable total of 13 potentially feasible reusable launcher concepts for further study. The characteristics of each of these selected vehicles are summarised in Table 3.5. A description of each vehicle and the rationale for its selection are presented later in Chapters 3.3.1, 3.3.2 and 3.3.4.

3.3.1 Characteristics of Reusable Launcher Concepts

The various operational modes, design variables and selected reusable concepts are now discussed in qualitative terms to show their inherent characteristics and the rationale for their selection. The quantitative analysis of the selected reusable launcher concepts in terms of their performance and costs are presented in Chapters 5 and 7 respectively.

Reusable Launcher Operational Modes

Launch Mode

Vertical Launch: This is the established method for launching the traditional, expendable, multi-stage, rocket-propelled, ballistic ascent launchers. The optimum configuration of these vehicles is a long cylinder which is inherently weak in bending. Vertical launch imposes low bending loads on the vehicle structure, allowing the minimisation of the

TABLE 3.5 REUSABLE LAUNCHER CONCEPTS EVALUATED IN THIS RESEARCH

	CONCEPT		STAGING MODE			PROPULSION MODE			LAUNCH MODE			LANDING MODE		ASCENT MODE		DESCENT MODE		UTILISATION MODE		
PROGENITOR	No	DESIGNATION	SSTO	TSTO Sub	TSTO Sup	ROCKET	ROCKET & AIR (Sub)	ROCKET & AIR (Sup)	VERT	HORIZ	INCL	VERT	HORIZ	BALL	LIFT	BALL	LIFT	CARGO	CREW	CARGO & CREW
ROCKET LAUNCHER	1	SSTO-R-VLVL	X			X			X			X		X		X		X		X
	2	SSTO-R-VLHL	X			X			X				X	X			X	X		X
	3	TSTO-R-VLHL			X	X			X				X	X			X	X		X
AIRCRAFT	4	SSTO-RA (Sub)-HLHL(u/c)	X				X			X			X		X		X	X	X	X
	5	SSTO-RA (Sub)-HLHL(Sled)	X				X			X			X		X		X	X	X	X
	6	SSTO-RA (Sub)-ILHL(Ramp)	X				X				X		X		X		X	X	X	X
	7	SSTO-RA (Sup)-HLHL(u/c)	X					X		X			X		X		X	X	X	X
	8	TSTO-RA (Sub)-HLHL(Air-Lau)		X			X			X			X		X		X	X	X	X
	9	TSTO-RA (Sub)-HLHL(u/c)			X		X			X			X		X		X	X	X	X
ROCKET LAUNCHER & AIRCRAFT	10	SSTO-R-HLHL(u/c)	X			X				X			X		X		X	X	X	X
	11	SSTO-R-HLHL(Sled)	X			X				X			X		X		X	X	X	X
	12	TSTO-R-HLHL(u/c)			X	X				X			X		X		X	X	X	X
	13	SSTO-RA-VLVL	X				X		X			X		X		X		X		X

structural mass. Vertical launch also allows easy access to trajectories at any desired azimuth. However, vertical launch necessitates that the thrust level at lift-off must be greater than the weight of the launcher, with the resulting penalty of high engine mass. Vertical launch also imposes high gravity losses: for a typical thrust/launch weight ratio at lift-off of 1.3, and neglecting drag forces which are small in the early phase of the ascent, only 23% of the engine thrust is available to accelerate the vehicle!

Horizontal Launch: The horizontal launch mode is the conventional aircraft type take-off from a runway. The vehicle accelerates itself on its own under carriage using its own jet thrust until sufficient speed is achieved to allow vehicle rotation and aerodynamic lift-off. The penalty for this launch mode is the high mass of the undercarriage, which must be sized to support the gross weight of the fully loaded vehicle. The mass of such an undercarriage is high, statistically, being about 3.5 % of the vehicle gross mass. To reduce the mass of the undercarriage, the vehicle may be mounted on a sled which is then accelerated up to take-off velocity along a tracked runway using the sleds own propulsive thrust or that of the vehicle's. The self-propelled sled also allows to save the mass of vehicle propellants that would otherwise be required to be carried in the launcher for the take-off run. However, such a sled would be a large, complex and expensive device.

Inclined Launch: This launch mode uses an inclined launch ramp to support the vehicle at angles between about 30 and 60 degrees. The vehicle is then launched by accelerating it along the ramp by jet thrust. Aerodynamic lift is then required to sustain lifting flight. This approach avoids the need for a runway or launch sled for vehicles employing aerodynamic lift. This launch mode has been extensively used for missile applications because they can tolerate high

launch acceleration levels of about 10g, allowing a typical velocity of about 100 m/s, which is adequate to develop enough aerodynamic lift, to be achieved within about 1 second, thus avoiding an unacceptable dropping of the vehicle on to the launch ramp. For space launchers however, where the acceleration must be limited to about 3g for structural strength reasons, lifting engines would be necessary to alleviate the normal component of the vehicle's weight acting on the ramp. For a launch acceleration of about 1 g, these engines would then be shut down within about 10 seconds with a vehicle velocity of about 100 m/s, which is adequate to develop aerodynamic lift to maintain lifting flight.

Landing Mode

Vertical Landing: This concept comprises the controlled ballistic descent of the returning launcher through the atmosphere to a gentle vertical landing at the launch site. The vehicle attitude has to be controlled throughout the descent using reaction control thrusters. The descent rate has to be controlled by retro-propulsion using the vehicles main engines. This landing mode is a completely new and somewhat startling concept for space launchers. However, such vertical landings have been successfully performed by NASA in the Moon landings of the Apollo programme using the Lunar Module as long ago as 1966. Much relevant experience on retro-propulsion vertical landings has also been gained from the Harrier fighter aircraft. This experience base gives high confidence that this landing method can be successfully developed.

Horizontal Landing: This is the classical unpowered gliding approach and landing on a runway. This method has been fully developed for space launchers by NASA with its NSTS Orbiter vehicle.

Ascent Mode

Ballistic Ascent: This is the fully developed, conventional, zero-lift ascent mode for vertically-launched rocket-propelled vehicles. The launcher is programmed to fly at nominally zero incidence (zero-lift) along a selected trajectory that has been designed to minimise the velocity losses due to atmospheric drag and gravity forces.

Lifting Ascent: Aerodynamic lifting ascent allows the vehicle to climb at relatively low flight path angles of about 20 degrees. This results in substantial reductions in the gravity loss, but incurs an increase in the drag loss. The drag losses can be very large for lifting vehicles using air-breathing propulsion because they must maximise their flight velocity whilst flying at low altitudes and along high dynamic pressure trajectories to develop sufficient thrust.

Descent Mode

Ballistic Descent: Ballistic descent and lifting descent with small lift/drag ratios give virtually no control on the down range motion and give very limited cross range capabilities. This implies tight requirements on the vehicle's re-entry longitude and latitude coordinates, velocity and attitude, to ensure landing at the desired location. The resulting trajectory dispersions caused by re-entry inaccuracies and wind effects are large, and necessitate landing in the sea, as used by the USA in its Mercury, Gemini and Apollo re-entry programmes, or on the ground in remote areas as used by the Soviets in their space programme (which are still used today for the current return missions from the Mir Space Station).

Lifting Descent: Aerodynamic lifting descent allows to control easily the vehicles down range and cross range motions. This allows to relax the re-entry conditions and to

fly very precisely to the required landing site. The merits of lifting descent have been demonstrated very successfully by the USA with its Orbiter vehicle.

Staging Mode

SSTO: Single stage vehicles have operational advantages compared to two stage vehicles. Complex and hazardous in-flight stage separation manoeuvres are obviated and ground operations are also much simplified because there are no stage mating operations. Costs should also be lower because there is only one vehicle to develop, procure and operate.

TSTO with Subsonic Staging: Subsonic staging of two stage vehicles does not allow to maximise the payload mass ratio advantage of the staging concept. However, subsonic staging for horizontally launched vehicles allows to use a conventional aircraft as the first stage, thus saving substantial costs in the development, procurement and operation of the first stage.

TSTO with Supersonic Staging: Supersonic staging allows to optimise the staging velocity and altitude to maximise the payload mass. The disadvantage is that the first stage becomes a complex and therefore expensive vehicle. For an air-breathing propelled first stage, performance limitations of the air-breathing propulsion may reduce the payload mass maximisation benefits of supersonic staging.

Propulsion Mode

Rocket Propulsion: Rocket propulsion systems for space launchers are fully developed and operational and there is a well established technology and experience base. Rocket engines have a very high thrust/weight ratio (typically 80 to 100) but suffer from a rather low specific impulse (typically

400 s) compared to air-breathing engines. Rocket engines can operate at all altitudes and speeds and are almost independent of the atmosphere. Their unique advantages for space propulsion makes it worthwhile to invest in further developments to improve their specific impulse and to increase their thrust/weight ratio. Potentially attractive ways to achieve these improvements are discussed in Chapter 6.

Air-Breathing Propulsion (Subsonic Combustion): The vehicle's flight speed for subsonic combustion ramjet propulsion systems is limited to about Mach 6.8 at 30 km altitude. At higher flight speeds, the compression of the free-stream air by diffusion in the engine's air intake system, results in excessively high combustion temperatures in the combustion chamber, causing, in turn, a high level of dissociation of the combustion products in endothermic reactions. Thus, the combustion efficiency can be substantially reduced, to the point where virtually no thrust is produced.

Air-Breathing Propulsion (Supersonic Combustion): Supersonic combustion for ramjet propulsion systems allows to use air-breathing propulsion beyond the Mach 6.8 limit of subsonic ramjet systems. However, such supersonic combustion ramjets (scramjets) are difficult to design because the current knowledge base is not developed. Furthermore, the development of full scale engines in ground based facilities is difficult and expensive because of the large air mass flow requirements at very high temperatures and velocities.

Utilisation Mode

Cargo Vehicle: Reusable Launchers developed for the transport of cargo only, can have more relaxed design requirements and reliability and safety margins. They may also be flown at

higher acceleration levels, typically 4g, to minimise gravity losses.

Crew Vehicle: Reusable Launchers developed to transport crews will have demanding safety and reliability requirements, necessitating a safe abort capability during all phases of the ascent and descent flights.

Combined Cargo and Crew Vehicle: Because they must carry crew, these vehicles will require the same high safety and reliability and safe abort requirements as for the crew-only transport vehicles. However, for these combined function vehicles, the crew may be carried as live passive cargo, thereby simplifying the vehicle and thereby reducing its costs.

3.3.2 Rocket Launcher Derivatives

There are major advantages for reusable launcher concepts which are derivatives of the current expendable, rocket-propelled space launchers. These are:

- there is an extensive engineering data base for expendable and partially reusable launchers, which is of direct relevance for the design of these vehicles;
- there is an established manufacturing, assembly, testing and operational infrastructure, which can be used for such vehicles. This should result in substantial cost savings in a procurement and operation programme for such vehicles.

The apparent major disadvantage of these vehicles, when assessed at the superseded technology level of their expendable rocket launcher progenitor, is their payload mass marginality. To make such vehicles technically feasible, major improvements in the propulsive performance of their rocket engines and major decreases in their dry masses will be essential. The application of recent advances in all the key launcher technologies now substantially improves the feasibility potential of these vehicles, making them serious contenders for future reusable launchers. These key technologies are: propulsion; aerodynamics and aerothermodynamics; materials and structures; trajectories and guidance; avionics. The status of these technologies is presented and discussed in Chapter 6.

The special characteristics, advantages and disadvantages of each rocket launcher-derived reusable launcher candidates are now presented.

Reusable Launcher No.1: This is defined as a single-stage-to-orbit, rocket-propelled, vertical launch, vertical landing vehicle, designated as **SSTO-R-VLVL.**

Like all SSTO launcher concepts, this vehicle offers the intuitive advantage of lower procurement and operational costs compared to TSTO vehicles because only one vehicle stage is required. SSTO vehicles also offer major operational advantages and inherently higher reliability because there are no stage separation operations and no spent stages to be dropped, allowing more performance-optimum trajectories to be flown without regard for the geographical location of safe dropping zones.

The SSTO-R-VLVL vehicle offers the ultimate in configuration and operational simplicity and is therefore the most fundamental launcher concept. Its aerodynamic interfaces are minimal, requiring only a low lift/drag ratio to achieve the required down range and re-entry cross range to its landing site, which ideally, should also be its launch site to avoid costs for return transportation to the launch base. The cross range constraint of this low lift/drag vehicle is probably its major disadvantage.

Reusable Launcher No.2: This is defined as a single-stage-to-orbit, rocket-propelled, vertical launch, horizontal landing vehicle, designated as **SSTO-R-VLHL.**

This vehicle differs from Vehicle No.1 only in its descent and landing modes which are now lifting descent and horizontal landing. These requirements necessitate the use of wings to generate enough lift, aerodynamic control surfaces to control the decent flight and an undercarriage. Compared to Vehicle No.1, the dry mass is expected to be higher because of the wings, control surfaces and landing gear, which would result in a lower payload mass ratio for the same gross lift-off mass. Its merit however is the inherently higher cross range capability compared to Vehicle No.1.

Reusable Launcher No.3: This is defined as a two-stage-to-orbit, rocket-propelled, vertical launch, horizontal landing vehicle, designated as **TSTO-R-VLHL.**

This vehicle is intuitively conceived to retain the reentry cross range capabilities of Vehicle No.2 whilst compensating for its high dry mass by means of the staging concept. The penalty to be paid will be higher costs because two stages have to be procured, recovered and mated.

3.3.3 Aircraft-Derived Reusable Launchers

There is a strong intuitive perception among launcher technologists that the highly developed, modern high speed aircraft can be developed into a space launcher to benefit from the following aircraft characteristics:

- the convenience of horizontal launch and landing;
- the energy savings resulting from the use of aerodynamic lifting ascent and descent;
- increased mission flexibility resulting from the high down-range and cross-range performance on re-entry;
- minimisation of the mass of on-board oxidiser by the use of air-breathing propulsion for the launch and early flight phase of the ascent;
- improved mission flexibility resulting from the cruising capability that air-breathing propulsion and lifting flight allow.

These apparent intuitive advantages make it well worthwhile to quantify the achievable benefits of aircraft-derived space launchers. The selected candidate reusable launcher concepts that are aircraft-derived are now presented.

Reusable Launcher No.4: This is defined as a single-stage-to-orbit, rocket and air-breathing propelled, horizontal launch and horizontal landing vehicle. The air-breathing combustion mode is subsonic. The vehicle is undercarriage-launched. The vehicle is designated as:
SSTO-RA(Sub)-HLHL (Undercarriage-Launched).

This launcher is the most fundamental and therefore the first of the candidate aircraft-derived vehicles selected for this analysis because it resembles most its aircraft progenitor: being single-staged, undercarriage-launched and landed and employing subsonic combustion air-breathing propulsion. Because air-breathing propulsion systems cannot operate at high altitude because of the low air density, rocket propulsion is also necessary for any type of air-breathing launcher, to propel the vehicle into orbit after the air-breathing phase. Rocket propulsion may also be necessary to augment the air-breathing thrust needed to overcome the high aerodynamic drag which occurs during the transonic flight on ascent. Rocket propulsion may also be used in parallel burn with the air-breathing engines to augment thrust.

Reusable Launcher No.5: This is defined as a single-stage-to-orbit, rocket and air-breathing propelled, horizontal launch and horizontal landing vehicle. The air-breathing combustion mode is subsonic. The vehicle is sled-launched on a rail-guided sled propelled by its own rocket engines but using propellants carried in the sled. The vehicle is designated as: **SSTO-RA(Sub)-HLHL (Sled-Launched).**

The sled-launch concept of this vehicle is intended to improve the payload mass ratio of the fundamental Vehicle No.4 by a mass reduction of its undercarriage, which now has to be sized only for the re-entry mass of the vehicle and also by a reduction of the take-off propellant mass that is now carried in the sled.

Reusable Launcher No.6: This vehicle is a single-stage-to-orbit, rocket and air-breathing propelled, inclined launch and horizontal landing vehicle. The air-breathing propulsion mode is subsonic. The vehicle is ramp-launched from an inclined ramp. The vehicle is designated as:
SSTO-RA(Sub)-ILHL (Ramp-Launched).

The ramp-launch concept of this vehicle is intended to improve the payload mass ratio of Vehicle No.4 in an alternative way to that of Vehicle No.5 for which the sled-launch concept was adopted. Thus, as for Vehicle No.5, the undercarriage mass can be reduced because it can now be sized for the re-entry mass of the vehicle. However, unlike Vehicle No.5, the take-off propellant mass for this vehicle is carried by the vehicle.

Reusable Launcher No.7: This is defined as a single-stage-to-orbit, rocket and air-breathing propelled, horizontal launch and horizontal landing vehicle. The air-breathing propulsion mode is supersonic. The vehicle is undercarriage-launched. The vehicle is designated as:
SSTO-RA(Sup)-HLHL (Undercarriage-Launched).

The concept of this vehicle is identical to that of Vehicle No.4, except that the air-breathing propulsion mode is now supersonic. Again, the intention here is to improve the payload mass ratio compared to the subsonic combustion Vehicle No.4 by the use of air-breathing propulsion beyond the subsonic combustion Mach Number limit of about 6.8, to very high Mach Numbers of 12 to 15, thus hopefully, maximising the benefits of air-breathing propulsion.

Reusable Launcher No.8: This is defined as a two-stage-to-orbit, rocket and air-breathing propelled, horizontal launch and horizontal landing vehicle. The air-breathing propulsion

mode is subsonic. The first stage of this vehicle is a conventional large aircraft propelled by turbojet engines. The second stage is an entirely rocket-propelled vehicle. The stages are separated at an altitude of about 8 km and a speed of about Mach 0.8. Thus, this TSTO vehicle can also be considered as an air-launched SSTO vehicle. The vehicle is designated as: **TSTO-RA(Sub)-HLHL (Air-Launched).**

The intention with this vehicle concept is to improve the payload mass ratio of the fundamental Vehicle No.4 by effectively air-launching it at altitude and with a small forward velocity, thus saving propellant mass and the undercarriage mass of the vehicle's second stage because this now needs to be sized only for the re-entry mass of the second stage.

Reusable Launcher No.9: This is defined as a two-stage-to-orbit, rocket and air-breathing propelled, horizontal launch and horizontal landing vehicle. The air-breathing combustion mode is subsonic. The vehicle is undercarriage-launched. The vehicle is designated as:
TSTO-RA(Sub)-HLHL (Undercarriage-Launched).

This is the last vehicle in the group of aircraft-derived launchers. The intention with this vehicle concept is to improve the payload mass ratio of the fundamental Vehicle No.4 by the use of the staging concept.

3.3.4 Rocket and Aircraft Hybrid Vehicles

In this group of vehicles, the benefits of rocket propulsion are added to the benefits of aircraft type characteristics in an effort to improve launcher costs whilst maintaining the operational flexibility of winged, lifting vehicles. These vehicles are presented below.

Reusable Launcher No.10: This is defined as a single-stage-to-orbit, rocket-propelled, horizontal launch and horizontal landing vehicle. The vehicle is undercarriage-launched. The designation is: **SSTO-R-HLHL (Undercarriage-Launched).**

This is the most fundamental vehicle in this group of rocket launcher/aircraft-derived hybrid vehicles. It has all the characteristics of Vehicle No.4, which is the fundamental vehicle of the aircraft-derived group, but the propulsion is performed entirely by rocket propulsion. The intention with this vehicle concept is to see if the use of rocket propulsion introduces any payload mass ratio penalties compared to Vehicle No.4, whilst retaining all its other operational advantages.

Reusable Launcher No.11: This is defined as a single-stage-to-orbit, rocket-propelled, horizontally launched and horizontally landed vehicle. The vehicle is sled-launched. The vehicle is designated as: **SSTO-R-HLHL (Sled-Launched).**

This vehicle concept is identical to that of the previous Vehicle No.10, except that it is launched on a rail-guided sled like that of Vehicle No.5. The sled is propelled by the vehicle's rocket engines but the propellants for the take-off run are stored in the sled.

The intention with this vehicle concept is to improve the payload mass ratio compared to the previous Vehicle No.10, its undercarriage-launched equivalent, by a saving in its undercarriage mass and in the take-off propellant mass.

Reusable Launcher No.12: This is defined as a two-stage-to-orbit, rocket-propelled, horizontally launched and horizontally landed vehicle. The vehicle is undercarriage-launched. The vehicle is designated as:
TSTO-R-HLHL (Undercarriage-Launched).

The intention with this vehicle concept is to determine the payload mass ratio gain over that of Vehicle No.11 because of the staging concept.

Reusable Launcher No.13: This is defined as a single-stage-to-orbit, rocket and air-breathing propelled, vertically launched and vertically landed vehicle. This vehicle is designated as: **SSTO-RA(Sub)-VLVL.**

This vehicle concept is identical to that of Vehicle No.1, the fundamental vehicle of the rocket launcher-derived group and indeed of this whole series of launchers, except that the rocket propulsion is now augmented by air-breathing propulsion for the lift-off and early ascent phase of the flight. The intention with this vehicle concept is to determine whether air-breathing thrust augmentation results in an improved payload mass ratio compared to that of Vehicle No.1.

Finally, Figure 3.4 is a Family Tree which has been produced to show clearly the evolution and relationships between the 13 reusable launcher concepts that have been selected for this research as described above.

FIGURE 3.4

FAMILY TREE OF THE SELECTED REUSABLE LAUNCHER CONCEPTS

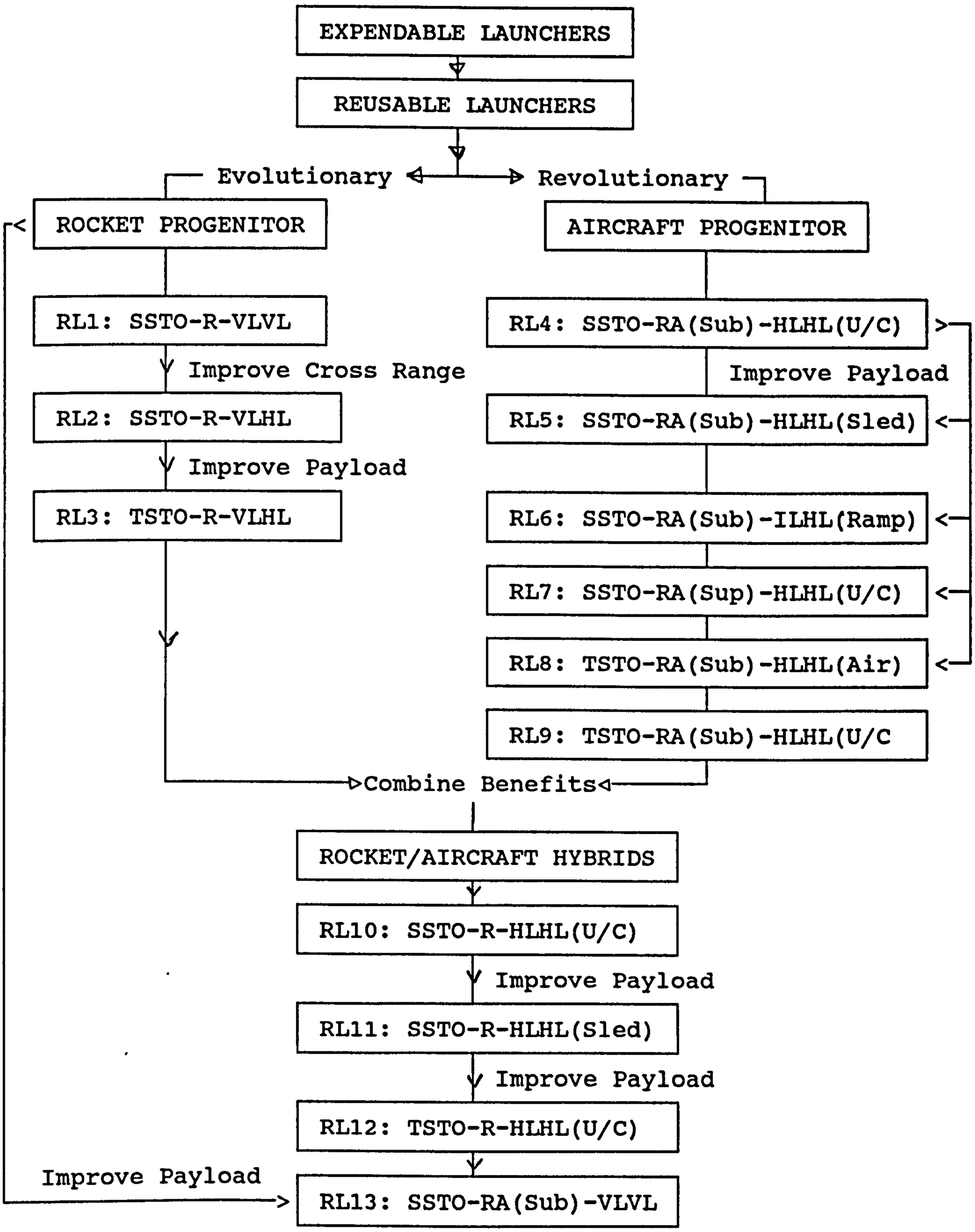

4 PERFORMANCE ANALYSIS OF REUSABLE LAUNCHERS

4.1 Synopsis

In this chapter, the important launcher performance parameters are first defined. Then, only to identify clearly the significance of these parameters, a set of analytical launcher performance equations are derived for each class of reusable launcher. Because the parameter values required for the solution of these analytical performance equations are themselves complex functions of many other parameters, all of which vary with the flight time, the use of these analytical equations for the accurate calculation of launcher performance, is deemed by the author to be inappropriate. Instead, it has been necessary to derive launcher performance by integrating the ascent differential equations of motion along the flight time. These differential and integral equations are then derived and transposed to a convenient form to allow the influence of propulsive, aerodynamic and gravity forces on the motion of the vehicle to be seen clearly. These equations of motion have then been modelled in several computer programs, described in Chapter 5, for the accurate performance calculation of the 13 different types of vehicles studied in this research.

4.2 Nomenclature

A_r = Aerodynamic reference area (m^2)
A_z = Azimuth angle (degrees)
C_d = Aerodynamic drag coefficient (-)
C_{di} = Aerodynamic drag coefficient due to lift (-)
C_{do} = Aerodynamic drag coefficient at zero lift (-)
C_l = Aerodynamic lift coefficient (-)
D = Aerodynamic drag force (N)
F_N = Net normal force along the lift vector (N)
F_T = Net tangential force along the velocity vector (N)
H = Vehicle altitude (m)
I_s = Specific impulse (s)
I_{sa} = Air-breathing specific impulse (s)
I_{sav} = Average specific impulse (Ns/kg)
I_{sc} = Cruise phase specific impulse (s)
I_{sr} = Rocket specific impulse (s)
I_{sr1} = Rocket specific impulse for stage 1 (s)
I_{sr2} = Rocket specific impulse for stage 2 (s)
I_t = Total impulse (Ns)
I_{tc} = Total impulse for cruise phase (Ns)
K = Induced drag factor (-)
L = Aerodynamic lift force (N)
M = Instantaneous mass of vehicle (kg)
M_l = Launch mass of vehicle (kg)
M_{l1} = Launch mass of stage 1 (kg)
M_{l2} = Launch mass of stage 2 (kg)
M_o = Orbital mass of vehicle (kg)
M_p = Propellant mass (kg)
M_{pa} = Air-breathing fuel mass (kg)
M_{pa1} = Air-breathing fuel mass for stage 1 (kg)
M_{pc} = Cruise phase fuel mass (kg)
M_{pl} = Payload mass (kg)
M_{pl1} = Payload mass of stage 1 (kg)
M_{pl2} = Payload mass of stage 2 (kg)
M_{pr} = Rocket propellant mass (kg)

M_{pr1} = Rocket propellant mass for stage 1 (kg)
M_{pr2} = Rocket propellant mass for stage 2 (kg)
M_v = Net mass of vehicle (kg)
M_{v1} = Net mass of first stage of TSTO vehicle (kg)
M_{v2} = Net mass of second stage of TSTO vehicle (kg)
S = Horizontal range of vehicle (m)
T = Thrust force (N)
V = Relative velocity of vehicle along motion axis (m/s)
V_i = Inertial velocity of vehicle along motion axis (m/s)
W = Instantaneous weight of vehicle (N)
W_l = Launch weight of vehicle (N)
W_{l1} = Launch weight of first stage of TSTO vehicle (N)
W_{l2} = Launch weight of second stage of TSTO vehicle (N)
g = Earth's gravitational acceleration (m/s^2)
g_0 = Earth's gravitational acceleration at sea level (m/s^2)
m_p = Propellant mass flow rate (kg/s)
r = Radial distance (m)
r_e = Earth's radius (6370×10^3 m)
r_a = Apogee radius (m)
r_{a1} = Apogee radius of orbit 1 (m)
r_{a2} = Apogee radius of orbit 2 (m)
r_p = Perigee radius (m)
r_{p1} = Perigee radius of orbit 1 (m)
r_{p2} = Perigee radius of orbit 2 (m)
t = Time (s)
α = Vehicle incidence angle measured from the motion axis (angle of attack) (degrees)
α_1 = Vehicle thrust angle measured from motion axis (degrees)
γ = Flight path angle measured from the local horizontal (degrees)
θ = longitude of vehicle (degrees)
ι = inclination of orbit (degrees)
σ = roll or bank angle of vehicle (degrees)
ϕ = latitude of vehicle (degrees)
λ_L = latitude of launch site (degrees)
μ = Earth's gravitational parameter (3.986×10^5 kg^3/s^2)

ρ = air density (kg/m^3)

ψ = heading of vehicle (degrees)

ω = rotation rate of the Earth (rad/s)

Δv = Velocity increment (m/s)

Δv_a = Air-breathing phase velocity increment (m/s)

Δv_{a1} = Air-breathing phase velocity increment for stage 1

Δv_{cf} = Velocity increment due to centrifugal force (m/s)

Δv_{dl} = Velocity increment due to aerodynamic drag (m/s)

Δv_{gl} = Velocity increment due to gravity force (m/s)

Δv_{rot} = Velocity increment due to Earth's rotation (m/s)

Δv_r = Rocket phase velocity increment (m/s)

Δv_{r1} = Rocket phase velocity increment for stage 1 (m/s)

Δv_{r2} = Rocket phase velocity increment for stage 2 (m/s)

4.3 Definition of Reusable Launcher Performance Parameters

The mass ratios of launchers are a valuable guide to their performance capabilities and provide a useful basis for comparing the performance of different launchers. However, before defining the mass ratios, the individual important mass elements are first defined.

The launcher mass elements of importance are:

- the launch mass (M_l): this is the mass of the launcher at engine ignition for vertically launched vehicles and at the start of the take-off run for horizontally launched vehicles.

- the propellant mass (M_p): this is the total on-board mass of propellant consumed by the launcher during its propulsive phases. It comprises the mass of on-board fuel for both the air-breathing and rocket-propelled phases and also the mass of on-board oxidiser for the rocket-propelled phase. The air-breathing fuel mass is denoted as M_{pa} and the rocket-propelled phase propellant (fuel plus oxidiser) is denoted as M_{pr}). Thus $M_p = M_{pa} + M_{pr}$.

- the orbital mass (M_o): this is the mass of the launcher at injection into the target orbit. Thus $M_o = M_l - M_p$.

- the vehicle mass (M_v): this is the mass of the empty launcher (without ascent-phase propellant and payload). Thus $M_v = M_o - M_{pl}$, where M_{pl} is the payload mass. However, M_v includes all the launcher operational subsystem masses and also the propellants needed for orbit and attitude control whilst in the target orbit and for re-entry retro-propulsion and descent control.

- the payload mass (M_{pl}): this is the mass of the payload delivered to the target orbit. It can comprise any percentage combination of cargo and crew. If crew are carried, the mass of their life-support systems are included in the payload mass.

The important mass ratios can now be defined. These are:

- the propellant mass ratio (M_p/M_l): this is the total propellant mass divided by the launch mass.

- the air-breathing phase propellant mass ratio (M_{pa}/M_l): this is the air-breathing phase propellant mass divided by the launch mass.

- the rocket phase propellant mass ratio (M_{pr}/M_l): this is the rocket phase propellant mass divided by the launch mass.

- the orbital mass ratio (M_o/M_l): this is the orbital mass divided by the launch mass.

- the vehicle mass ratio (M_v/M_l): this is the vehicle mass divided by the launch mass. For a TSTO vehicle, the first stage vehicle mass ratio is denoted by M_{v1}/M_{l1}) and the second stage vehicle mass ratio is denoted by M_{v2}/M_{l2}.

- the payload mass ratio (M_{pl}/M_l): this is the payload mass divided by the launch mass. For a TSTO vehicle, the payload ratio is denoted by M_{pl}/M_{l1}.

- the payload/vehicle mass ratio (M_{pl}/M_v): this is the payload mass divided by the vehicle mass. It indicates the payload-carrying capability of the empty vehicle.

4.4 Derivation of Analytical Performance Equations

A set of analytical performance equations are derived here because, although they are only approximate and therefore less accurate than the differential and integral equations derived in Chapter 4.6, their simplicity makes them useful to illustrate the significance and dependence of launcher performance on the various parameters and to show clearly the performance trends of individual launchers. These analytical equations are therefore used frequently in the discussion of the launcher performance results in Chapter 5, which have been derived by numerical analysis.

For the purposes of deriving the launcher performance equations, the reusable launchers studied in this research are classified as follows:

- the vehicles may be SSTO or TSTO;

- the vehicles may be 'accelerators' or cruise/accelerators';

- the vehicles may be entirely rocket-propelled or air-breathing and rocket-propelled;

This leads to six sets of performance equations, one set for each class of vehicle as shown below:

Equation Set 1: SSTO Accelerator: Rocket-propelled

Equation Set 2: SSTO Accelerator: Air Breathing + Rocket

Equation Set 3: SSTO Cruise/Accelerator: AB + Rocket

Equation Set 4: TSTO Accelerator: Stages 1 and 2 Rocket

Equation Set 5: TSTO Accelerator: Stage 1 AB; Stage 2 Rocket

Equation Set 6: TSTO Cruise/Accelerator: Stage 1 AB; Stage 2 Rocket

To date, all launchers have been rocket-propelled 'accelerator' vehicles, in which the propulsive phases have been used to accelerate the vehicle throughout its ascent trajectory. The use of air-breathing propulsion in future winged launchers, would allow to economically introduce cruise phases into launcher ascent trajectories. This cruise capability would significantly extend the versatility of such vehicles, enabling them to be flown in cruising flight from the launch site to the required latitude and longitude before accelerating into the target orbit. Thus, cruising capability of launchers makes the so called 'off-set'launch possible.

Equation Set 1: SSTO Accelerator: Rocket-Propelled

Summation of the launcher mass elements gives:

$$M_l = M_{pr} + M_v + M_{pl} \qquad (1)$$

and summing the orbital mass elements gives:

$$M_o = M_v + M_{pl} \qquad (2)$$

Substituting (2) into (1) and solving for M_o gives:

$$M_o = M_l - M_{pr} \qquad (3)$$

Using the transposed form of the rocket equation gives:

$$M_{pr} = M_l(1-e^{-\frac{\Delta V_r}{I_{sr}g_0}}) \qquad (4)$$

Substituting (4) into (3) gives:

$$M_o = M_l - M_l(1-e^{-\frac{\Delta V_r}{I_{sr}g_0}}) \qquad (5)$$

Dividing both sides of (5) by M_l to get mass ratios gives:

$$\frac{M_0}{M_l} = e^{-\frac{\Delta V_r}{I_{sr}g_0}} \qquad (6)$$

Substituting (2) into (6) and solving for M_{pl}/M_l gives:

$$\frac{M_{pl}}{M_l} = (e^{-\frac{\Delta V_r}{I_{sr}g_0}} - \frac{M_v}{M_l}) \qquad (7)$$

Equation Set 2: SSTO Accelerator: Air Breathing + Rocket

Summation of the launcher mass elements gives:

$$M_1 = M_{pa} + M_{pr} + M_v + M_{pl} \qquad (8)$$

and summation of the orbital mass elements gives:

$$M_0 = M_v + M_{pl} \qquad (9)$$

Substituting (9) into (8) and solving for M_o gives:

$$M_o = M_1 - M_{pa} - M_{pr} \qquad (10)$$

Dividing both sides of (10) by M_1 to give mass ratios:

$$\frac{M_o}{M_1} = 1 - \frac{M_{pa}}{M_1} - \frac{M_{pr}}{M_1} \qquad (11)$$

$$M_{pa} = M_1(1-e^{-\frac{\Delta V_a}{I_{sa}g_0}}) \qquad (12)$$

Dividing (12) by M_1 gives:

$$\frac{M_{pa}}{M_1} = (1 - e^{-\frac{\Delta V_a}{I_{sa}g_0}}) \qquad (13)$$

$$M_{pr} = (M_1 - M_{pa})(1 - e^{-\frac{\Delta V_r}{I_{sr}g_0}}) \qquad (14)$$

Dividing both sides of (14) by M_1 gives:

$$\frac{M_{pr}}{M_1} = (1 - \frac{M_{pa}}{M_1})(1 - e^{-\frac{\Delta V_r}{I_{sr}g_0}}) \qquad (15)$$

Substituting (9) into (11) and solving for M_{pl}/M_1 gives:

$$\frac{M_{pl}}{M_1} = 1 - \frac{M_{pa}}{M_1} - \frac{M_{pr}}{M_1} - \frac{M_v}{M_1} \qquad (16)$$

Equation Set 3: SSTO Cruise/Accelerator: AB + Rocket

Summation of the launcher mass elements gives:

$$M_l = M_{pa} + M_{pc} + M_{pr} + M_v + M_{pl} \qquad (17)$$

and summation of the orbital mass elements gives:

$$M_o = M_v + M_{pl} \qquad (18)$$

Substituting (18) into (17) and solving for M_o gives:

$$M_o = M_l - M_{pa} - M_{pc} - M_{pr} \qquad (19)$$

Dividing both sides of (19) by M_l to give mass ratios:

$$\frac{M_o}{M_l} = 1 - \frac{M_{pa}}{M_l} - \frac{M_{pc}}{M_l} - \frac{M_{pr}}{M_l} \qquad (20)$$

$$\frac{M_{pa}}{M_l} = (1 - e^{-\frac{\Delta V_a}{I_{sa} g_0}}) \qquad (21)$$

$$\frac{M_{pc}}{M_l} = \frac{I_{tc}}{I_{sc} M_l} \qquad (22)$$

$$\frac{M_{pr}}{M_l} = (1 - \frac{M_{pa}}{M_l} - \frac{M_{pc}}{M_l})(1 - e^{-\frac{\Delta V_r}{I_{sr} g_0}}) \qquad (23)$$

$$\frac{M_{pl}}{M_l} = (1 - \frac{M_{pa}}{M_l} - \frac{M_{pc}}{M_l} - \frac{M_{pr}}{M_l} - \frac{M_v}{M_l}) \qquad (24)$$

Equation Set 4: TSTO Accelerator: Stages 1 and 2 Rocket

First Stage Equations:

$$M_{l1} = M_{pr1} + M_{v1} + M_{pl1} \qquad (25)$$

and the payload of the first stage is the launch mass of the second stage:

$$M_{pl1} = M_{l2} \qquad (26)$$

Transposing (25) to solve for M_{pl1} and dividing by M_{l1} to give mass ratios:

$$\frac{M_{pl1}}{M_{l1}} = \left(1 - \frac{M_{pr1}}{M_{l1}} - \frac{M_{v1}}{M_{l1}}\right) \qquad (27)$$

$$\frac{M_{pr1}}{M_{l1}} = \left(1 - e^{-\frac{\Delta V_{r1}}{I_{sr1} g_0}}\right) \qquad (28)$$

Second Stage Equations:

$$M_{l2} = M_{pr2} + M_{v2} + M_{pl2} \qquad (29)$$

Dividing (29) by M_{l2} to give mass ratios:

$$\frac{M_{pl2}}{M_{12}} = \left(1 - \frac{M_{pr2}}{M_{12}} - \frac{M_{v2}}{M_{12}}\right) \qquad (30)$$

$$\frac{M_{pr2}}{M_{12}} = \left(1 - e^{-\frac{\Delta V_{r2}}{I_{sr2} g_0}}\right) \qquad (31)$$

For mathematical convenience, the overall payload mass ratio can be expressed as:

$$\frac{M_{pl2}}{M_{11}} = \frac{M_{pl2}}{M_{12}} \times \frac{M_{12}}{M_{11}} \qquad (32)$$

Substituting (26) into (32) gives:

$$\frac{M_{pl2}}{M_{11}} = \frac{M_{pl2}}{M_{12}} \times \frac{M_{pl1}}{M_{11}} \qquad (33)$$

The orbital mass ratio is given by:

$$\frac{M_{o2}}{M_{11}} = \frac{M_{pl2}}{M_{11}} + \frac{M_{v2}}{M_{11}} \qquad (34)$$

Equation Set 5: TSTO Accelerator: Stage 1 AB; Stage 2 Rocket

First Stage Equations:

$$\frac{M_{pl1}}{M_{11}} = \left(1 - \frac{M_{pa1}}{M_{11}} - \frac{M_{v1}}{M_{11}}\right) \qquad (35)$$

$$\frac{M_{pa1}}{M_1} = \left(1 - e^{-\frac{\Delta V_{a1}}{I_{sa1} g_0}}\right) \qquad (36)$$

Second Stage Equations:

$$\frac{M_{pl2}}{M_{12}} = \left(1 - \frac{M_{pr2}}{M_{12}} - \frac{M_{v2}}{M_{12}}\right) \qquad (37)$$

and the overall mass ratio is given by:

$$\frac{M_{pl2}}{M_{11}} = \frac{M_{pl2}}{M_{12}} \times \frac{M_{pl1}}{M_{11}} \qquad (38)$$

and the orbital mass ratio is given by:

$$\frac{M_{o2}}{M_{11}} = \frac{M_{pl2}}{M_{11}} + \frac{M_{v2}}{M_{11}} \qquad (39)$$

Equation Set 6: TSTO Cruise/Accel: Stage 1 AB; Stage 2 Rocket

First Stage Equations:

$$\frac{M_{pl1}}{M_{11}} = \left(1 - \frac{M_{pa1}}{M_{11}} - \frac{M_{pc1}}{M_{11}} - \frac{M_{v1}}{M_{11}}\right) \qquad (40)$$

$$\frac{M_{pa1}}{M_{11}} = \left(1 - e^{-\frac{\Delta V_{a1}}{I_{sa1} g_0}}\right) \qquad (41)$$

$$\frac{M_{pc1}}{M_{11}} = \frac{I_{tc1}}{I_{sc1} M_{11}} \qquad (42)$$

Second Stage Equations:

$$\frac{M_{pl2}}{M_{12}} = \left(1 - \frac{M_{pr2}}{M_{12}} - \frac{M_{v2}}{M_{12}}\right) \qquad (43)$$

The overall payload ratio is given by:

$$\frac{M_{pl2}}{M_{11}} = \frac{M_{pl2}}{M_{12}} \times \frac{M_{pl1}}{M_{11}} \qquad (44)$$

and the orbital mass ratio is given by:

$$\frac{M_{o2}}{M_{11}} = \frac{M_{pl2}}{M_{11}} + \frac{M_{v2}}{M_{11}} \qquad (45)$$

4.5 Derivation of Equations for Velocity increments and Average Specific Impulse

It can be seen readily from the analytical equations derived for each class of reusable launcher in Chapter 4.4 above, that the accuracy of the calculated values of the payload ratio depends on the accuracy of the values of the following three performance parameters:

- velocity increment (Δv);
- average specific impulse (I_s);
- vehicle mass ratio (M_v/M_l).

The accurate calculation of the velocity increments and the average specific impulse are presented below. The accurate calculation of the vehicle mass ratio is a difficult problem and is discussed in Chapter 5.2.4.

The total velocity increment Δv for any required orbit is calculated from:

$$\Delta v = \Delta v_{pt} + \Delta v_{circ} + \Delta v_{dl} + \Delta v_{gl} - \Delta v_{cf} \mp \Delta v_{rot} \qquad (46)$$

The perigee velocity of the target orbit Δv_{pt} is calculated from:

$$\Delta v_{pt} = \left[\frac{2\mu}{r_{p1}}\left(\frac{r_{a1}}{r_{a1}+r_{p1}}\right)\right]^{\frac{1}{2}} \qquad (47)$$

The velocity to circularise an elliptic orbit Δv_{circ}, if required, is calculated from:

$$\Delta v_{circ} = \left[\frac{2\mu}{r_{a2}}\left(\frac{r_{p2}}{r_{a2}+r_{p2}}\right)\right]^{\frac{1}{2}} - \left[\frac{2\mu}{r_{a1}}\left(\frac{r_{p1}}{r_{a1}+r_{p1}}\right)\right]^{\frac{1}{2}} \qquad (48)$$

The velocity loss due to aerodynamic drag Δv_{dl} and the velocity loss due to gravity force Δv_{gl} are complex functions of the aerodynamic design of the vehicle and the selected ascent trajectory. The derivation of these velocity loss equations is presented in Chapter 4.6. These equations are given below:

The velocity loss due to aerodynamic drag Δv_{dl} is given by:

$$\Delta v_{dl} = \int_0^t \left(\left(C_{d0}+\frac{\alpha^2}{K}\right) A_r \frac{\rho V^2}{2M}\right) dt \qquad (49)$$

The velocity loss due to gravity force Δv_{gl} is given by:

$$\Delta v_{gl} = \int_0^t \left(g_0\left(\frac{r_e^2}{r^2}\right)\sin\gamma\right) dt \qquad (50)$$

The Earth's rotation contributes a velocity gain for prograde orbits and a velocity loss for retrograde orbits. The value of Δv_{rot} is a function of the launch site latitude and launch azimuth angle, being a maximum for an easterly launch from the equator (prograde orbit) and a minimum for westerly launches from the equator (retrograde orbit). The value of Δv_{rot} is calculated from:

$$\Delta v_{rot} = \omega r_e \cos\lambda_L \sin A_Z \qquad (51)$$

The launch azimuth angle A_z required to achieve a selected orbit inclination from any launch site latitude is calculated from:

$$\sin A_Z = \frac{\cos i}{\cos\lambda_L} \qquad (52)$$

The calculation of an accurate value of the average specific impulse I_{sav} requires integration of the thrust F and propellant mass flow rate m_p over the selected ascent trajectory. The value of I_{sav} in Ns/kg (or m/s) is calculated by numerical integration from:

$$I_{sav} = \frac{\int_0^t T dt}{\int_0^t m_p dt} \qquad (53)$$

4.6 Derivation of Launcher Ascent Integral Equations of Motion

An exact analysis of the performance of a launcher as it ascends through the atmosphere, requires the solution of the equations of motion for a non-rigid vehicle with six degrees of freedom (horizontal, vertical and lateral translations; pitch, yaw and roll rotations), for a rotating oblate Earth model. However, for this system-level study, where the primary objective is to use the equations of motion to establish the comparative orbital mass ratios for a large number of reusable launcher concepts, the full six-degree of freedom model is deemed by the author to be unnecessarily complex and the numerical solution of the equations of motion would require massive computational efforts, even when using a modern high speed computer, running at speeds exceeding 25 MHz. Instead, a simplified approach, using a point-mass two-degree of freedom model (horizontal and vertical motion only), for a non-rotating spherical Earth, is deemed to be sufficiently accurate for this comparative performance study. The use of this simplified model is therefore justified to substantially reduce computational time and effort.

The equations of motion for such a two-degree of freedom model are derived in this Section and transposed to a form that is convenient for illustrating the velocity and flight path angle contributions due to propulsive, aerodynamic and gravity forces. However, to be able to trace the loss of accuracy incurred by use of the two-degree of freedom model, the equations of motion are first derived for a point-mass three-degree of freedom model (horizontal, vertical and lateral translations) for a rotating spherical Earth. These equations, identified here as the root equations, are then successivly simplified according to the following steps:

Step 1:
Derivation of a second set of equations of motion: These are derived for a **point-mass three-degree of freedom, non-rotating spherical Earth model** by simplification of the root equations of motion.

Step 2:
Derivation of a third (final) set of equations of motion: These are derived for a **point-mass two-degree of freedom, non-rotating spherical Earth model** by further simplification of the second set of equations.

4.6.1 Derivation of the Equations of Motion for a Point-Mass Three-degree of Freedom, Rotating Spherical Earth Model

The motion of a vehicle, considered as a point mass, ascending through the atmosphere, is defined by:
- its position vector $\vec{r}(t)$;
- its velocity vector $\vec{V}(t)$;
- its instantaneous mass M.

At each instant, the vehicle is subjected to a total force $\vec{F}$, which results from the combined action of the thrust force $\vec{T}$ provided by the propulsion system, the aerodynamic force $\vec{A}$ and the gravity force (weight) $\vec{W}$. Thus:

$$\vec{F} = \vec{T} + \vec{A} + \vec{W} \qquad (54)$$

For an inertial system, by Newton's Second Law of Motion, the total force $\vec{F}$ is:

$$M\frac{d\vec{V}}{dt} = \vec{F} \qquad (55)$$

Because we need to know the motion of the vehicle with respect to a reference frame and a coordinate system within that frame, it is then necessary to select the reference frame and coordinate system and then to develop the scalar equations of motion from the vector force equations (54) and (55).

Reference Frame and Coordinate System

Figure 4.1 shows the adopted reference frames and coordinate system. OXYZ is defined as an inertial reference frame, taken such that O is at the centre of the gravitational field of the spherical Earth and the OXY plane is the equatorial plane. The ascending vehicle has a rotating reference frame Oxyz. The Earth is rotating at constant angular velocity ω directed along its Z axis. The atmosphere is assumed to be at rest with respect to the Earth and therefore rotates with the same angular velocity ω. Figure 4.1 also shows the curvilinear path of an ascending vehicle. The various vectors and angles that define the instantaneous position M of the vehicle in its flight path are also shown. These vectors and angles are now defined:

V is the velocity vector of the vehicle M. The position vector is $\vec{r}$, which is defined by its magnitude r, its longitude θ measured from the X axis, in the equatorial plane, positively eastward, and its latitude ϕ, measured from the equatorial plane along a meridian, positively northwards. The flight path angle is γ, which is the angle between the local horizontal plane and the velocity vector V. γ is positive when V is above the horizontal plane. The angle ψ is the vehicle heading and is the angle between the local parallel of the latitude and the projection of V on the horizontal plane, measured positively in the right-hand

direction about the x axis. The vectors $\vec{i}$, $\vec{j}$ and $\vec{k}$ are unit vectors along the axes of the rotating system Oxyz.

Force Diagrams

Figure 4.2 shows a vector diagram of the instantaneous aerodynamic, propulsive and gravitational forces acting on the vehicle. The vehicle is flying with velocity $\vec{V}$ at a flight path angle γ measured from the local horizontal plane and at an angle of attack α. The aerodynamic force is decomposed into the drag force $\vec{D}$ opposite to the velocity vector, and the lift force $\vec{L}$ acting orthogonal to the velocity vector. The propulsive thrust force $\vec{T}$ is always in the lift-drag plane and acts at an angle α_1 between the thrust and the velocity vectors. $\vec{W}$ is the weight of the vehicle, acting along the radius vector towards the gravitational centre.

Because of the three degrees of freedom, lateral aerodynamic forces will occur if the lift-drag plane is rotated from the vertical plane which is the $(\vec{r}, \vec{V})$ plane. Figure 4.3 illustrates the vector diagram when the lift-drag plane is rotated through an angle σ, which is defined as the roll or bank angle. Axes x', y', z' are the axes from the position M of the vehicle, parallel to the rotating axes x, y, z respectively. Axes x_1, y_1, z_1 are the axes from the point M, along the direction of the normal force vector $\overrightarrow{F_N \cos \sigma}$, V and the vector $\overrightarrow{F_N \sin \sigma}$ respectively. The axes system $Mx_1y_1z_1$ is deduced from the axes system $Mx'y'z'$ by a rotation ψ in the horizontal plane, followed by a rotation γ in the vertical plane.

Scalar Force Equations of Motion

Transformation of the vector force equations of motion (54) and (55) into a set of three useful scalar force equations

has been performed using the mathematical procedure described in Chapter 3 of Reference 38. These three equations are:

$$M\frac{dV}{dt} = F_T - W\sin\gamma + M\omega^2 r\cos\phi(\sin\gamma\cos\phi - \cos\gamma\sin\psi\sin\phi) \quad (56)$$

$$MV\frac{d\gamma}{dt} = F_N\cos\sigma - W\cos\gamma + \frac{MV^2}{r}\cos\gamma + 2M\omega V\cos\psi\cos\phi + M\omega^2 r\cos\phi(\cos\gamma\cos\phi + \sin\gamma\sin\psi\sin\phi) \quad (57)$$

$$MV\frac{d\psi}{dt} = -\frac{F_N\sin\sigma}{\cos\gamma} - \frac{MV^2}{r}\cos\gamma\cos\psi\tan\phi + 2M\omega V(\tan\gamma\sin\psi\cos\phi - \sin\phi) - \frac{M\omega^2 r}{\cos\gamma}\cos\psi\sin\phi\cos\phi \quad (58)$$

Equation (56) gives the rate of change of velocity along the vehicle's motion axis. Equation (57) gives the rate of change of the vehicle's flight path angle. Equation (58) gives the rate of change of the vehicle's heading angle. In these equations, F_T is the net tangential force along the velocity vector and F_N is the net normal force along the lift vector. These forces, derived from Figure 4.2 are:

$$F_T = T\cos\alpha_1 - D \quad (59)$$

$$F_N = T\sin\alpha_1 + L \quad (60)$$

The presence of the ω terms in equations (56), (57) and (58) is due to the rotation of the Earth. The term $\omega^2 r$ in Equations (56) and (57) is the centripetal acceleration, which, for a given value of r, depends on the direction of r and therefore on the latitude of the vehicle. This acceleration is zero when r is collinear with ω, that is, for

flight paths over the poles of the Earth and is a maximum for flight paths over the equator. As an example, for a flight altitude of 100 km over the equator, the value of the centripetal acceleration is very small with a value of about 3.5×10^{-3} g_0, and can therefore be neglected. The term $2\omega V$ in Equation (57) is the Coriolis acceleration and depends on both the magnitude and direction of the velocity of the vehicle with respect to the Earth. It is zero when the flight path is parallel to the polar axis and a maximum when the flight path is orthogonal to the polar axis. For example, for an orbital speed of 8 km/s at zero inclination, the Coriolis acceleration has a value of about 0.12 g_0. Thus, it can be seen, that for high accuracy in trajectory calculations, the Coriolis acceleration is significant and cannot be neglected. However, for this research, where the comparative performance of different vehicles is of most importance, the use of a simpler, two-degree-of-freedom, non-rotating spherical Earth trajectory model has been adopted. This simpler model, as shown in Chapters 4.6.2 and 4.6.3 below, excludes both the centripetal and Coriolis acceleration terms because of the assumption of a non-rotating Earth.

The velocity V is the relative velocity with respect to the Earth. This is the velocity value used in the calculation of aerodynamic drag and lift forces in the equations developed later in this Section. The inertial velocity V_i is calculated by the vector addition of the Earth's rotational velocity.

4.6.2 Derivation of the Equations of Motion for a Point-Mass Three-Degree of Freedom, Non-rotating Spherical Earth Model

These equations are readily derived from the rotating Earth root equations (56), (57) and (58), by simply deleting all the terms containing the Earth's rotation vector ω. The resulting equations are:

$$M\frac{dV}{dt} = F_T - W\sin\gamma \qquad (61)$$

$$MV\frac{d\gamma}{dt} = F_N\cos\sigma - W\cos\gamma + \frac{MV^2}{r}\cos\gamma \qquad (62)$$

$$MV\frac{d\psi}{dt} = \frac{F_N\sin\sigma}{\cos\gamma} - \frac{MV^2}{r}\cos\gamma\cos\psi\tan\phi \qquad (63)$$

4.6.3 Derivation of the Equations of Motion for a Point-Mass Two-degree of Freedom, Non-rotating Spherical Earth Model

These equations are readily derived from the three-degree of freedom, non-rotating spherical Earth equations (61), (62) and (63), by simply putting the bank angle σ to zero in Equation (62) and by deleting Equation (63) because there is no lateral motion. This yields two simple equations:

$$M\frac{dV}{dt} = F_T - W\sin\gamma \qquad (64)$$

$$MV\frac{d\gamma}{dt} = F_N - W\cos\gamma + \frac{MV^2}{r}\cos\gamma \qquad (65)$$

Equations (64) and (65) are the final equations. Before solving them, they are elaborated further as follows:

$$D = C_d A_r \frac{\rho V^2}{2} \qquad (66)$$

$$C_d = C_{do} + C_{di} \tag{67}$$

$$C_{di} = \frac{\alpha^2}{K} \tag{68}$$

Substituting (68) into (67) gives:

$$C_d = C_{do} + \frac{\alpha^2}{K} \tag{69}$$

Substituting (69) into (66) gives:

$$D = (C_{do} + \frac{\alpha^2}{K}) A_r \frac{\rho V^2}{2} \tag{70}$$

$$W = Mg \tag{71}$$

Substituting (59), (70) and (71) into (64) gives:

$$\frac{MdV}{dt} = T\cos\alpha_1 - (C_{do} + \frac{\alpha^2}{K}) A_r \frac{\rho V^2}{2} - Mg\sin\gamma \tag{72}$$

$$g = g_o \frac{r_e^2}{(r_e+H)^2} \tag{73}$$

$$(r_e+H) - r \qquad (74)$$

Substituting (74) into (73) gives:

$$g = g_o\frac{r_e^2}{r^2} \qquad (75)$$

Therefore substituting (75) into (72) gives:

$$\frac{MdV}{dt} = T\cos\alpha_1 - ((C_{do}+\frac{\alpha^2}{K})A_r\frac{\rho V^2}{2}) - Mg_o(\frac{r_e^2}{r^2})\sin\gamma \qquad (76)$$

Dividing both sides of (76) by M gives:

$$\frac{dV}{dt} = \frac{T}{M}\cos\alpha_1 - ((C_{do}+\frac{\alpha^2}{K})A_r\frac{\rho V^2}{2M}) - g_o(\frac{r_e^2}{r^2})\sin\gamma \qquad (77)$$

Equation (77) can now be integrated to give the velocity change as a function of time:

$$\Delta v = \int_0^t \frac{T}{M}\cos\alpha_1 dt - \int_0^t ((C_{do}+\frac{\alpha^2}{K})A_r\frac{\rho V^2}{2M})\,dt - \int_0^t (g_0(\frac{r_e^2}{r^2})\sin\gamma)\,dt \qquad (78)$$

Equation (78) has been derived in this form to identify clearly the various velocity gains and losses:

Term 1 gives the velocity gain due to propulsive thrust:

$$\int_0^t \frac{T}{M}\cos\alpha_1 dt \qquad (79)$$

Term 2 gives the velocity loss due to aerodynamic drag:

$$\int_0^t ((C_{do}+\frac{\alpha^2}{K})A_r\frac{\rho V^2}{2M})dt \qquad (80)$$

Term 3 gives the velocity loss due to gravity force:

$$\int_0^t (g_0(\frac{r_e^2}{r^2})\sin\gamma)dt \qquad (81)$$

Elaboration of Equation (65):

$$L = C_l A_r \frac{\rho V^2}{2} \qquad (82)$$

$$C_l = \frac{\alpha}{K} \qquad (83)$$

Substituting (83) into (82) gives:

$$L = \frac{\alpha}{K} A_r \frac{\rho V^2}{2} \qquad (84)$$

Substituting (60), (71), (75) and (84) into (65) gives:

$$MV\frac{d\gamma}{dt} = \frac{\alpha}{K}A_r\frac{\rho V^2}{2}+T\sin\alpha_1-Mg_0\left(\frac{r_e^2}{r^2}\right)\cos\gamma+\frac{MV^2}{r}\cos\gamma \qquad (85)$$

Dividing both sides of (85) by MV gives:

$$\frac{d\gamma}{dt} = \left(\frac{\frac{\alpha}{K}A_r\frac{\rho V^2}{2}}{MV}\right)+\left(\frac{T\sin\alpha_1}{MV}\right)-\left(\frac{g_0}{V}\left(\frac{r_e^2}{r^2}\right)\cos\gamma\right)+\left(\frac{V\cos\gamma}{r}\right) \qquad (86)$$

Equation (86) can now be integrated to give the flight path angle as a function of time:

$$\Delta\gamma = \int_0^t\left(\frac{\frac{\alpha}{K}A_r\frac{\rho V^2}{2}}{MV}\right)dt + \int_0^t\left(\frac{T\sin\alpha_1}{MV}\right)dt - \int_0^t\left(\frac{g_0}{V}\left(\frac{r_e^2}{r^2}\right)\cos\gamma\right)dt + \int_0^t\left(\frac{V\cos\gamma}{r}\right)dt \qquad (87)$$

Equation (87) consists of four terms which comprise the resulting flight path angle (FPA):

Term 1 is the FPA change due to lift:

$$\int_0^t\left(\frac{\frac{\alpha}{K}A_r\frac{\rho V^2}{2}}{MV}\right)dt \qquad (88)$$

Term 2 is the FPA change due to thrust:

$$\int_0^t \left(\frac{T\sin\alpha_1}{MV}\right) dt \qquad (89)$$

Term 3 is the FPA change due to gravity force:

$$\int_0^t \left(\frac{g_0}{V}\left(\frac{r_e^2}{r^2}\right)\cos\gamma\right) dt \qquad (90)$$

Term 4 is the FPA change due to the centrifugal effect:

$$\int_0^t \left(\frac{V\cos\gamma}{r}\right) dt \qquad (91)$$

In addition to the velocity and flight path angle differential equations (77) and (86), there are two more coupled equations which are needed in the trajectory program. These are the altitude and range equations given below:

$$\frac{dH}{dt} = V\sin\gamma \qquad (92)$$

$$\frac{dS}{dt} = V\cos\gamma \qquad (93)$$

The derivation of the velocity and flight path angle integral equations in the final forms given in equations (78) and (87) has been intentional: to allow the individual terms of each equation to be closely monitored in the computer solution. This allows the interaction of aerodynamic, propulsion and trajectory parameters to be readily assessed.

Figure 4.1: Reference Frame and Coordinate System (Reference 38)

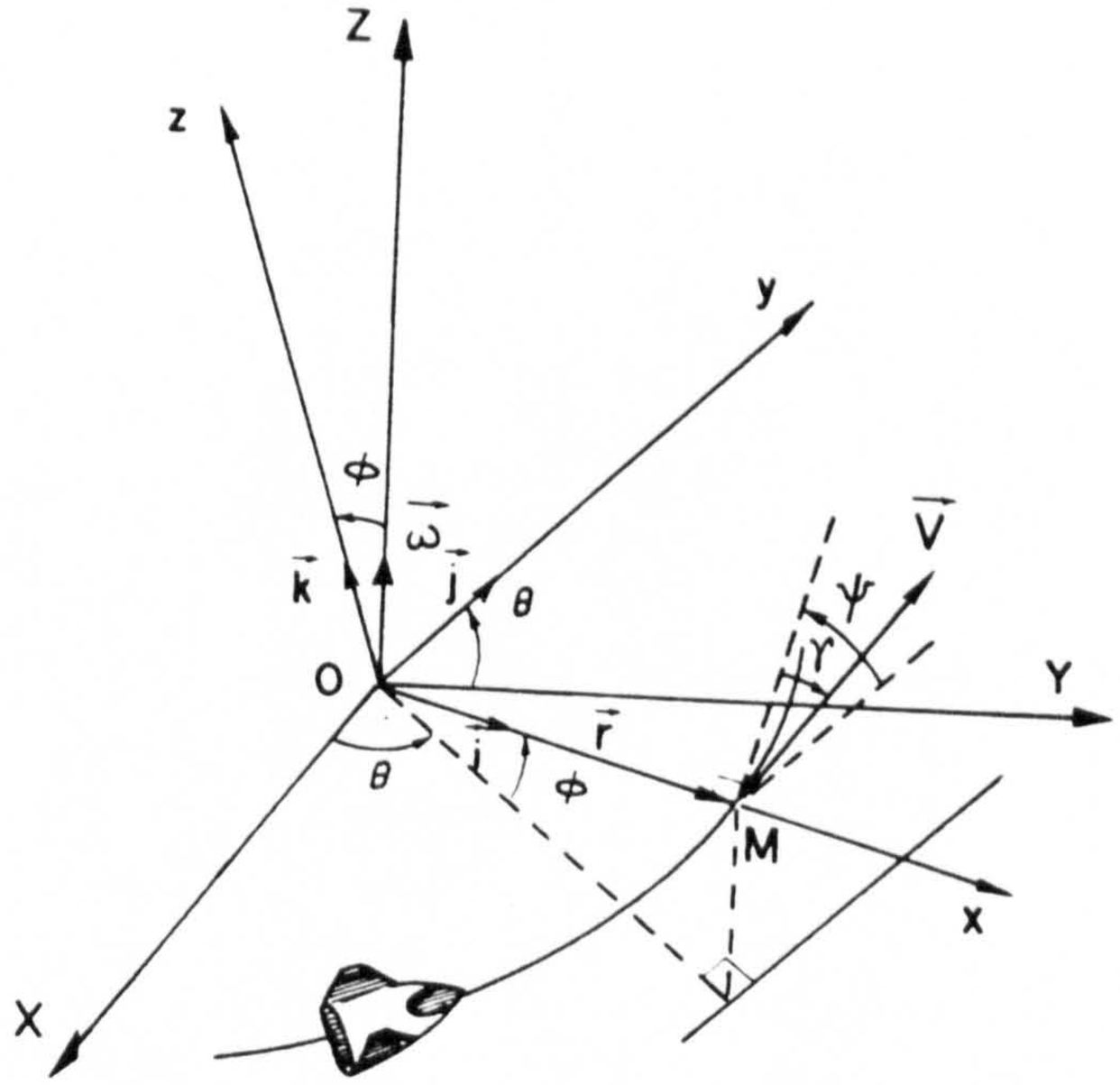

Figure 4.2: Forces Acting on the Vehicle

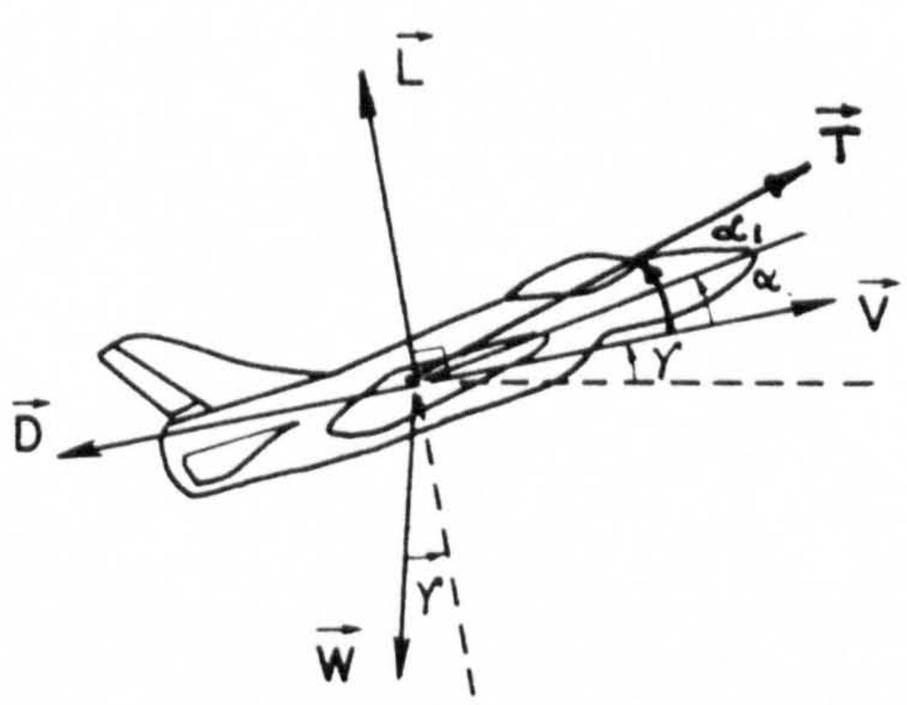

Figure 4.3: Aerodynamic Forces in the Lift-Drag Plane

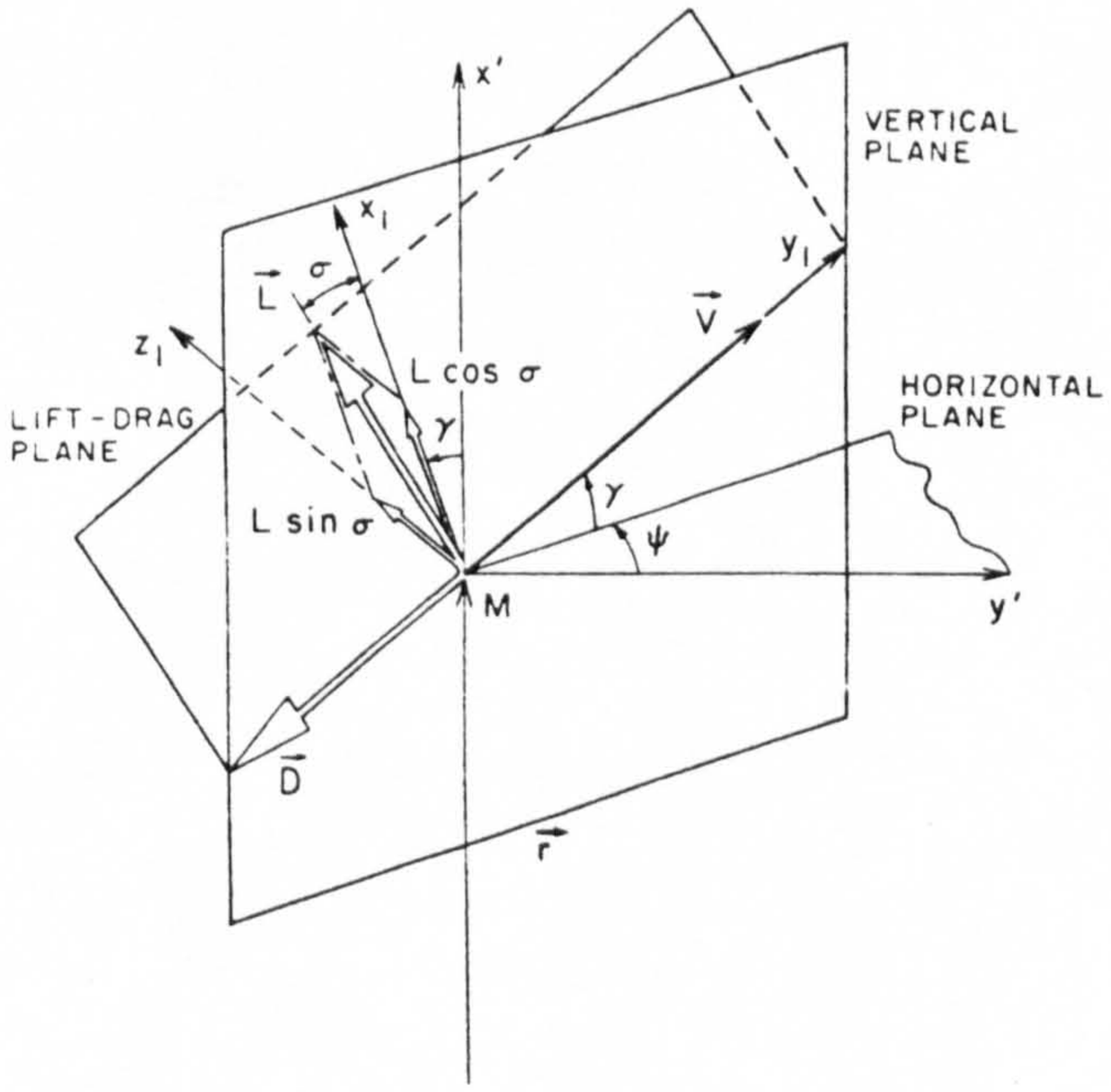

5 CALCULATED PERFORMANCE OF REUSABLE LAUNCHERS

5.1 Synopsis

The derivation of a standard calculation methodology for the performance of each of the candidate launchers is first described. A typical payload-delivery mission is then defined and adopted as a standard reference mission. The performance of each candidate reusable launcher is then calculated for the reference mission, using the standard calculation methodology. The performance results for each launcher are then presented and discussed. A comparative analysis of the performance of all the candidate launchers is then performed and the results are discussed. Finally, performance results from other system studies are presented and compared with those from this research.

5.2 Standard Performance Calculation Methodology

To be able to compare, on a fair basis (apples with apples), the performance of candidate reusable launchers, it was deemed to be essential to use consistently, a standard set of performance analysis tools for each vehicle. The required tools are:

- a trajectory analysis computer code;
- an aerodynamic analysis computer code;
- a propulsion analysis computer code;
- a vehicle mass analysis model;
- a graphical presentation of launcher performance.

Furthermore, to be able to compare the performance results of this research with those from other system studies, wherever possible, the vehicle configuration adopted for each vehicle was that used in the comparative reference system study.

A major effort in this research was the preparation by the author of this set of standard performance analysis tools. These tools are discussed below:

5.2.1 Trajectory Analysis Computer Code

Early in this research in 1989, the author discovered that there were no trajectory analysis computer codes available which were suitable for use in the research. Trajectory analysis codes were found to be existing in the European Aerospace companies, but all of these were large and complex codes, designed for trajectory optimisation of well defined, current, multi-stage expendable, rocket-propelled launchers, No codes were found, either complex trajectory optimising codes, or simple trajectory simulation codes, that could be used for vehicles employing aerodynamic lifting ascent and/or air-breathing propulsion. The author was then compelled to expend a major effort to develop his own ascent trajectory analysis codes to cover the various new operational characteristics of the candidate launchers: vertical and horizontal launch; rocket and/or air-breathing propelled; lifting and/or ballistic flight; single and two-stage-to-orbit vehicles. The codes, which were developed as trajectory simulation codes, are able to simulate user-defined ascent trajectories. Optimisation of the trajectory, for any user-defined cost function like maximum injected mass or payload mass, must then be performed by the user, using a reiterative process, and the adjustment of parameters, to converge rapidly to the maximum value of the selected cost function. The principal features of these codes are described below.

5.2.1.1 Specific Trajectory Analysis Codes

Because the development of a single, large, generic ascent trajectory code that could be used for any type of launcher proved to be a complex and inefficient approach, the author decided instead, to split this large code into the following specific codes, each one being focused on a particular category of launcher:

- Code SSTOVL: this code covers the ascent of single-stage-to-orbit vehicles which can be rocket-propelled and/or air-

breathing propelled, ascending either on non-lifting flight and/or lifting flight. For the non-lifting flight case, the vehicle flight controls are the magnitude and direction of the thrust vector. Thus, the vehicle acceleration is controlled by engine throttling and the flight path angle is controlled by engine thrust vectoring. For the lifting-flight case, the vehicle flight controls are the magnitude of the thrust and the incidence angle (angle of attack) of the vehicle. Thus, the acceleration level is controlled by engine throttling and the flight path angle is controlled by the angle of attack. This program also, uniquely, allows to fly a vehicle under a combination of thrust vectoring and angle of attack, both controls being used simultaneously. This allows to explore possible gains in orbital mass by this unusual combination of flight controls.

- Code SSTOHL: this code covers the ascent of single-stage-to-orbit vehicles which are launched horizontally and ascend under lifting flight, using rocket propulsion and/or air-breathing propulsion. The flight controls are thrust magnitude to control the acceleration level and angle of attack to control the flight path angle

- Code TSTOVL: this code covers the ascent of two-stage-to-orbit vehicles which are vertically launched and propelled by rocket propulsion and/or air-breathing propulsion and may ascend under non-lifting flight and/or lifting flight. The code is a derivative of Code SSTOVL, developed specifically for two stage vehicles, allowing to optimise the staging parameters of Mach number and altitude. The flight controls are thrust magnitude and thrust vector angle for the non-lifting flight case and thrust magnitude and angle of attack for the lifting flight case. Like Code SSTOVL, this code may also be used to examine trajectories simultaneously using thrust vectoring and angle of attack to control the flight path angle.

- Code TSTOHL: this code covers two-stage-to-orbit vehicles which are horizontally launched and propelled by rocket propulsion and/or air-breathing propulsion, ascending under lifting flight. The code is a derivative of Code SSTOHL, developed specifically for two stage vehicles to allow the optimisation of the staging Mach number and altitude. The flight controls are thrust magnitude and angle of attack.

5.2.1.2 Equations of Motion Used in the Trajectory Programs
The shape of the trajectory is determined by four coupled differential equations of motion, which must therefore be solved simultaneously. The derivation of these equations has already been presented in Chapter 4. These equations are: the velocity equation (77); the flight path angle equation (86); the altitude equation (92) and the range equation (93). The significance of these equations are described below:

- Equation (77): this gives the vehicle velocity along the flight path angle as a function of time. The deliberate casting of this equation in this form, which comprises three terms, allows the individual velocity contributions of propulsive thrust, aerodynamic drag and gravity force to be identified and accounted for separately. Thus the comparative significance of each of these forces can be readily assessed, aiding the user to converge to an optimum trajectory.

- Equation (86): this gives the vehicle flight path angle as a function of time. Again, the deliberate casting of the equation in this form, which comprises four terms, allows the individual flight path angle contributions of aerodynamic lift, propulsive thrust, gravity force and the centrifugal effect, to be identified and accounted for separately. Again, the comparative significance of each of these forces can be readily assessed, aiding the user to converge to an optimum trajectory.

- Equation (92): the integration of this equation gives the altitude from the launch site as a function of time;

- Equation (93): the integration of this equation gives the slant range from the launch site as a function of time.

5.2.1.3 Solution Scheme for the Equations of Motion

Because the equations of motion are all first order differential equations, their integration has been possible using simple numerical methods. Three methods have been developed and there are versions of each program with each of these three numerical schemes. These schemes, in order of ascending accuracy and computational time are:
- a finite difference scheme;
- a second order Runge-Kutta scheme;
- a fourth order Runge-Kutta scheme.

The Finite Difference Scheme: This method uses a very small time step (typically of 0.1 s), over which the values of all variables are assumed to be constant. Thus, starting with specified initial values of all the variables, the change in the value of each variable is calculated over the time step, where the time step simply becomes a multiplicand in each term of the integrand. These changes are then added to the initial values to give the new input values for the next time step. In this way, the values of all variables are integrated with flight time along the trajectory. Input values of relevant parameters are changed at specified elapsed flight times, in accordance with the user-specified flight plan and constraints which are input into the programme at its start. The accuracy and stability of the scheme has been tested by the integration of standard first order differential equations with closed-form solutions and found to be surprisingly accurate. A time step of 0.1 s was found to be a good compromise between accuracy and computer execution time.

The Second Order and Fourth Order Runge-Kutta Schemes: These integration schemes differ from the finite difference scheme only in the use of standard second and fourth order Runge-Kutta integration algorithms. These schemes were also tested by integrating the same standard set of first order differential equations with closed form solutions as used to test the finite difference scheme. The accuracy improvements obtained using Runge-Kutta to solve the equations of motion, were found to be too small to warrant the longer computer execution times, especially because the programs have to be run many times to arrive at an optimum trajectory for each vehicle case.

5.2.1.4 Data Requirements for the Trajectory Programs

The programs require user-defined data to be input into three data files, which are accessed automatically by the program. These files are :

- a standard atmosphere data file;
- a vehicle aerodynamic data file;
- a vehicle propulsion data file.

The standard atmosphere data file used is the 1976 US Standard Atmosphere (Reference 5) for altitudes up to 100 km. For higher altitudes up to 140 km, the Jacchia Model (Reference 6) has been used. These models give tabular data of air pressure, temperature and density as functions of altitude. These tables have been used in the programs: the required values being found automatically using a table look-up algorithm developed by the author. Intermediate values are calculated using linear interpolation. Any user-defined standard atmosphere, for example, the Kourou Launch site standard, can be readily substituted in the data file.

The Vehicle Aerodynamic Model: For each vehicle, values are required to be input into this data file by the user. This data comprises a table of drag and lift coefficients as

functions of Mach number and angle of attack. Again, an automatic table look-up and linear interpolation algorithm is used to find the required values.

The Vehicle Propulsion Model:

For rocket-propelled vehicles, the performance can be readily calculated from closed-form equations. Thus, the first step is to select the number of engines, the combustion chamber pressure, the initial sea level thrust, the vacuum specific impulse and, for fixed geometry engines, the nozzle area ratio of the engine. The thrust and specific impulse values as a function of altitude are then calculated by the program by accounting for the change in the pressure thrust term as the vehicle ascends. Alternatively, for a user-selected option for optimum expansion over the ascent trajectory, the program is directed to calculate the thrust and specific impulse as functions of altitude for full expansion. The algorithm for this calculation has been developed by the author and the derived equations are presented below:

A_e = nozzle exit area (m^2)

A_t = nozzle throat area (m^2)

C_f = thrust coefficient (-)

F = thrust force (N)

F_i = initial value of thrust force (N)

I_s = specific impulse (Ns/kg)

I_{si} = initial value of specific impulse (Ns/kg)

P_a = ambient static pressure (N/m^2)

P_{ai} = initial value of ambient pressure (N/m^2)

P_c = combustion chamber pressure (N/m^2)

γ = specific heat ratio of nozzle gases (-)

λ = nozzle divergence loss coefficient (-)

Ω = Vandenkerckhove Function (-)

ϵ = nozzle area ratio (-)

$$C_f = \lambda\Omega\left(\frac{2\gamma}{\gamma-1}Z\right)^{\frac{1}{2}} \qquad (1)$$

$$\Omega = \gamma^{\frac{1}{2}}\left(\frac{2}{\gamma+1}\right)^{\frac{\gamma+1}{2(\gamma-1)}} \qquad (2)$$

$$Z = 1 - \left(\frac{P_a}{P_c}\right)^{\frac{\gamma-1}{\gamma}} \qquad (3)$$

$$A_t = \frac{F}{C_f P_c} \qquad (4)$$

$$\varepsilon = \frac{A_e}{A_t} \qquad (5)$$

For complete nozzle expansion:

$$\varepsilon = \frac{\left(\frac{P_c}{P_a}\right)^{\frac{1}{\gamma}}}{\left(\frac{\gamma+1}{2}\right)^{\frac{1}{\gamma-1}}\left[\frac{\gamma+1}{\gamma-1}(Z)\right]^{\frac{1}{2}}} \qquad (6)$$

$$A_e = \varepsilon A_t \qquad (7)$$

$$F = F_1 + (P_{a1} - P_a)A_e \qquad (8)$$

$$I_s = I_{s1}\frac{F}{F_1} \qquad (9)$$

These equations allow the thrust coefficient (C_f) and the nozzle throat area (A_t) of each engine to be calculated. The area ratio of the nozzle (ϵ) for full expansion of the nozzle discharging to the atmospheric pressure at the vehicle altitude can then be calculated. The exit area for optimum expansion can then be calculated. The thrust and specific impulse values at any altitude can then be calculated.

For air-breathing propulsion systems, the model must show the gross thrust and gross specific impulse as functions of Mach Number, altitude, vehicle incidence angle and equivalence ratio. These values must be obtained from detailed engine performance calculations.

5.2.1.5 Description of the Trajectory codes

The trajectory codes calculate various performance parameters for user defined launch and target orbit coordinates and a flight plan. The flight plan covers up to 5 flight phases, but can be readily extended for any number of phases. The performance parameters calculated are: instantaneous values of flight time; thrust level; vehicle mass; propellant mass, flight altitude; flight range; relative velocity; inertial velocity; vehicle acceleration; gravitational acceleration; centrifugal acceleration; angle of attack, thrust vector angle; Mach Number; dynamic pressure; velocity gain from propulsive thrust; velocity loss from aerodynamic drag; velocity loss from gravity force; velocity gain from centrifugal force; various velocity and vehicle mass budgets. A choice of three thrust control modes are provided: no thrust control; progressive throttling of all engines to maintain axial acceleration and dynamic pressure constraints; or progressive shut down of each engine to maintain the axial acceleration and dynamic pressure constraint. User-specified flight modes of constant, or decreasing or increasing flight path angle and gravity turn manoeuvres may be used for any of the flight phases. Constraints of axial acceleration and

dynamic pressure are built into the program and the limits can be specified and used optionally, either singly or together. Three data files are built into the programme: a standard atmosphere; an aerodynamic performance model for the vehicle; a propulsion model for the vehicle. The data for these files has to be input by the user for his specific vehicle and launch site.

5.2.1.6 Flight Path Constraint Algorithms

The acceleration control algorithm is a simple one: the control variable is the thrust level. The acceleration is computed at each integration step and then compared with the user-defined acceleration limit. If the acceleration limit has been reached, the thrust level is reduced by successive iterative steps of 0.1 % for the next integration step, until the computed acceleration is less than the required acceleration limit, within 0.5 %. This algorithm works very well and convergence to the required acceleration normally requires no more than three iterations. The dynamic pressure control algorithm is more complex: the control variable is the thrust level and this must be reduced early enough so that the user-defined dynamic pressure limit is not exceeded, but ideally, is just reached. This is achieved by computing the rate of change of the dynamic pressure at each integration step and then reducing the thrust level by a percentage, typically 1 %, which is proportional to the rate of change of dynamic pressure, in the next integration step. This algorithm works well but requires user experience to set the thrust level reduction value on the first few runs of the program for each new vehicle case.

5.2.1.7 Computer Requirements

The trajectory programs have been written in Microsoft Quick Basic, Version 4.5. The programs can be run on any IBM AT or compatible personal computer (PC), using the Microsoft Operating System, Version 3.2 or higher. Two versions of each

program are available: Version 1 produces all outputs on the computer screen and these can be read to a computer file in real time, for subsequent preparation of graphs using a graphics programme like Harvard Graphics; Version 2 gives all outputs on a line printer, to provide a permanent record. A typical run duration is 150 seconds on a PC equipped with an INTEL 386 Processor with a Maths coprocessor, running at 25 MHz. However, because the programs cannot optimise a trajectory, but can only simulate a user-defined trajectory, in practice, many runs (typically up to 30 runs), are needed for the user to converge to an optimum trajectory.

5.2.2 Aerodynamic Analysis Computer Codes

The aerodynamic coefficients as functions of Mach number and incidence angle for each of the candidate vehicle configurations were calculated using the NLR AERO code (Reference 3) for the speed range up to Mach 1.3 and the SHABP code (Reference 4) for the speed range Mach 1.3 to 25. Both these codes are well developed and are accepted industry standards.

5.2.3 Propulsion Analysis Computer Codes

Similar to the situation concerning the availability of suitable trajectory analysis codes, the author found at the start of this research in 1989, that no suitable propulsion analysis codes were available in Europe for air-breathing propulsion. The available performance codes for rocket propulsion were found to comprise data from existing rocket engines only. The author therefore had to develop his own generalised propulsion performance algorithms for rocket propulsion, based on input values of the combustion chamber pressure and mixture ratio (See Chapter 5.2.1.4). For air-breathing propulsion, performance algorithms for hydrogen-fuelled turbojets, ramjets, scramjets and air-ejector engines became available through European industry studies sponsored

by ESA during this research period. These algorithms gives tables of the thrust, fuel flow and specific impulse as functions of Mach Number, altitude, equivalence ratio and vehicle incidence angle. These data have been used in this research.

5.2.4 Vehicle Mass Analysis Model

The author realised early in this research, that to be able to calculate the payload mass into orbit for any launcher, that simple analytical equations could be used, but only if accurate values (which are difficult to calculate) of the following performance parameters were used: the total velocity increment (ΔV); the average specific impulse (I_s); the vehicle dry mass (M_v). The significance of these parameters is illustrated by the simple equation below:

$$\frac{M_{pl}}{M_l} = \left(e^{-\frac{\Delta V}{I_s g_0}} - \frac{M_V}{M_l}\right)$$

This equation shows that to maximise the payload ratio M_{pl}/M_l, that the velocity increment ΔV must be minimised, the specific impulse I_s must be maximised and most importantly, that the vehicle net mass M_v must be minimised.

Now, for the purposes of vehicle comparative studies, what are the possibilities to achieve these requirements? We can with high confidence, minimise the velocity increment by flying along an optimised ascent trajectory with aerodynamically efficient vehicles, for which we have well developed trajectory analysis and aerodynamic analysis tools. Similarly, we can maximise the specific impulse by using the best available propulsion systems whose performance we can accurately predict because we also have good propulsion analysis capabilities. However, to minimise the vehicle dry mass, we must be able to accurately calculate the vehicle mass.

The vehicle mass depends on its size, the selected materials of construction **and most importantly, on the designer's skill to minimise mass.** Thus, the only accurate method to establish vehicle mass, is to undertake a detailed design of the vehicle. Clearly, such detailed designs cannot be established during vehicle comparative and feasibility studies. Instead, for such studies, there are two other methods by which the vehicle mass be may be estimated. The are:

- by a statistical/analytical method using data from existing launch vehicles, modified, as necessary, to account for mass reductions made possible by the use of advanced materials.
- by adopting the vehicle mass ratio as a parameter. Then, to give a point of reference within the parameter range, to seek for nominal values of the Vehicle Mass Ratio for each vehicle type from other vehicle system studies, where the vehicle net mass has been accurately calculated from detailed engineering design.

This second approach has been adopted in this research because Vehicle Net Mass ratio values based on detailed engineering design were indeed found for most of the vehicle types that have been studied in this research. The reference studies from which this data were derived, are discussed in Chapter 5.19: Comparison of the Calculated Performance Results with those from other System Studies.

5.2.5. Graphical Presentation of Launcher Performance

Having decided to adopt the Vehicle Mass Ratio as a parameter because we do not know its exact valve, the next problem was to devise a simple, standard graphical method that would allow to show clearly the absolute achievable limits of the Payload Mass Ratio for any launcher, and thus to be able to compare easily the performances of all the candidate launchers. Such a graphical method has been devised by the author and is based on the following simple analytical equations for SSTO and TSTO vehicles respectively, as demonstrated below;

For SSTO vehicles, the Orbital Mass Ratio M_o/M_l, the Vehicle Mass Ratio M_v/M_l and the Payload Mass Ratio M_{pl}/M_l are related by the equation:

$$\frac{M_o}{M_1} = \frac{M_v}{M_1} + \frac{M_{pl}}{M_1} \qquad (1)$$

For TSTO launchers, the relationship is given by:

$$\frac{M_o}{M_1} = \frac{M_{v2}}{M_1} + \frac{M_{pl}}{M_1} \qquad (2)$$

where suffix 2 denotes Second Stage parameters.

Adding the First Stage Vehicle Mass Ratio M_{v1}/M_l to both sides of Equation (2) gives:

$$\frac{M_0}{M_1} + \frac{M_{v1}}{M_1} = \frac{M_{v2}}{M_1} + \frac{M_{pl}}{M_1} + \frac{M_{v1}}{M_1} \qquad (3)$$

The Overall Vehicle Mass Ratio M_v is:

$$\frac{M_v}{M_1} = \frac{M_{v1}}{M_1} + \frac{M_{v2}}{M_1} \qquad (4)$$

Therefore, substituting (4) into (3) gives:

$$\frac{M_o}{M_1} + \frac{M_{v1}}{M_1} = \frac{M_v}{M_1} + \frac{M_{pl}}{M_1} \qquad (5)$$

Equation (5) for TSTO vehicles is now analogous to Equation (1) for SSTO vehicles.

Thus, from Equations (1) and (5), the absolute limits of the Payload Mass Ratio for both SSTO and TSTO vehicles respectively can be determined as follows:

For SSTO Vehicles:

The value of the Orbital Mass M_o is calculated by the ascent trajectory program and is therefore known. The launch mass M_l is also known, allowing the value of the Orbital Mass Ratio M_o/M_l to be calculated. Using Equation (1), if we now set the the Vehicle Mass Ratio M_v/M_l to zero, the absolute maximum value of the Payload Mass Ratio M_{pl}/M_l is then equal to the Orbital Mass Ratio M_o/M_l. Similarly, if we set the Payload Mass Ratio M_{pl}/M_l to zero, the absolute maximum value of the Vehicle Mass Ratio is then equal to the Orbital Mass Ratio. The straight line joining these two values is then the locus of all SSTO vehicle Payload Mass Ratio values, ranging from its absolute maximum value, through zero payload, to negative values.

For TSTO Vehicles:

The value of the Orbital Mass M_o is calculated from the trajectory program. The Launch Mass M_l is also known, allowing the value of the Orbital Mass Ratio M_o/M_l to be calculated. Thus, for any given value of the First Stage Vehicle Mass Ratio M_{v1}/M_l, the value of the left-hand side of Equation (5) can be calculated. Then, using Equation (5), if we now set the the Vehicle Mass Ratio M_v/M_l to zero, the absolute maximum value of the Payload Mass Ratio M_{pl}/M_l is then equal to the left-hand side $(M_o/M_l + M_{v1}/M_l)$. Similarly, if we set the Payload Mass Ratio M_{pl}/M_l to zero, the absolute maximum value of the Overall Vehicle Mass Ratio M_v/M_l is then equal to the left-hand side $(M_o/M_l + M_{v1}/M_l)$. The straight line joining these two values is then the locus of all TSTO vehicle Payload Mass Ratio values, ranging from its absolute maximum value, through zero payload, to negative values.

Thus, the same standard graphical presentation can be conveniently used to display the performance of both SSTO and TSTO vehicles. This graphical method, although beguiling because of its simplicity, is a powerful tool to display the limits of launcher performance. It has been used consistently in the Thesis to display the individual absolute performance limits of the candidate launchers and then also to compare their performances. A sketch of the generalised graph is given below.

Standardised Graphical Presentation of Results

Payload Mass Ratio Versus Vehicle Mass Ratio

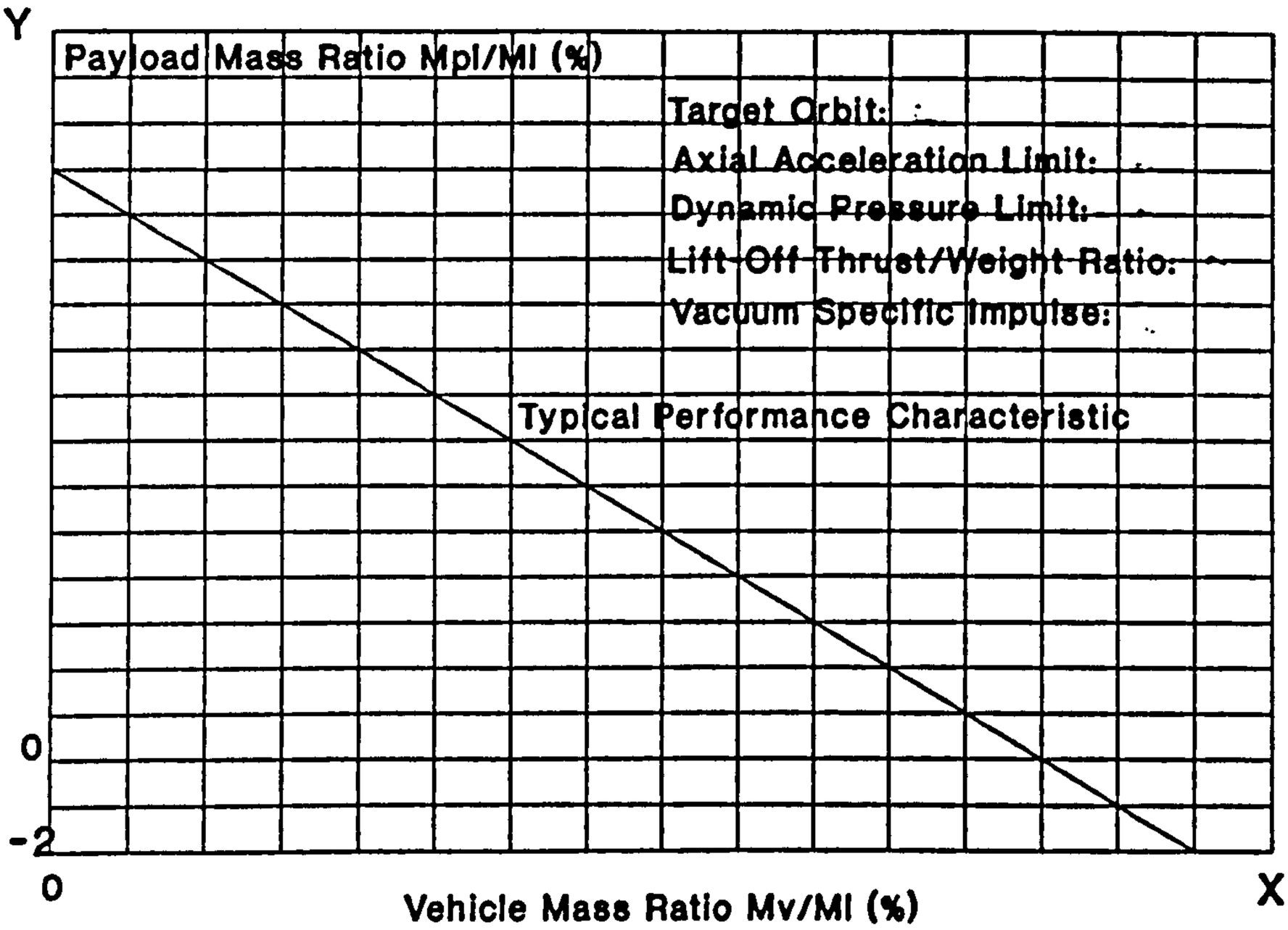

5.3 Reference Mission

The reference mission that has been selected for this performance analysis is a typical payload-delivery mission to a low Earth orbit. The launch site is the Kennedy Space Centre (28.5 degrees north). The target orbit is a low Earth circular orbit, at an altitude of 200 km and an orbital inclination of 28.5 degrees. This orbit is achieved by a circularisation manoeuvre at the apogee of an elliptic transfer orbit with a perigee altitude of 100 km, an apogee altitude of 200 km and an inclination of 28.5 degrees. Thus, the launch azimuth is directly East, allowing to benefit fully from the Earth's rotation to minimise the required total velocity increment. This reference mission is also the minimum energy mission of the three identified orbits of interest for future launchers as presented in Chapter 3.2, and thus yields the maximum payload mass ratio performance for each of the candidate launchers. Smaller payload mass ratios will of course result for the other two higher energy missions: the Space Station Freedom mission (450 km x 450 km x 28.5 degrees), the Sun-synchronous polar mission (850 km x 850 km x 97 degrees) and these reduced values can then be readily calculated.

For this target orbit:

- the perigee velocity ΔV_{pt}, calculated from Equation 47 is 7879 m/s.
- the velocity increment required to circularise this orbit, calculated from Equation 48, is 30 m/s.
- Earth's rotational velocity at the latitude of the launch site ΔV_{rot}, calculated from Equation 51 is 407 m/s.

5.4 Standard Mission Design Criteria

For the purposes of a fair comparison between the candidate launchers, the following standard mission design criteria were adopted for all the candidate launchers:

- the launch mass;

- the maximum axial acceleration;
- the maximum dynamic pressure.

Launch Mass: Because of the scale effect of the launch mass on payload performance (the larger the launch mass, the larger the payload mass), it was deemed essential to select a standard value of the launch mass for all the launchers. The selected launch mass used in this comparative performance is 350 tonnes. This value was assessed as being large enough to yield a design aim payload mass target of 7 tonnes, which is 2 % of the launch mass. A 2 % Payload Mass Ratio is the current performance capability of expendable launchers and is assessed by the author to be a realistic design aim for reusable launchers.

Maximum Axial Acceleration: A standard value of 3g is selected, which is a typical maximum value for manned launchers and which also allows to reduce structural mass because of the lower acceleration loads on the vehicle.

Maximum Dynamic Pressure: A standard value of 85 kPa is selected. Although this is a rather high value for current expendable rocket-propelled vehicles, which typically have design maximum dynamic pressures in the range 30 kPa to 50 kPa, reusable launchers using air-breathing propulsion, require higher dynamic pressures to improve their engine performance and to reduce engine size. For reusable rocket-propelled vehicles, these can accommodate this higher dynamic pressure and associated heat load on ascent because they must have thermal protection systems which are sized for the higher heat loads of re-entry and descent.

All other mission design criteria like lift-off thrust/weight ratio, staging inertial velocity, were selected for each launcher type based on optimisation studies, using the trajectory models to maximise the payload mass ratio.

5.5 Performance of Reusable Launcher No.1: SSTO-R-VLVL

This launcher is a single-stage-to-orbit, rocket-propelled, vertically launched and vertically landed vehicle.

5.5.1 Vehicle Configuration

Figure 5.1 shows the configuration and overall dimensions of the vehicle, sized for a payload mass of 7000 kg and a lift-off mass of 350000 kg. This configuration is identical to the MBB Beta 2 vehicle described in Reference 10, and has been adopted in this research for comparative reasons.

The vehicle configuration has been made as simple as possible to minimise manufacturing costs. It comprises a cylindrical body which houses the propellant tanks and rocket engines. The payload is positioned on top of the vehicle under a conical aerodynamic fairing, which is longitudinally split. The fairing is not jettisoned, because this is a reusable launcher. Instead, it is opened up in space to release the payload by rotating the two longitudinal halves around hinges located at the base of the fairing. The fairing is then closed again before re-entry of the vehicle for a ballistic descent to Earth. This vehicle re-enters the atmosphere in a tail-first orientation, using a heat shield around the engine bay to absorb the re-entry heating. This tail-first reentry mode has been selected to avoid the longitudinal aerodynamic stability problem which results from the centre of pressure being well forward of the centre of gravity of the vehicle, which is far-aft because of the high mass of the rocket engines which are mounted at the aft end of the vehicle. At an altitude of about 10 km, the rate of descent is controlled by operating the rocket engines to provide a braking thrust. Figure 5.2 shows the zero-lift drag coefficient C_{do} as a function of Mach number. This data has been used in the trajectory model;

5.5.2 Ascent and Descent Trajectories

The ascent trajectory programs have been used reiteratively, to find a trajectory that yields a maximum value of the injected mass into the reference transfer orbit, whilst ensuring that only simple and practical flight operational procedures are necessary. This effort has resulted in selecting a simple ascent trajectory comprising two non-lifting flight phases: Flight Phase 1 comprises vertical flight for 10 seconds to gain a high enough altitude for launch range safety; Phase 2 comprises flight at a variable, optimised, pitch-over rate at an azimuth angle of 90 degrees (due East). This pitch-over rate has been optimised so that the vehicle is flying horizontally and at the required inertial velocity when the perigee altitude of the transfer orbit (100 km) is reached. The optimisation has been done by converging to the final trajectory by successive, finer and finer modifications of the trajectory in many successive runs of the program. The required flight path angle profiles are achieved by thrust vectoring. Constraints imposed on the flight are the adopted standard values: a maximum axial acceleration of 3g (29.43 m/s2); a maximum dynamic pressure of 85 KPa. These constraints are achieved by engine throttle control.

5.5.3 Performance Results

The performance results are shown graphically in Figures 5.3, 5.4 and 5.5.

Figure 5.3 shows the Payload Mass Ratio (M_{pl}/M_l) versus the Vehicle Mass Ratio (M_V/M_l) with the Vacuum Specific Impulse as a parameter. This is the standard graphical method for presenting launcher performance that has been adopted in this Thesis, as described in Chapter 5.2.5.

Examination of Figure 5.3 shows that:
- the Payload Mass Ratio is a linear function of the Vehicle Mass Ratio;
- the Payload Mass Ratio is highly sensitive to the specific impulse. For example, if we select a Payload Mass Ratio of 2 %, which is a typical realistic value for current expendable launchers, and if we have a low performing propulsion system with a vacuum specific impulse of 400 s, it can be seen that the Vehicle Mass Ratio must not be more than 9 % (Point A on Figure 5.3). If however, we can use a higher performing propulsion system with a vacuum specific impulse of 440 s, it can be seen that the Payload Mass Ratio is doubled to 4%, for a modest increase in specific impulse of 10 %. (Point B on Figure 5.3). Thus, the high slope of the performance curves, shows that there is high potential to increase the payload mass ratio for this vehicle by increasing the propulsive performance. In fact, if we can guarantee a vacuum specific impulse value of 464 s, which is demonstrated in Chapter 6.1 as being a typical current maximum achievable value for advanced hydrogen/oxygen rocket engines, and if we can build a vehicle with a Vehicle Mass Ratio of 9 %, which is probably quite demanding, we could achieve a Payload Mass Ratio of 5.3 % for this vehicle (Point C on Figure 5.3). Alternatively, and probably much more realistically, if we keep our Payload Mass Ratio value at a modest value of 2 % and if we can achieve a vacuum specific impulse of 464 s, we can alleviate substantially the Vehicle Mass Ratio constraint of 9 % to a value of 12.3 % (Point D1 on Figure 5.3). Thus, point D1 on Figure 5.3 can be adopted as a realistic design point for this vehicle: 2 % payload ratio; 464 s vacuum specific impulse; 12.3 % vehicle mass ratio; 1.4 lift-off thrust/weight ratio; 3g axial acceleration limit; 85 kPa dynamic pressure limit.

To show the detailed performance results for this vehicle and to demonstrate the capabilities of the trajectory programme,

the evolution of various parameters as functions of the flight time are shown in Figures 5.4A to 5.4J respectively: Altitude; Relative Velocity; Dynamic Pressure; Drag Force; Throttle Factor; Total Thrust; Relative Flight Path Angle; Angle of Attack; Mach Number; Instantaneous Total Mass; Axial Acceleration;

Figures 5.5A and 5.5B show the evolution with the flight time of the Gravity and Drag losses respectively. The Figures show clearly that the major loss is due to gravity force and that the drag loss is quite small. These results are expected, being typical for vertically launched, non-lifting ascent, rocket-propelled vehicles. The gravity loss amounts to 1200 m/s, which is 16.05 % of the ideal velocity increment of 7472 m/s. The drag loss is 120 m/s, which is 1.61 % of the ideal velocity increment. Thus, the total losses are 17.66 % of the ideal velocity increment.

Figure 5.1

Configuration of Reusable Launcher No.1: SSTO-R-VLVL

(Derived from Reference 10)

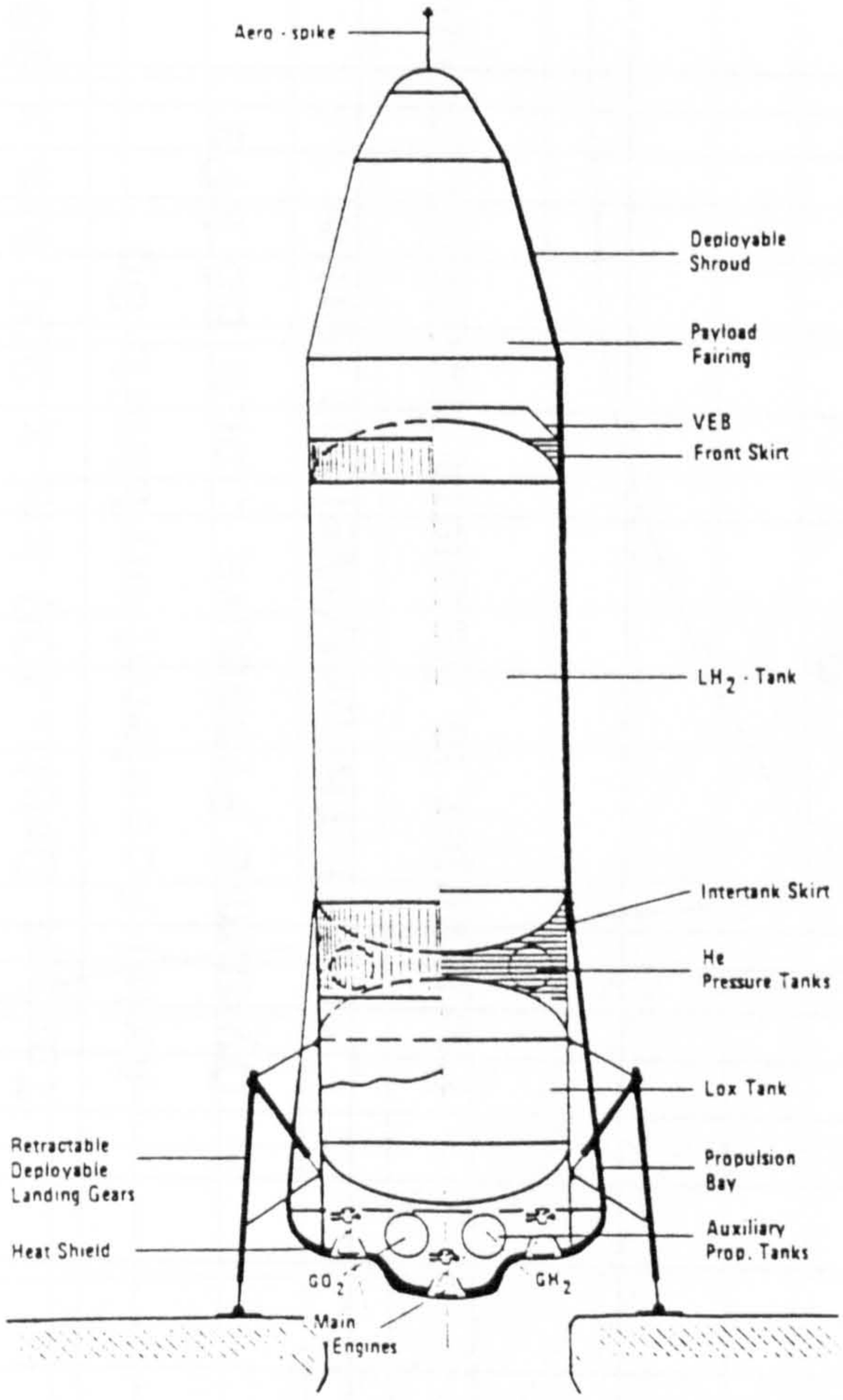

Height: 41.5 m.

Diameter: 8 m.

Lift-Off Mass: 350 tonnes

Lift-Off Thrust: 4900 KN

Aerodynamic Reference Area: 50.26 m^2

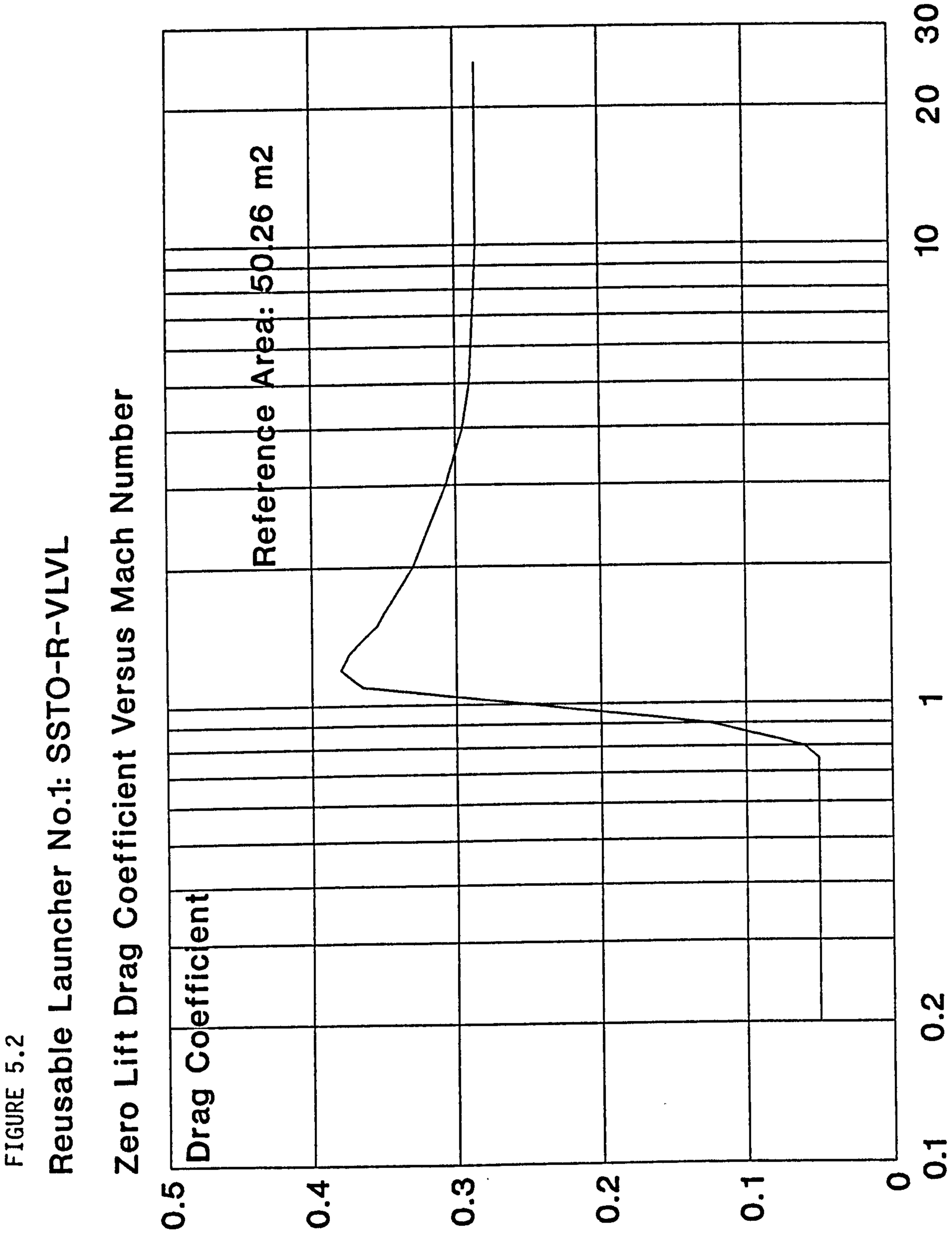
Zero Lift Drag Coefficient Versus Mach Number
Reusable Launcher No.1: SSTO-R-VLVL
Reference Area: 50.26 m2
Drag Coefficient
0.5
0.4
0.3
0.2
0.1
0
0.1
0.2
1
10
20
30
Mach Number

FIGURE 5.2

FIGURE 5.3

Reusable Launcher No.1: SSTO-R-VLVL

Payload Mass Ratio Versus Vehicle Mass Ratio

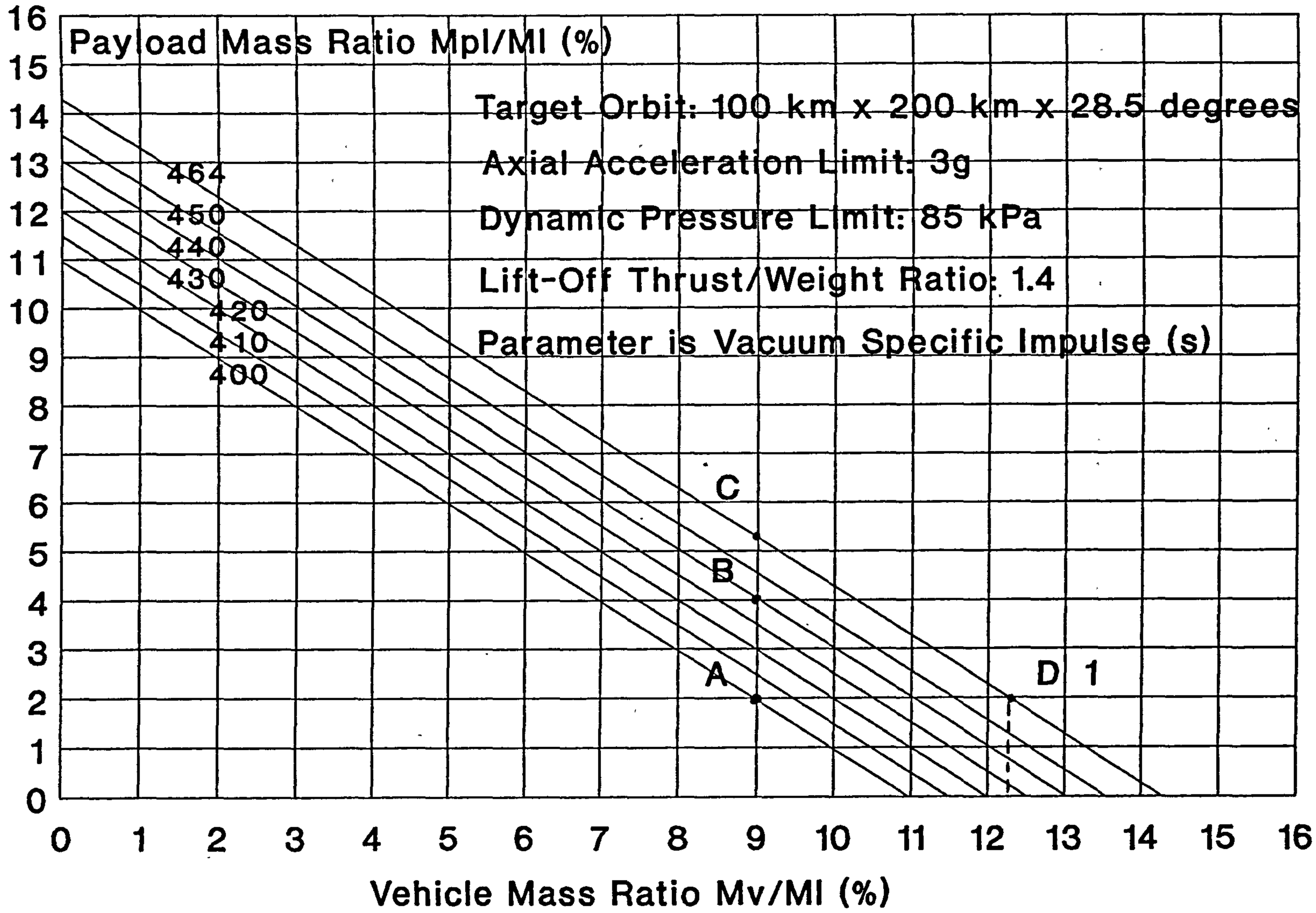

Figures 5.4A and 5.4B

Performance Results:

Reusable Launcher No.1: SSTO-R-VLVL:

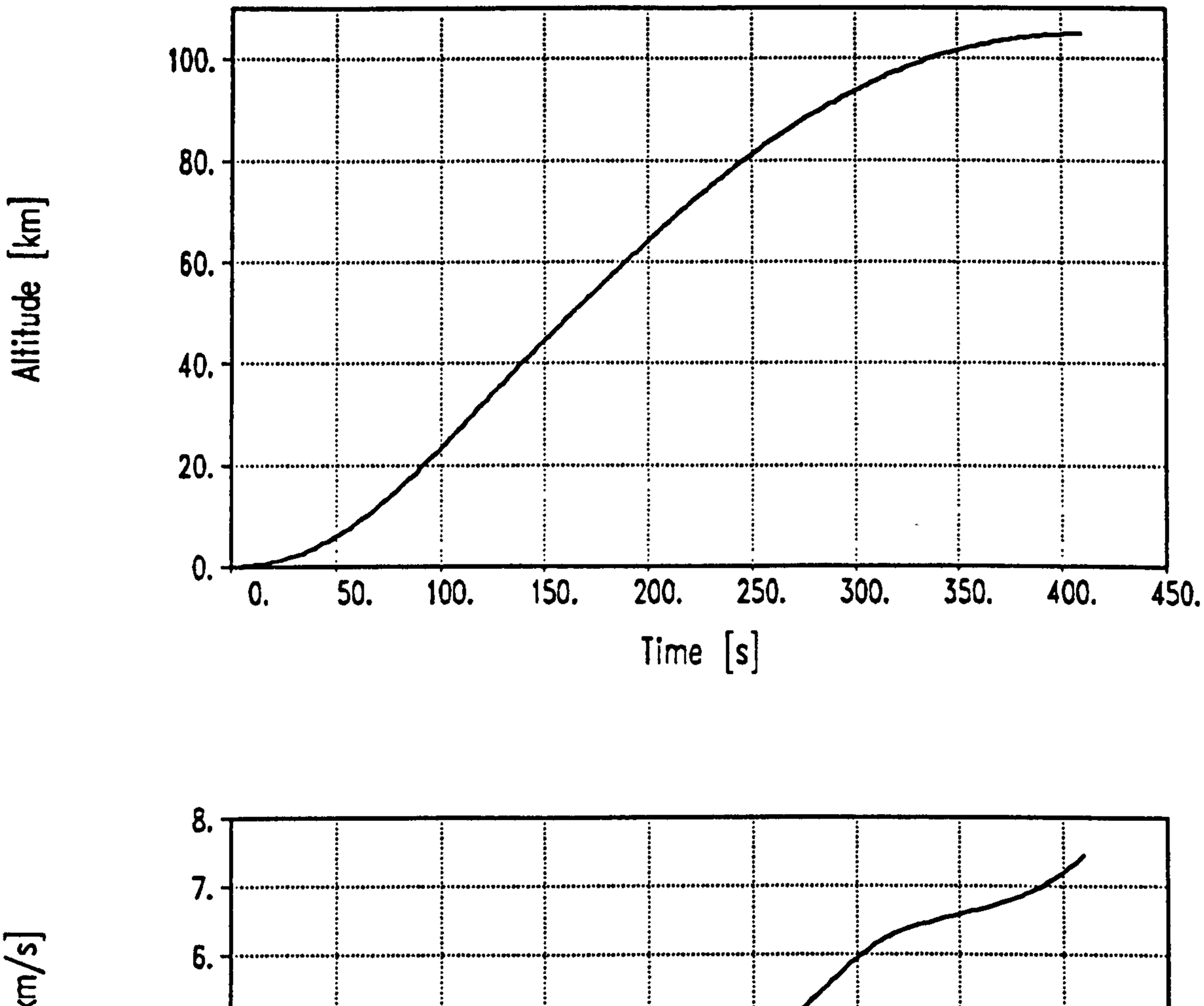

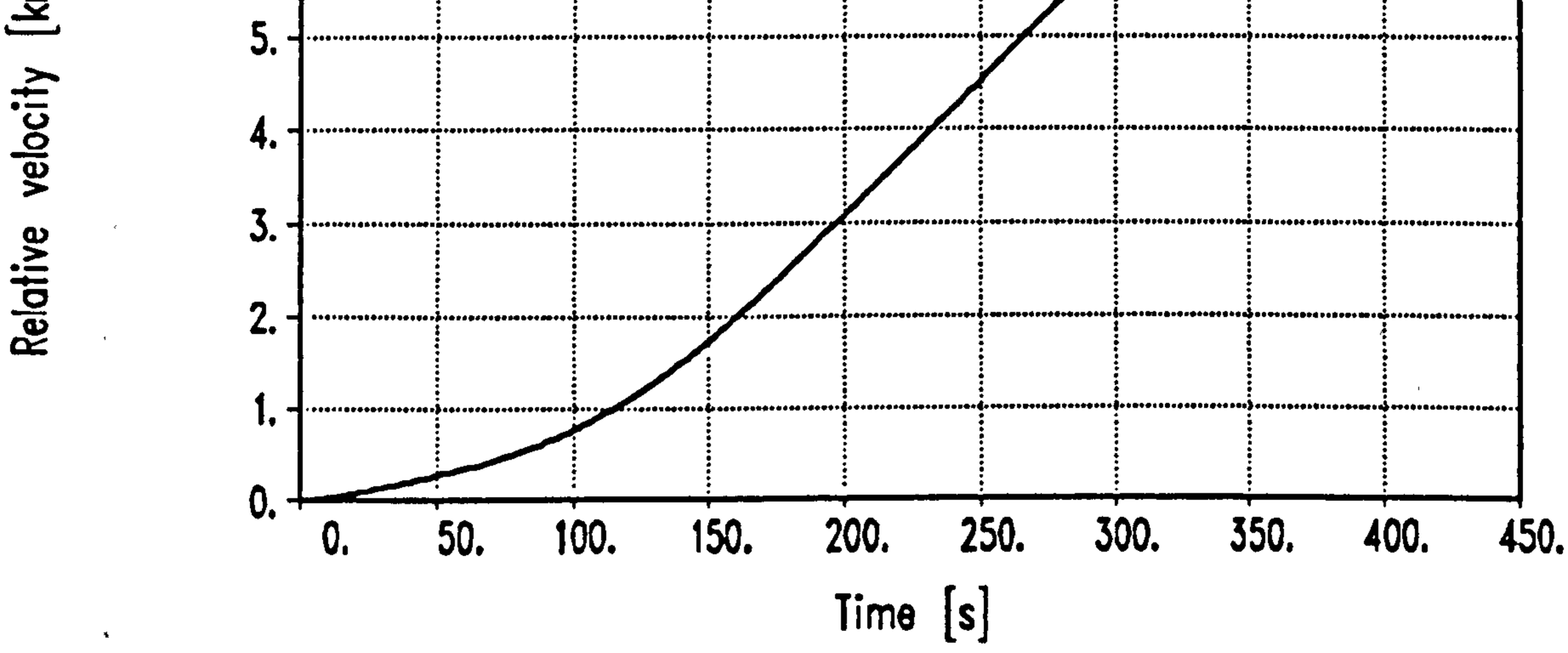

Figures 5.4C and 5.4D

Performance Results:

Reusable Launcher No.1: SSTO-R-VLVL:

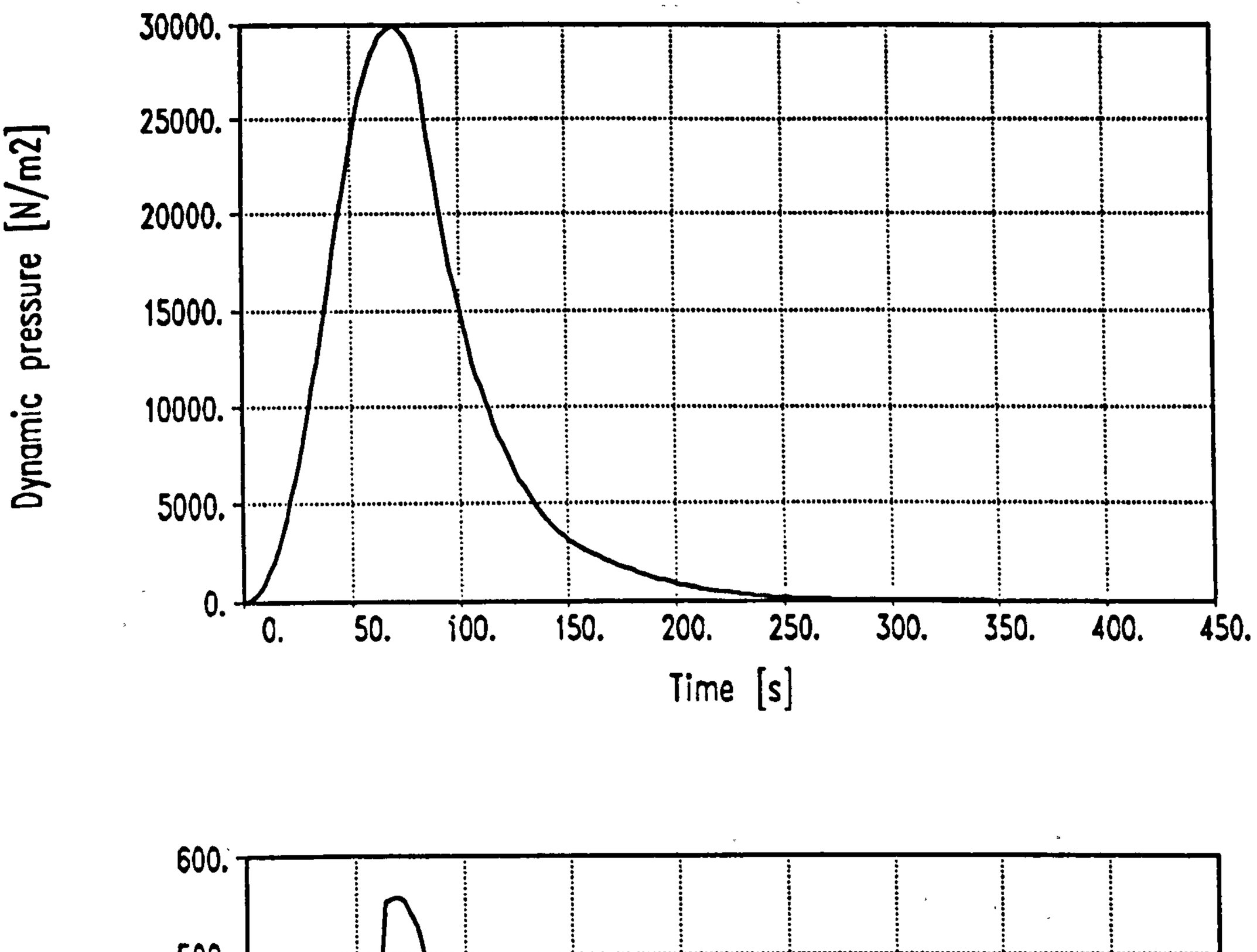

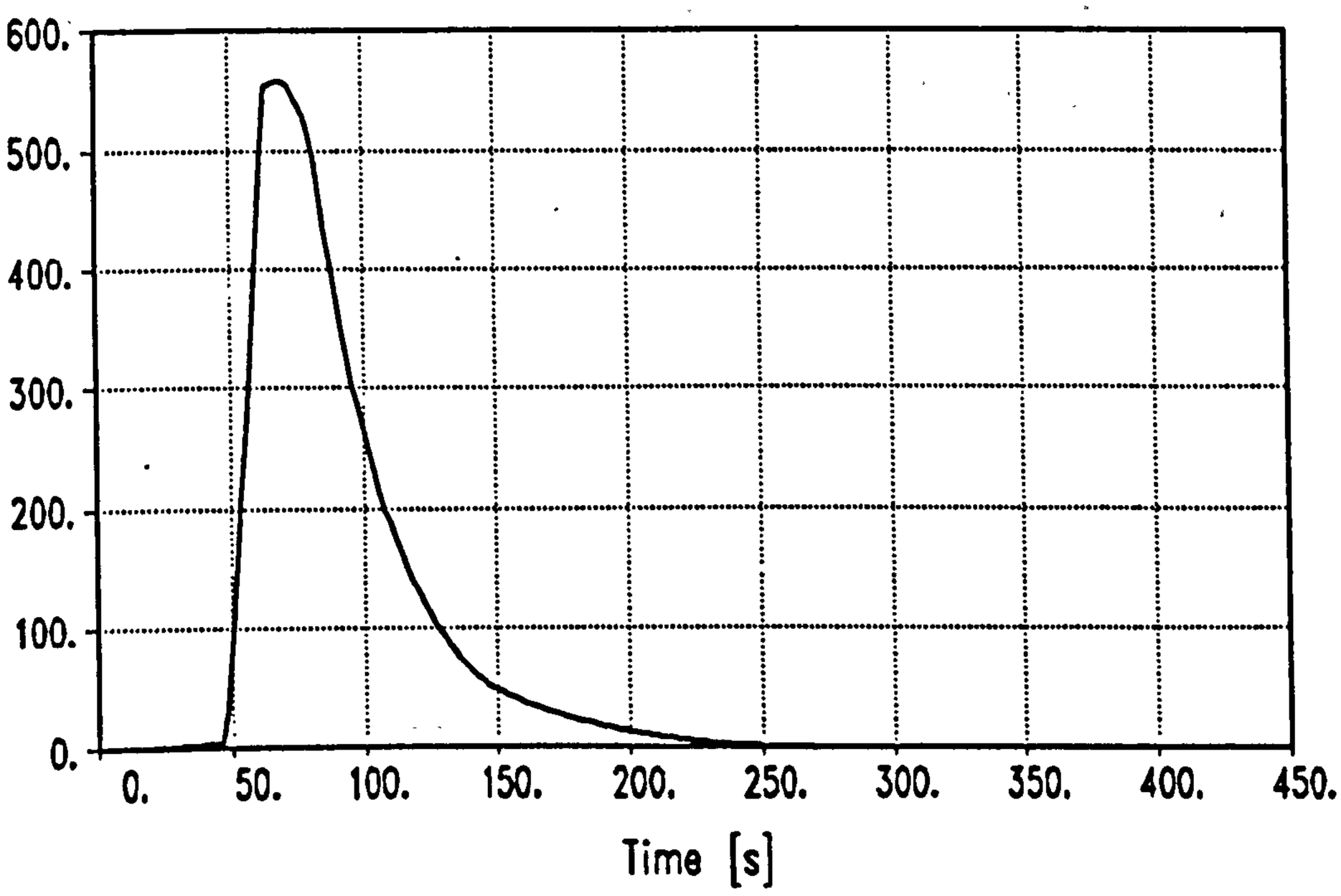

Figures 5.4E and 5.4F

Performance Results:

Reusable Launcher No.1: SSTO-R-VLVL:

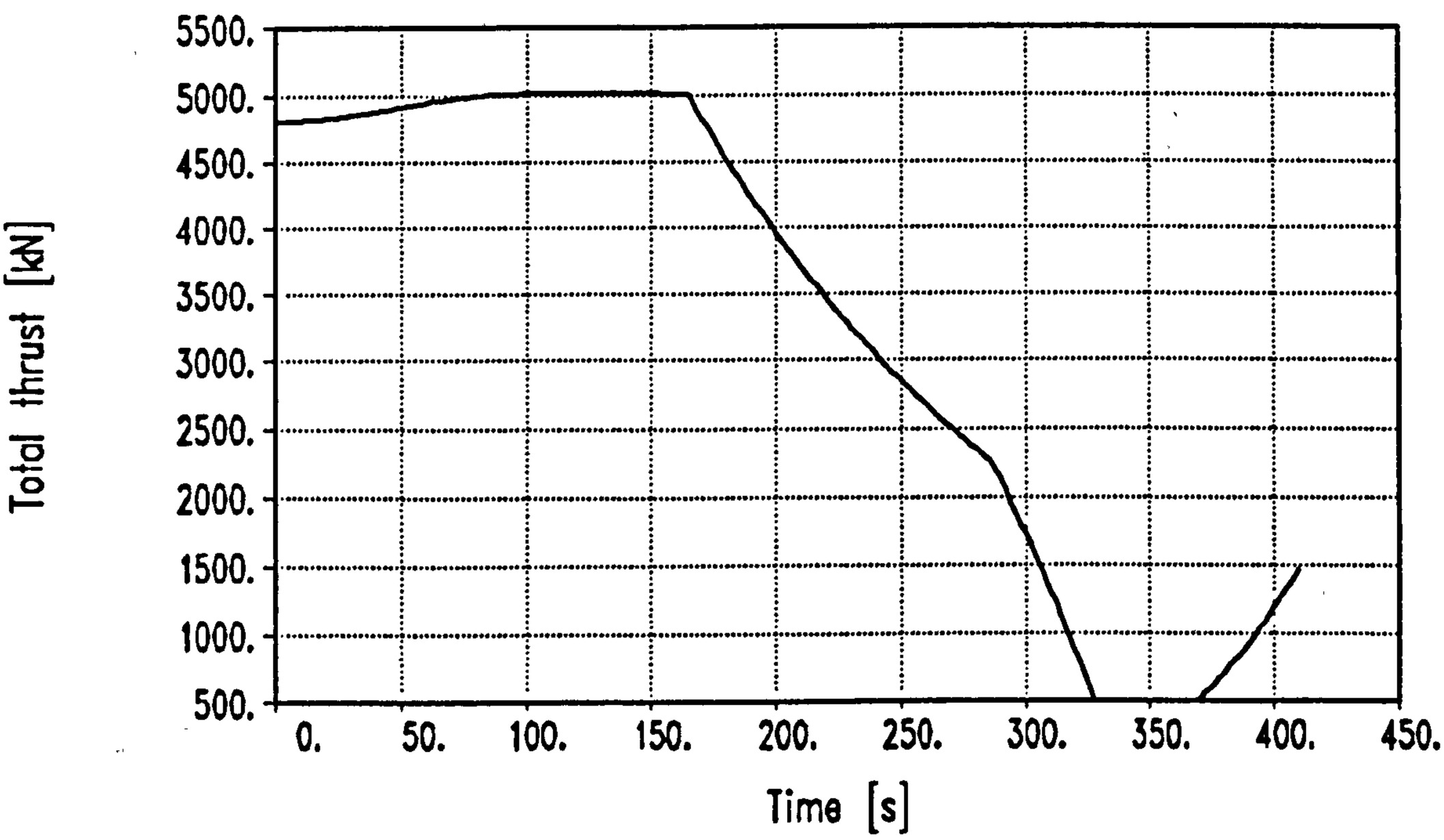

Figures 5.4G and 5.4H

Performance Results:

Reusable Launcher No.1: SSTO-R-VLVL:

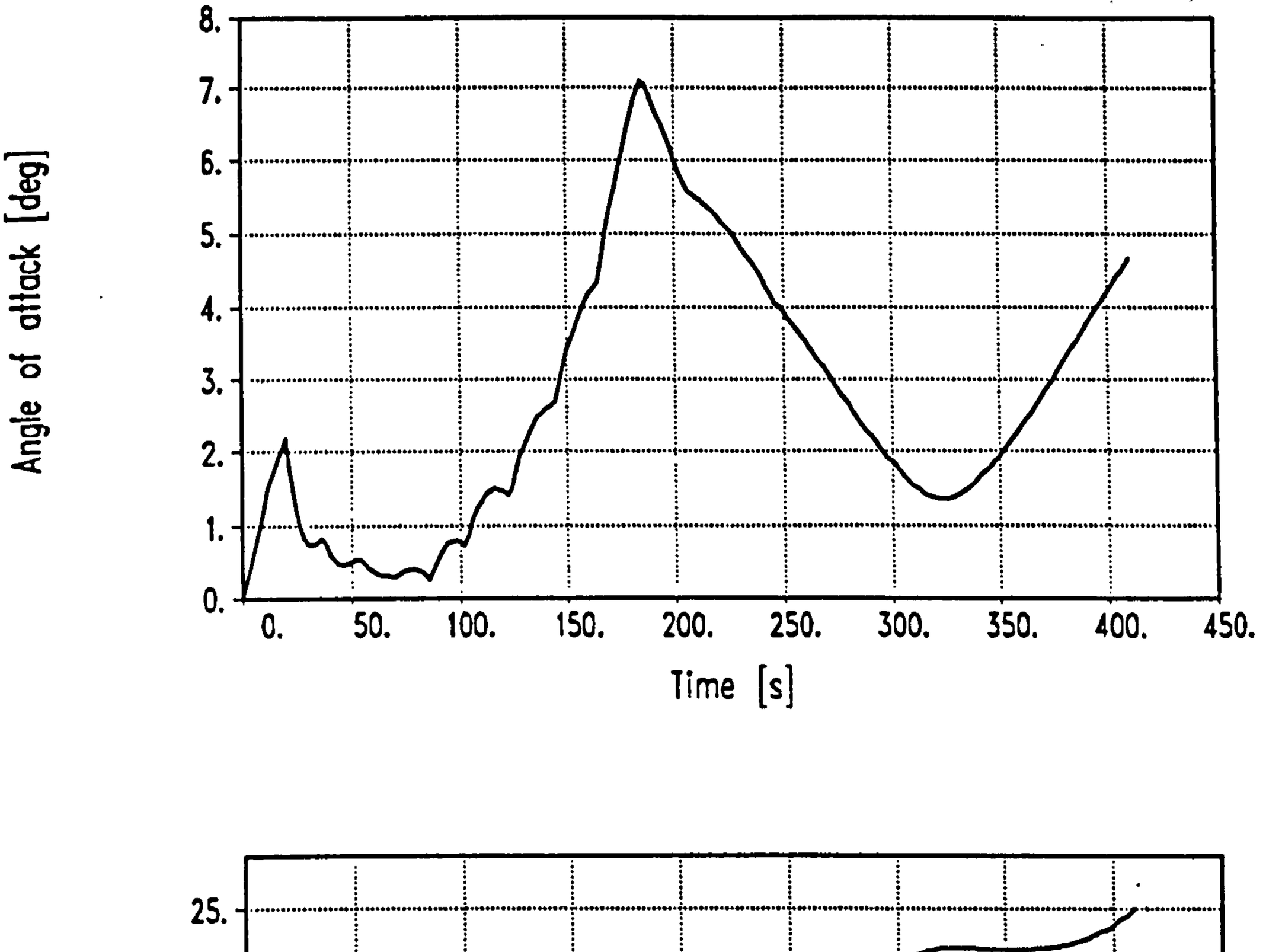

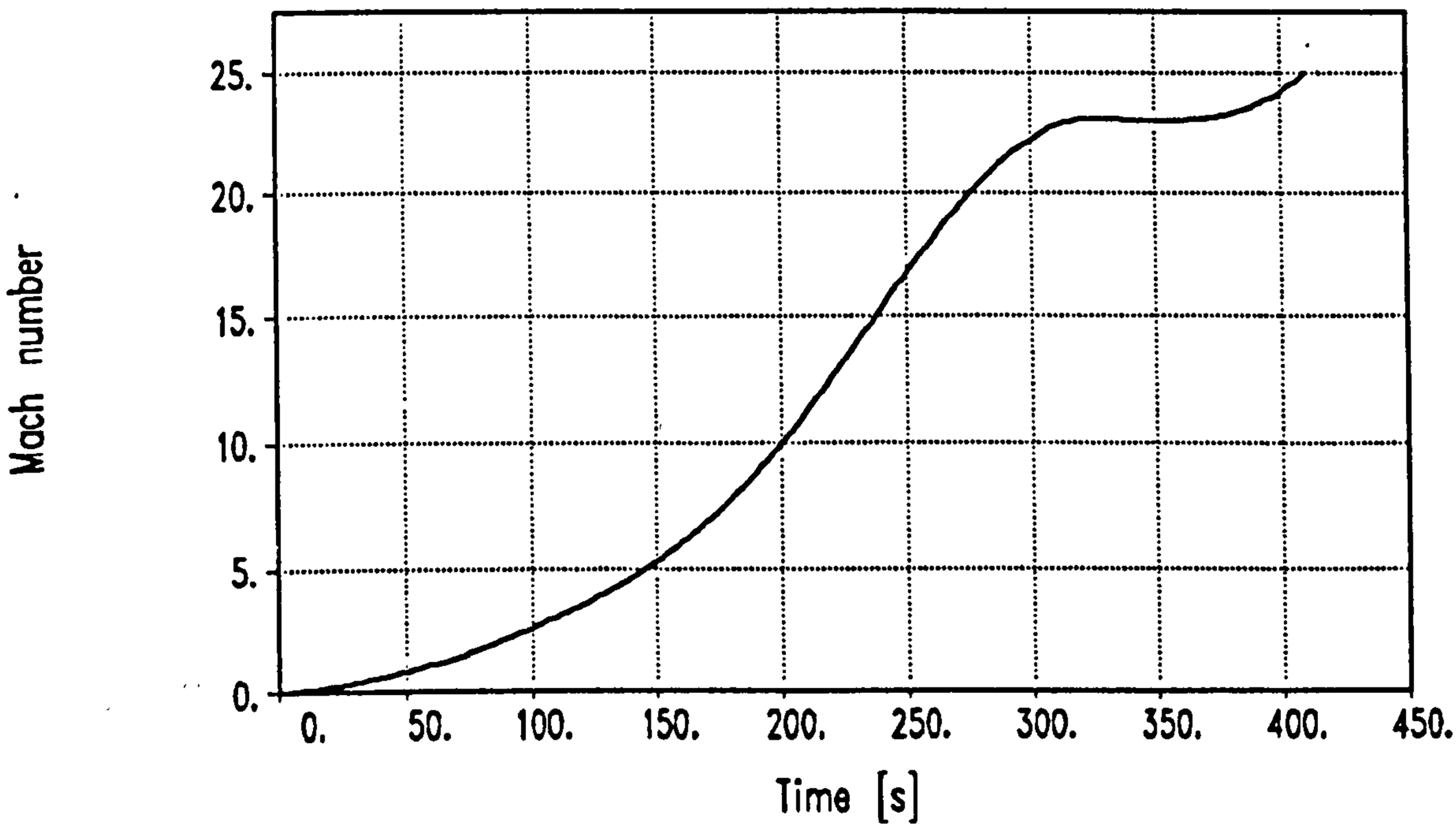

Figures 5.4I and 5.4J

Performance Results:

Reusable Launcher No.1: SSTO-R-VLVL:

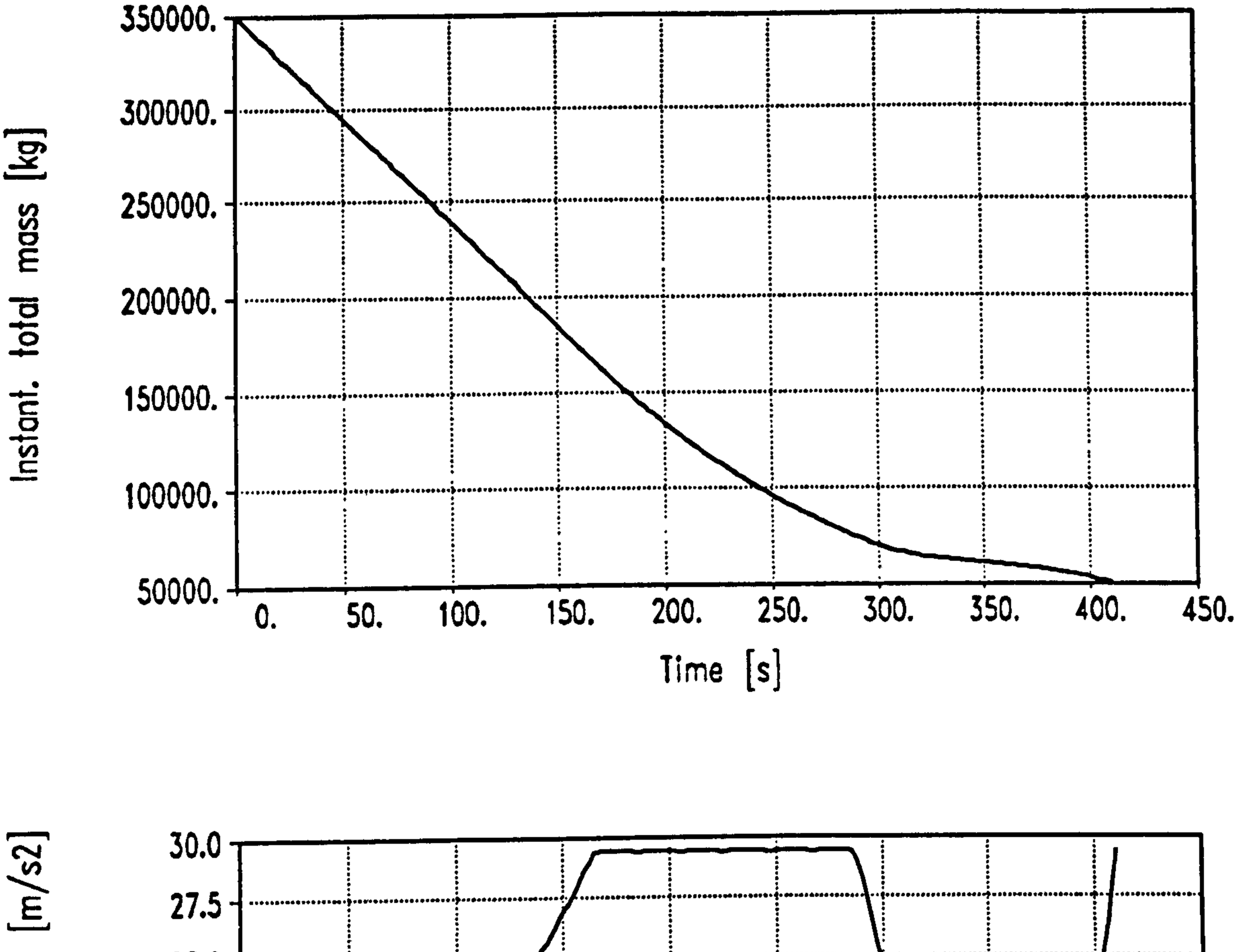

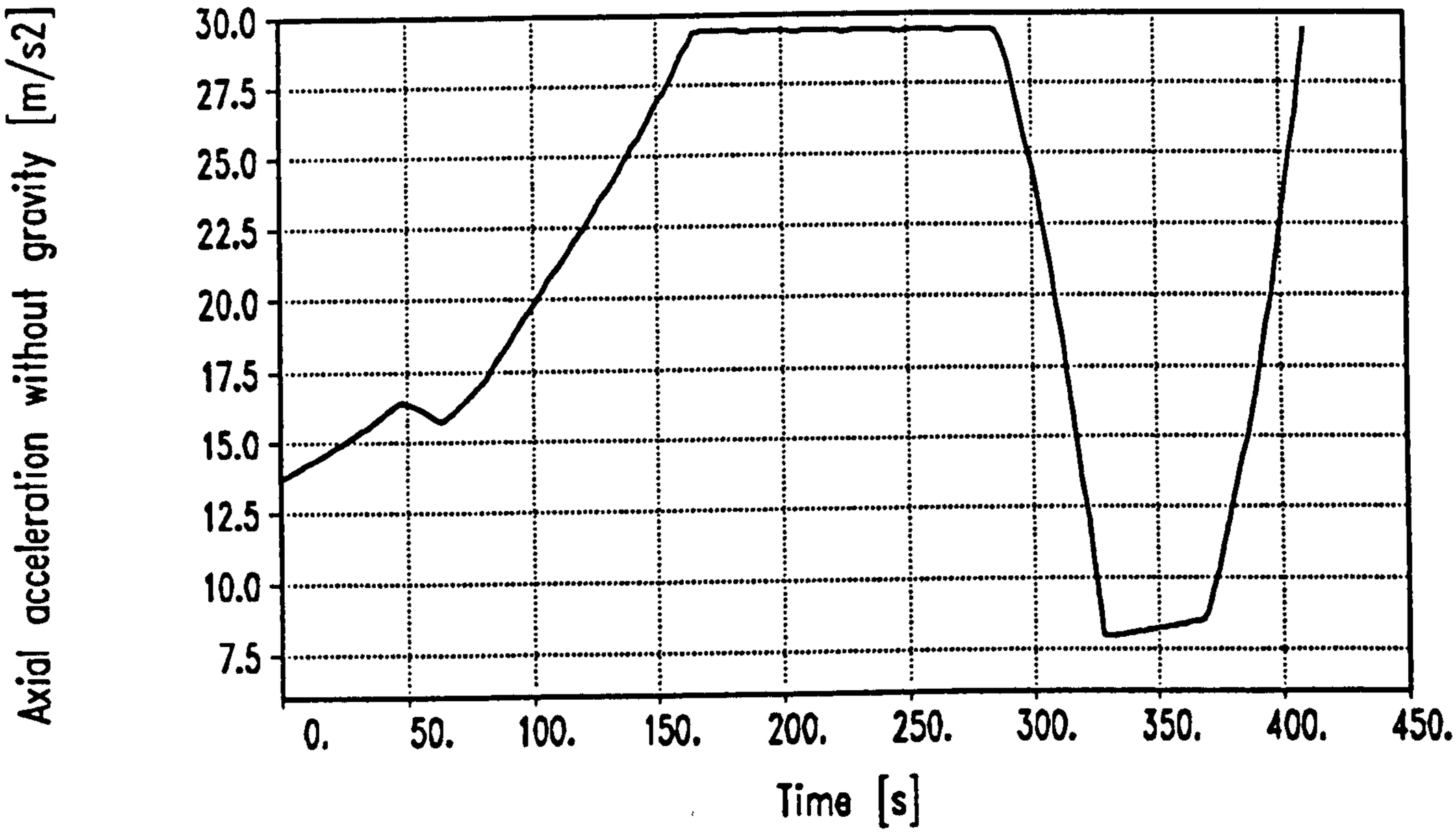

Figure 5.5A

Performance Results:

Reusable Launcher No.1: SSTO-R-VLVL:

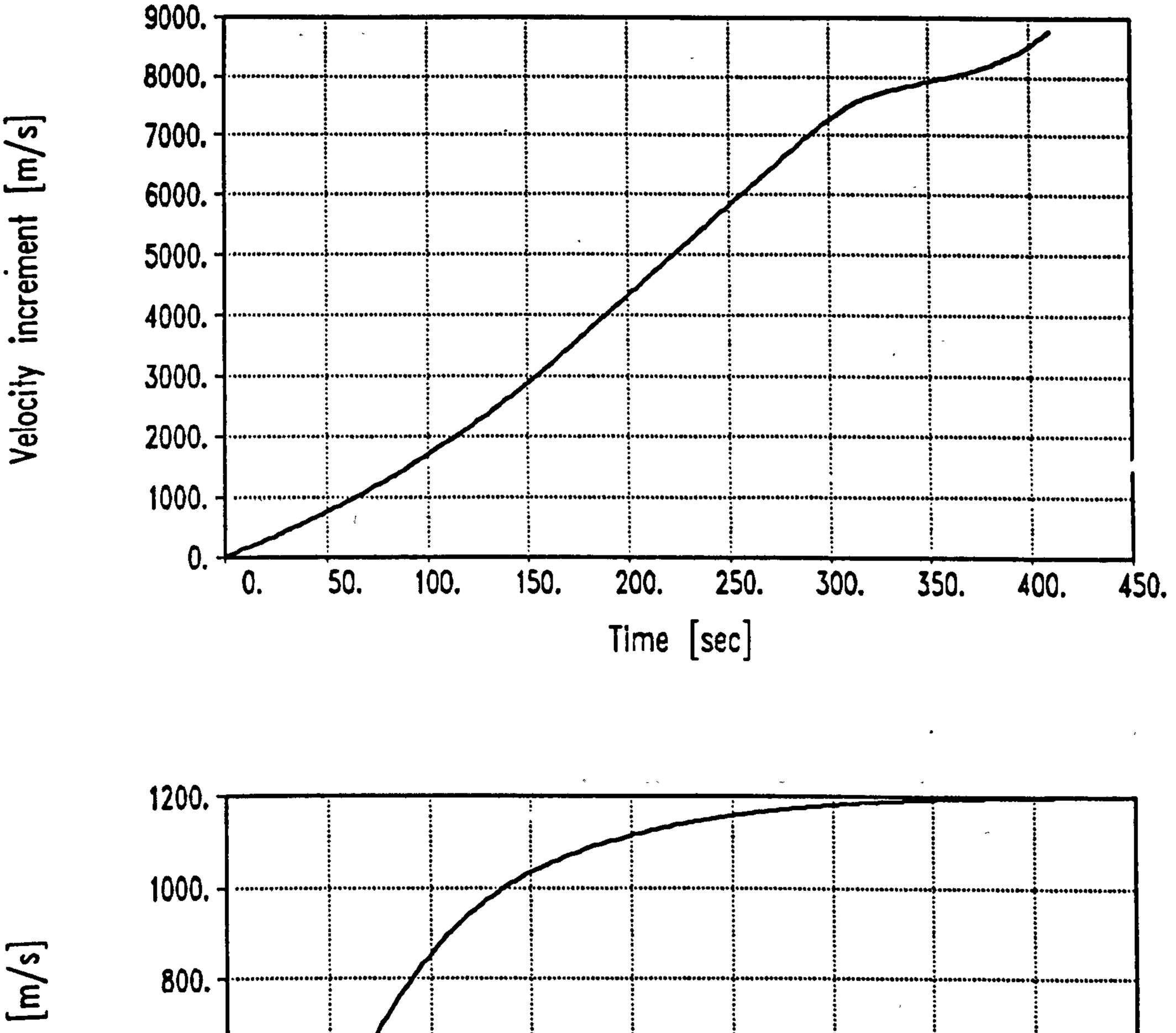

Figure 5.5B

Performance Results:

Reusable Launcher No.1: SSTO-R-VLVL

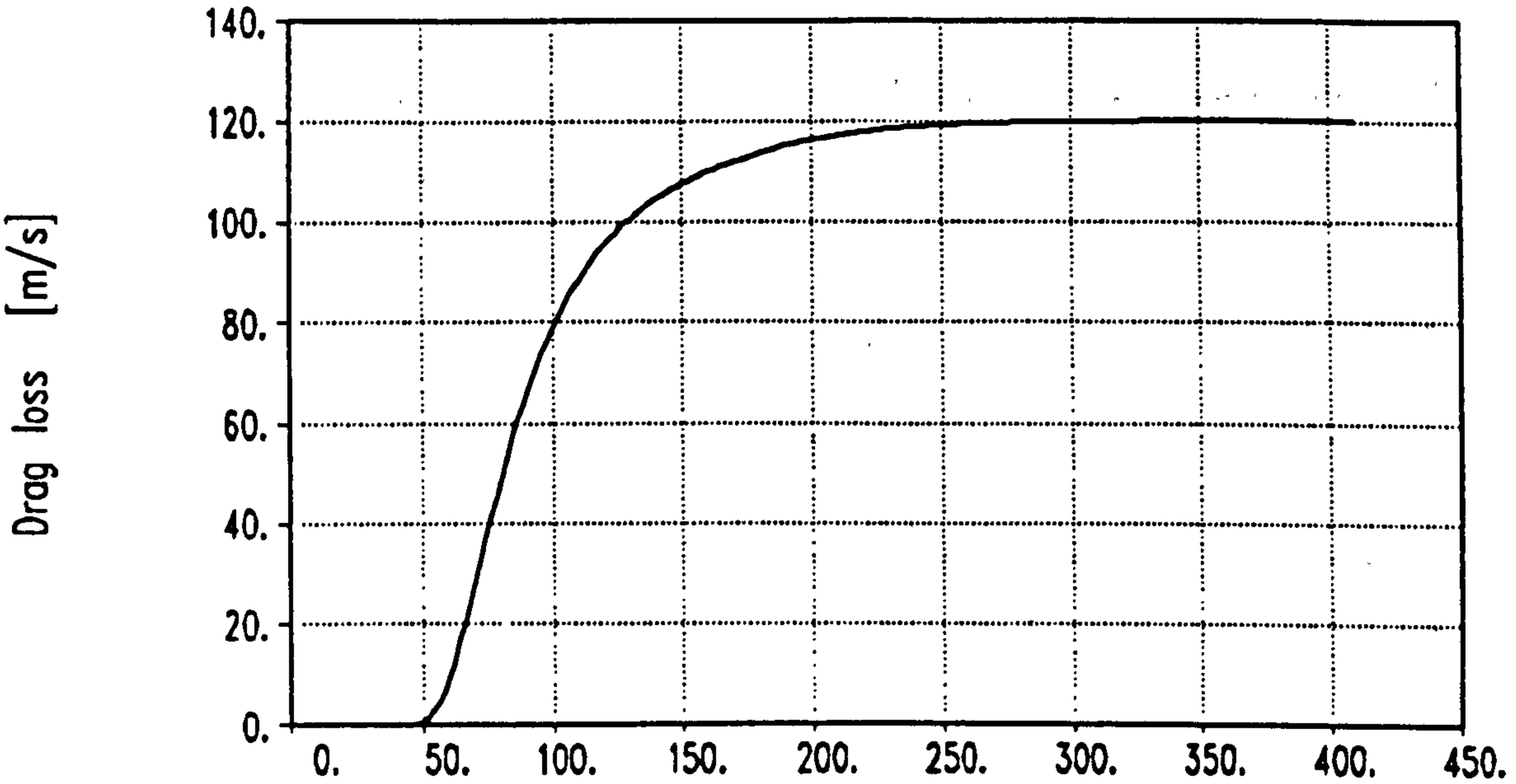

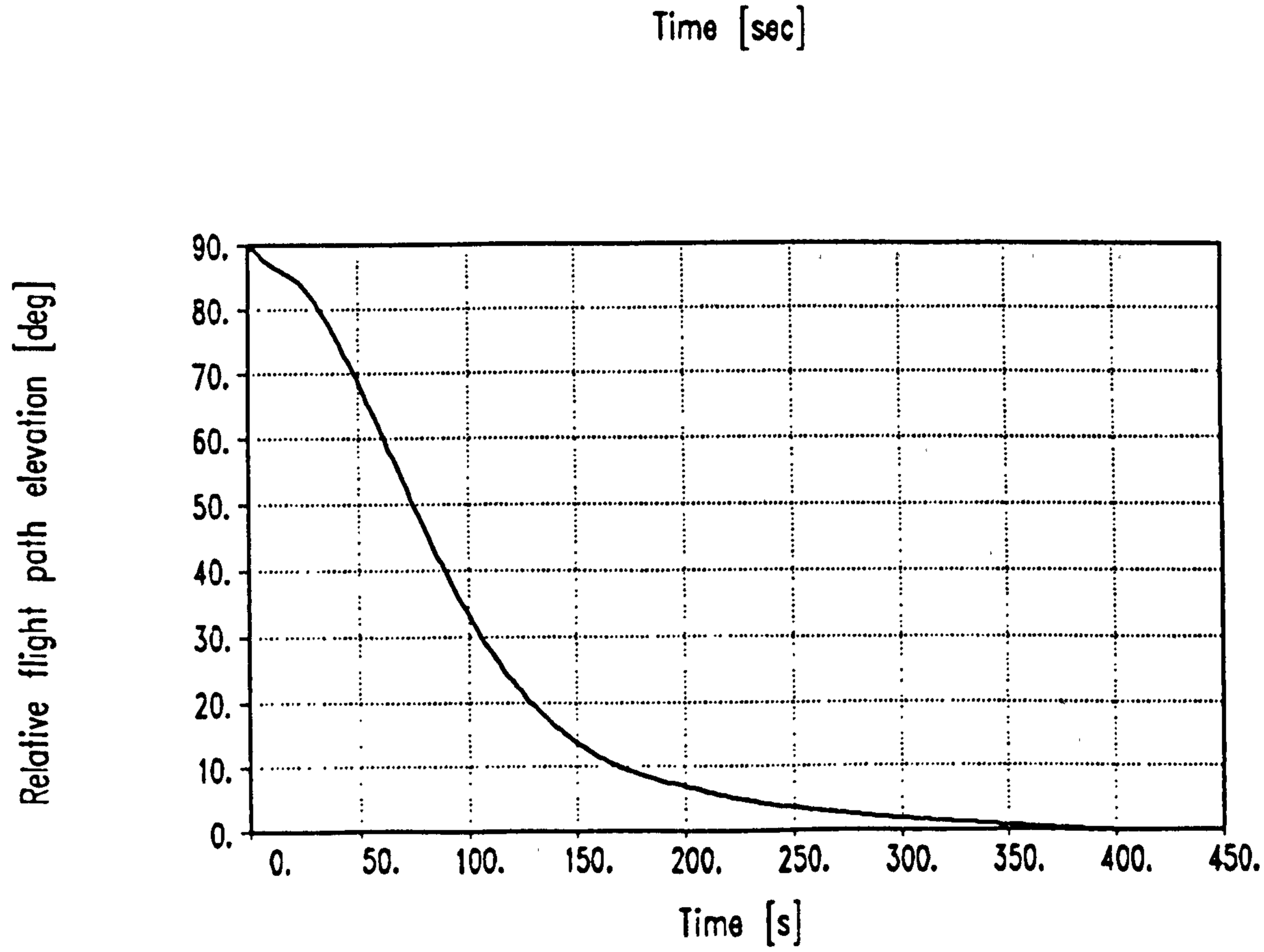

5.6 Performance of Reusable Launcher No.2: SSTO-R-VLHL

This launcher is a single-stage-to-orbit, rocket-propelled, vertically launched and horizontally landed vehicle.

5.6.1 Vehicle Configuration

Figure 5.6 shows the general configuration of the vehicle. This configuration is that used in Reference 11 and has been adopted in this research for comparative purposes.

The similarity of this vehicle to Vehicle No.1 is that it is also rocket-propelled and is launched vertically. The descent and landing modes are however, completely different. This vehicle reenters nose first and descends as a glider under aerodynamic control and lands horizontally on a runway. These differences necessitate a completely different vehicle configuration to that of Vehicle No.1, which reenters tail first and descends ballistically and lands vertically. This vehicle therefore needs a set of wings and aerodynamic control surfaces and control actuators for aerodynamic descent control. Additionally, the vehicle must be equipped with an integral wheeled undercarriage for horizontal landing. This undercarriage must be sized to accommodate the landing loads corresponding to the vehicle mass at re-entry. Therefore, to minimise aerodynamic drag, the configuration derived for this vehicle is a cylindrical body with a sharper nose and a higher slenderness ratio to that of Vehicle No.1. The wings, sized for the landing case, are a double-delta shape and are blended into the body. The tail is a vertical fin. Aerodynamic control is achieved by means of a tail rudder and wing ailerons. The payload and propellant tanks are housed in the cylindrical body and the rocket engines are located at the aft end of the vehicle. The payload is deployed via a pair of payload bay doors located on top of

the cylindrical body. Figure 5.7 shows the drag and lift coefficients as functions of the Mach Number.

5.6.2 Ascent and Descent Trajectories

The design philosophy and operational constraints adopted for the ascent trajectory for this vehicle are identical to those adopted for Vehicle No.1, as described in Chapter 5.5.2: Flight Phase 1 comprises vertical flight for 10 seconds. Flight Phase 2 comprises a variable, optimised pitch-over manoeuvre until the perigee altitude and inertial velocity of the transfer orbit (100 km and 7879 m/s) are reached. The prescribed flight path angle is achieved by thrust vector control. No aerodynamic lift is used and the vehicle is constrained to fly at zero angle of attack.

5.6.3 Performance Results

Comprehensive performance results, similar to those presented in Figures 5.4 and 5.5 for Vehicle No.1 are also available for this vehicle. However, the results presented here have been limited to the most significant one, which is the Payload Mass Ratio versus Vehicle Mass Ratio characteristic, presented in the standard graphical presentation, under the same design conditions as for Vehicle No.1. These results are shown in Figure 5.8, together with those of Vehicle No.1 to facilitate a comparison.

Examination of Figure 5.8 shows that the Payload Mass Ratio for this vehicle is slightly lower than that for Vehicle No.1. For the design point Payload Mass Ratio of 2%, the required Vehicle Mass Ratio is 11 % (point D2 on Figure 5.8), compared to 12.3 % for Vehicle No.1 (point D1 on Figure 5.8).

We must now examine the significance of the apparently achievable design point Vehicle Mass Ratio of 11 %.
Unlike that of Vehicle No.1, for this vehicle, the additional masses of the wings, aerodynamic control surfaces and

actuators and the undercarriage must be included. A statistical analysis, based on a literature review, of the masses of wings, control surfaces and undercarriages for this type of launcher, reveals the following typical values:
- mass of wings, control surfaces and actuators: 14.5 % of vehicle landing mass;
- mass of undercarriage and actuation system: 3.5 % of vehicle landing mass.

Thus, the design point value of 11 % Vehicle Mass Ratio, although marginally lower than that of Vehicle No.1 at 12.3 %, inherently includes an additional total mass of 18 % of 11 %, which is nearly 2 %. This effectively leaves a Vehicle Mass Ratio of (11 - 2) %, which is 9 % for the remainder of the vehicle, and this is now much lower than the corresponding value of 12.3 % for Vehicle No.1.

Figure 5.6
Configuration of Reusable Launcher No.2:
SSTO-R-VLHL
(Derived from Reference 11)

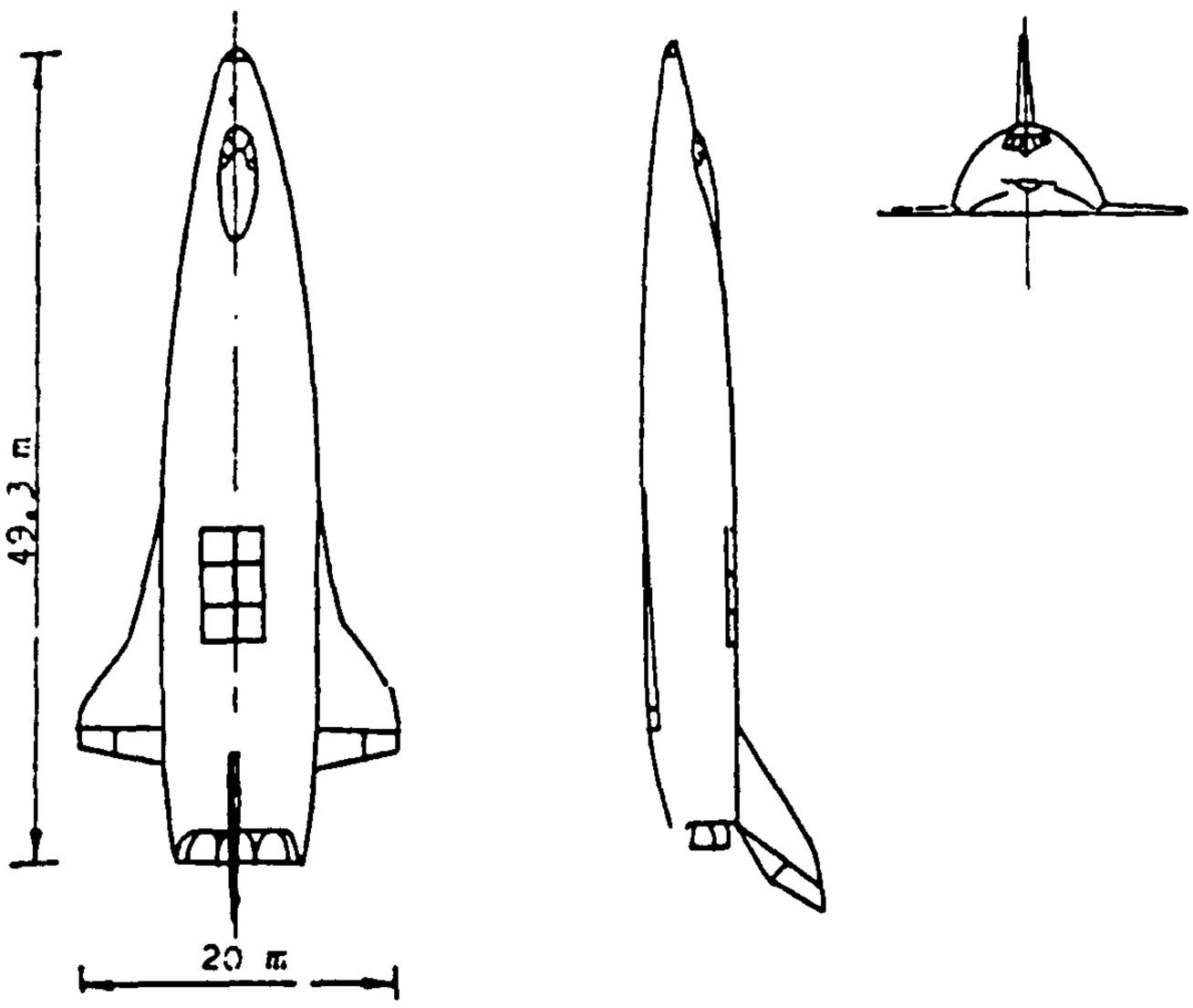

Height: 49.3 m.
Width: 20 m.
Lift-Off Mass: 350 tonnes
Lift-Off Thrust: 4900 KN
Aerodynamic Reference Area: 227 m²

Figure 5.7

Lift and Drag Coefficients for Reusable Launcher No.2

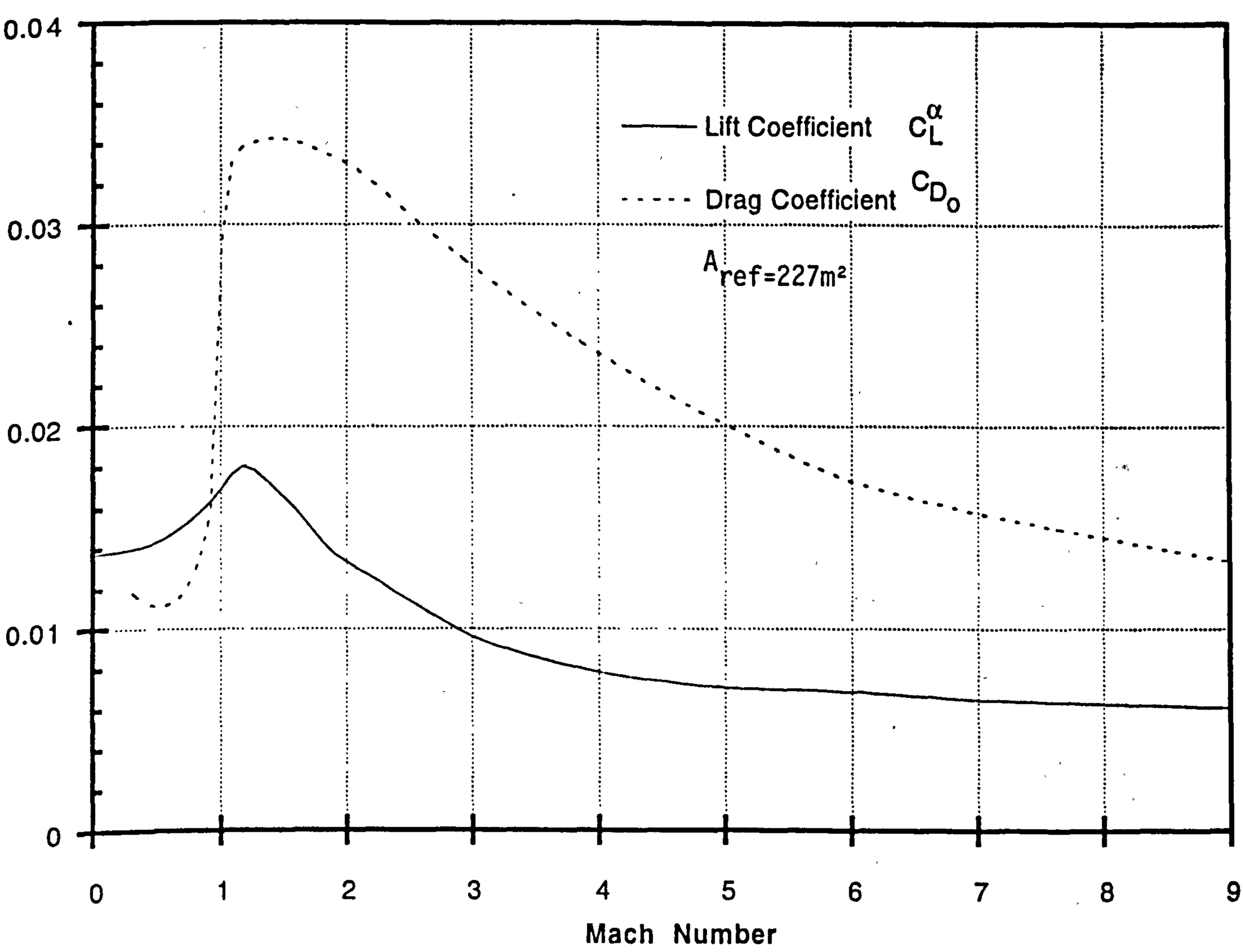

Figure 5.8

Reusable Launcher No.2: SSTO-R-VLHL

Payload Mass Ratio Versus Vehicle Mass Ratio

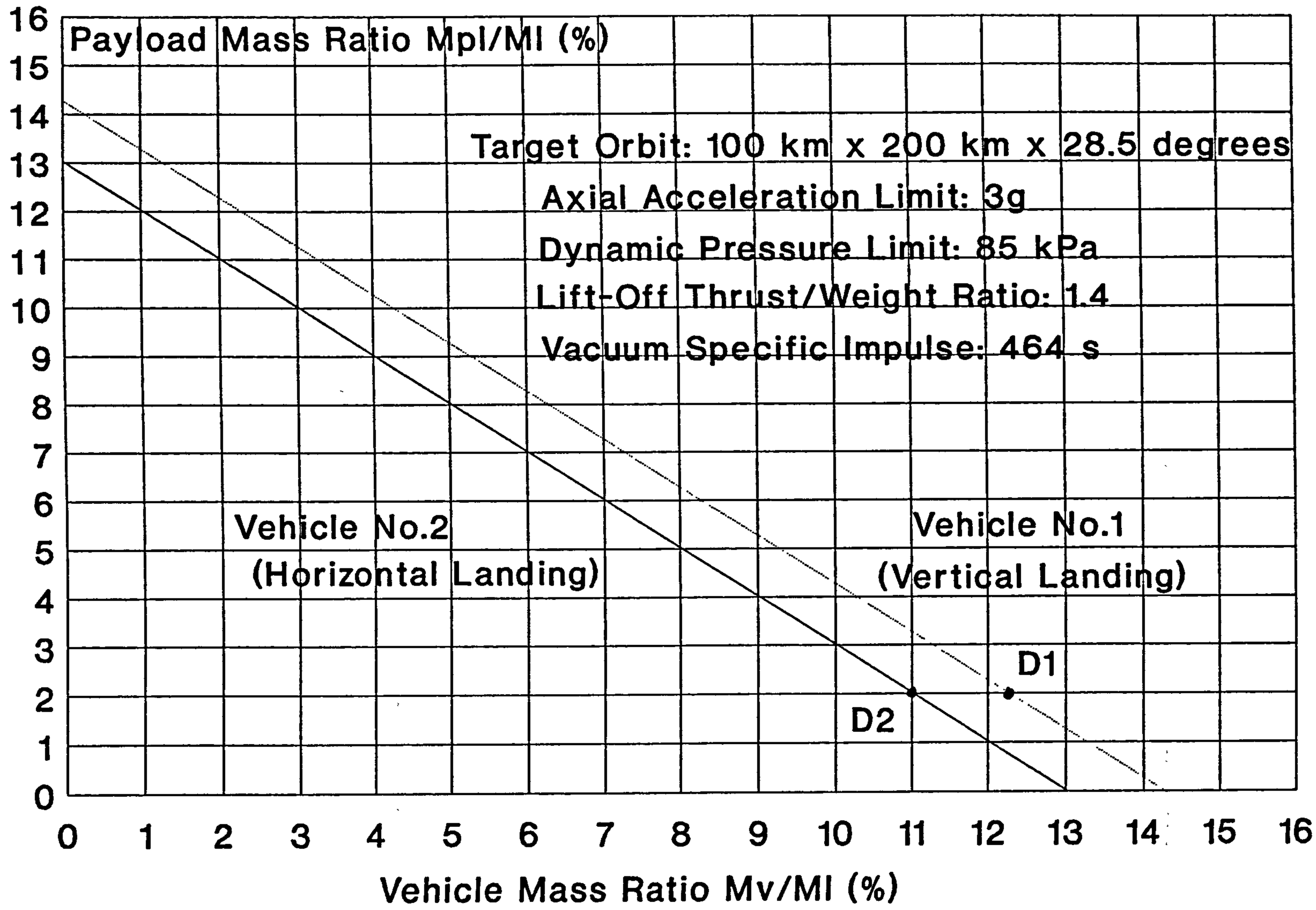

5.7 Performance of Reusable Launcher No.3: TSTO-R-VLHL

This launcher is a two-stage-to-orbit, rocket-propelled, vertically launched and horizontally landed vehicle.

5.7.1 Vehicle Configuration

Figure 5.9 shows the configuration and overall dimensions of the composite vehicle for the launch mode. This configuration is that of the comparative vehicle of Reference 11.

In common with Vehicles 1 and 2, this vehicle is also rocket-propelled and launched vertically. The major difference however, is that this is a two stage vehicle. Both stages ascend on a non-lifting trajectory and descend under aerodynamically controlled gliding flight to land horizontally on their own integral undercarriages. Thus, each stage is a winged vehicle of almost identical configuration: each being very similar to Vehicle No.2, which is intentional, for commonality reasons in this comparative study. During launch, the Second Stage is mounted on the back of the First Stage and the rocket engines in both stages are operated simultaneously in parallel burn. However, the Second Stage engines are fed with propellant from the First Stage tanks, thus ensuring that the Second Stage tanks are full at stage separation. To give clearance for accommodating the Second Stage on the back of the First Stage, the First Stage has twin tails and rudders. The Second Stage has a single central tail. The aerodynamic characteristics for each stage are almost identical to those of Vehicle No.2 as shown in Figure 5.10.

5.7.2 Ascent and Descent Trajectories

The ascent trajectory adopted is very similar to that described for the closely related Vehicles 1 and 2: the trajectory comprises three flight phases: Flight Phase 1 is a vertical ascent for 10 seconds; Flight Phase 2 comprises a variable, optimised pitch-over until the required altitude and velocity for separation of the stages is reached; Flight Phase 3 is the Second Stage flight along a variable, optimised pitch-over trajectory until the altitude and velocity at perigee of the required transfer orbit is achieved.

5.7.3 Performance Results

Using the trajectory model, considerable computational efforts were expended firstly to select the optimum staging inertial velocity that gave the highest Orbital Mass Ratio. This resulted in a staging inertial velocity of 3000 m/s. Secondly, an optimum trajectory was then found by computing the variable pitch-over turning rate angle that maximised the Orbital Mass Ratio for the Second Stage. The performance results, shown in the standard graphical presentation, are given in Figure 5.11.

Examination of Figure 5.11 shows that the Payload Mass Ratio characteristics for this vehicle are substantially higher than those of the almost identical but single-staged Vehicle No.2. This result is expected because of the staging concept. For Vehicle No.2, whilst a Vehicle Mass Ratio value of 11 % yields our design point Payload Mass Ratio of 2 % (point D2 on Figure 5.11), for Vehicle No.3, under the same design conditions, the Payload Mass Ratio is substantially increased to 8.5 % (point A on Figure 5.11). Alternatively, and much more realistically, at our design point Payload Mass Ratio of 2 %, the Vehicle Mass Ratio can be increased to a more feasible value of 17.5 % (point D3 on Figure 5.11).

Figure 5.9

Configuration of Reusable Launcher No.3:

TSTO-R-VLHL

(Derived from Reference 11)

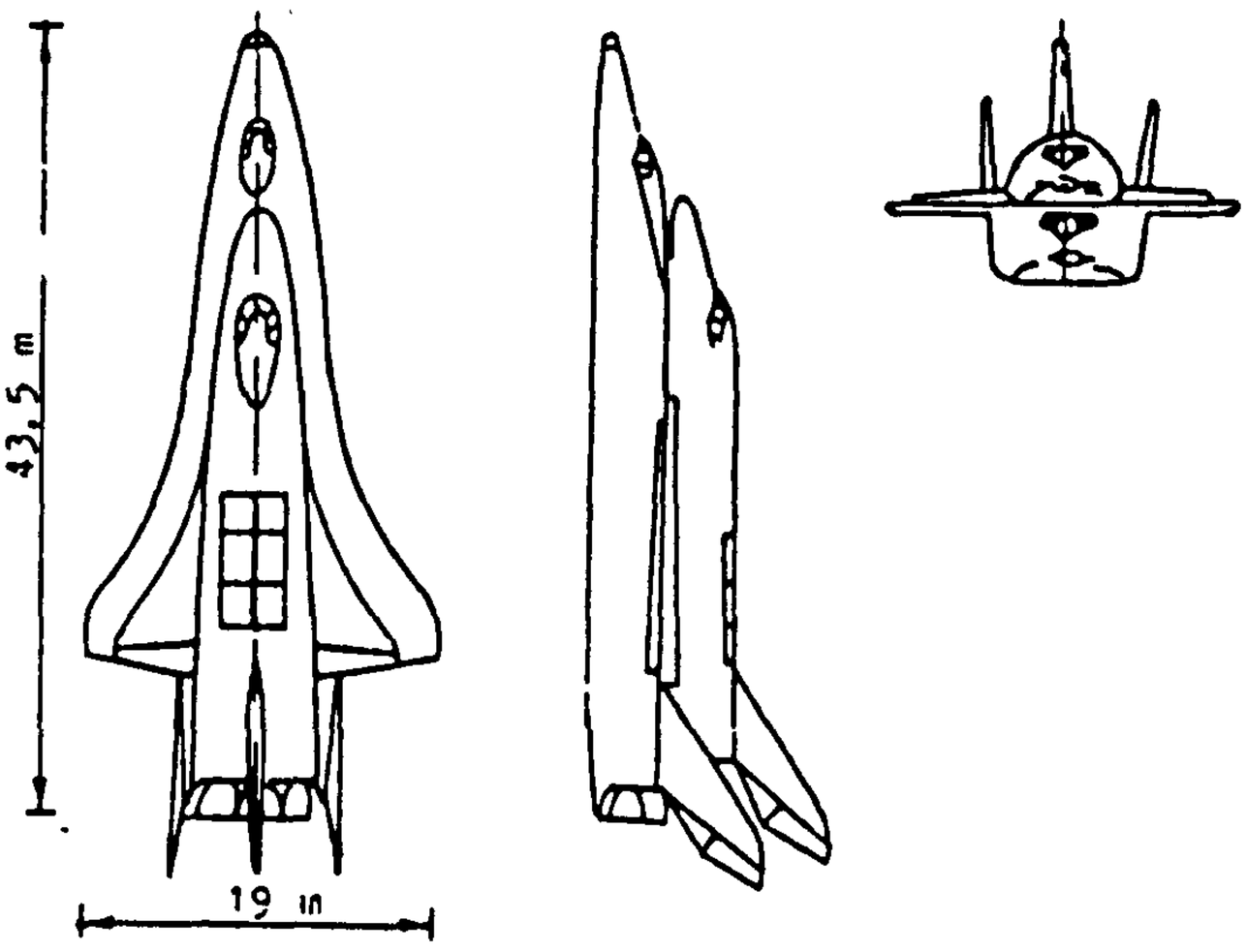

Height: 43.5 m.
Width: 19 m.
Lift-Off Mass: 350 tonnes
Lift-Off Thrust: 4900 KN
Aerodynamic Reference Area Stage 1: 185 m²
Stage 2: 131 m²

Figure 5.10 A

Lift and Drag Coefficients for Stage 1 of reusable Launcher No.3

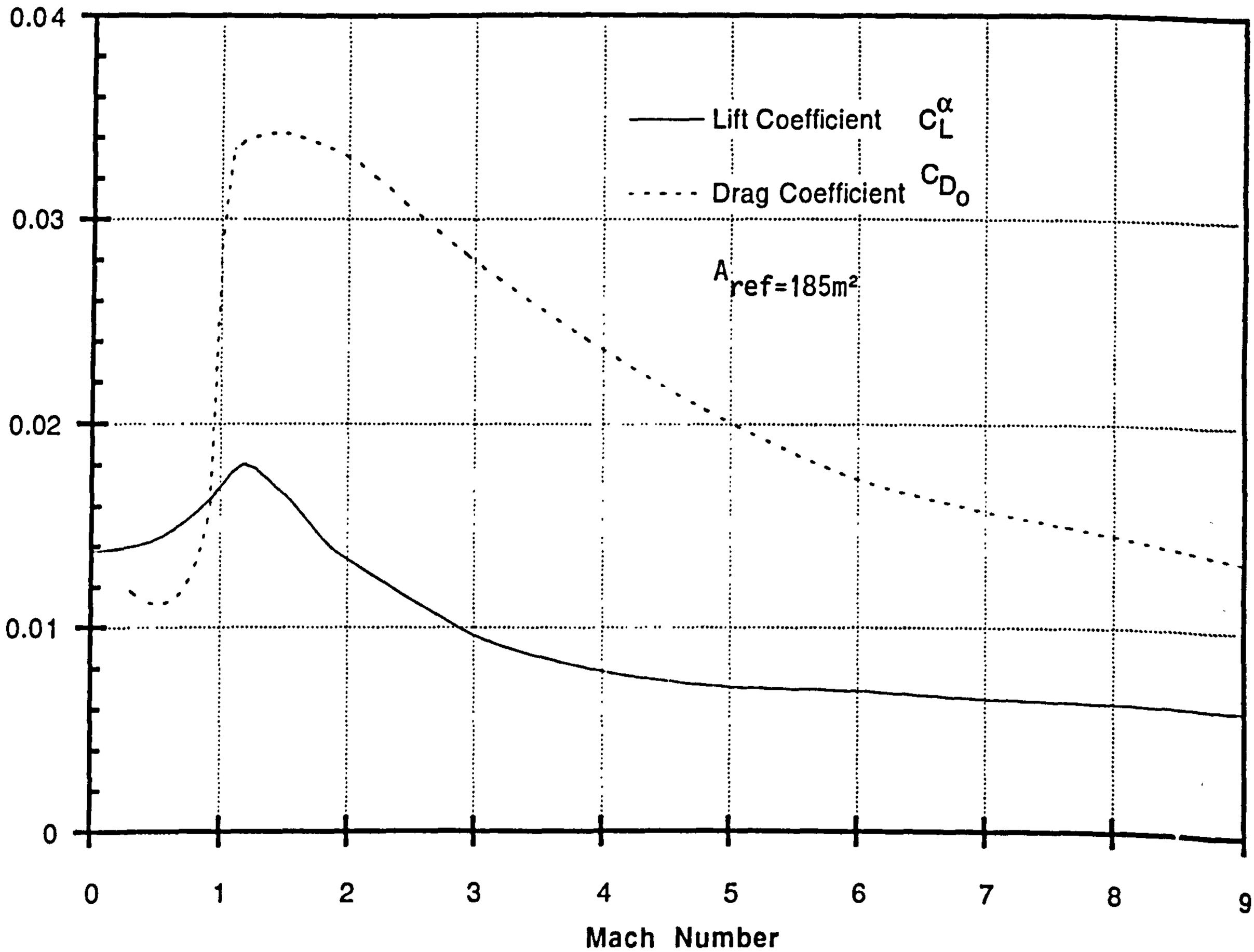

Figure 5.10 B

Lift and Drag Coefficients for Stage 2
of Reusable Launcher No.3

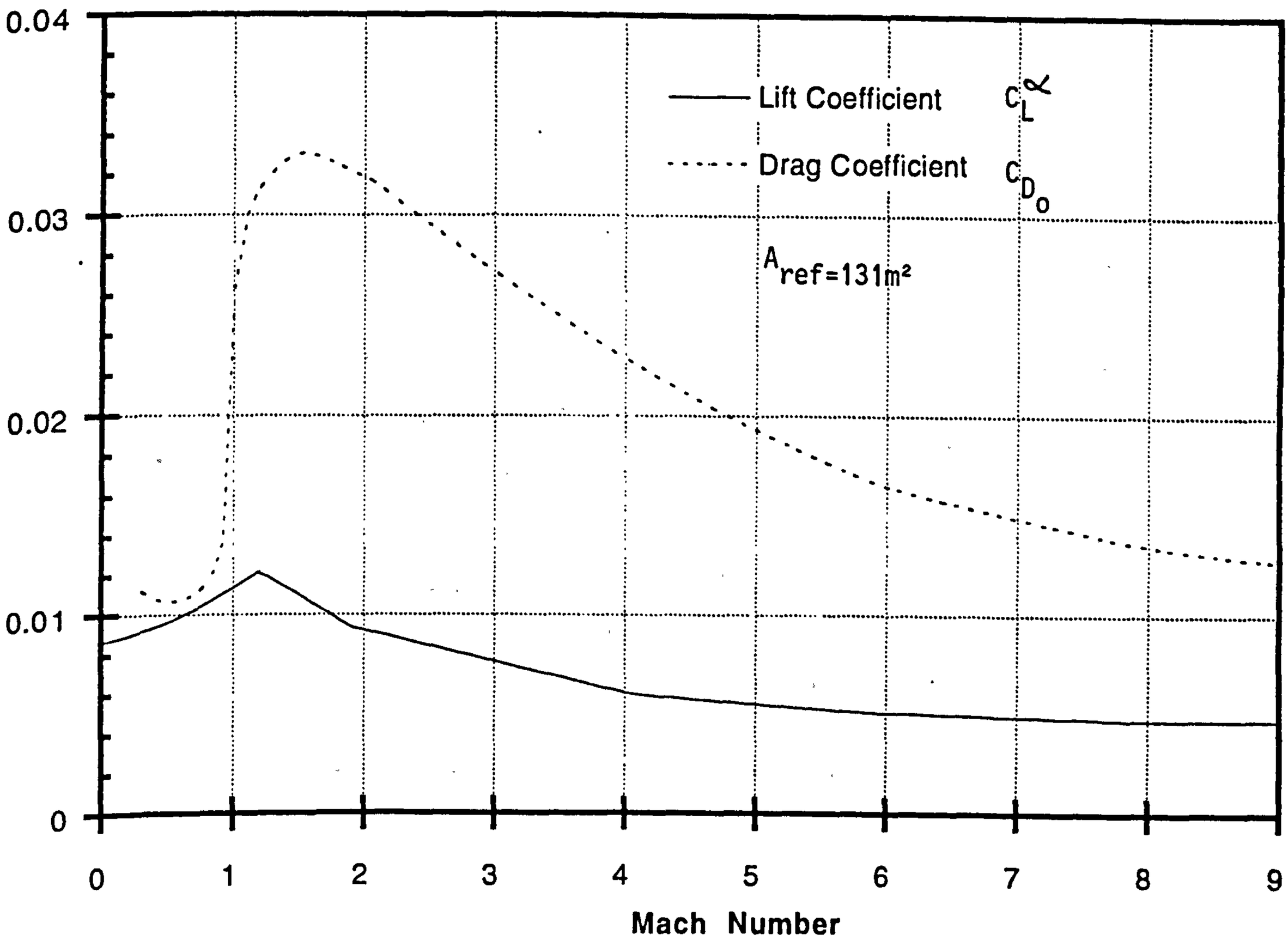

FIGURE 5.11

Reusable Launcher No.3: TSTO-R-VLHL

Payload Mass Ratio Versus Vehicle Mass Ratio

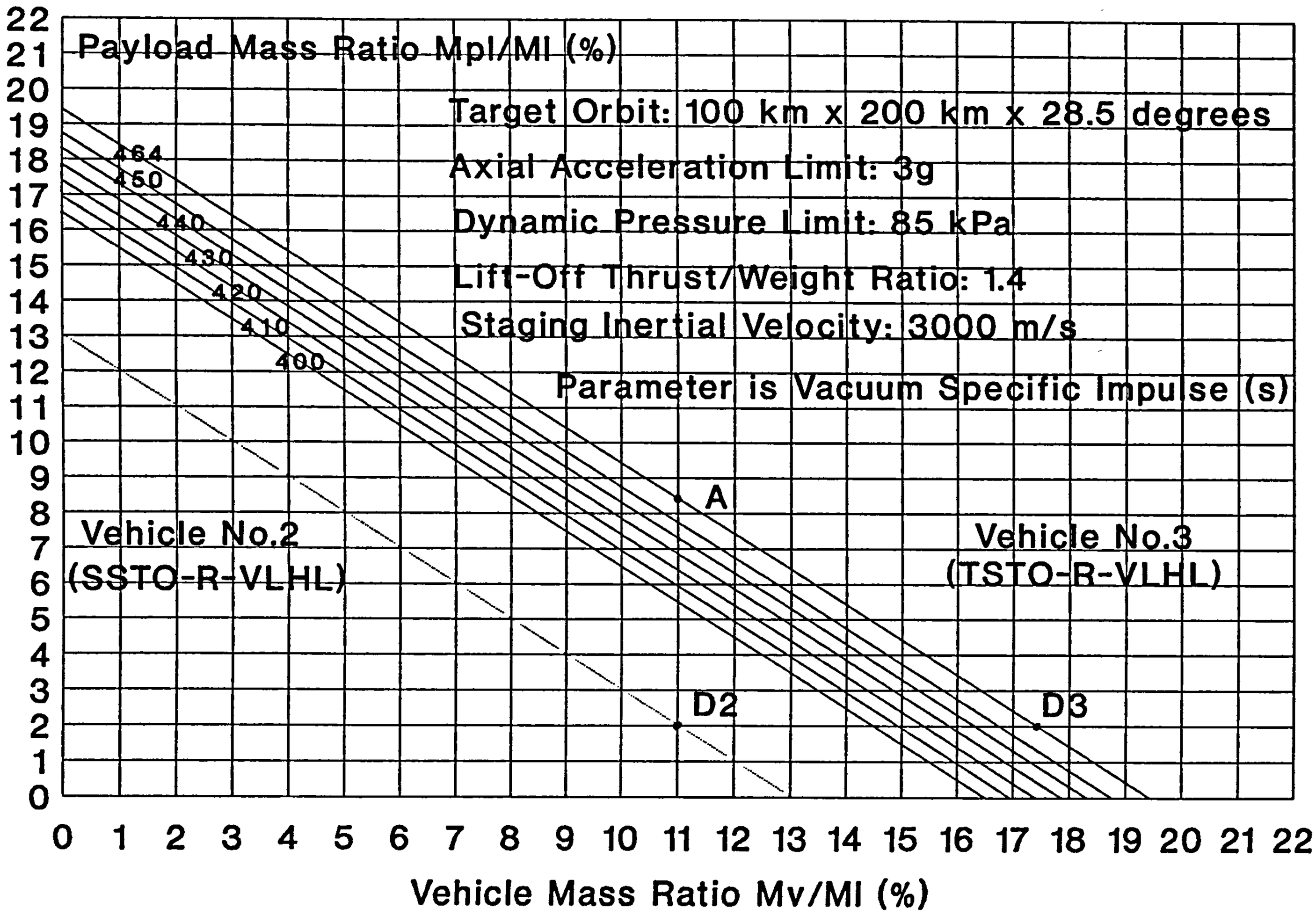

5.8 Performance of Reusable Launcher No.4: SSTO-RA(Sub)-HLHL (Undercarriage-Launched)

This launcher is a single-stage-to-orbit, rocket and air-breathing propelled, horizontally launched and horizontally landed vehicle. The air-breathing combustion mode is subsonic. The Vehicle is undercarriage-launched.

5.8.1 Vehicle Configuration

This is the first of the candidate vehicles that is launched horizontally and that employs both rocket propulsion and air-breathing propulsion. Rocket propulsion is used for the take-off and initial flight phase. Subsonic Combustion ramjets are used for the intermediate flight phase. Rocket propulsion is used again for the final flight phase into orbit.

The vehicle configuration adopted is that developed by British Aerospace in Phase 2 of the ESA Study on Winged Launcher Configurations (Reference 7). The vehicle configuration is shown in Figure 5.12. The vehicle has a conical body of circular cross section, with a long forebody, to provide a high degree of external compression of the air for the ramjet engines. The wing is a delta configuration placed low at the aft end of the vehicle. Aerodynamic control is achieved by a body-mounted fin located on the forward end of the body and by wing ailerons. The rocket engines are located at the aft end of the vehicle. The subsonic combustion ramjets are located in a pod under the rear of the body and utilise the underside of the body as an external expansion nozzle. The payload bay is located in the body towards its rear end. The drag and lift coefficients of the vehicle as functions of Mach number and incidence angle are shown in Figures 5.13 and 5.14 respectively.

5.8.2 Ascent and Descent Trajectories

The ascent trajectory comprises 5 phases. Phase 1 starts with the take-off run of the vehicle propelled by its rocket engines. Phase 2 begins with the rotation in pitch of the vehicle until it lifts off under rocket propulsion. Phase 3 begins with the ignition of the ramjet engines in parallel burn with the rocket engines until sufficient thrust is developed by the ramjets. Phase 4 is the propulsion phase using the ramjet engines only. Phase 5 begins with the final transition from ramjet engines to rocket engines, which then propel the vehicle into orbit. After re-entry, the vehicle descends in an aerodynamically controlled gliding flight to a horizontal runway landing.

5.8.3 Performance Results

The performance analysis of this vehicle, as for all the air-breathing propelled vehicles, has required an immense amount of reiterative computational effort to derive an ascent trajectory that maximised the Orbital Mass. This effort resulted from: the modelling difficulties for the ramjet engines; the parallel burn of both rocket and ramjet engines in Phase 3 of the flight; the optimisation of the transition points between each phase. The ramjet performance data has been derived from the ESA Winged Launcher Configuration Study (Reference 7). The fuel flow and thrust characteristics as functions of Mach number, incidence angle and equivalence ratio are shown in Figures 5.15 and 5.16 respectively. The specific impulse is derived by the trajectory program by the ratio of thrust/fuel flow rate.

The optimised ascent trajectory transition points for this vehicle are:

- Phase 1 to Phase 2 transition: Mach 0.5; Altitude 0 km;
- Phase 2 to Phase 3 transition: Mach 1; Altitude 1.62 km;

- Phase 3 to Phase 4 transition: Mach 2.83; Altitude 15.8 km;
- Phase 4 to Phase 5 transition: Mach 5.6; Altitude 25.2 km;

The Payload Mass Ratio calculated for this vehicle and plotted in the standard graphical form, is shown in Figure 5.17.

Examination of Figure 5.17 shows that to achieve our Payload Mass Ratio design point of 2 %, that the Vehicle Mass Ratio must not exceed 9.1 % (point D4 on Figure 5.17). This value is 3.93 % smaller than the Vehicle Mass Ratio of 11.03 % that is required for the, so far, most comparable vehicle in this analysis, which is Reusable Launcher No.2, the SSTO-R-VLHL (point D2 on Figure 5.17). This result indicates that for this undercarriage-launched vehicle, that the use of subsonic combustion ramjets with rocket propulsion results in a unrealistically small Vehicle Mass Ratio of only 9.1 %. This 9.1 % Vehicle Mass Ratio must now include an undercarriage sized for the take-off mass of the vehicle, which has a statistical mass ratio of 3.5 %. This leaves a Vehicle Mass Ratio of only 5.6 % for the rest of the vehicle. We can therefore already predict that it is unlikely that this vehicle can deliver a positive payload mass.

Figure 5.12
Configuration of Reusable Launcher No.4:
SSTO-RA(Sub)-HLHL (Undercarriage-Launched)
(Derived from Reference 7)

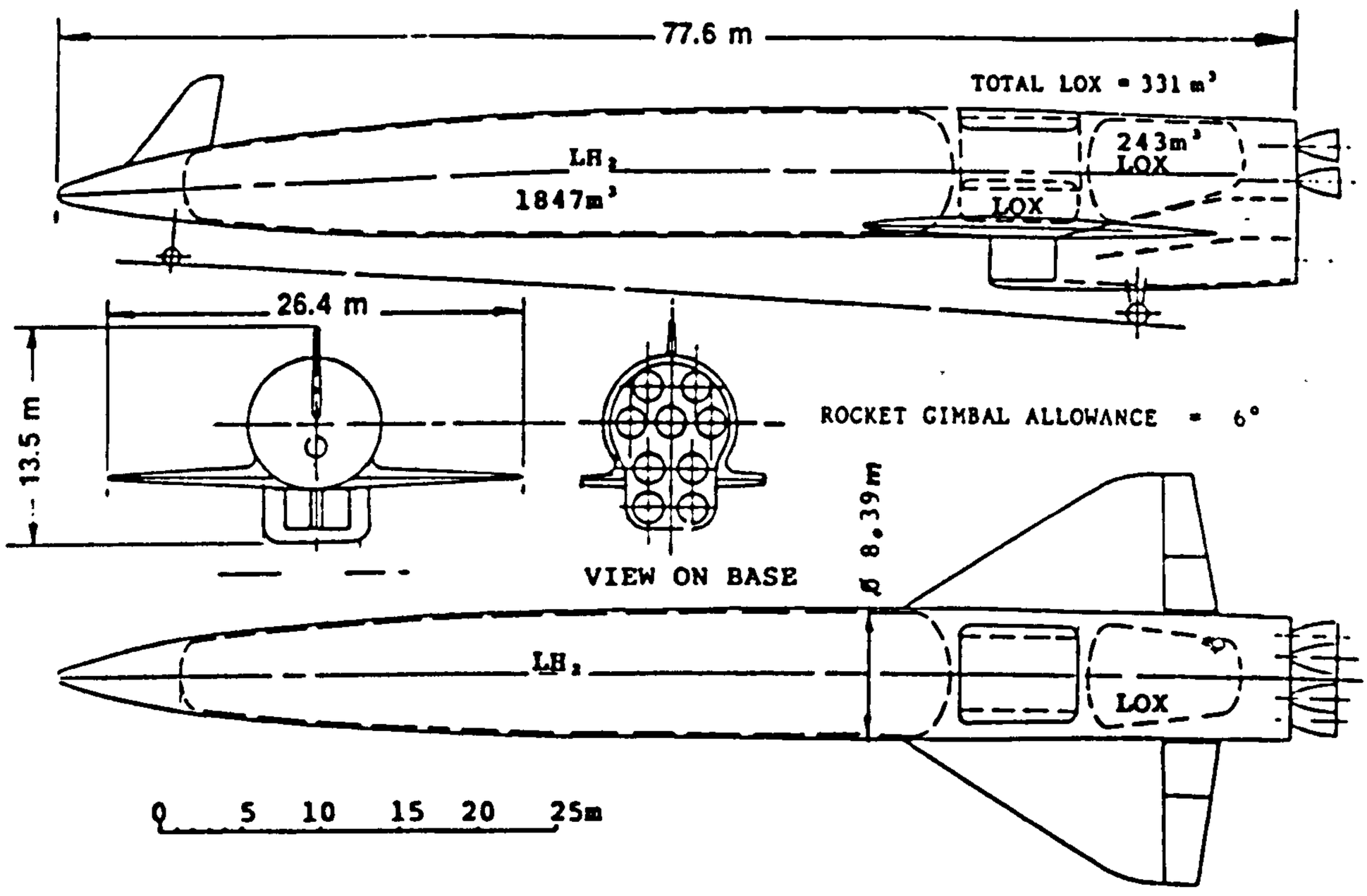

Length: 77.6 m.
Width: 26.4 m.
Lift-Off Mass: 350 tonnes
Lift-Off Thrust: 1750 KN
Aerodynamic Reference Area = 356.9 m²

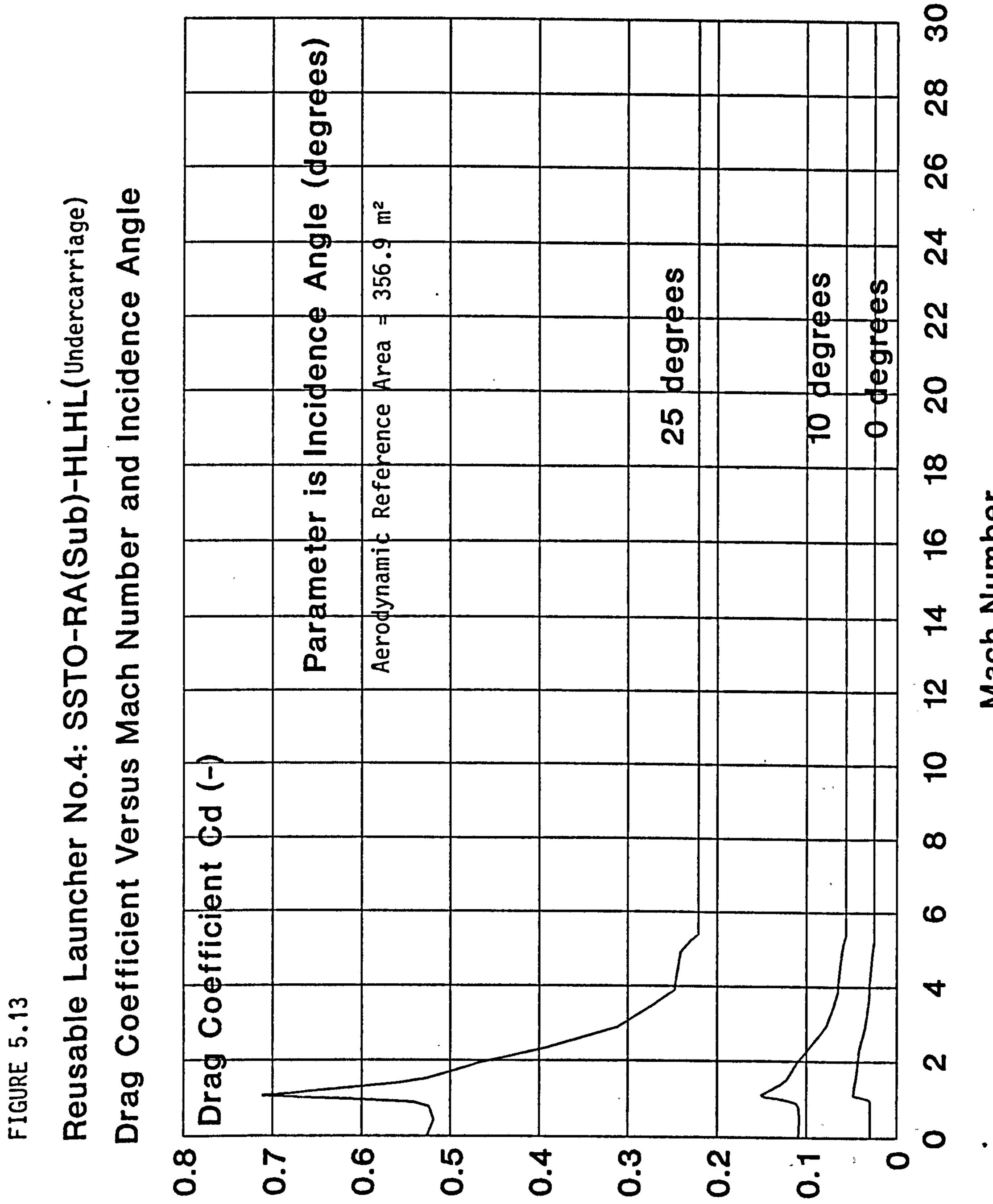
FIGURE 5.13
Reusable Launcher No.4: SSTO-RA(Sub)-HLHL(Undercarriage)
Drag Coefficient Versus Mach Number and Incidence Angle
Parameter is Incidence Angle (degrees)
Aerodynamic Reference Area = 356.9 m²
25 degrees
10 degrees
0 degrees
Drag Coefficient Cd (-)
Mach Number
0.8 0.7 0.6 0.5 0.4 0.3 0.2 0.1 0
0 2 4 6 8 10 12 14 16 18 20 22 24 26 28 30

FIGURE 5.14

Reusable Launcher No.4: SSTO-RA(Sub)-HLHL(Undercarriage)

Lift Coefficient Versus Mach Number And Incidence Angle

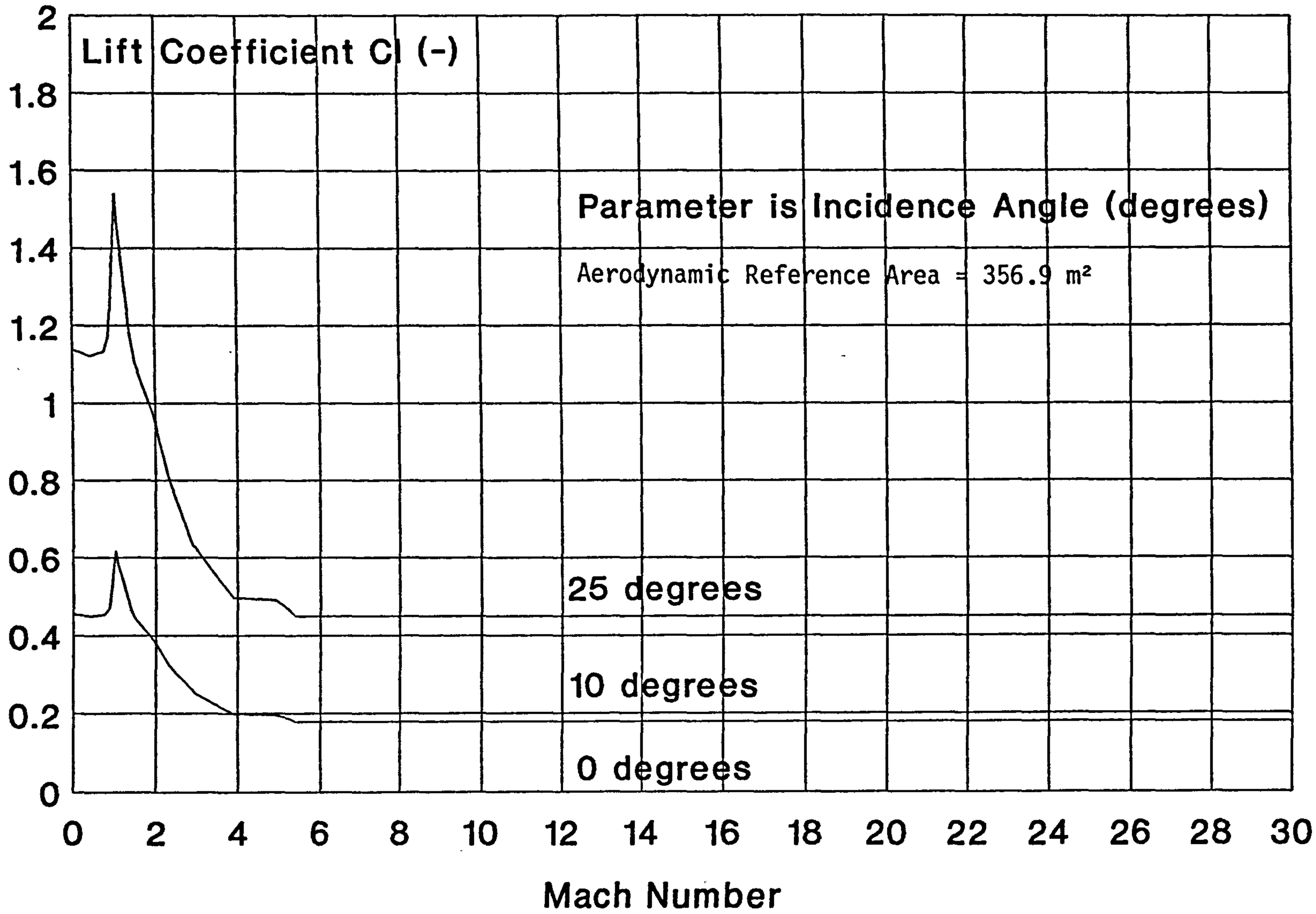

Figure 5.15

Reusable Launcher No.4:

SSTO-RA (Sub)-HLHL (Undercarriage-Launched)
Ramjet Engine: Fuel Flow versus Mach Number
(Data from Reference 7)

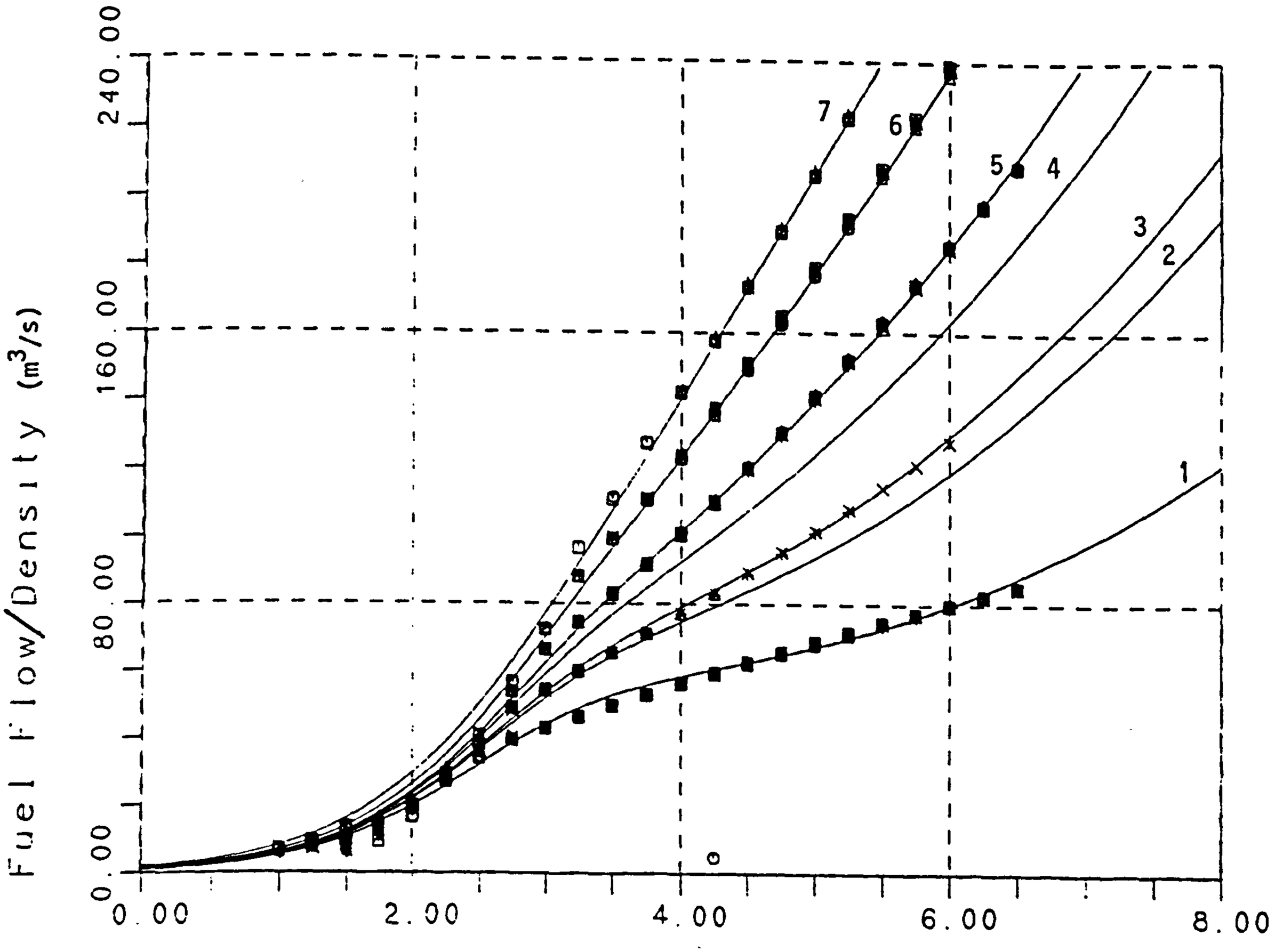

1 alfa=0 EQR=1.0
2 alfa=4 EQR=1.0
3 alfa=5 EQR=1.0
4 alfa=8 EQR=1.0
5 alfa=10 EQR=1.0
6 alfa=15 EQR=1.0
7 alfa=20 EQR=1.0

- Points are calculated values
- Curves are from best-fit equations
- alfa = angle of attack (degrees)
- EQR = equivalence ratio
- Fuel Flow in (Kg/s)
- Density is Air Density (Kg/m³)

Figure 5.16

Reusable Launcher No.4:

SSTO-RA (Sub)-HLHL (Undercarriage-Launched)
Ramjet Engine: Thrust versus Mach Number

(Data from Reference 7)

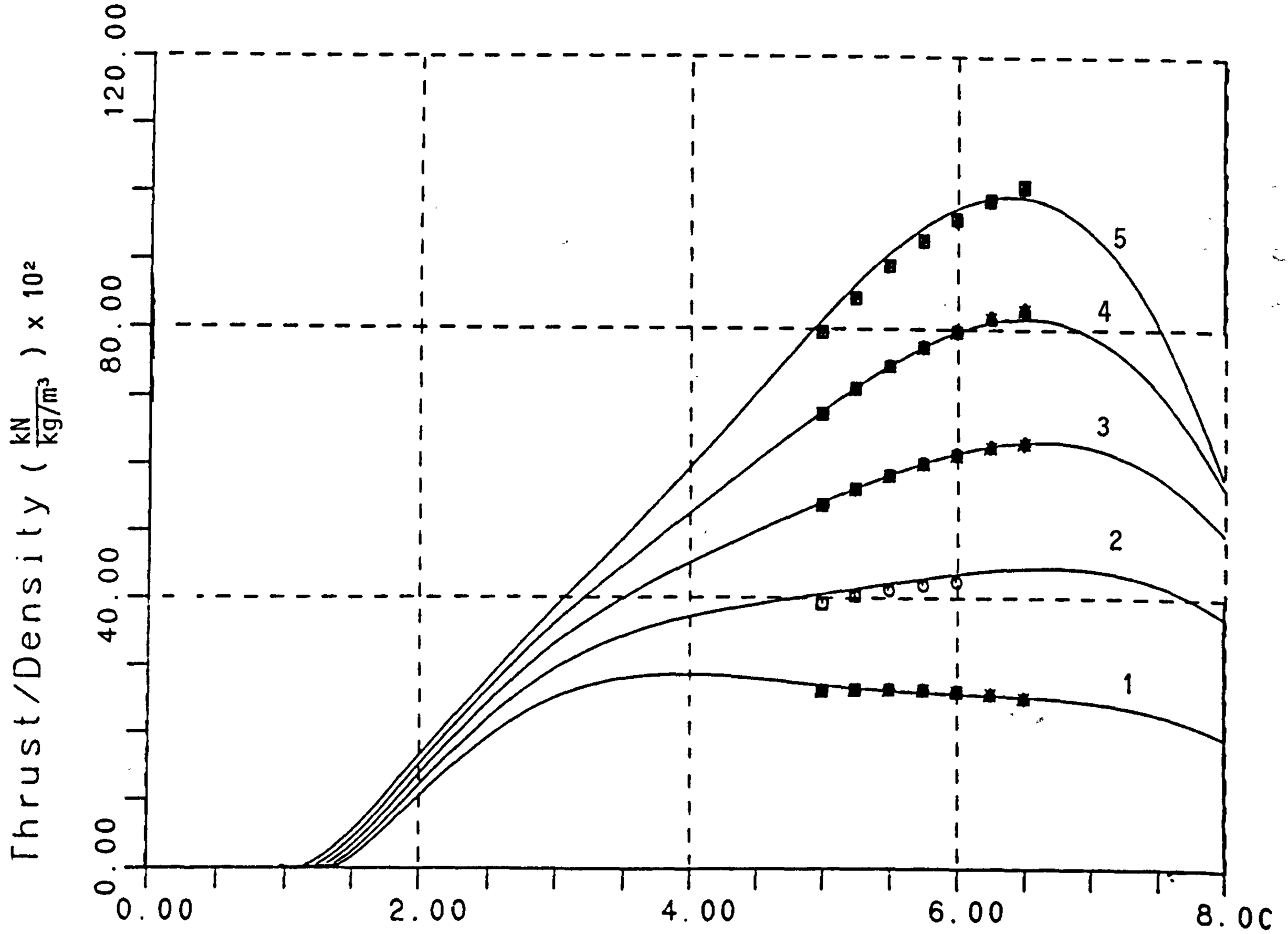

1 alfa=0 EQR=4.0
2 alfa=5 EQR=4.0
3 alfa=10 EQR=4.0
4 alfa=15 EQR=4.0
5 alfa=20 EQR=4.0

- Points are calculated values
- Curves are from best-fit equations
- alfa = angle of attack (degrees)
- EQR = equivalence ratio
- Thrust in kN
- Density is Air Density (Kg/m³)

FIGURE 5.17

Reusable Launcher No 4: SSTO-RA(Sub)-HLHL(Undercarriage)

Payload Mass Ratio Versus Vehicle Mass Ratio

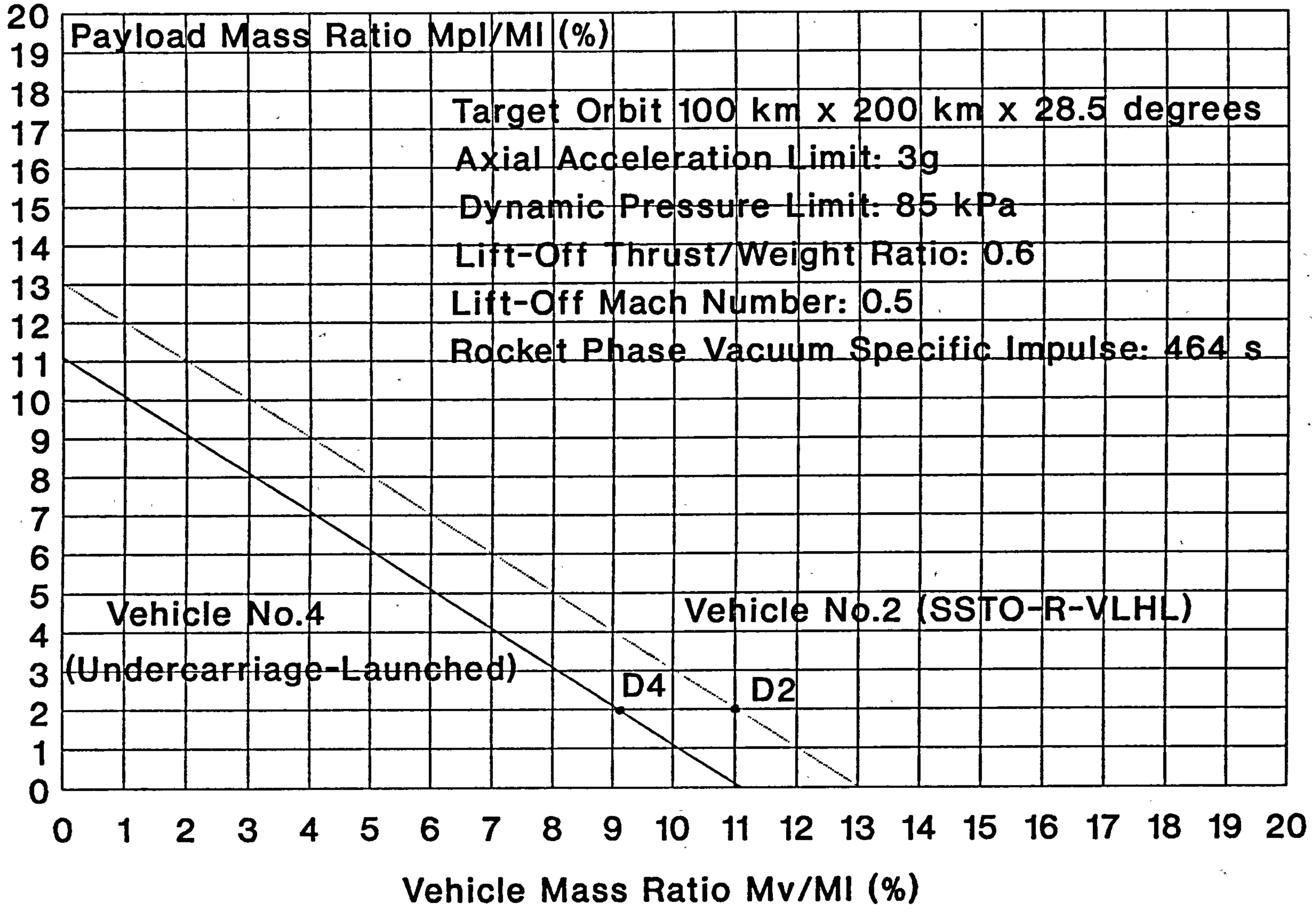

5.9 Performance of Reusable Launcher No.5: SSTO-RA(Sub)-HLHL (Sled-Launched)

This launcher is a single-stage-to-orbit, rocket and air-breathing propelled, horizontally launched and horizontally landed vehicle. The air-breathing combustion mode is subsonic. The vehicle is sled-launched.

5.9.1 Vehicle Configuration

The configuration of this vehicle and its propulsion systems are the same as that of Vehicle No.4, except for two major differences:

- the vehicle, propelled by its rocket engines, takes off on a sled which carries the propellants required for the take-off run;
- the vehicle, because of its sled launch, requires less rocket propellants. Hence, the tankage volume of the vehicle is correspondingly smaller than that of Launcher No.4, the equivalent undercarriage-launched vehicle.

5.9.2 Ascent and Descent Trajectories

Except for Flight Phase 1, this vehicle has a similar ascent trajectory to that of Vehicle No.4, comprising 5 flight phases. Phase 1 starts with the take-off run of the vehicle on its sled, propelled by its own rocket engines. Phase 2 begins with the rotation in pitch of the vehicle on the sled until it lifts off. Phase 3 begins with the ignition of the ramjet engines in parallel burn with the rocket engines until sufficient thrust is developed by the ramjets. Phase 4 is the propulsion phase with the ramjet engines only. Phase 5 begins with the final transition from ramjet engines to rocket engines, which then propel the vehicle into orbit. The descent mode is also identical to that of Vehicle No.4,

comprising an aerodynamically controlled gliding flight and a horizontal landing.

5.9.3 Performance Results

The performance results, shown in the standard graphical presentation are given in Figure 5.18. The Payload Mass Ratio characteristic of Vehicle No.4, which is the most directly comparable vehicle, is also shown on Figure 5.19 as a dotted line.

Examination of Figure 5.18 shows that the reduced rocket propellant mass that is carried by this vehicle because of its sled launch, is reflected clearly in the calculated Payload Mass Ratio. The increase in Payload Mass Ratio between that of Vehicle No.4 (sled-launched) and that of Vehicle No.5 (undercarriage-launched) is a very large value of 3.9 %, which is the vertical distance between lines D4 and D5 on Figure 5.18. The significance of this increased value is demonstrated by the fact that it is twice the value of our target design point Payload Mass Ratio of 2 %. Succinctly put, the mass of the rocket propellant saved by using a sled for the take-off run is double the mass of the specified payload!

Figure 5.18 also shows that to achieve the 2 % Payload Mass Ratio value for this vehicle, the Vehicle Mass Ratio must not exceed 13 %. However, at this stage of the analysis, it is not possible to conclude that for this vehicle, or indeed for any of the vehicles, that the required Vehicle Mass Ratios can actually be achieved. The assessment of actually achievable Vehicle Mass Ratio values for each vehicle is addressed later in this Chapter.

FIGURE 5.18

Reusable Launcher No.5: SSTO-RA(Sub)-HLHL(Sled)

Payload Mass Ratio Versus Vehicle Mass Ratio

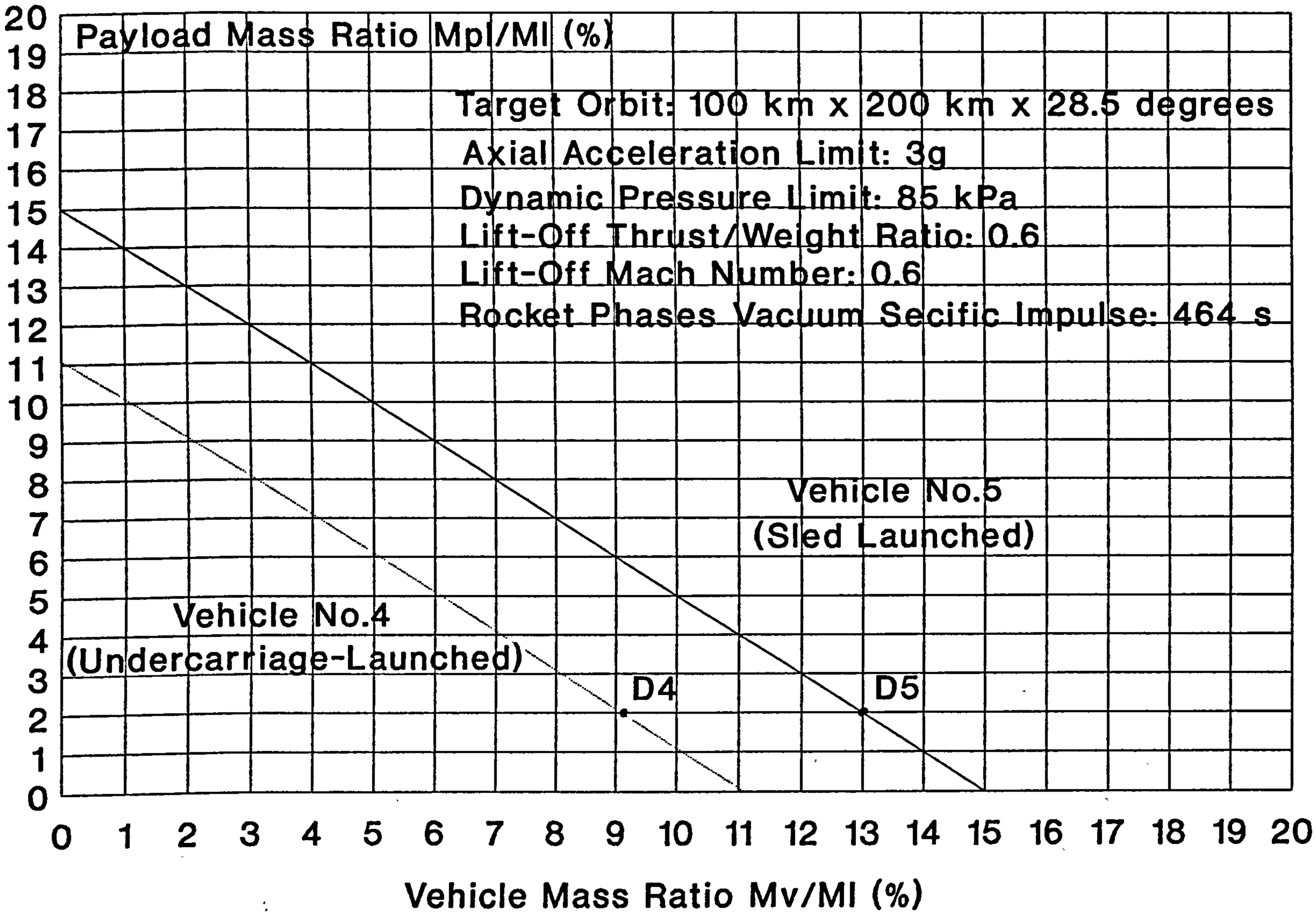

5.10 Performance of Reusable Vehicle No.6: SSTO-RA(Sub)-ILHL (Ramp-Launched)

This launcher is a single-stage-to-orbit, rocket and air-breathing propelled, inclined launched and horizontally landed vehicle. The air-breathing combustion mode is subsonic. The vehicle is ramp-launched.

5.10.1 Vehicle Configuration

This vehicle is similar to Vehicle No.5 except for the two following major differences:

- the vehicle is launched from a short inclined ramp;
- the vehicle, because of its ramp launch mode, has an additional set of rocket engines to lift it off the ramp at launch, by alleviating the weight component of the vehicle acting normal to the ramp. Without these lift engines, the vehicle would drop on to the ramp because of the relatively low thrust/vehicle weight ratio, typically 0.6, that must be used for launch vehicles

The motivation for investigating this inclined ramp launch mode is the payload mass ratio gain that would be made possible by a reduction of the mass of the undercarriage that would otherwise be required for take-off, as is the case for the undercarriage-launched Vehicle No.4. An undercarriage is still needed for the landing phase, but this can now be sized for the substantially smaller re-entry landing mass of the vehicle. The significance of reducing the undercarriage mass is illustrated in this typical vehicle sizing example:

- For our standard design point vehicle Launch Mass of 350 tonnes and Payload Mass Ratio of 2% , the Payload Mass is 7 tonnes. The undercarriage mass for a horizontally launched vehicle is, statistically, 3.5% of the launch mass, which gives an undercarriage mass of 12.25 tonnes. It

can be seen that the undercarriage mass is almost twice that of the desired payload mass!

5.10.2 Ascent and Descent Trajectories

Except for Flight Phase 1, this vehicle has a similar ascent trajectory to that of Vehicle No.5, comprising 5 flight phases. Phase 1 starts with the lift-off from the inclined ramp using both the axial and lift rocket engines. Phase 2 begins with the rotation in pitch of the vehicle until it is flying under aerodynamic lift and axial engine rocket thrust, with the lift rocket engines shut down. Phase 3 begins with the ignition of the ramjet engines in parallel burn with the rocket engines until sufficient thrust is developed by the ramjets. Phase 4 is the propulsion phase using the ramjet engines only. Phase 5 begins with the final transition from ramjet engines to rocket engines, which then propel the vehicle into orbit. The descent mode is also identical to that of Vehicle No.5, comprising an aerodynamically controlled gliding flight and a horizontal landing.

5.10.3 Performance Results

The first step in the performance assessment is to investigate the vehicle mass savings that would be achieved for a launch from an inclined ramp compared to a launch on an undercarriage as used for Vehicle No.4. To illustrate the savings clearly, an analytical approach has been used and is presented here:

The sketch below shows the force diagram for the vehicle on the ramp.

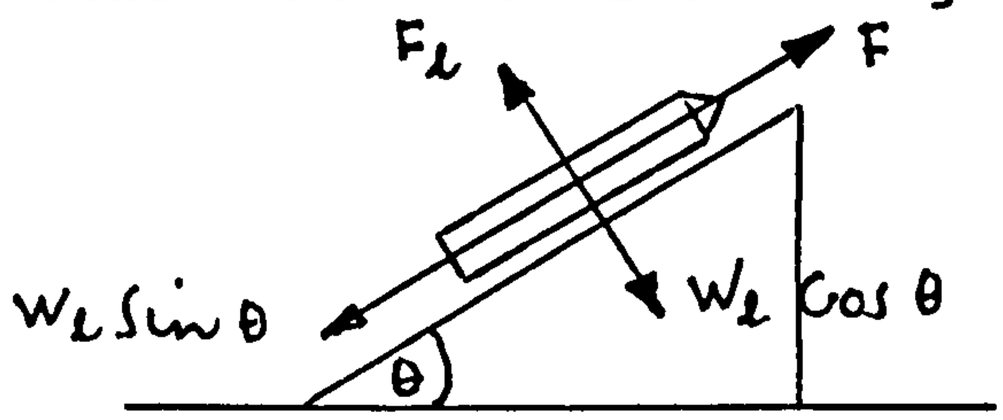

W_l is the vehicle launch weight; F is the vehicle axial thrust; F_L is the lift force required to compensate the

normal component of the vehicle weight on the ramp $W_l\cos\theta$, where θ is the ramp angle; $W_l\sin\theta$ is the vehicle weight component acting down the ramp.

The launch procedure is envisaged as follows: the initial condition prior to launch is that the vehicle is clamped to the launch ramp. The lift engines and thrust engines are then started and verified for proper functioning and delivery of the required thrust. The clamps are then released and the vehicle is accelerated off the ramp at a flight path angle equal to the ramp angle. The vehicle is allowed to accelerate until a velocity of 170 m/s (Mach 0.5), which is the same velocity used for lift-off of the undercarriage-launched Vehicle No.4, is reached. This is achieved within about 29 seconds with an axial thrust/vehicle weight ratio of 0.6, giving an axial acceleration of about 5.9 m/s2, as for Vehicle No.5. The vehicle is then rotated in pitch to give the angle of attack needed to develop enough aerodynamic lift to sustain flight. The lift engines are then shut down and the vehicle accelerates in climbing flight under axial thrust and aerodynamic lift.

The lift engine mass ratio M_L/M_l is calculated as follows:

$F_L = W_l\cos\theta$ (1)

$W_l = M_l g$ (2)

$F_L/W_L = c$ (3) where W_L is the lift engine weight and c is the lift engine thrust/weight ratio

$W_L = M_L g$ (4) where M_L is the lift engine mass

Substituting (2), (3) and (4) into (1) gives:

$cM_L g = M_l g\cos\theta$ (5)

Dividing both sides of (5) by M_l to get mass ratios:

$M_L/M_l = \cos\theta/c$ (6)

For example: for a ramp angle θ of 30 degrees and a lift engine thrust/weight ratio c of 80, the Lift Engine Mass Ratio is:

$M_L/M_l = \cos 30/80 = 0.01082 = 1.08\%$

The lift engine propellant mass ratio M_{pL}/M_l is calculated as follows:

$I_{tL} = F_L t_L$ (7) where I_{tL} is the total impulse delivered by the lift engines over their thrusting time t_L

$M_{pL} = I_{tL}/I_{sL}g$ (8) where I_{sL} is the average specific impulse of the lift engines

Substituting (7) into (8) gives;

$M_{pL} = F_L t_L / I_{sL}g$ (9)

Now $F_L = cW_L = cM_L g$ (10)

Substituting (10) into (9) gives:

$M_{pL} = cM_L g t_L / I_{sL} g$ (11)

Dividing both sides of (11) by M_l to give mass ratios:

$M_{pL}/M_l = (ct_L/I_{sL})(M_L/M_l)$ (12)

For example: for c = 80; t_L = 29 s; I_{sL} = 400 s; M_L/M_l = 0.0108, the Lift Engine Propellant Mass Ratio is:

$M_{pL}/M_l = 0.06275 = 6.275\ \%$

The potential reduction in the undercarriage mass ratio $\Delta M_{uo}/M_l$ is calculated as follows:

$M_{uo}/M_{ul} = 0.035M_o/0.035M_l$ (13)

where M_{uo} is the undercarriage mass sized for the vehicles landing (orbital) mass and M_{ul} is the undercarriage mass sized for the vehicles launch mass and the coefficient 0.035 is the statistical value for undercarriage mass.

From (13):

$M_{uo} = M_{ul}(M_o/M_l)$ (14)

$\Delta M_u = M_{ul} - M_{uo}$ (15)

Substituting (14) into (15) gives;

$\Delta M_u = M_{ul} - M_{ul}(M_o/M_l)$ (16)

Dividing both sides of (16) to get mass ratios:

$\Delta M_u/M_l = M_{ul}/M_l(1 - M_o/M_l)$ (17)

Now $M_o/M_l = (M_l - M_p)/M_l$ (18)

Substituting (18) into (17) gives;

$\Delta M_u/M_l = M_{ul}/M_l(M_p/M_l)$ (19)

For example: for $M_{ul}/M_l = 0.035$; $M_p/M_l = 0.91$ (which is the calculated value for Vehicle No.5), the difference in undercarriage mass is :

$\Delta M_u/M_l = 0.035(0.91) = 0.03185 = 3.185$ %

Therefore, for an inclined ramp launch, the vehicle mass ratio is decreased by the smaller undercarriage mass and increased by the mass of the additional lift engines. For this vehicle, the propellant mass needed by the lift engines contributes fully to the gain in potential energy of the vehicle. Similarly, for Vehicle No.4, the propellant mass needed for the runway take-off contributes fully to the gain in kinetic energy of the vehicle. Thus, the take-off propellant masses are not relevant for calculating the difference in the Vehicle Mass Ratios of the two vehicles, which is given by:

$$\Delta M_v/M_l = \Delta M_u/M_l - M_L/M_l \qquad (20)$$

Thus, in our example, it can be seen that the Vehicle Mass Ratio reduction resulting from an inclined ramp launch at 30 degrees is:

$\Delta M_v/M_l = (0.03185 - 0.01082) = 0.02103 = 2.1$ %

This is a very significant Vehicle Mass Ratio reduction, being about the same as our standard Payload Mass Ratio target of 2 %. This Vehicle Mass Ratio reduction translates directly into a corresponding increase in the Payload Mass Ratio.

The Payload Mass Ratio performance of this inclined launch vehicle is therefore identical to that of the undercarriage-launched Vehicle No.4. The savings in the Vehicle Mass Ratio resulting from the reduced undercarriage mass, cannot, at this stage of our performance analysis, be accounted for in the reduction of the Payload Mass Ratio, but will of course

reflect in the accounting of the actual vehicle mass and thus on the feasibility of actually being able to achieve the required Vehicle Mass Ratio. This is discussed later in this Chapter. The Payload Mass Ratio results are shown in Figure 5.19, which although identical to those for Vehicle No.5 as given in Figure 5.18, are reproduced in Figure 5.19 for completeness and consistency in the presentation.

Figure 5.19

Reusable Launcher No.6: SSTO-RA(Sub)-ILHL (Ramp)

Payload Mass Ratio Versus Vehicle Mass Ratio

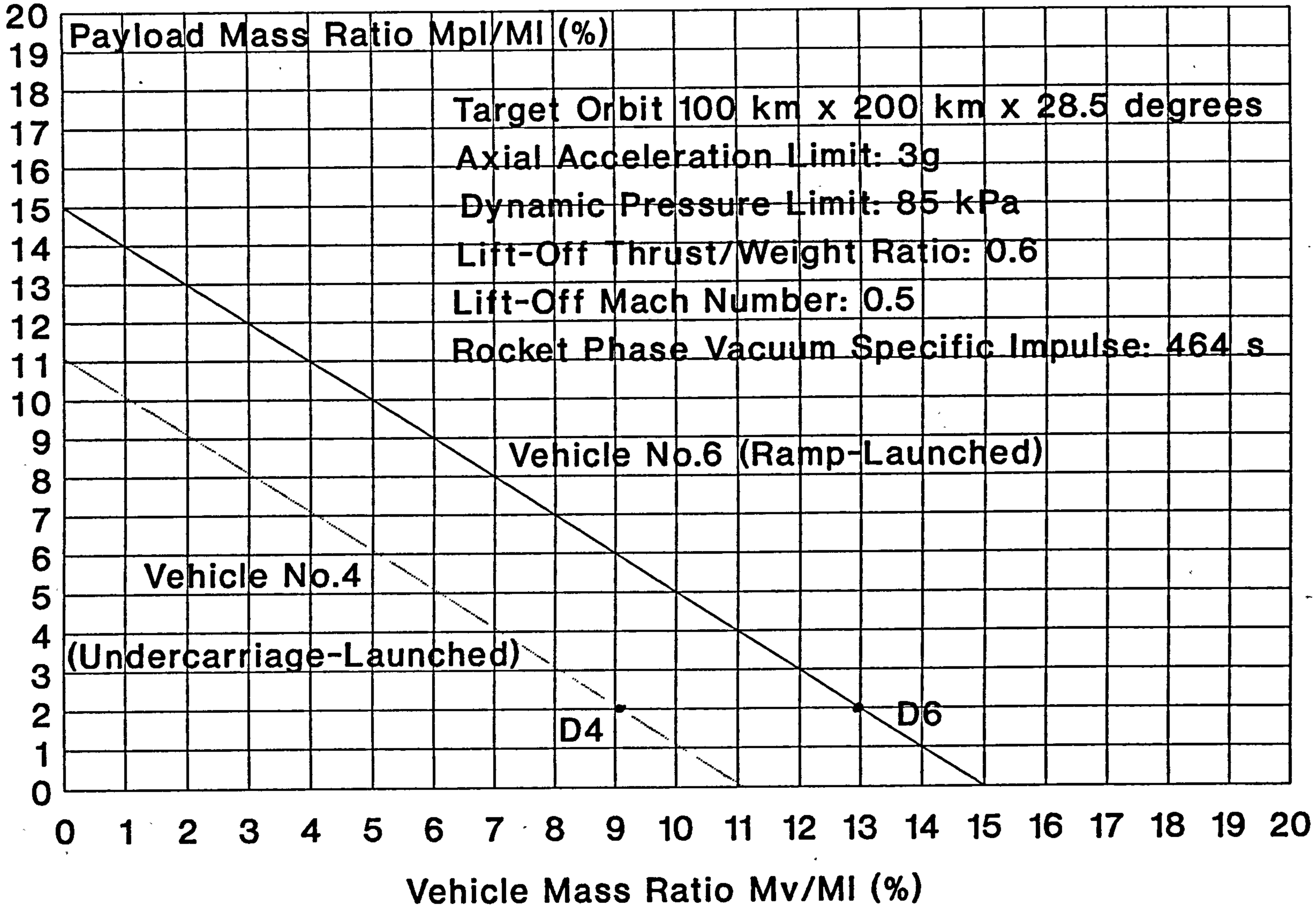

5.11 Performance of Reusable Launcher No.7: SSTO-RA(Sup)-HLHL (Undercarriage-Launched)

This launcher is a single-stage-to-orbit, rocket and air-breathing propelled, horizontally launched and horizontally landed vehicle. The combustion mode is supersonic. The vehicle is undercarriage-launched.

5.11.1 Vehicle Configuration

This vehicle is a most important one in this analysis simply because it is the vehicle that has been adopted by the USA as their X30 experimental vehicle within their National Aerospace Plane Programme (NASP). The unique feature of this vehicle is that it is the only one in this list of candidate vehicles that uses air-breathing propulsion which includes supersonic combustion.

Because the performance of this vehicle type is closely guarded by the USA, resulting in virtually no performance data being available in the published literature, and because, at an intuitive level, the use of air-breathing propulsion to very high Mach numbers of 12 to 15 should result in payload mass increases compared with similar vehicles propelled by air-breathing engines employing subsonic combustion up to the subsonic combustion limit of about Mach 6.8, this vehicle concept has been adopted by the author from Phase 5 of the ESA Winged Launcher Configuration Study (Reference 8). For this research therefore, the vehicle configuration, its aerodynamic and propulsion performance characteristics, have been adopted from the ESA study. This adoption has been essential because of the difficulty in modelling the aerodynamic and propulsion performance of such a complex vehicle. The performance data used is unique in Europe and is the best available data, albeit that Europe has only a small capability in the analysis of supersonic combustion ramjets (scramjets) compared to the USA.

The vehicle configuration is shown in Figure 5.20. The aerodynamic characteristics are shown in Figure 5.21.
The vehicle is propelled by a combined cycle engine comprising four operating modes: an air ejector mode for take-off and initial climb, transitioning to a subsonic combustion ramjet mode, transitioning again to a supersonic combustion ramjet mode and finally transitioning to a rocket propulsion mode for the final flight phase to orbit. The propulsion performance data that has been generated for this vehicle is very extensive, covering each of the propulsion modes. Samples of this data for each engine mode are shown in Figures 5.22 to 5.24.

5.11.2 Ascent and Descent Trajectories

The ascent trajectory comprises five flight phases. Phase 1 starts with the take-off run of the vehicle on its own undercarriage, propelled by its air ejector engines. Phase 2 begins with the rotation in pitch of the vehicle until it lifts off at Mach 0.5. Phase 3 begins with the ignition of the subsonic ramjet engines in parallel burn with the air ejectors until sufficient thrust is developed by the ramjets to allow a progressive transition from the air ejector mode to ramjet mode at Mach 2.5. Phase 4 starts with the progressive transition from subsonic combustion to supersonic combustion in ramjet mode at Mach 6. Phase 5 starts with the initiation of rocket thrust and the progressive shut down of the scramjet engines at Mach 12. The vehicle is then propelled to orbit entirely by rocket propulsion. After re-entry, the vehicle descends under gliding flight to a runway landing on its own undercarriage.

5.11.3 Performance Results

The calculated Payload Mass Ratio is shown plotted in Figure 5.25 in the standard graphical presentation.

Examination of Figure 5.25 shows that to achieve our design point Payload Mass Ratio of 2 %, that the maximum allowable Vehicle Mass Ratio must not exceed 18.6 %. This value is more than double the Vehicle Mass Ratio value of 9 % for Vehicle No.4, which is the most comparable vehicle but which employs subsonic combustion air-breathing propulsion. Thus, at this stage of the analysis, it appears that the use of air-breathing propulsion to very high Mach numbers could alleviate considerably the vehicle mass ratio constraints. However, we know that such a vehicle must carry a very high volume of liquid hydrogen, which has a very low density. Thus, we can expect that the vehicle size, and therefore its mass, will also be larger and will consume the allowable higher vehicle mass ratio. Furthermore, because this vehicle has to fly at low altitude to very high Mach numbers to develop enough thrust, the aerodynamic drag losses are considerably high, amounting to 2250 m/s for this design case. The gravity loss amounts to 800 m/s. Thus, the total velocity losses amount to 3050 m/s, giving a total velocity increment of 10522 m/s, which is 41 % of the theoretical velocity increment of 7472 m/s for this mission, of which a massive 30.1 % comprises the drag loss. This value can be compared for example, with a total velocity loss of 17.66 %, equivalent to a total velocity increment of 8792 m/s for Vehicle No.1, which is the vertically launched, rocket-propelled vehicle. Furthermore, the low altitude flight to Mach 12 results in high aerodynamic heating and the vehicle has to have additional thermal protection. Again, this adds more mass to the vehicle. The impact on vehicle mass of using air-breathing propulsion to very high Mach numbers is quantified in Chapter 6.2: Air-Breathing Propulsion.

Figure 5.20
Configuration of Reusable Launcher No.7:
SSTO-RA(Sup)-HLHL (Undercarriage-Launched)

(Derived from Reference 8)

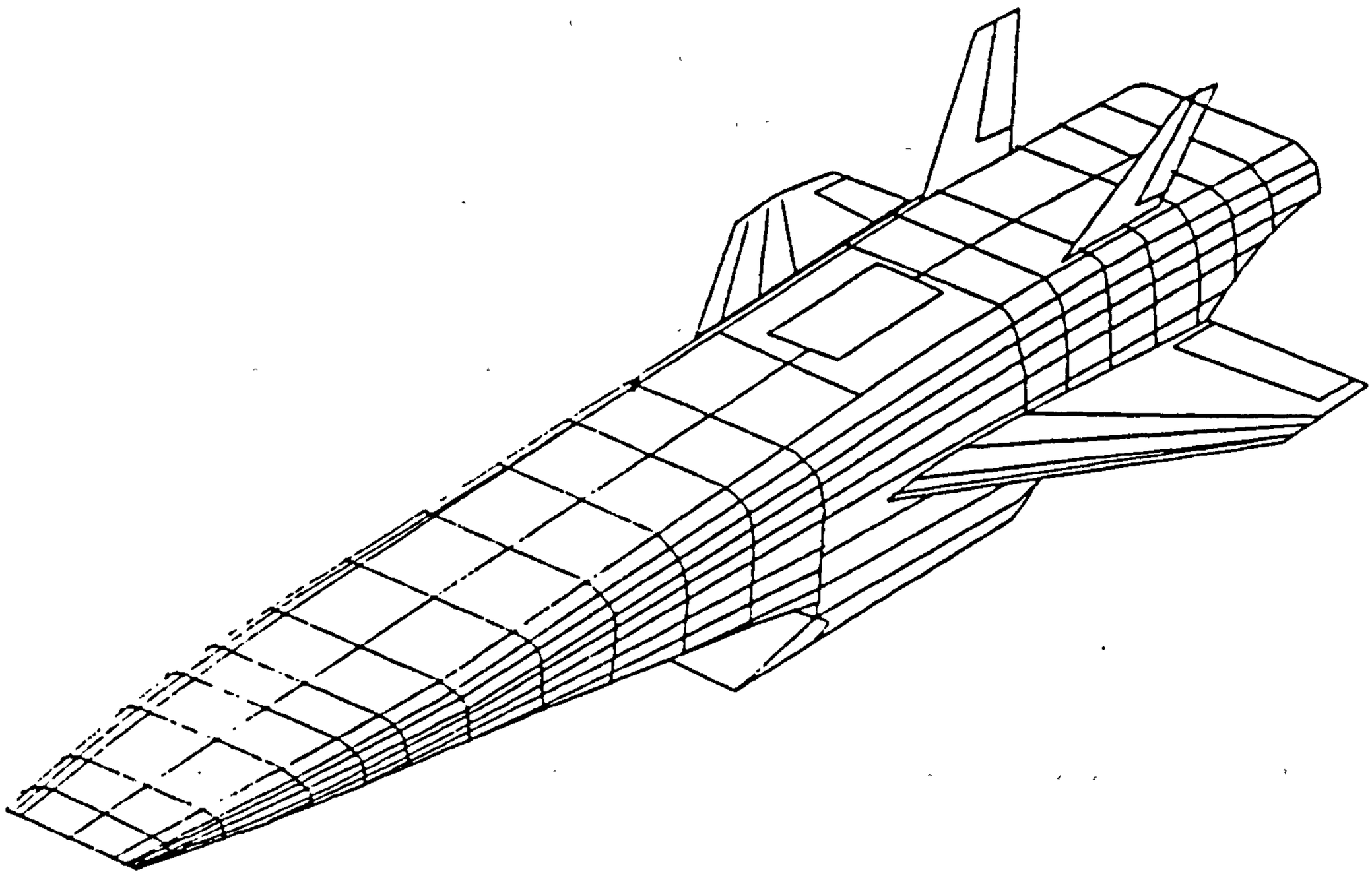

Length: 81.5 m.
Width: 23.5 m.
Lift-Off Mass: 350 tonnes
Lift-Off Thrust: 1750 KN
Aerodynamic Reference Area 649 m^2

Figure 5.21

Reusable Launcher No.7:

SSTO-RA(Sup)-HLHL (Undercarriage-Launched)

Aerodynamic Characteristics

Aerodynamic Reference Area = 649 m²

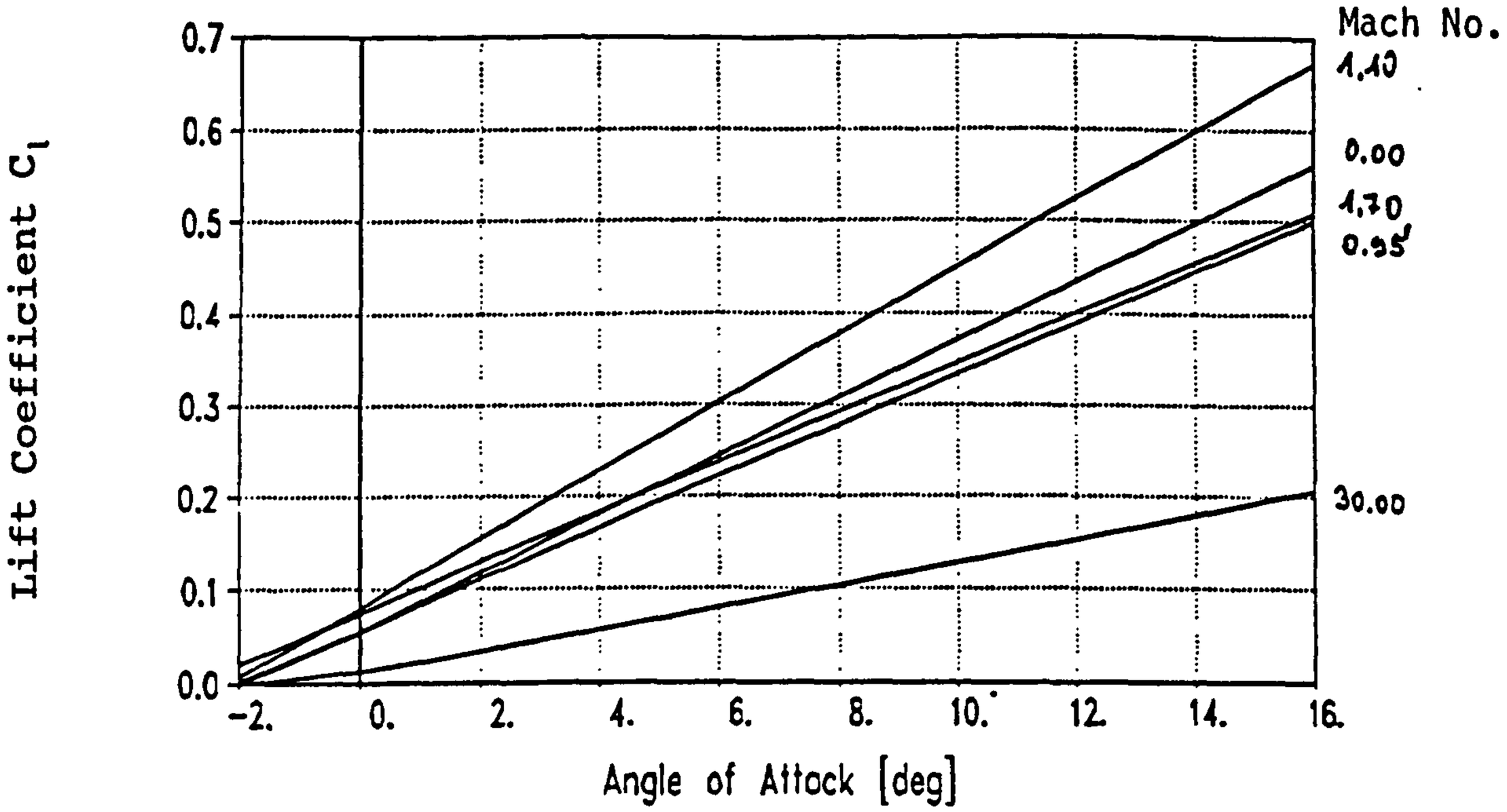

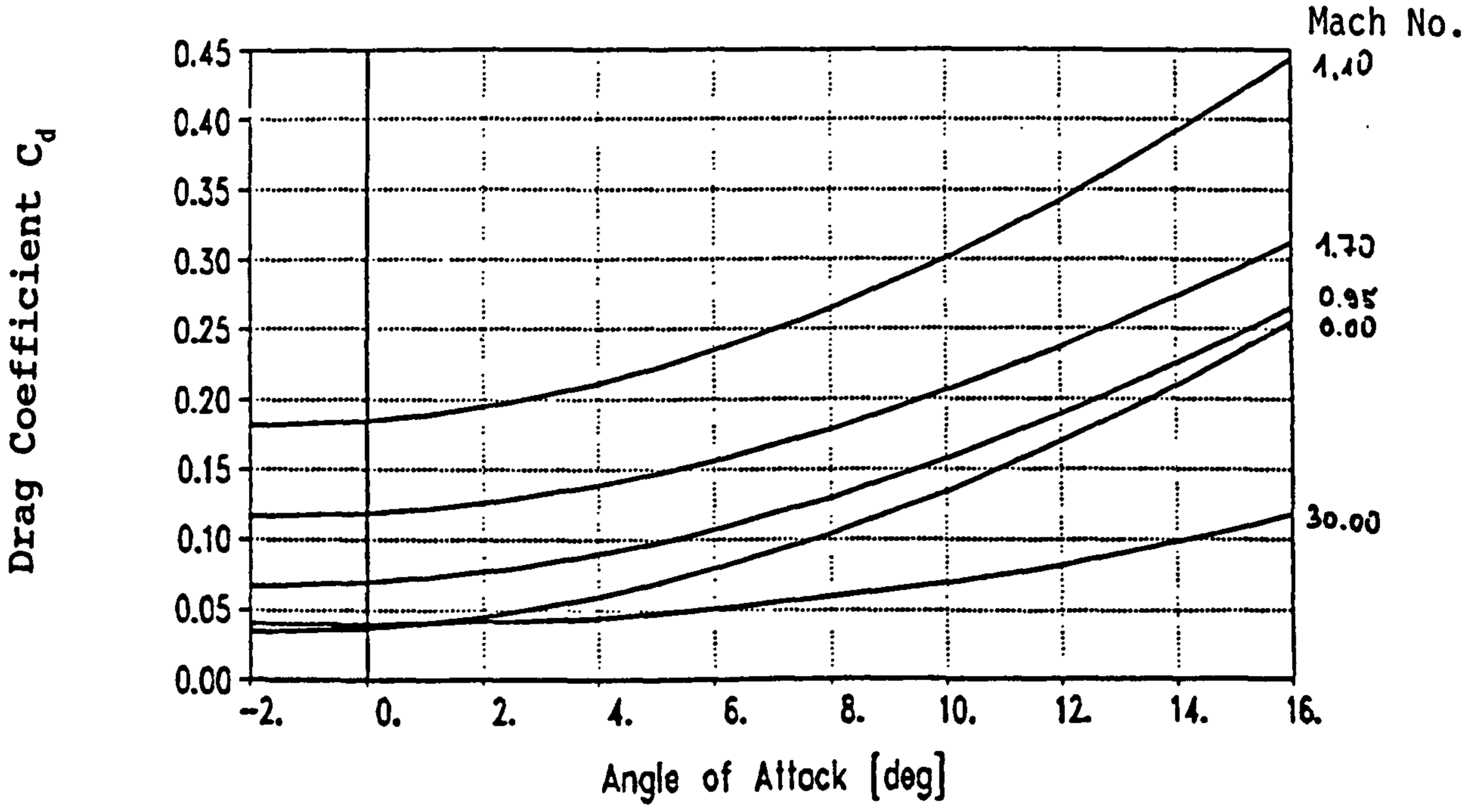

Figure 5.22

Reusable Launcher No.7:

SSTO-RA(Sup)-HLHL (Undercarriage-Launched)

Air Ejector Engine Performance Characteristics

(Data from Reference 8)

Mach Ma[-]	Incidence α[deg]	Dyn. Press. Q[kPa]	Ejector Mass Flow m_{ej}[kg/s]	Ejector Thrust. $F_{ej,x}$[kN]
0.0	2.0	45.0	300.0	811.6
0.0	2.0	45.0	600.0	1623.1
0.0	2.0	45.0	1000.0	2705.2
0.0	2.0	65.0	300.0	778.6
0.0	2.0	65.0	600.0	1557.1
0.0	2.0	65.0	1000.0	2595.2
0.0	6.0	45.0	300.0	1029.7
0.0	6.0	45.0	600.0	2059.4
0.0	6.0	45.0	1000.0	3432.3
0.0	6.0	65.0	300.0	987.8
0.0	6.0	65.0	600.0	1975.7
0.0	6.0	65.0	1000.0	3292.8
0.5	2.0	45.0	300.0	747.7
0.5	2.0	45.0	600.0	1559.2
0.5	2.0	45.0	1000.0	2641.3
0.5	2.0	65.0	300.0	692.7
0.5	2.0	65.0	600.0	1471.3
0.5	2.0	65.0	1000.0	2509.3
0.5	6.0	45.0	300.0	906.1
0.5	6.0	45.0	600.0	1935.8
0.5	6.0	45.0	1000.0	3308.8
0.5	6.0	65.0	300.0	819.9
0.5	6.0	65.0	600.0	1807.8
0.5	6.0	65.0	1000.0	3124.9
1.0	2.0	45.0	300.0	151.8
1.0	2.0	45.0	600.0	963.3
1.0	2.0	45.0	1000.0	2045.4
1.0	2.0	65.0	300.0	-108.6
1.0	2.0	65.0	600.0	670.0
1.0	2.0	65.0	1000.0	1708.0
1.0	6.0	45.0	300.0	-246.6
1.0	6.0	45.0	600.0	783.0
1.0	6.0	45.0	1000.0	2156.0
1.0	6.0	65.0	300.0	-746.8
1.0	6.0	65.0	600.0	241.0
1.0	6.0	65.0	1000.0	1558.2
1.5	2.0	45.0	300.0	414.5
1.5	2.0	45.0	600.0	1226.1
1.5	2.0	45.0	1000.0	2308.2
1.5	2.0	65.0	300.0	244.7
1.5	2.0	65.0	600.0	1023.3
1.5	2.0	65.0	1000.0	2061.4
1.5	6.0	45.0	300.0	261.7
1.5	6.0	45.0	600.0	1291.4
1.5	6.0	45.0	1000.0	2664.3
1.5	6.0	65.0	300.0	-56.0
1.5	6.0	65.0	600.0	931.9
1.5	6.0	65.0	1000.0	2249.0
2.0	2.0	45.0	300.0	543.5
2.0	2.0	45.0	600.0	1355.1
2.0	2.0	45.0	1000.0	2437.2

Figure 5.23A

Reusable Launcher No.7:

SSTO-RA(Sup)-HLHL (Undercarriage-Launched)
Ramjet Engine Fuel Flow versus Mach Number

(Data from Reference 8)

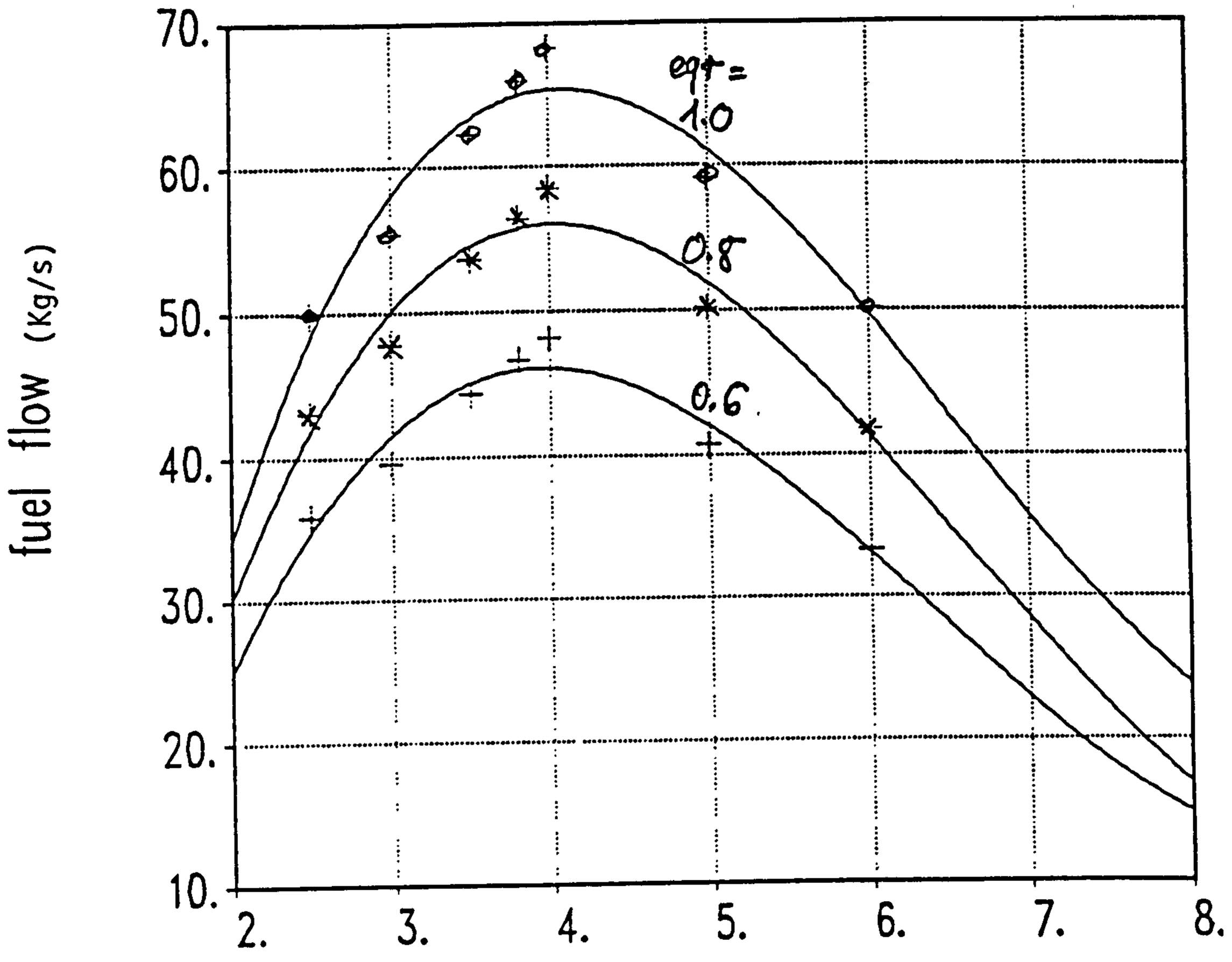

alfa = 2.000E+00 (degrees) qdyn = 4.500E+01 (kPa)

eqr =
⊕ 1.0
* 0.8
\+ 0.6

alfa = angle of attack (degrees)
qdyn = dynamic pressure (kPa)
eqr = equivalence ratio

Figure 5.23B

Reusable Launcher No.7:

SSTO-RA(Sup)-HLHL (Undercarriage-Launched)
Ramjet Engine Thrust versus Mach Number

(Data from Reference 8)

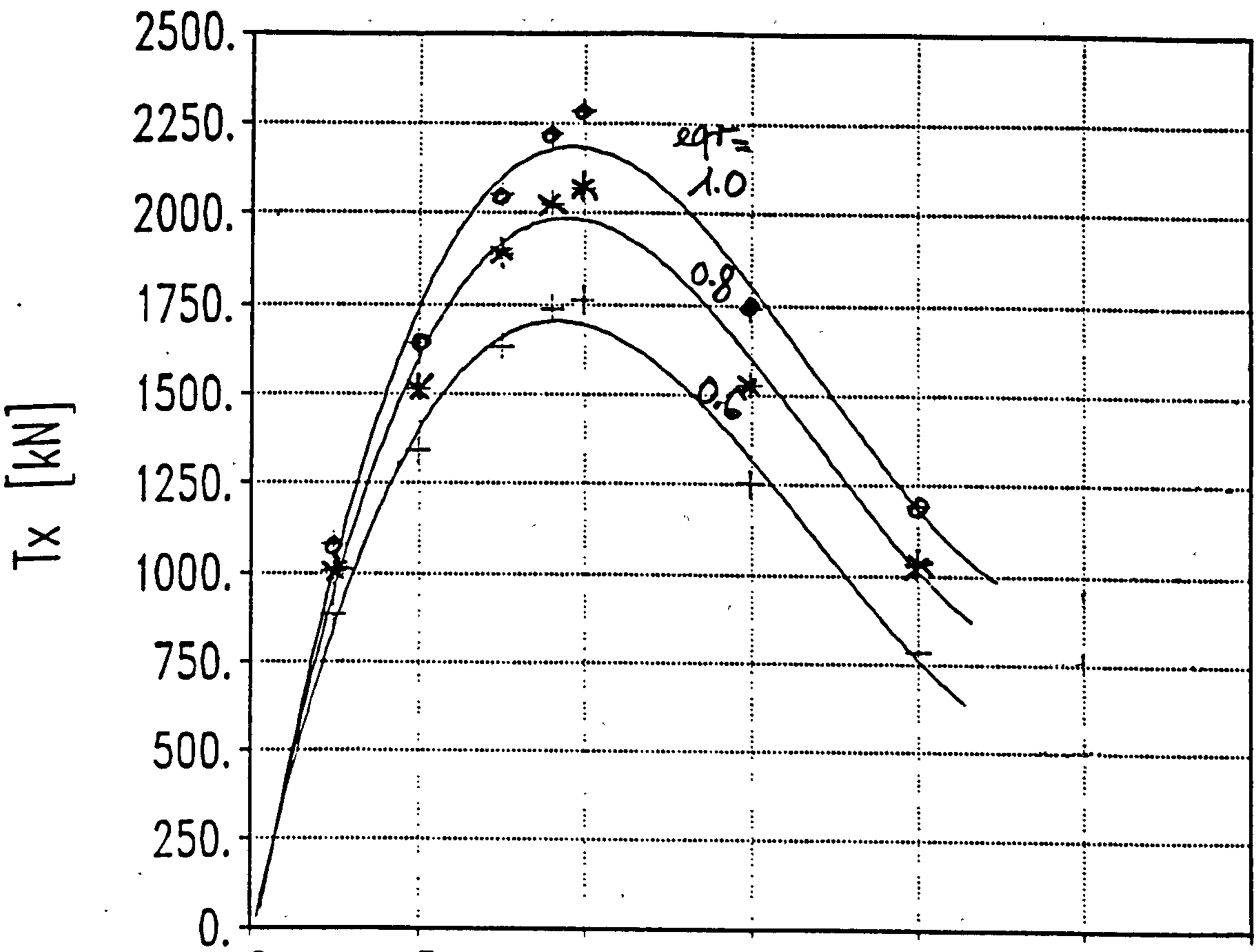

alfa = 2.000E+00 (degrees) qdyn = 4.500E+01 (kPa)

eqr =

◆ 1.0

✱ 0.8

\+ 0.6

alfa = angle of attack (degrees)
qdyn = dynamic pressure (kPa)
eqr = equivalence ratio

Figure 5.24A

Reusable Launcher No.7:

SSTO-RA(Sup)-HLHL (Undercarriage-Launched)
Scramjet Engine Fuel Flow versus Mach Number

(Data from Reference 8)

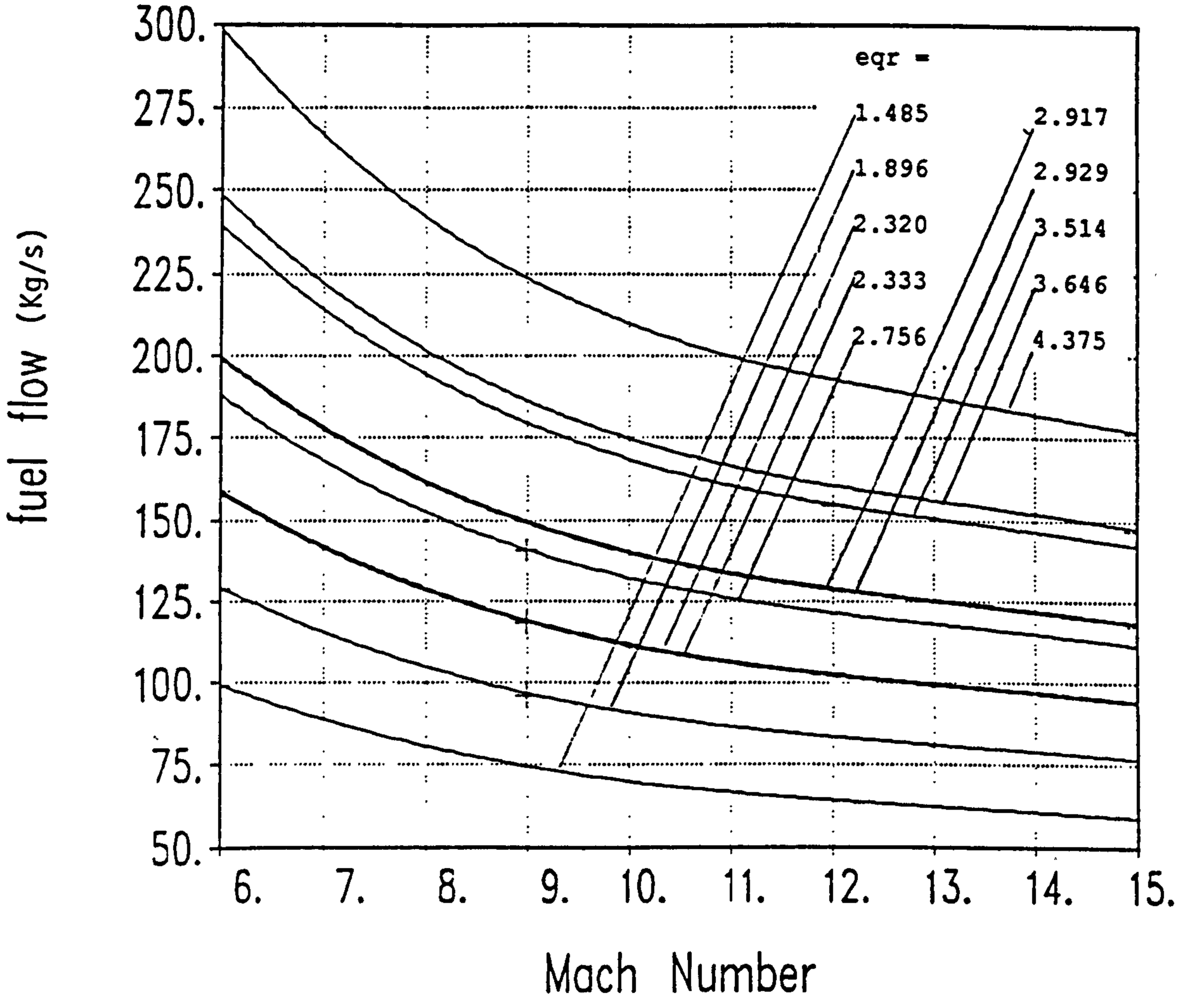

alfa = 2.000E+00 (degrees) qdyn = 4.500E+01 (kPa)

alfa = angle of attack (degrees)
qdyn = dynamic pressure (kPa)
eqr = equivalence ratio

Figure 5.24B

Reusable Launcher No.7:

SSTO-RA(Sup)-HLHL (Undercarriage-Launched)
Scramjet Engine Thrust versus Mach Number

(Data from Reference 8)

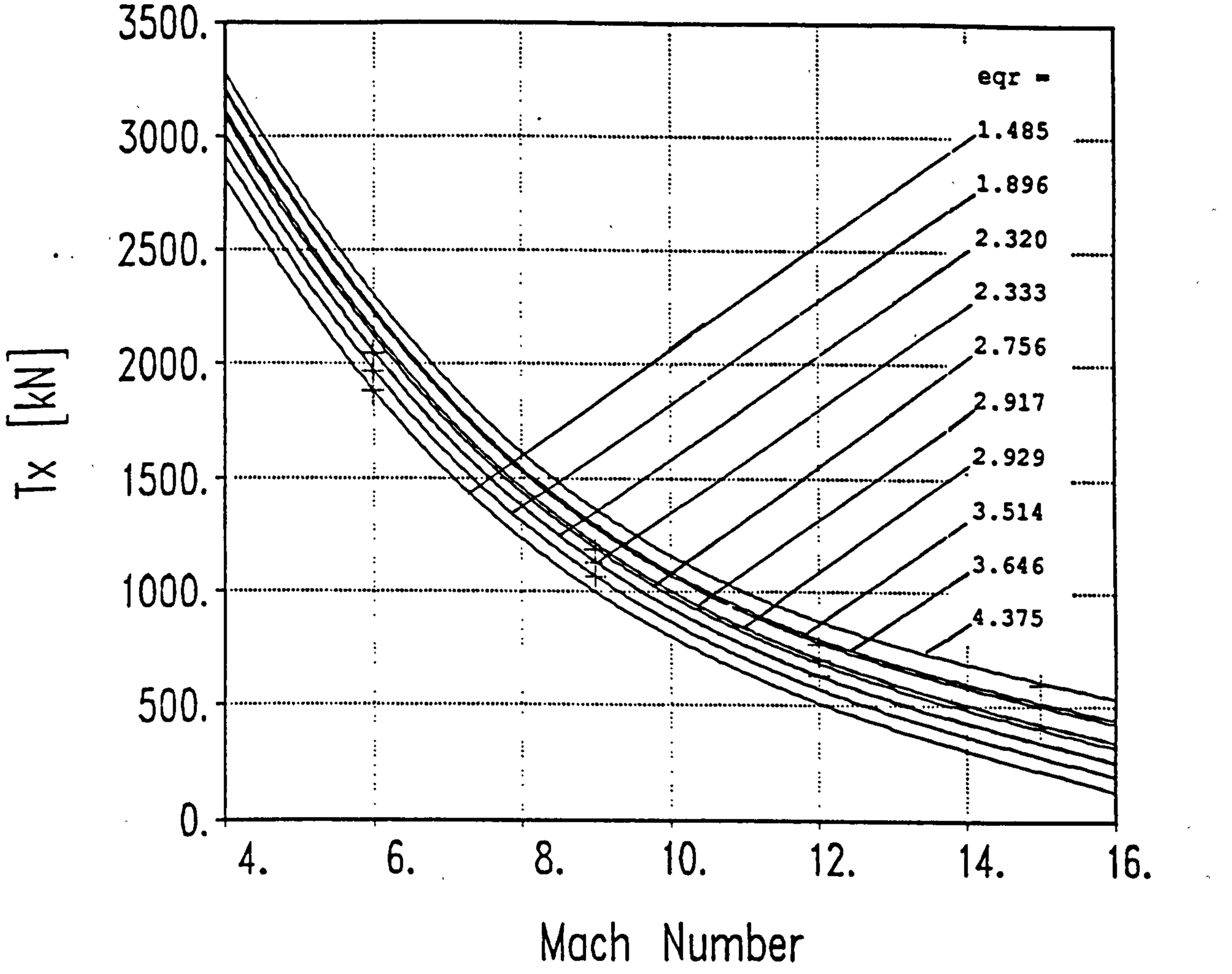

alfa = 2.000E+00 (degrees) qdyn = 4.500E+01 (kPa)

alfa = angle of attack (degrees)
qdyn = dynamic pressure (kPa)
eqr = equivalence ratio

Figure 5.25

Reusable Launcher No.7: SSTO-RA(Sup)-HLHL (Undercarriage)

Payload Mass Ratio Versus Vehicle Mass Ratio

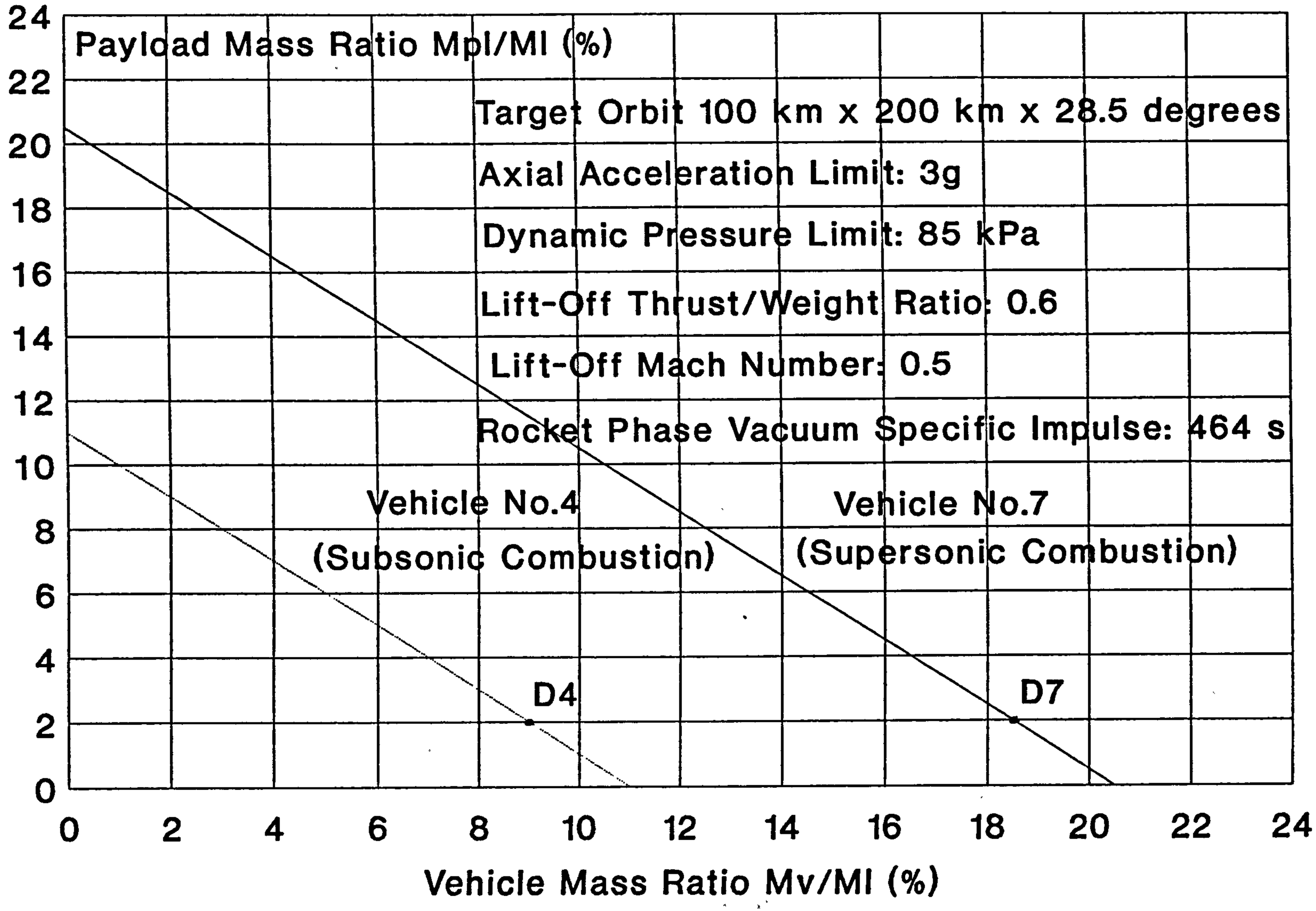

5.12 Performance of Reusable Launcher No.8: TSTO-RA(Sub)-HLHL(Sub) (Air-Launched)

This launcher is a two-stage-to-orbit, rocket and air-breathing propelled, horizontally-launched and horizontally landed vehicle. The air-breathing propulsion mode is subsonic. Separation of the stages is at subsonic speed. The vehicle is air-launched.

5.12.1 Vehicle Configuration

This is the first of the TSTO vehicles which employs both rocket and air-breathing propulsion and lifting flight. This vehicle is also unique amongst the candidate vehicles because, although it is a two stage vehicle, the lower stage is a conventional subsonic aircraft employing turbojet engines and the upper stage is entirely rocket propelled. Thus, this vehicle concept can also be classified as a single stage rocket-propelled vehicle which is air-launched. Therefore, in this performance analysis, this vehicle is treated simply as an air-launched, rocket-propelled, lifting, SSTO. For performance comparison reasons, the configuration of this vehicle is identical to that evaluated in Reference 11.

The motivation for investigating this vehicle is to determine the Payload Mass Ratio gains that could be achieved by launching the vehicle at altitude and with an initial velocity and also through savings in the undercarriage mass, which now needs only to be sized for the landing mass of the Second Stage.

The Second Stage is carried on the back of the First Stage, which is the carrier aircraft. The Second Stage vehicle configuration adopted for this analysis is shown in Figure 5.26. Because it is rocket-propelled and air launched, the body is less slender than that of the ground launched, rocket and air-breathing propelled Vehicles 4, 5 and 6. The aerodynamic characteristics are shown in Figure 5.27.

5.12.2 Ascent and Descent Trajectories

For the purposes of this analysis, the ascent trajectory starts at the separation point of the Second Stage from the carrier aircraft, flying due East, at an altitude of 8 km and a speed of Mach 0.6, which is 665 m/s at this altitude. The ascent then comprises three flight phases. Flight Phase 1 is a rapid pull-up manoeuvre from the nominal horizontal flight direction at separation, to a 20 degrees flight path angle. Flight Phase 2 is a climbing and accelerating flight with a variable, optimised pitch-over rate, until the perigee altitude and velocity of the transfer orbit are reached with the vehicle flying almost horizontally. The vehicle re-enters and descends under an aerodynamically controlled gliding flight and lands horizontally on its own undercarriage.

5.12.3 Performance Results

The calculated performance results are shown in the standard graphical presentation in Figure 5.28.
Examination of Figure 5.28 shows that for this air-launched vehicle, to achieve our design point Payload Mass Ratio of 2 %, the Vehicle Mass Ratio must not be more than 12.2 % (point D8 on Figure 5.28). This value can be compared with that of Vehicle No.4, which is the equivalent vehicle that is ground-launched on its own undercarriage, requiring a very demanding Vehicle Mass Ratio of 9.1 % (point D4 on Figure 5.28). This 4.1 % difference in the Vehicle Mass Ratios means that the

Figure 5.26
Configuration of Reusable Launcher No.8:
TSTO-RA(Sub)-HLHL (Air-Launched)

(Derived from Reference 11)

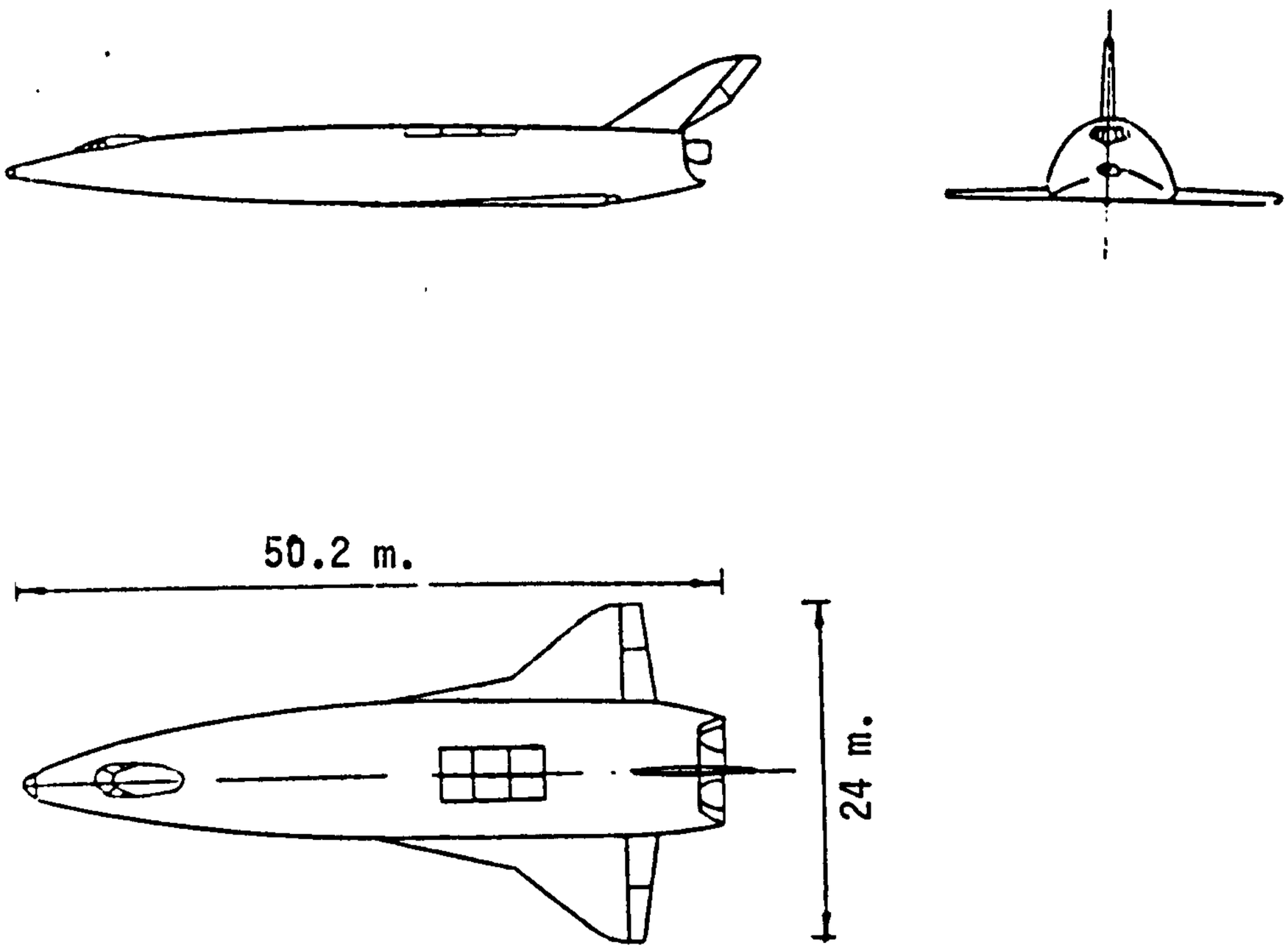

Length: 50.2 m.
Width: 24 m.
Lift-Off Mass: 350 tonnes
Lift-Off Thrust: 3500 KN
Aerodynamic Reference Area: 238 m^2

Figure 5.27

Lift and Drag Coefficients for Stage 2
of Reusable Launcher No.8

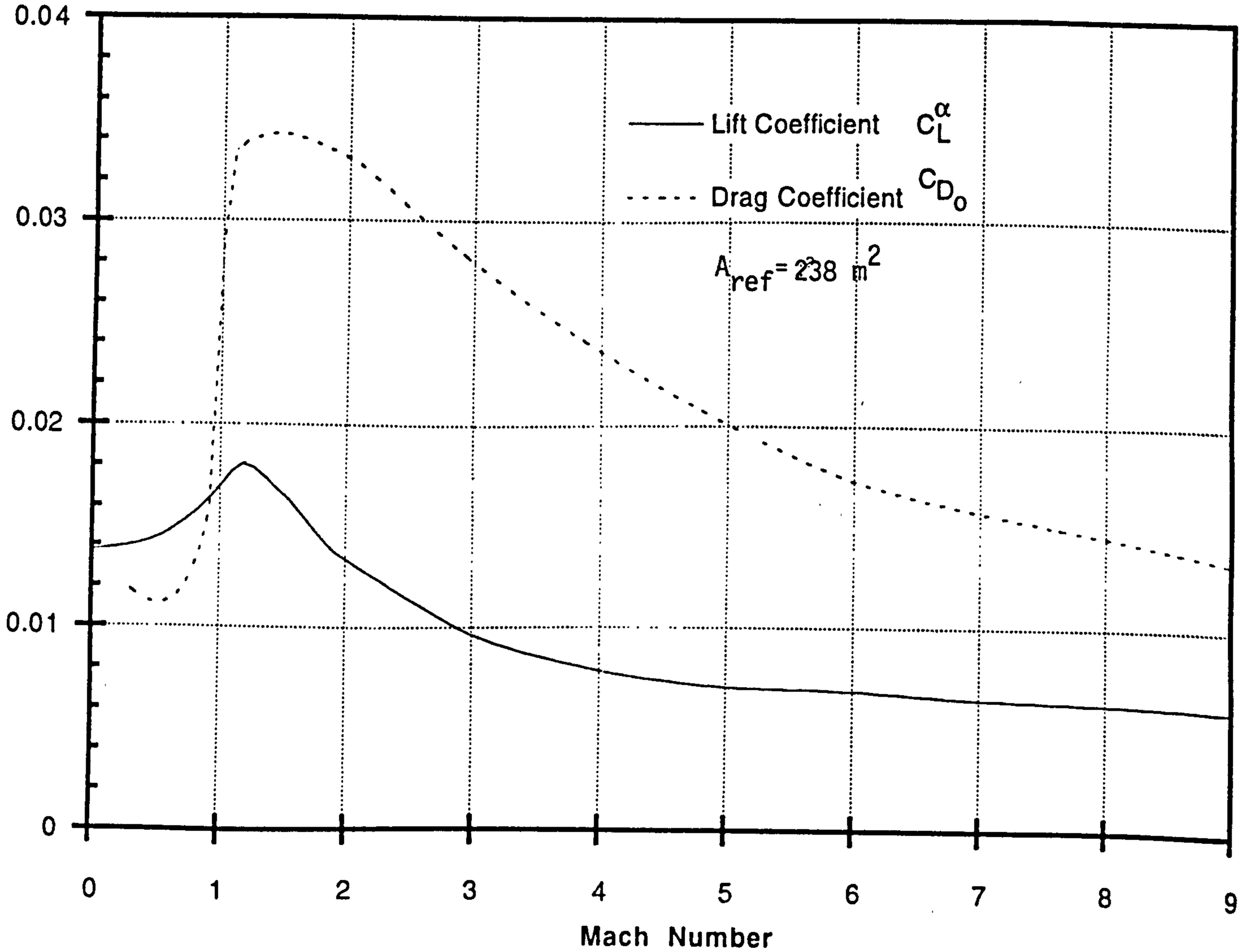

Figure 5.28

Reusable Launcher No.8: TSTO-RA(Sub)-HLHL (Air-Launch)

Payload Mass Ratio Versus Vehicle Mass Ratio

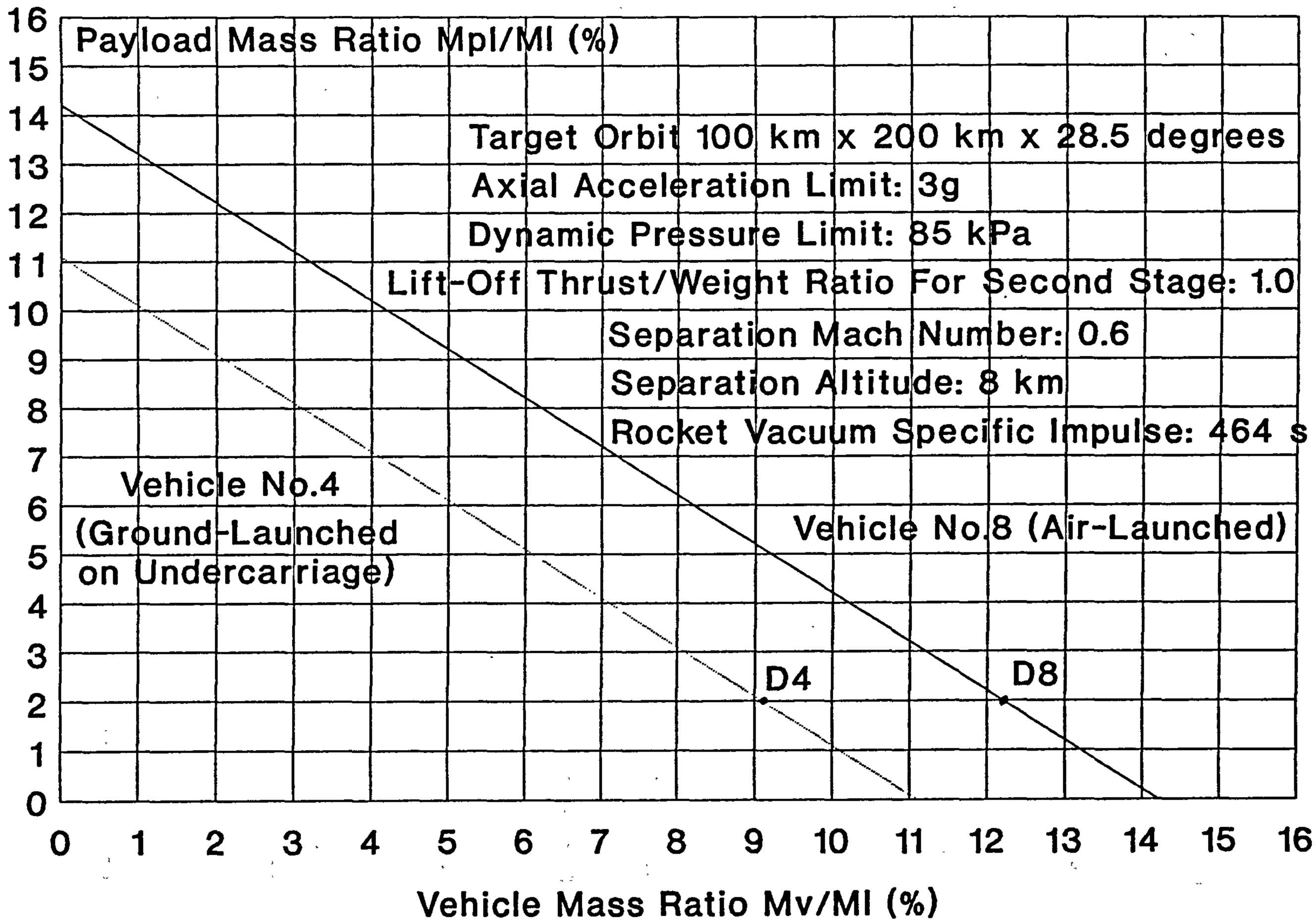

air-launched vehicle has a much higher potential to be able to deliver a positive payload mass and this is assessed later in this Chapter.

5.13 Performance of Reusable Launcher No.9: TSTO-RA(Sub)-HLHL(Sup) (Undercarriage-Launched)

This launcher is a two-stage-to-orbit, rocket and air-breathing propelled, horizontally launched and horizontally landed vehicle. The air-breathing combustion mode is subsonic. Separation of the stages is at supersonic speed. The vehicle is undercarriage-launched.

5.13.1 Vehicle Configuration

In common with Vehicle No.8, this vehicle is also a TSTO which employs both rocket and subsonic combustion air-breathing propulsion, takes-off and lands horizontally and employs lifting flight for both ascent and descent. The fundamental difference however, is that unlike Vehicle No.8, which separates its stages at subsonic speed, for this vehicle, the stage separation takes place at supersonic speed.

The First Stage is propelled by a set of combined cycle turbofan-ramjet engines (turboramjets). The Second Stage is propelled by rocket engines. In the launch configuration, the Second Stage is mounted on the back of the First Stage in a highly integrated, blended design. The composite vehicle takes-off horizontally on its own integral undercarriage. After stage separation, the First Stage flies back under its turboramjet power to make a runway landing. The Second Stage ascends to orbit under rocket propulsion and lifting flight. The descent mode of the Second Stage is a gliding flight under aerodynamic control and the landing mode is horizontal using its own integral undercarriage.

The vehicle configuration adopted is that developed by DASA in Phase 4 of the ESA Winged Launcher Configuration Study Reference 9). This configuration, shown in Figure 5.29, has itself been derived from the DASA Saenger vehicle. The First Stage has a conical body of elliptical cross section, with a long forebody, to provide a high degree of external compression of the air for the turboramjet engines. The wing is a delta configuration blended to the body. Aerodynamic control is achieved by twin tails and by wing ailerons. The turboramjet engines are located in a rectangular pod under the body and utilise the aft underside of the body as an external expansion nozzle. The Second Stage has a conical body of circular cross section and a delta wing mounted low on the body. Aerodynamic control is achieved by twin tails, rudders and wing ailerons. The drag and lift coefficients for the composite vehicle and for the separate stages are shown in Figures 5.30 and 5.31 respectively.

5.13.2 Ascent and Descent Trajectories

The ascent trajectory comprises 4 flight phases. Phase 1 starts with the take-off run of the vehicle on its own undercarriage, propelled by its turboramjet engines operating in the turbofan mode. Phase 2 begins with the rotation in pitch of the vehicle until it lifts off under turbofan propulsion. Phase 3 begins with the progressive transition from turbofan to ramjet mode. Phase 4 begins with the ascent of the Second Stage to orbit under rocket propulsion after its separation from the First Stage.

5.13.3 Performance Results

For this vehicle, a large computational effort has been necessary to derive an ascent trajectory that maximised the Orbital Mass. This effort resulted from the modelling difficulties for the ramjet engines. The turbojet and ramjet

performance data have been derived from Phase 4 of the ESA Winged Launcher Configuration Study (Reference 9). Samples of the fuel flow and thrust characteristics as functions of Mach number, incidence angle and equivalence ratio are shown in Figure 5.32 to Figure 5.35 respectively.

The optimised flight path results for this vehicle are:
- Phase 1 to Phase 2 transition: Mach 0.5; Altitude 0 km;
- Phase 2 to Phase 3 transition: Mach 3; Altitude 19.7 km;
- Phase 3 to Phase 4 transition: Mach 6.6; Altitude 33.7 km;

The Payload Mass Ratio calculated for this vehicle, plotted in the standard graphical form, is shown in Figure 5.36.

Examination of Figure 5.36 shows that to achieve our Payload Mass Ratio design point of 2 %, that the Vehicle Mass Ratio has an extremely high allowable value of 49.9 % (point D9 on Figure 5.36). This result can be compared with that of Vehicle No.3, the TSTO, rocket-propelled, vertically launched vehicle, in which the maximum allowable Vehicle Mass Ratio is 17.4 % for a 2 % design point Payload Mass Ratio value (point D3 on Figure 5.36).

Figure 5.26 also shows that although the slope of the performance curves is the same for Vehicles 3 and 9, that the Payload Mass Ratio of Vehicle 9 is very much larger over the whole of the Vehicle Mass Ratio range. The explanation for this is the use of air-breathing propulsion in the First Stage of Vehicle No.9, which has an average specific impulse about an order of magnitude higher than that of the rocket propulsion used in the First Stage of Vehicle No.3.

The very high allowable Vehicle Mass Ratio for Vehicle No.9, could, at first sight, lead one to conclude that this vehicle is much less sensitive to Vehicle Mass than all the other candidate vehicles. However, reflection on this matter

reveals that this vehicle must inherently have a much higher vehicle mass because air-breathing propulsion systems are very heavy, with thrust/weight ratios in the range of 5 to 10 compared with rocket engines which have thrust/weight values in the range 80 to 100. Furthermore, this vehicle also has an integral undercarriage for each stage and these are heavy systems with a statistical mass ratio value of 3.5 % of the stage launch mass. Thus, simply put, although Vehicle No.9 has a high allowable Vehicle Mass Ratio, most of it will be needed to make a practical vehicle. Just how much is needed, will be assessed later in this Chapter.

Figure 5.29
Configuration of Reusable Launcher No.9:
TSTO-RA(Sub)-HLHL (Undercarriage-Launched)
(Derived from Reference 9)

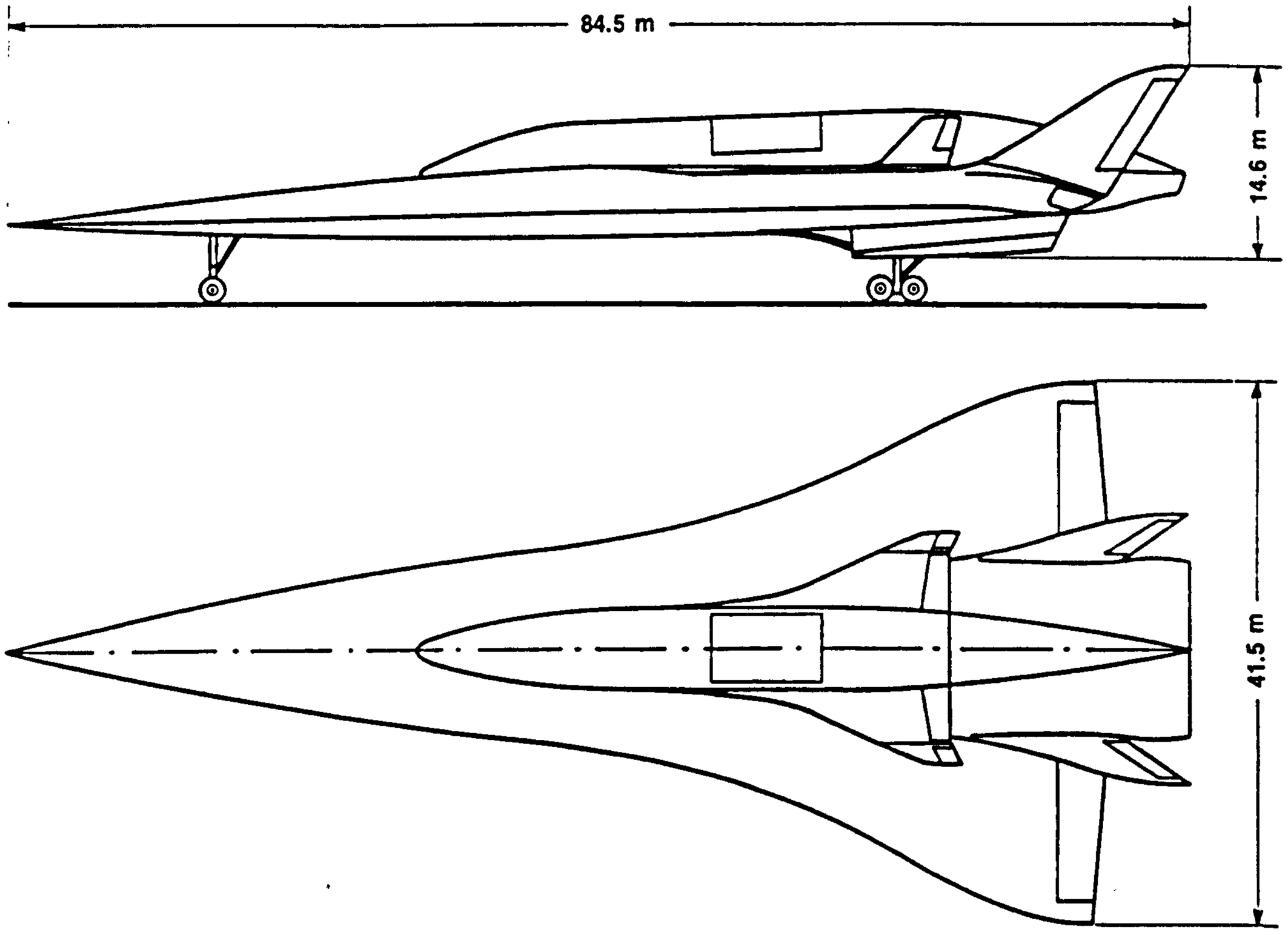

Length: 84.5
Width: 41.5 m.
Lift-Off Mass: 350 tonnes
Lift-Off Thrust: 1750 KN
Aerodynamic Reference Area Stage 1 = 1435m²
Stage 2 = 267.2m²
Combined Vehicle = 1550m²

Figure 5.30A

Aerodynamic Coefficients for Stage 1 and Composite Vehicle: Reusable Launcher No.9

(Data from Reference 9)

Ma Machnumber
α Incidence (AOA)
C_L Lift coefficient
C_D Drag coefficient
Aerodynamic Reference Area Stage 1 = 1435m²
Aerodynamic Reference Area Combined Vehicle = 1550m²

Ma	α[deg]	$C_{L,1}$	$C_{D,1}$	$C_{L,2}$	$C_{D,2}$
.300	1.20	.0000000	.0081000	.0000000	.0078000
	2.20	.0299200	.0085471	.0299200	.0082471
	3.20	.0608600	.0093600	.0608600	.0090600
	4.20	.0943500	.0110610	.0943500	.0107610
	5.20	.1298000	.0135500	.1298000	.0132500
	6.20	.1671000	.0168810	.1671000	.0165810
	8.70	.2678000	.0363100	.2678000	.0360100
	11.20	.3781000	.0747500	.3781000	.0744500
	13.70	.4962000	.1181000	.4962000	.1178000
	16.20	.6202000	.1743000	.6202000	.1740000
	21.20	.8781000	.3277000	.8781000	.3274000
	26.20	1.1350000	.5372000	1.1350000	.5369000
.600	1.20	.0000000	.0072000	.0000000	.0069000
	2.20	.0300300	.0076714	.0300300	.0073714
	3.20	.0610600	.0085070	.0610600	.0082070
	4.20	.0946000	.0102210	.0946000	.0099210
	5.20	.1300000	.0127310	.1300000	.0124310
	6.20	.1673000	.0161110	.1673000	.0158110
	8.70	.2679000	.0353800	.2679000	.0350800
	11.20	.3777000	.0738100	.3777000	.0735100
	13.70	.4952000	.1170000	.4952000	.1167000
	16.20	.6185000	.1730000	.6185000	.1727000
	21.20	.8744000	.3255000	.8744000	.3252000
	26.20	1.1290000	.5335000	1.1290000	.5332000

Suffix 1 = Stage 1, Suffix 2 = Combined Vehicle

Figure 5.30B

Aerodynamic Coefficients for Stage 1 and Composite Vehicle: Reusable Launcher No.9

(Data from Reference 9)

Ma	α[deg]	$C_{L,1}$	$C_{D,1}$	$C_{L,2}$	$C_{D,2}$
.900	1.20	.0000000	.0069000	.0000000	.0065000
	2.20	.0317700	.0073953	.0317700	.0069953
	3.20	.0645500	.0082870	.0645500	.0078870
	4.20	.0998800	.0101400	.0998800	.0097400
	5.20	.1371000	.0128440	.1371000	.0124440
	6.20	.1762000	.0164530	.1762000	.0160530
	8.70	.2814000	.0365200	.2814000	.0361200
	11.20	.3958000	.0766700	.3958000	.0762700
	13.70	.5177000	.1217000	.5177000	.1213000
	16.20	.6454000	.1798000	.6454000	.1794000
	21.20	.9093000	.3378000	.9093000	.3374000
	26.20	1.1700000	.5526000	1.1700000	.5522000
1.200	.00	-.0269500	.0161612	-.0269500	.0116612
	1.00	.0019260	.0157927	.0019260	.0112927
	2.00	.0284800	.0160308	.0284800	.0115308
	3.00	.0534200	.0170370	.0534200	.0125370
	4.00	.0773900	.0184530	.0773900	.0139530
	5.00	.1014000	.0203850	.1014000	.0158850
	7.50	.1632000	.0309200	.1632000	.0264200
	10.00	.2283000	.0509100	.2283000	.0464100
	12.50	.2897000	.0724200	.2897000	.0679200
	15.00	.3435000	.0973800	.3435000	.0928800
1.500	.00	-.0267900	.0161029	-.0267900	.0119029
	1.00	-.0034240	.0156270	-.0034240	.0114270
	2.00	.0183500	.0156887	.0183500	.0114888
	3.00	.0391300	.0164543	.0391300	.0122543
	4.00	.0592900	.0175940	.0592900	.0133940
	5.00	.0796200	.0192210	.0796200	.0150210
	7.50	.1323000	.0278300	.1323000	.0236300
	10.00	.1884000	.0441200	.1884000	.0399200
	12.50	.2455000	.0634300	.2455000	.0592300
	15.00	.2994000	.0870500	.2994000	.0828500
2.000	.00	-.0240900	.0132585	-.0240900	.0097585
	1.00	-.0030780	.0128246	-.0030780	.0093246
	2.00	.0165000	.0128809	.0165000	.0093809
	3.00	.0351800	.0135789	.0351800	.0100789
	4.00	.0533000	.0146180	.0533000	.0111180
	5.00	.0715800	.0161010	.0715800	.0126010
	7.50	.1190000	.0238600	.1190000	.0203600
	10.00	.1694000	.0384400	.1694000	.0349400
	12.50	.2207000	.0558000	.2207000	.0523000
	15.00	.2692000	.0770400	.2692000	.0735400

Figure 5.30C

Aerodynamic Coefficients for Stage 1 and Composite Vehicle: Reusable Launcher No.9

(Data from Reference 9)

Ma	α[deg]	$C_{L,1}$	$C_{D,1}$	$C_{L,2}$	$C_{D,2}$
3.000	.00	-.0244800	.0104557	-.0244800	.0079557
	1.00	-.0076980	.0099187	-.0076980	.0074187
	2.00	.0082230	.0097983	.0082230	.0072983
	3.00	.0237400	.0102466	.0237400	.0077466
	4.00	.0389900	.0109960	.0389900	.0084960
	5.00	.0545000	.0121540	.0545000	.0096540
	7.50	.0951600	.0183660	.0951600	.0158660
	10.00	.1390000	.0303100	.1390000	.0278100
	12.50	.1850000	.0454600	.1850000	.0429600
	15.00	.2316000	.0649800	.2316000	.0624800
5.000	.00	-.0222400	.0080053	-.0222400	.0059053
	1.00	-.0103600	.0074440	-.0103600	.0053440
	2.00	.0011810	.0071944	.0011810	.0050944
	3.00	.0127500	.0073940	.0127500	.0052940
	4.00	.0243000	.0078308	.0243000	.0057308
	5.00	.0361700	.0086030	.0361700	.0065030
	7.50	.0677700	.0130220	.0677700	.0109220
	10.00	.1024000	.0219000	.1024000	.0198000
	12.50	.1393000	.0336900	.1393000	.0315900
	15.00	.1786000	.0496000	.1786000	.0475000
7.000	.00	-.0213100	.0072580	-.0213100	.0052580
	1.00	-.0113500	.0065706	-.0113500	.0045706
	2.00	-.0015260	.0062099	-.0015260	.0042099
	3.00	.0085170	.0063370	.0085170	.0043370
	4.00	.0186700	.0067214	.0186700	.0047214
	5.00	.0291700	.0074790	.0291700	.0054790
	7.50	.0573900	.0114700	.0573900	.0094700
	10.00	.0886000	.0188000	.0886000	.0168000
	12.50	.1230000	.0295600	.1230000	.0275600
	15.00	.1606000	.0444500	.1606000	.0424500

Figure 5.31

Aerodynamic Coefficients for Stage 2 of Reusable Launcher No.9

(Data from Reference 9)

Aerodynamic Reference Area Stage 2 = 267.2m²
Suffix 3 = Stage 2

Ma	α[deg]	$C_{L,3}$	$C_{D,3}$
6.000	.00	-.0258800	.0274130
	2.00	-.0047570	.0259327
	4.00	.0184000	.0262027
	6.00	.0436600	.0284230
	8.00	.0707100	.0328330
	10.00	.0998700	.0396400
	15.00	.1816000	.0687500
	20.00	.2757000	.1185700
	25.00	.3776000	.1924400
8.000	.00	-.0246700	.0265150
	2.00	-.0057620	.0250349
	4.00	.0150900	.0251549
	6.00	.0380900	.0270750
	8.00	.0633400	.0310650
	10.00	.0909000	.0373600
	15.00	.1707000	.0652400
	20.00	.2644000	.1140900
	25.00	.3665000	.1870000
10.000	.00	-.0240100	.0258870
	2.00	-.0063600	.0244073
	4.00	.0131700	.0244373
	6.00	.0349500	.0262070
	8.00	.0592000	.0299670
	10.00	.0861000	.0360300
	15.00	.1654000	.0633900
	20.00	.2591000	.1117100
	25.00	.3613000	.1842400
30.000	.00	-.0178800	.0213200
	2.00	-.0103400	.0198204
	4.00	.0000777	.0192604
	6.00	.0137100	.0199504
	8.00	.0307300	.0222400
	10.00	.0514200	.0265100
	15.00	.1187000	.0483100
	20.00	.2054000	.0903600
	25.00	.3055000	.1570600

Figure 5.32

Turbojet Fuel flow Characteristics for Reusable Launcher No.9
(Data from Reference 9)

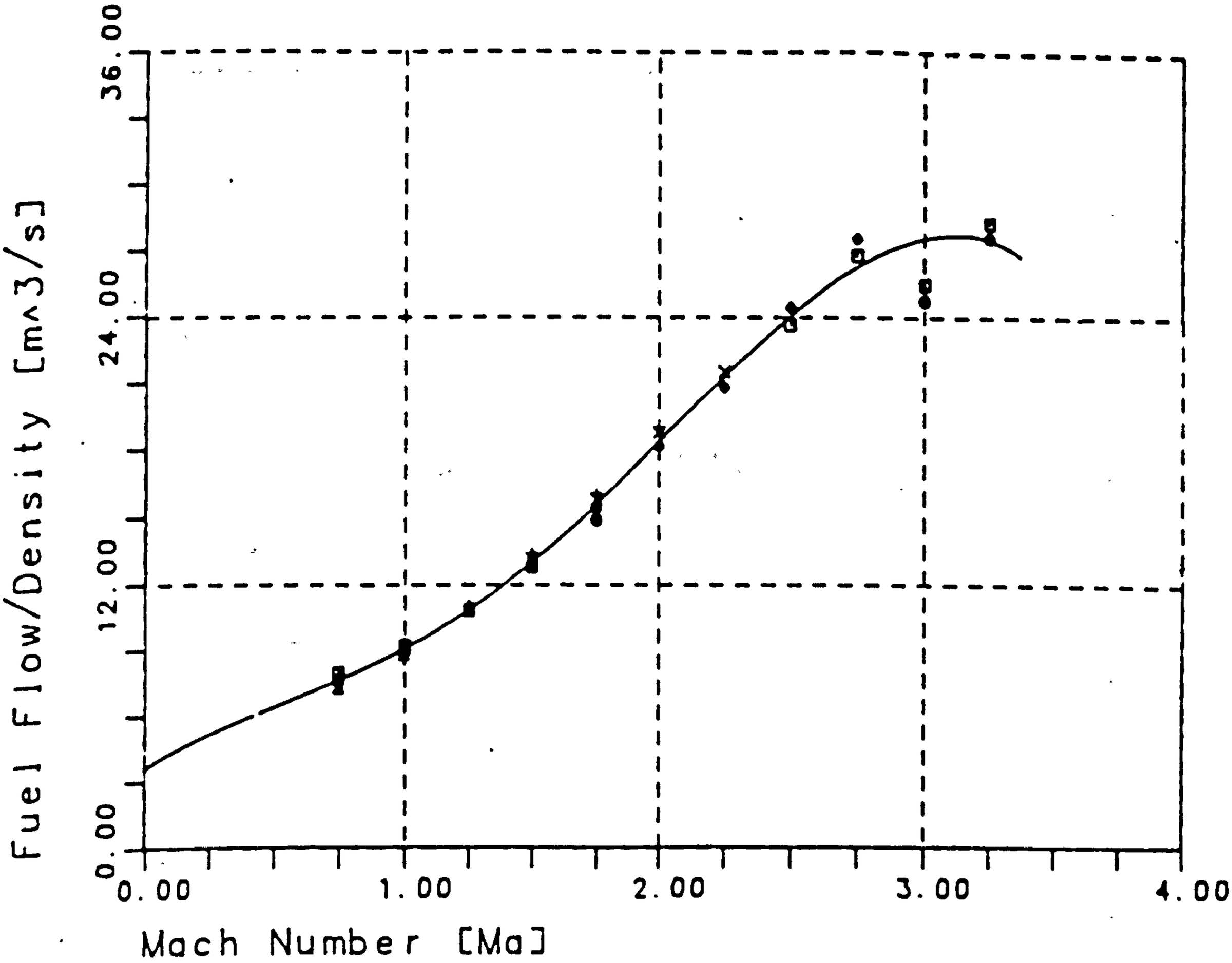

alfa: angle of attack (degrees)
EQR: equivalence ratio
Points are calculated values
Curve is from best-fit equations
Density is Air Density (Kg/m^3)

Figure 5.33

Turbojet Specific Impulse Characteristics for Reusable Launcher No.9
(Data from Reference 9)

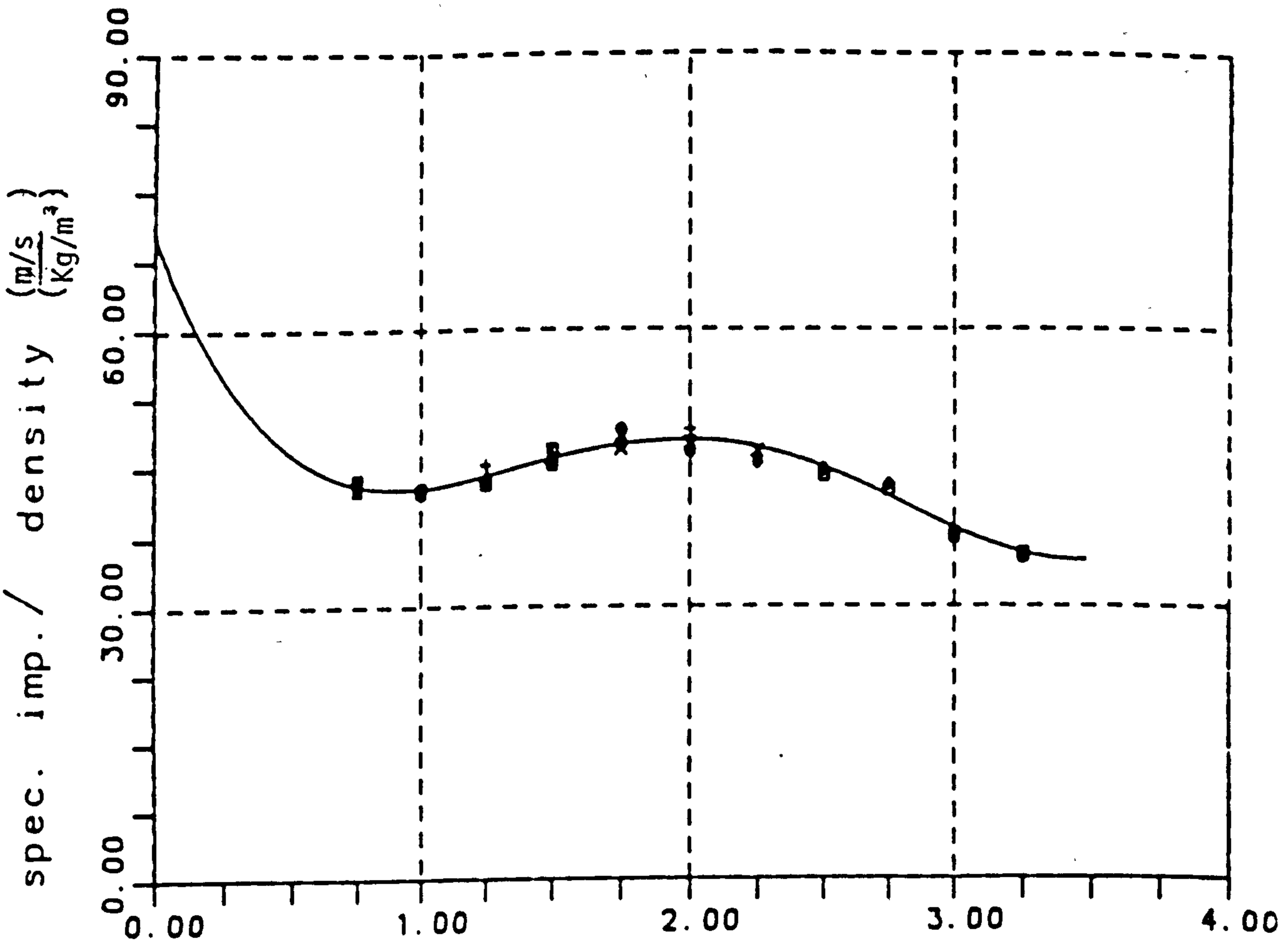

alfa = angle of attack (degrees)
EQR = equivalence ratio
Points are calculated values
Curve is from best-fit equation
Specific Impulse in m/s
Density is Air Density in Kg/m^3

Figure 5.34

Ramjet Fuel Flow Characteristics for Reusable Launcher No.9

(Data from Reference 9)

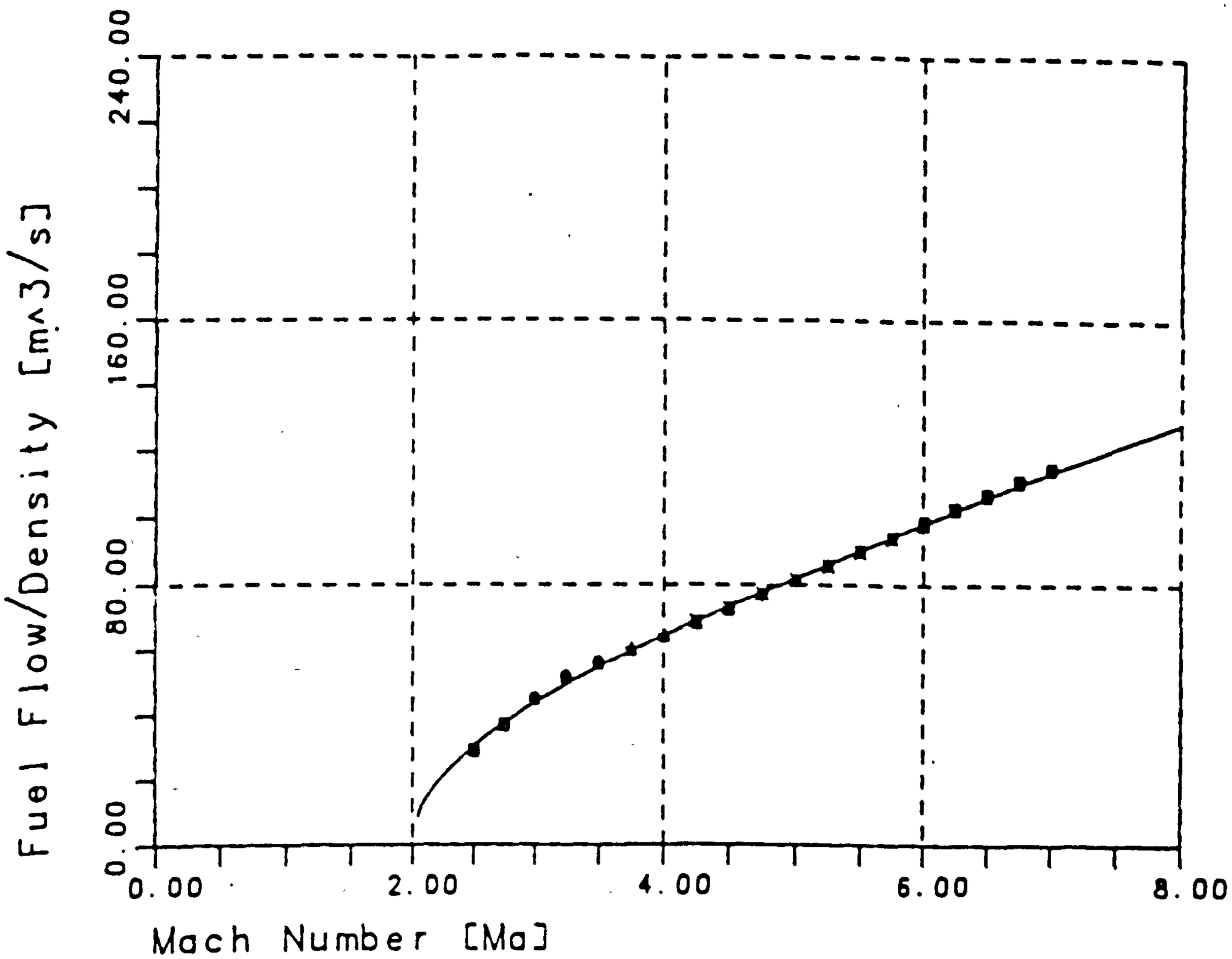

alfa=2 EQR=1

alfa = angle of attack (degrees)
EQR = equivalence ratio
Points are calculated values
Curve is from best-fit equation
Fuel Flow in Kg/s
Density is Air Density (Kg/m^3)

Figure 5.35

Ramjet Thrust Characteristics for Reusable Launcher No.9

(Data from Reference 9)

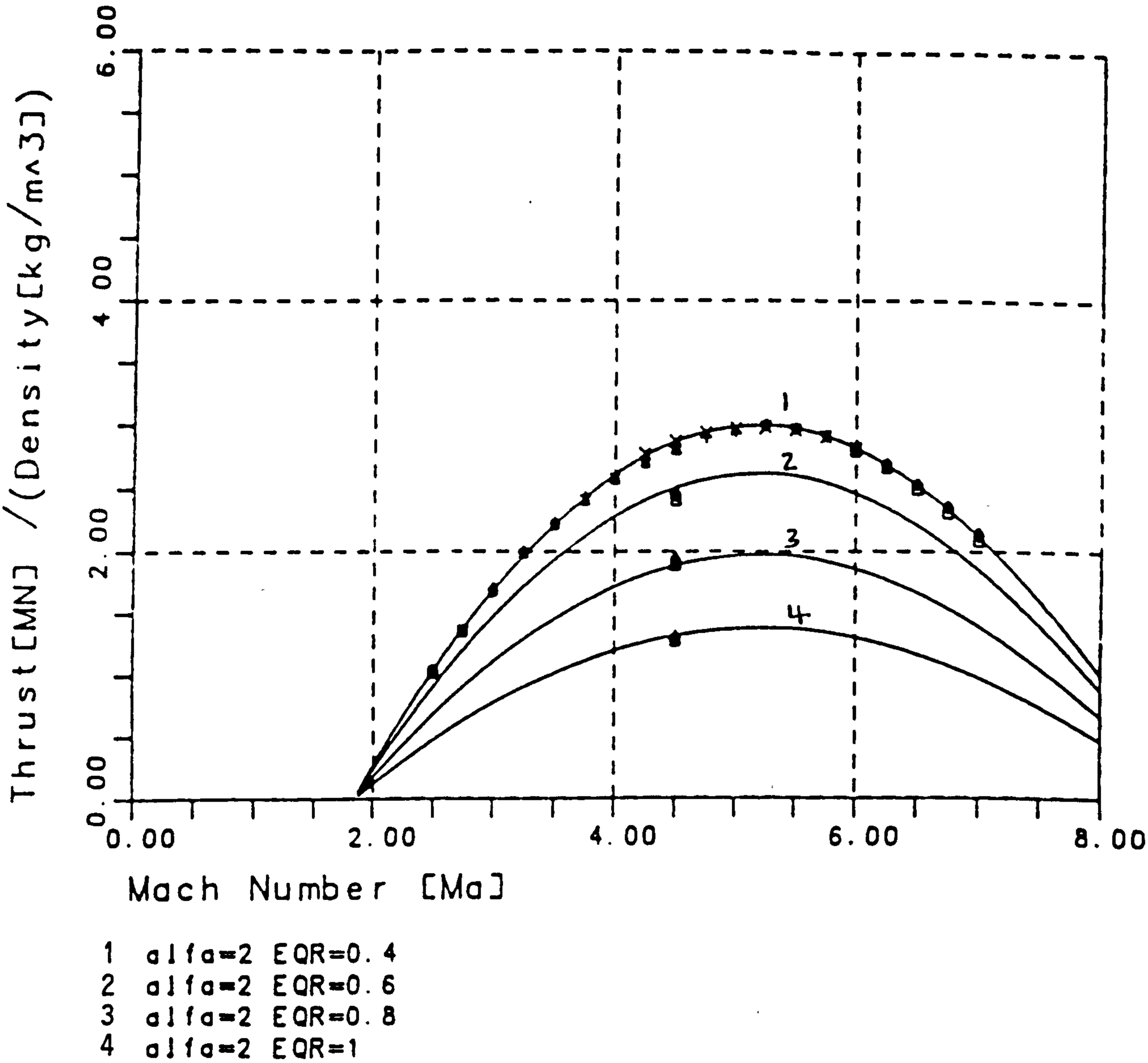

1 alfa=2 EQR=0.4
2 alfa=2 EQR=0.6
3 alfa=2 EQR=0.8
4 alfa=2 EQR=1

alfa = angle of attack (degrees)
EQR = equivalence ratio
Points are calculated values
Curve is from best-fit equation
Density is Air Density (Kg/m^3)

FIGURE 5.36

Reusable Launcher No.9: TSTO-RA(Sub)-HLHL (Undercarriage)

Payload Mass Ratio Versus Vehicle Mass Ratio

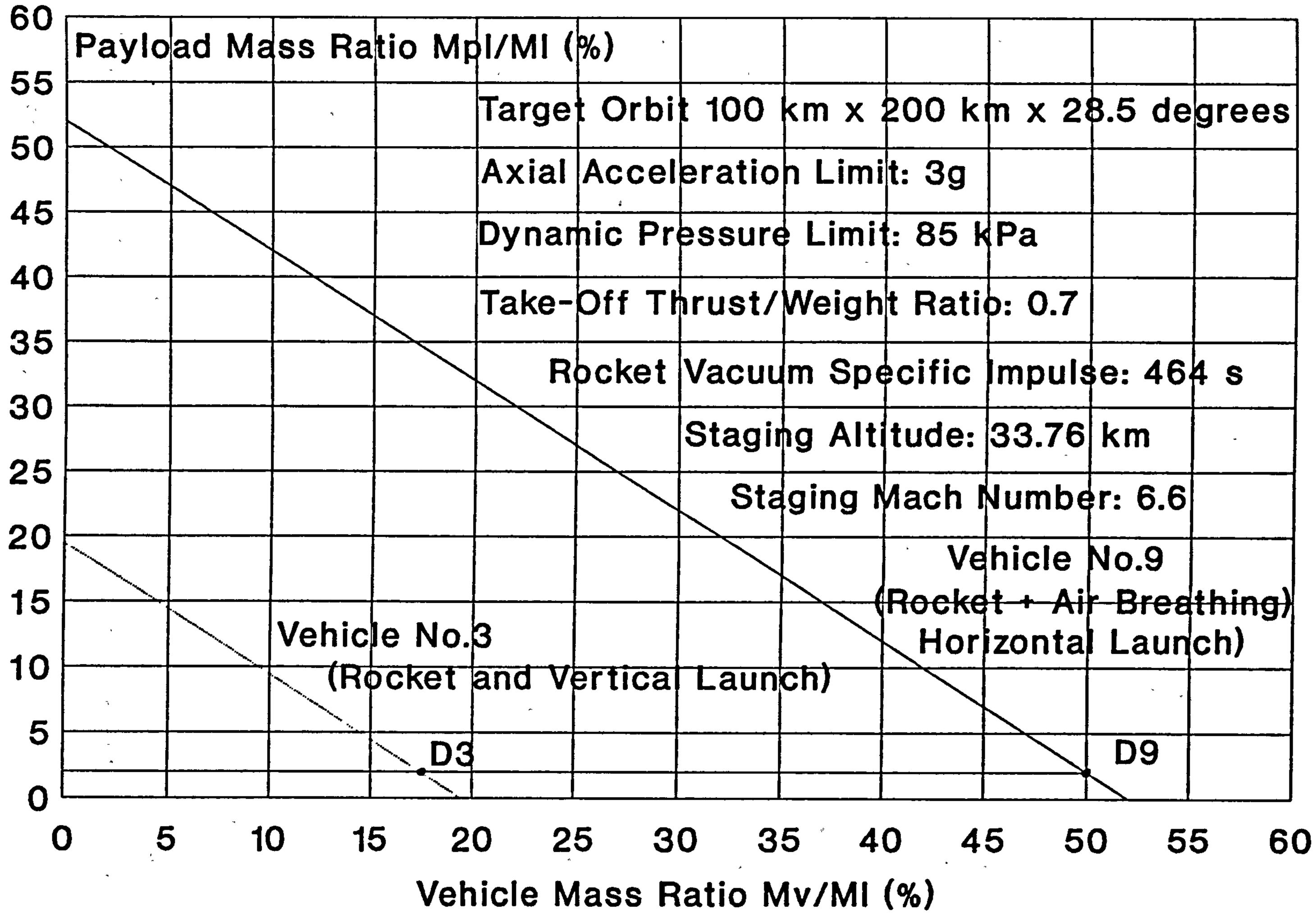

5.14 Performance of Reusable Launcher No.10: SSTO-R-HLHL (Undercarriage-Launched)

This launcher is a single-stage-to-orbit, rocket-propelled, horizontally launched and horizontally landed vehicle. The vehicle is undercarriage-launched.

5.14.1 Vehicle Configuration

This launcher is the first of the candidate vehicles which are entirely rocket-propelled but which are launched and landed horizontally and use aerodynamic lift. For performance comparison reasons, the configuration of this vehicle is that evaluated in Reference 11.

The motivation for studying this vehicle is to see whether rocket propulsion, with its order of magnitude lower specific impulse and order of magnitude higher thrust/weight ratio than air-breathing propulsion, can deliver a higher Payload Mass Ratio than similar vehicles employing air-breathing and rocket propulsion. Thus, this vehicle is directly comparable with Reusable Launcher No.4, which is also undercarriage-launched.

The vehicle configuration is shown in Figure 5.37. the aerodynamic characteristics are shown in Figure 5.38.

5.14.2 Ascent and Descent Trajectories

The ascent trajectory comprises 3 phases. Phase 1 starts with the take-off run of the vehicle on its undercarriage, propelled by its own rocket engines. Phase 2 begins with the rotation in pitch of the vehicle until it lifts off under rocket propulsion. Phase 3 comprises a climbing, accelerating and lifting flight under rocket propulsion using an optimised, variable flight path trajectory until the altitude

and inertial velocity are achieved for injection at the perigee of the transfer orbit. The descent trajectory is a gliding flight under aerodynamic control, to a runway landing on its own integral undercarriage.

5.14.3 Performance Results

The Payload Mass Ratio results, plotted in the standard graphical presentation, are shown in Figure 5.39.

Examination of Figure 5.39 shows that at our design point Payload Mass Ratio value of 2 %, that the maximum allowable Vehicle Mass Ratio is 11 % (point D10 on Figure 5.39). This value is 1.9 % higher than the 9.1 % Vehicle Mass Ratio required for the equivalent undercarriage-launched but air-breathing propelled vehicle, which is Launcher No.4 (point D4 on Figure 5.39). At this stage of the performance analysis, this result is very encouraging and indicates that this rocket-propelled vehicle has a higher potential to deliver a positive payload than the equivalent air-breathing/rocket-propelled vehicle No.4. A major contributor to this higher performance potential is the lower drag of the purely rocket-propelled vehicle because of the absence of air-breathing engine nacelles. Indeed, all air-breathing vehicles suffer from higher drag because of their air intakes. The high drag of air-breathing vehicles, which substantially degrades their performance is discussed further in Chapter 6.2: Air Breathing Propulsion.

Figure 5.37
Configuration of Reusable Launcher No.10:
SSTO-R-HLHL (Undercarriage-Launched)
(Derived from Reference 11)

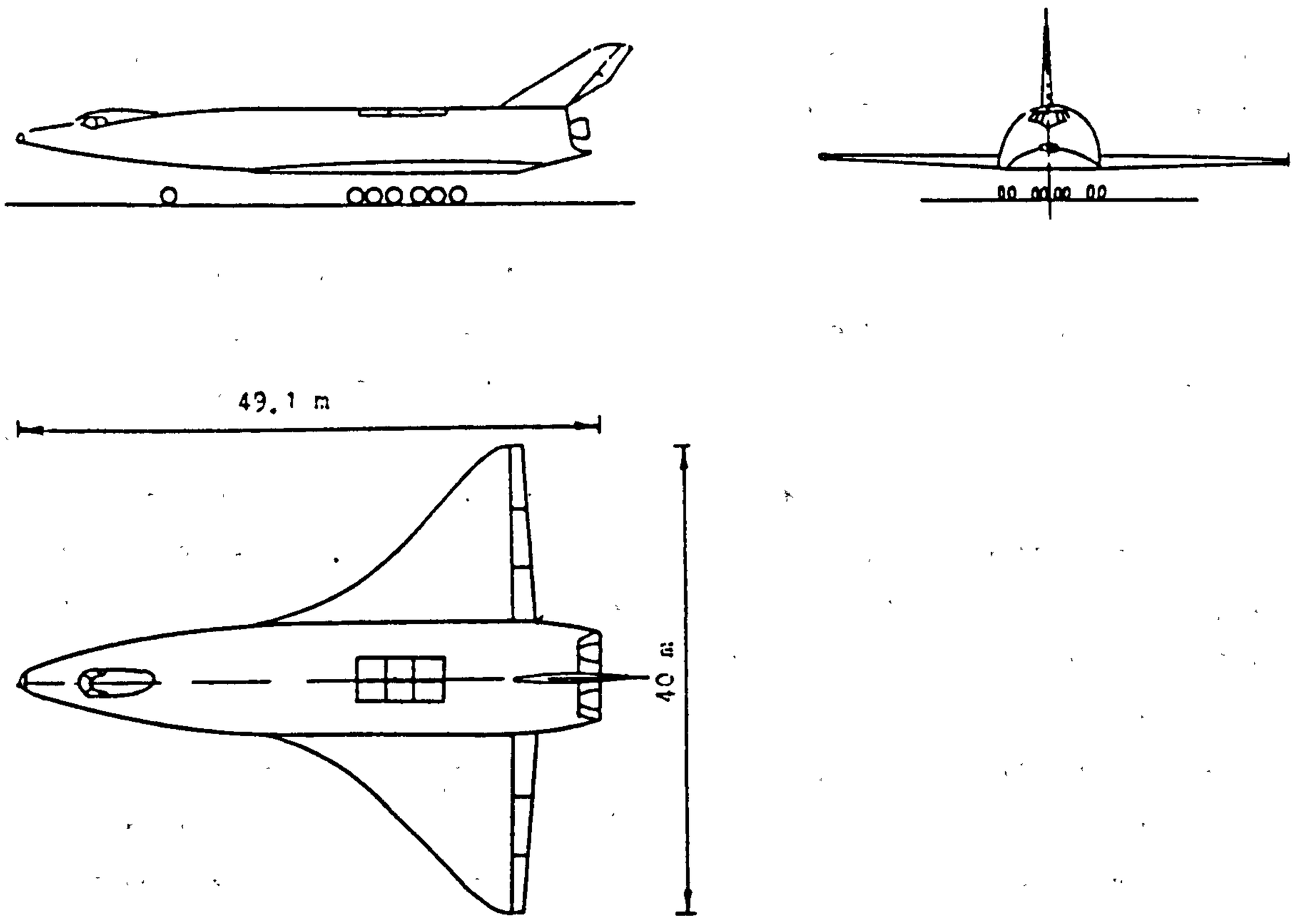

Length: 49.1 m.
Width: 40 m.
Lift-Off Mass: 350 tonnes
Lift-Off Thrust: 3500 KN
Aerodynamic Reference Area: 744 m^2

Figure 5.38

Lift and Drag Coefficients for Reusable Launcher No.10

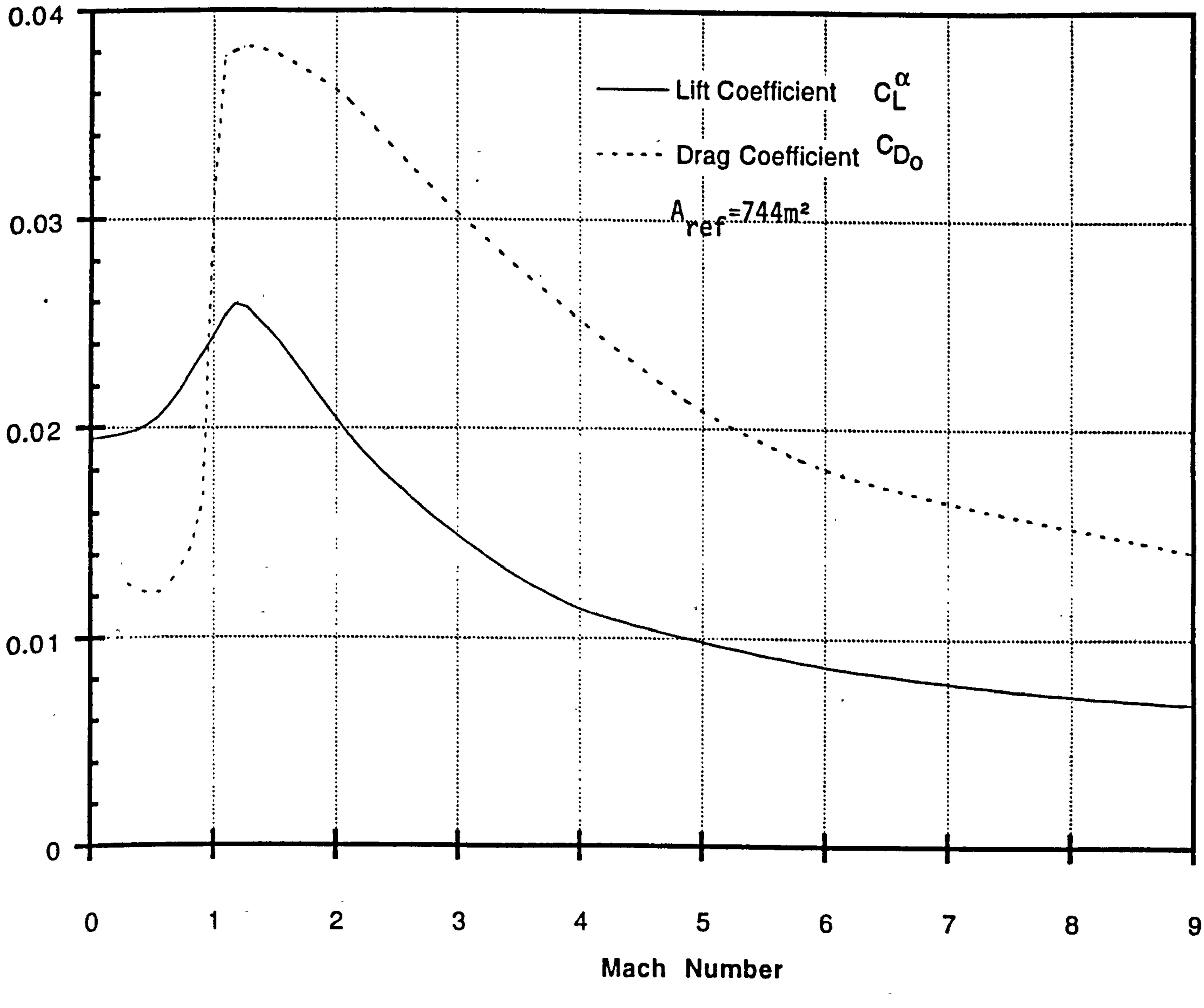

FIGURE 5.39

Reusable Launcher No.10: SSTO-R-HLHL(Undercarriage)

Payload Mass Ratio Versus Vehicle Mass Ratio

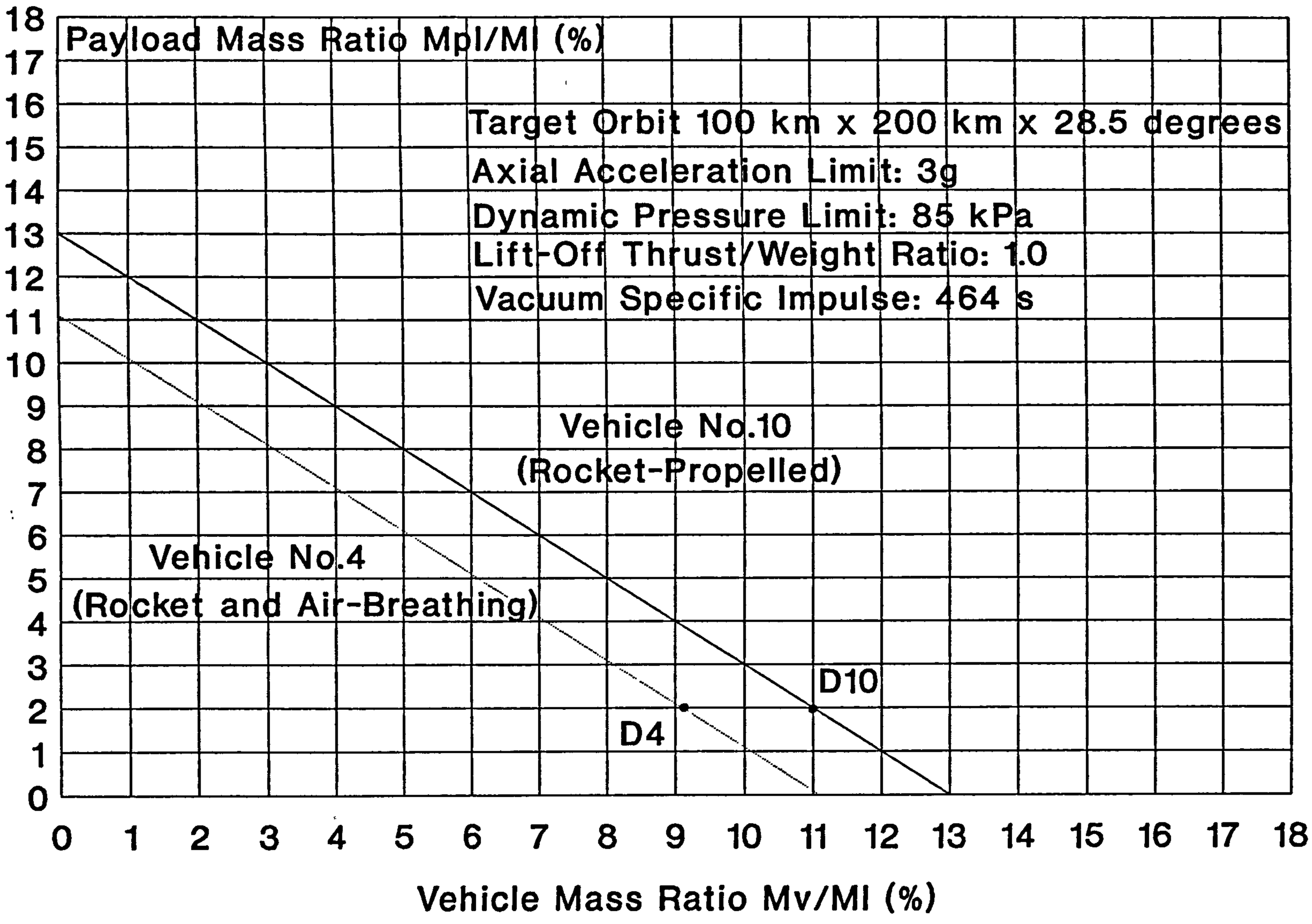

5.15 Performance of Reusable Launcher No.11: SSTO-R-HLHL (Sled-Launched)

This launcher is a single-stage-to-orbit, rocket-propelled, horizontally launched and horizontally landed vehicle. The vehicle is sled-launched.

5.15.1 Vehicle Configuration

This vehicle is very similar to Vehicle 10, except that it is launched on a sled. Figure 5.40 shows the configuration, which, for performance comparison reasons, is that of the vehicle evaluated in Reference 11. It can be seen that this vehicle is much smaller than Vehicle 10 because it does not have to accommodate the rocket propellant needed for its take-off run. The aerodynamic characteristics are shown in Figure 5.41.

The motivation for investigating this vehicle is to compare its performance capabilities with that of the equivalent air-breathing/rocket-propelled Vehicle No.5, which is also launched on a sled. It is also interesting to determine the mass saving that is expected to result from the undercarriage mass of this vehicle, which has to be sized for a much lower landing mass, compared to that of Vehicle No.10, which has its undercarriage sized for its take-off mass.

5.15.3 Ascent and Descent Trajectories

The ascent and descent trajectories are similar to that described for Vehicle No.10, the undercarriage-launched, rocket-propelled vehicle. The major difference is that this vehicle is launched on a sled.

5.15.4 Performance Results

The Payload Mass Ratio results, plotted in the standard graphical presentation, are shown in Figure 5.42.

Examination of Figure 5.42 shows that at our design point Payload Mass Ratio value of 2 %, that the required maximum Vehicle Mass Ratio is 12 % (point D11 on Figure 5.42). This value is only 1 % lower than the maximum allowable Vehicle Mass Ratio of 13 % that is required for the comparable sled-launched, air-breathing/rocket-propelled Vehicle No.5 (point D5 on Figure 5.42). Again, this result shows that this rocket-propelled vehicle has a better potential to deliver a positive payload than the equivalent air-breathing/rocket-propelled Vehicle No.5, which has to carry inherently heavy air-breathing engines all the way to orbit.

Figure 5.40
Configuration of Reusable Launcher No.11:
SSTO-R-HLHL (Sled-Launched)
(Derived from Reference 11)

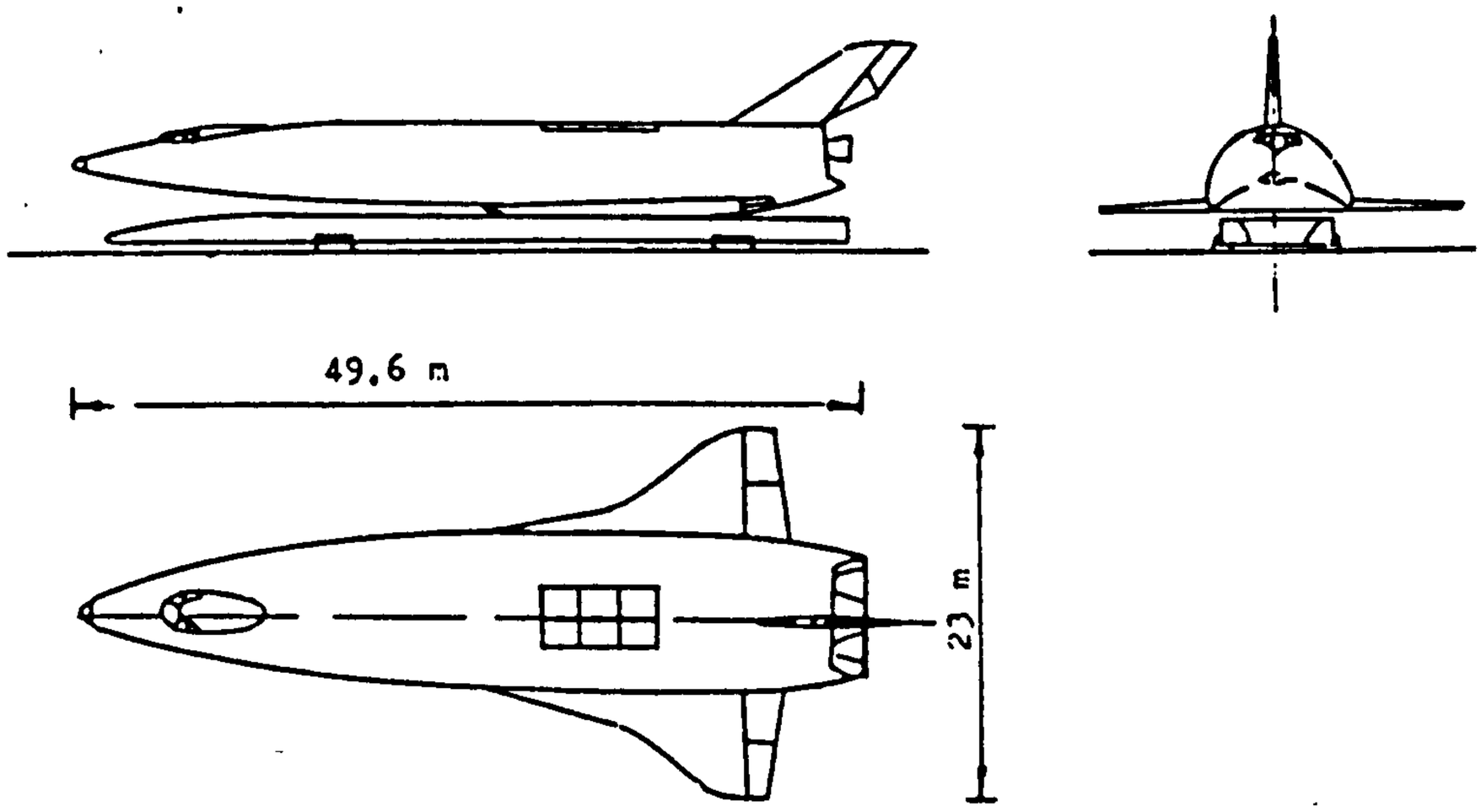

Length: 49.6 m.
Width: 23 m.
Lift-Off Mass: 350 tonnes
Lift-Off Thrust: 3500 KN
Aerodynamic Reference Area: 312 m^2

Figure 5.41

Lift and Drag Coefficients for Reusable Launcher No.11

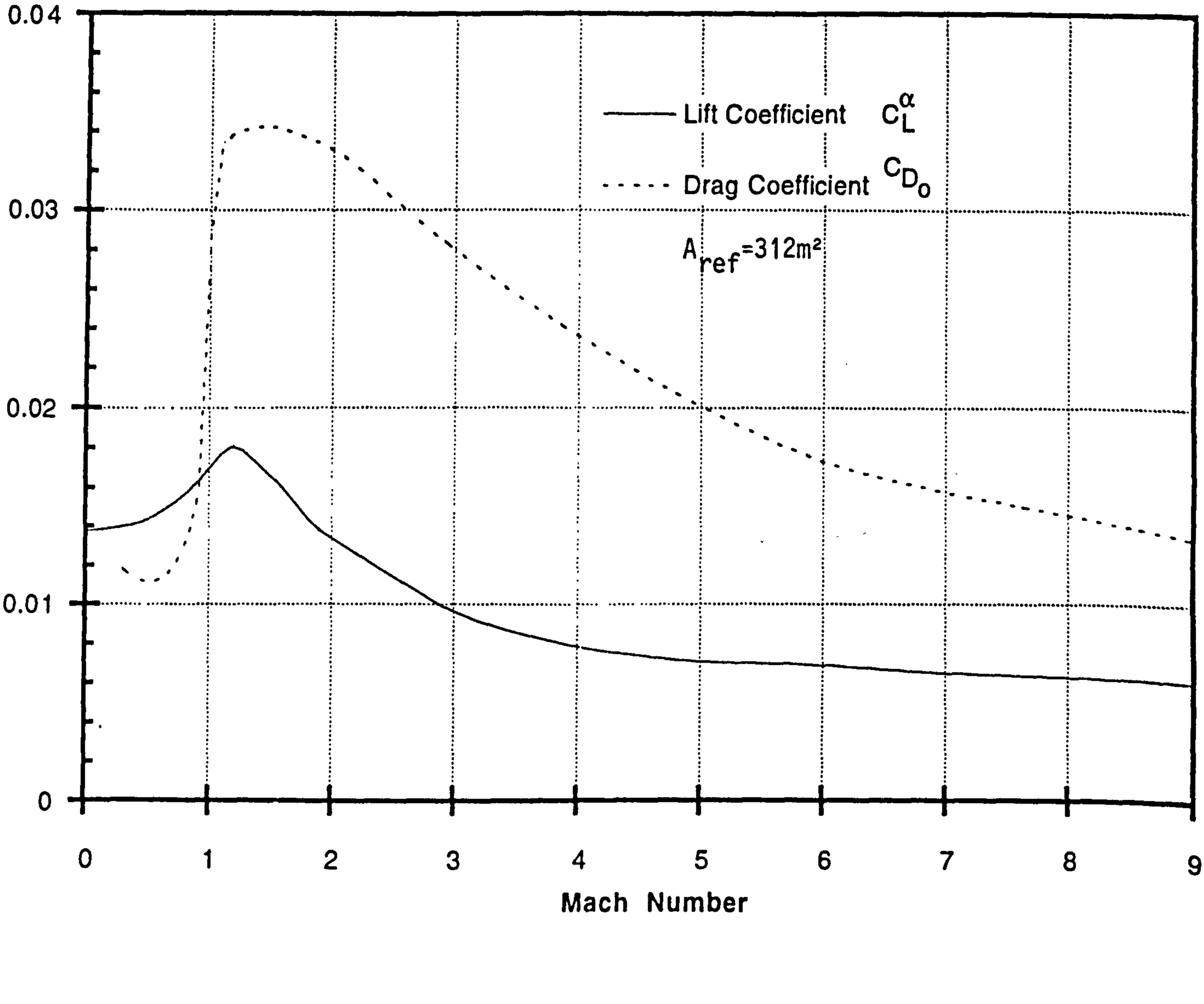

FIGURE 5.42

Reusable Launcher No.11: SSTO-R-HLHL(Sled-Launched)

Payload Mass Ratio Versus Vehicle Mass Ratio

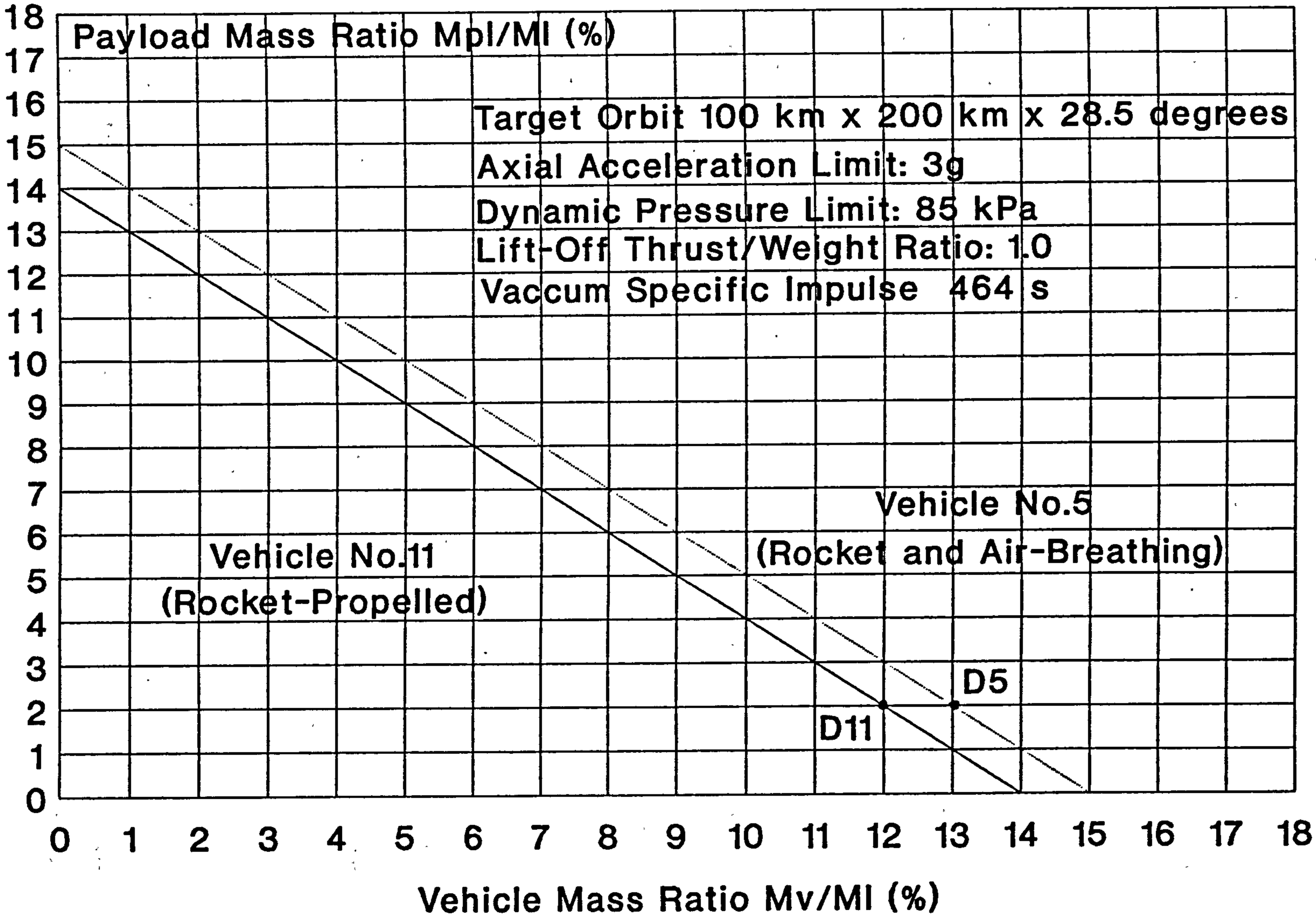

5.16 Performance of Reusable Launcher No.12: TSTO-R-HLHL (Undercarriage-Launched)

This launcher is a two-stage-to-orbit, rocket-propelled, horizontally launched and horizontally landed vehicle. The vehicle is undercarriage-launched.

5.16.1 Vehicle Configuration

The vehicle configuration is shown in Figure 5.43, which for performance comparison reasons is idential to that evaluated in Reference 11, The aerodynamic characteristics are shown in Figure 5.44.

The motivation for investigating this vehicle is to examine whether rocket propulsion can yield an improved Payload Mass Ratio compared to the equivalent air-breathing/rocket-propelled Vehicle No.9. It is also interesting to see the increase in Payload Mass Ratio of this two stage vehicle compared with Vehicle No.11, which is the equivalent single stage vehicle.

5.16.2 Ascent and Descent Trajectories

This vehicle takes-off on its own undercarriage under rocket propulsion. It then climbs and accelerates at an optimised, variable flight path until the optimised staging altitude and inertial velocity are reached. The Second Stage then climbs and accelerates at an optimised flight path until the required altitude and inertial velocity for insertion at the perigee of the transfer orbit are reached. At stage separation, the First Stage returns to the launch base under gliding flight, to land horizontally on its own undercarriage. After re-entry, the second stage also descends under gliding flight to land horizontally on its own undercarriage.

5.16.3 Performance Results

The Payload Mass Ratio results are shown plotted in the standard graphical presentation in Figure 5.45.

Examination of Figure 5.45 shows that at our design point Payload Mass Ratio value of 2 %, that the allowable maximum Vehicle Mass Ratio is 24 % (point D12 on Figure 5.45). This is about half that of the 50 % Vehicle Mass Ratio value required for Vehicle No.9, which is the equivalent air-breathing/rocket-propelled launcher. The significance of this result will be examined later in this Chapter.

Figure 5.43
Configuration of Reusable Launcher No.12:
TSTO-R-HLHL (Undercarriage-Launched)

(Derived from Reference 11)

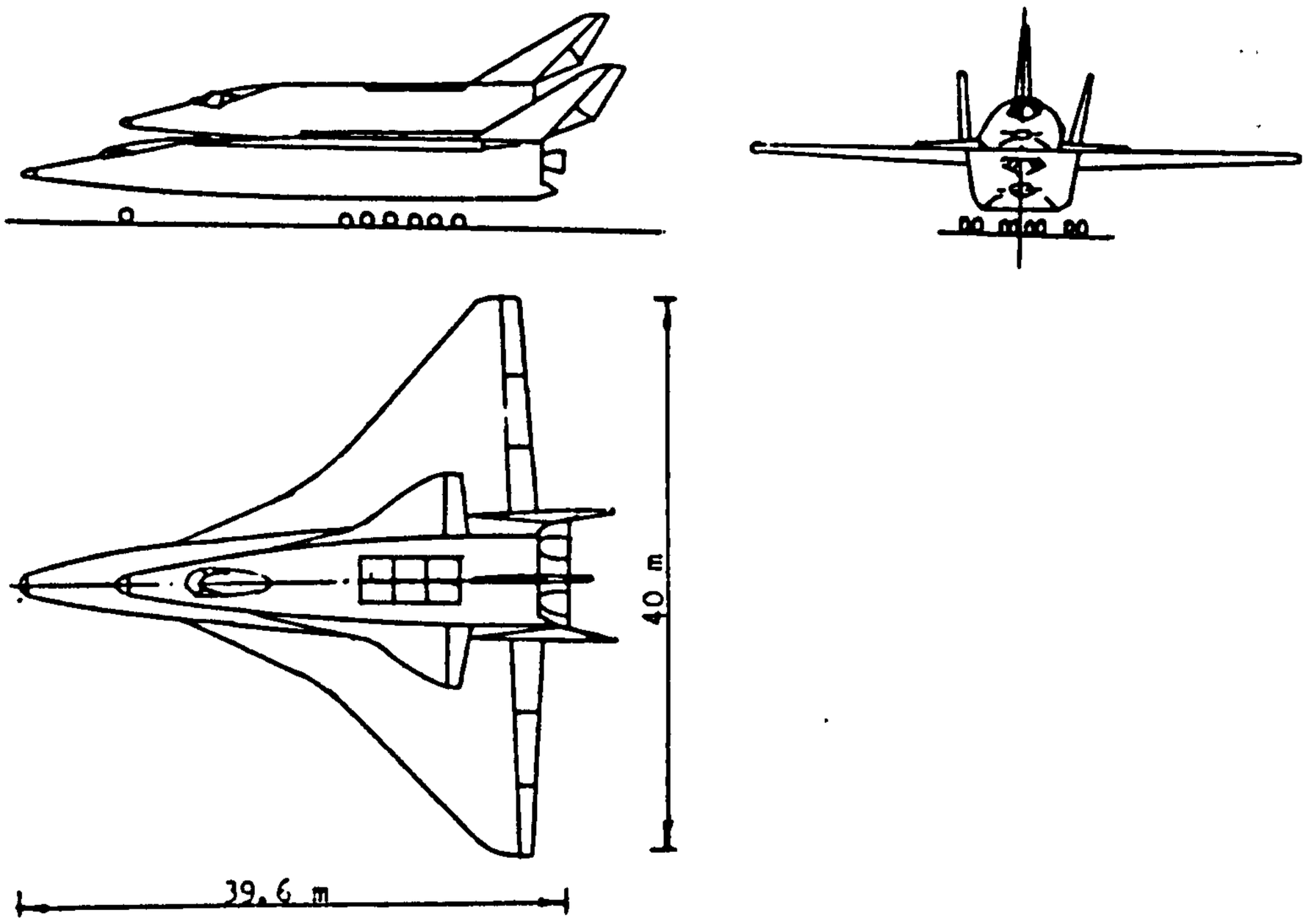

Length: 39.6 m.
Width: 40 m.
Lift-Off Mass: 350 tonnes
Lift-Off Thrust: 3500 KN
Aerodynamic Reference Area Stage 1: 744 m^2
Stage 2: 123 m^2

Figure 5.44 A

Lift and Drag Coefficients for the First Stage of Reusable Launcher No.12

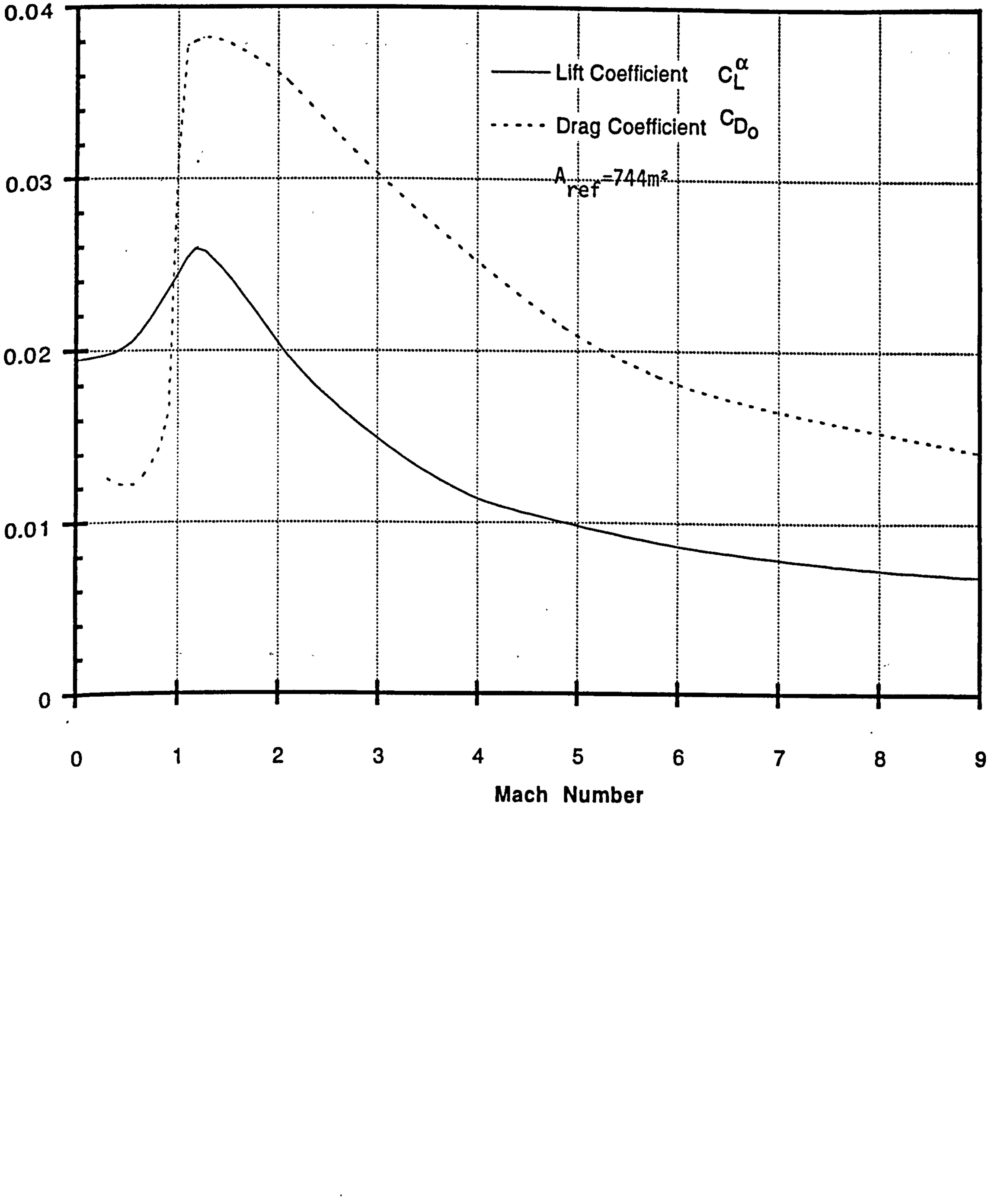

Figure 5.44 B

Lift and Drag Coefficients for the Second Stage of Reusable Launcher No.12

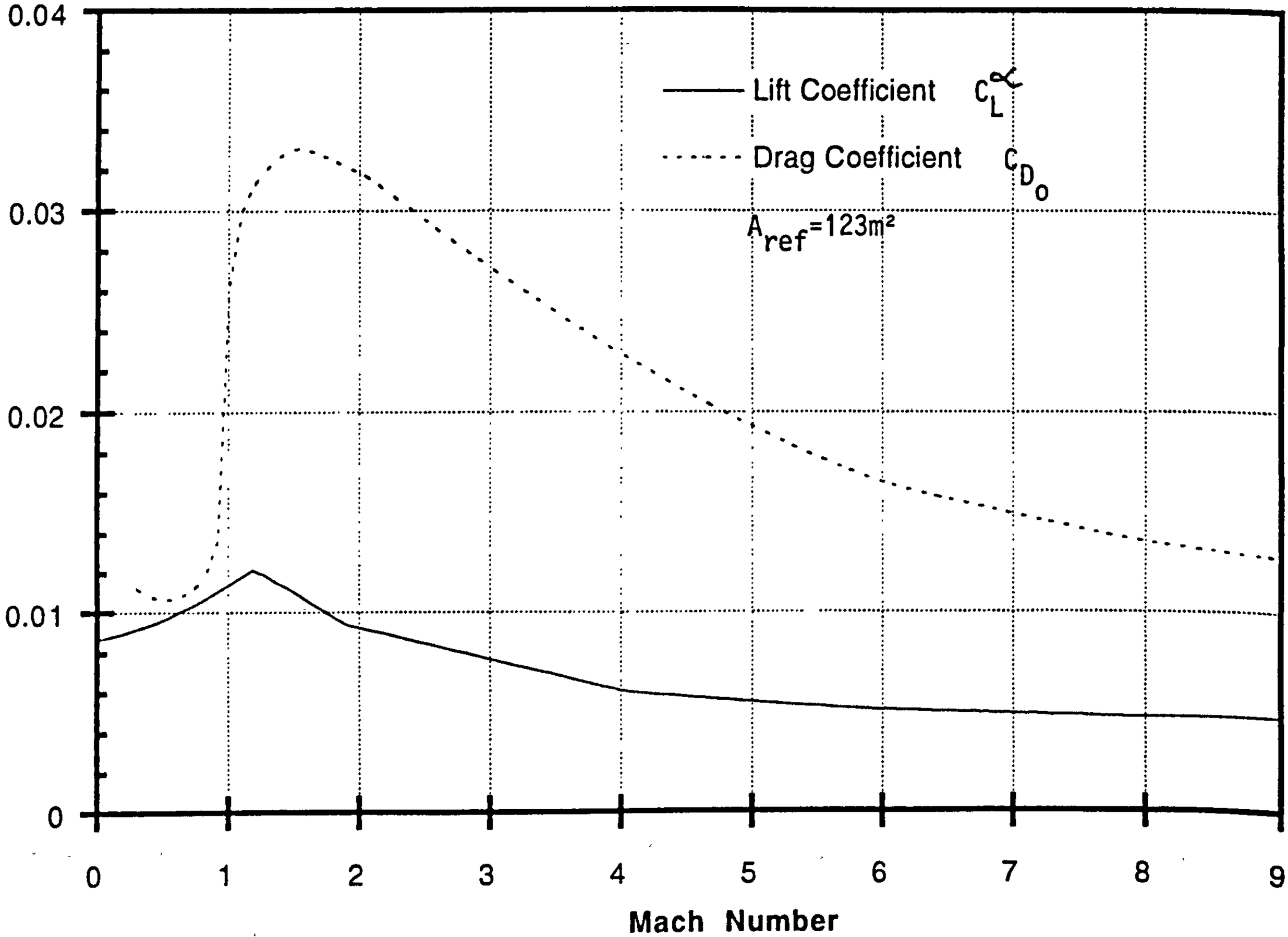

FIGURE 5.45

Reusable Launcher No.12: TSTO-R-HLHL(Sup) (Undercarriage)

Payload Mass Ratio Versus Vehicle Mass Ratio

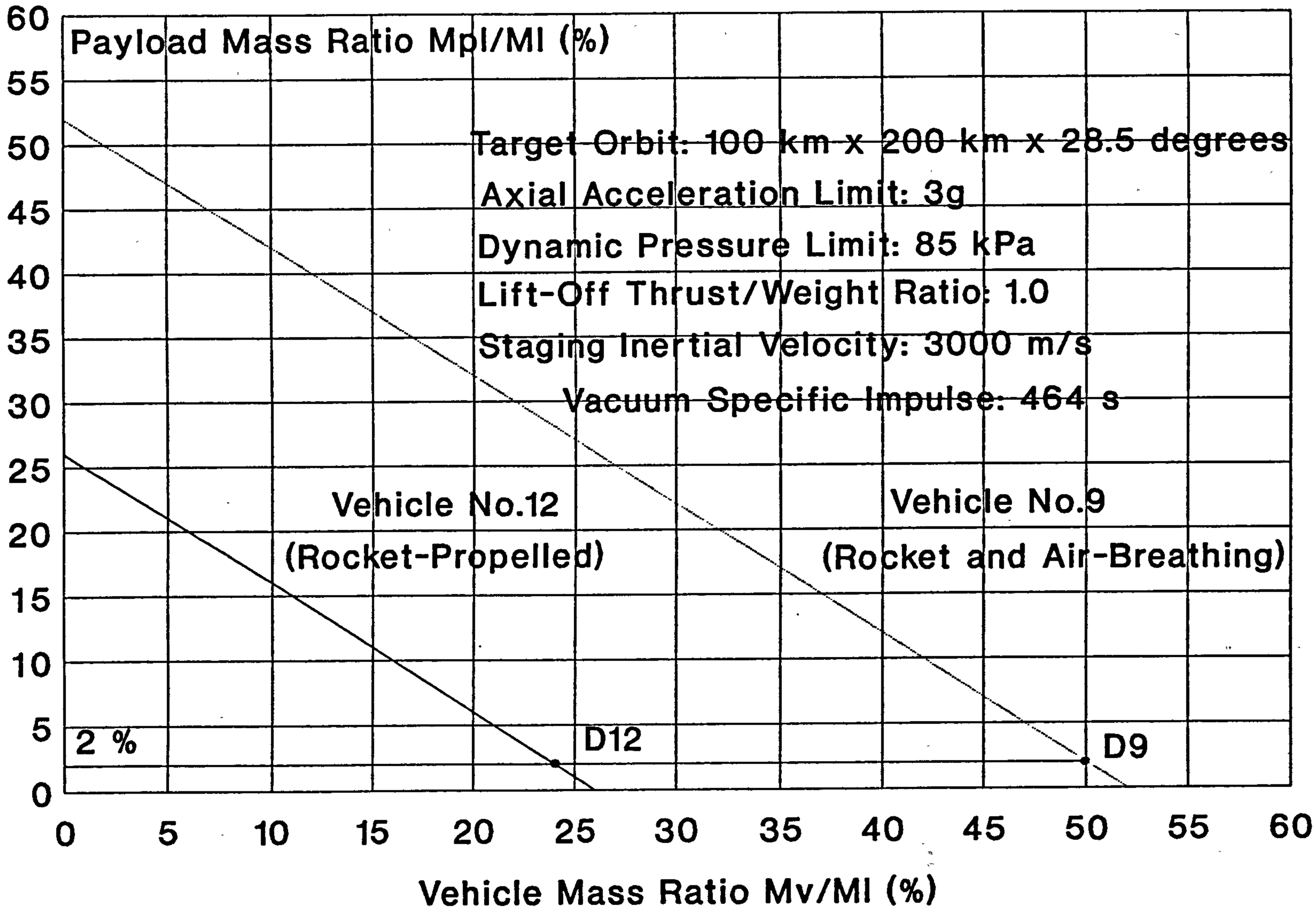

5.17 Performance of Reusable Launcher No.13: SSTO-RA(Sub)-VLVL

This launcher is a single-stage-to-orbit, rocket and air-breathing propelled, vertically launched and vertically landed vehicle. The air-breathing combustion mode is subsonic.

5.17.1 Vehicle Configuration

The configuration of this vehicle is identical to that of Vehicle No.1 as shown in Figure 5.1. The aerodynamic characteristics are also identical to that of Vehicle No.1, as shown in Figure 5.2. The only difference to Vehicle No.1 is that this vehicle uses air-breathing propulsion to augment the rocket propulsion during the lift-off and early flight phase of the vehicle. Hence, the motivation for investigating this vehicle is to examine whether the use of air-breathing propulsion to augment the rocket propulsion results in an improved Payload Mass Ratio. The air-breathing engine type selected for this vehicle is a turbojet burning hydrogen fuel and designed for operation up to Mach 3 at 20 km altitude.

5.17.2 Ascent and Descent Trajectories

The ascent trajectory of this vehicle is similar to that of Vehicle No.1, but with three flight phases. Phase 1 comprises lift-off and vertical flight for 10 seconds using rocket and air-breathing propulsion in parallel burn. Phase 2 comprises flight at a variable, optimised, pitch-over rate using rocket and air-breathing propulsion in parallel burn until an inertial speed of Mach 3 is reached at 20 km altitude. The air-breathing engines are then shut down. Phase 3 comprises the remaining flight under rocket propulsion only until the required altitude and inertial velocity are reached for insertion into the transfer orbit at its perigee.

5.17.3 Performance Results

The use of air-breathing propulsion to augment rocket propulsion on a vertically launched vehicle is a concept that is worth exploring, based on the following rationale:

- Rocket propulsion has a specific impulse which is typically one order of magnitude lower than that of air-breathing propulsion (400 s at sea level for a hydrogen/oxygen rocket engine, versus 4000 s at sea level for a hydrogen-fuelled turbojet). On the other hand, rocket propulsion has a thrust/weight ratio that is typically one order of magnitude larger than that of air-breathing propulsion (a thrust/weight of 80 for a large hydrogen/oxygen rocket engine, versus a thrust/weight of 8 for an advanced hydrogen-fuelled turbojet). Thus, it can be seen that if air-breathing propulsion only was used to propel the vehicle during its lift-off and low altitude flight, that the propellant mass savings that would be achieved because of the high specific impulse could be negated entirely by the high mass of the air-breathing engines. Furthermore, the low density of the hydrogen fuel that would be required for the air-breathing propulsion mode, would result in a very large vehicle to accommodate the fuel, resulting in a higher vehicle mass, which for a single stage vehicle, offsets directly the payload mass. If however, air-breathing propulsion is used to partially augment the thrust of the rocket propulsion for such a vehicle, and if the air-breathing thrust/weight ratio can be substantially increased, it is hypothesised that it might be possible to achieve a gain in the payload mass ratio.

This hypothesis has been examined in this research and the results are shown in Figure 5.46, in which the influence of air-breathing propulsion on the performance of the standard rocket-propelled Vehicle No.1 is presented.

Examination of Figure 5.46 shows, firstly, that as expected because of the higher specific impulse, the Orbital Mass Ratio increases slightly and linearly as the fraction of air-breathing thrust augmentation is increased over the full thrust augmentation range from 0 % to 100 %. However, Figure 5.46 also shows that because of the higher mass of the air-breathing engines, that the Engine Mass Ratio increases steeply and linearly. The net result then is that the Orbital Mass minus the Engine Mass ratio (Mo-Me)/Ml decreases steeply and linearly as the fraction of air-breathing thrust increases. The reason for the rather small increase in the Orbital Mass Ratio is that, despite the high specific impulse of the air-breathing engines (4000 s in this example), the resulting average specific impulse during the air-augmented phase increases exponentially as the air-augmentation ratio is increased. Thus, at low values of air-augmentation ratio, the average specific impulse is only slightly higher than that of the pure rocket-propelled case. This average specific impulse characteristic can be seen on Figure 5.46. Thus, this example shows that, for a typical air-breathing thrust/weight ratio of 8, that air-breathing augmentation will not result in an increase in the Payload Mass Ratio.

The resulting decreased performance of the entirely rocket-propelled Vehicle No.1 by the use of a 10 % value of air-breathing thrust augmentation is shown in Figure 5.47.

Examination of Figure 5.47 shows that at our design point Payload Mass Ratio value of 2 %, that the maximum allowable Vehicle Mass Ratio is 12.6 % (point D13 on Figure 5.47). This is a minor increase of 0.3 % over the Vehicle Mass Ratio value of 12.3 % (point D1 on Figure 5.47) that is required for the entirely rocket-propelled vehicle No.1.

Figure 5.46

Reusable Launcher No.13: SSTO-RA(sub)-VLVL

Performance Influence of Air-Breathing Propulsion

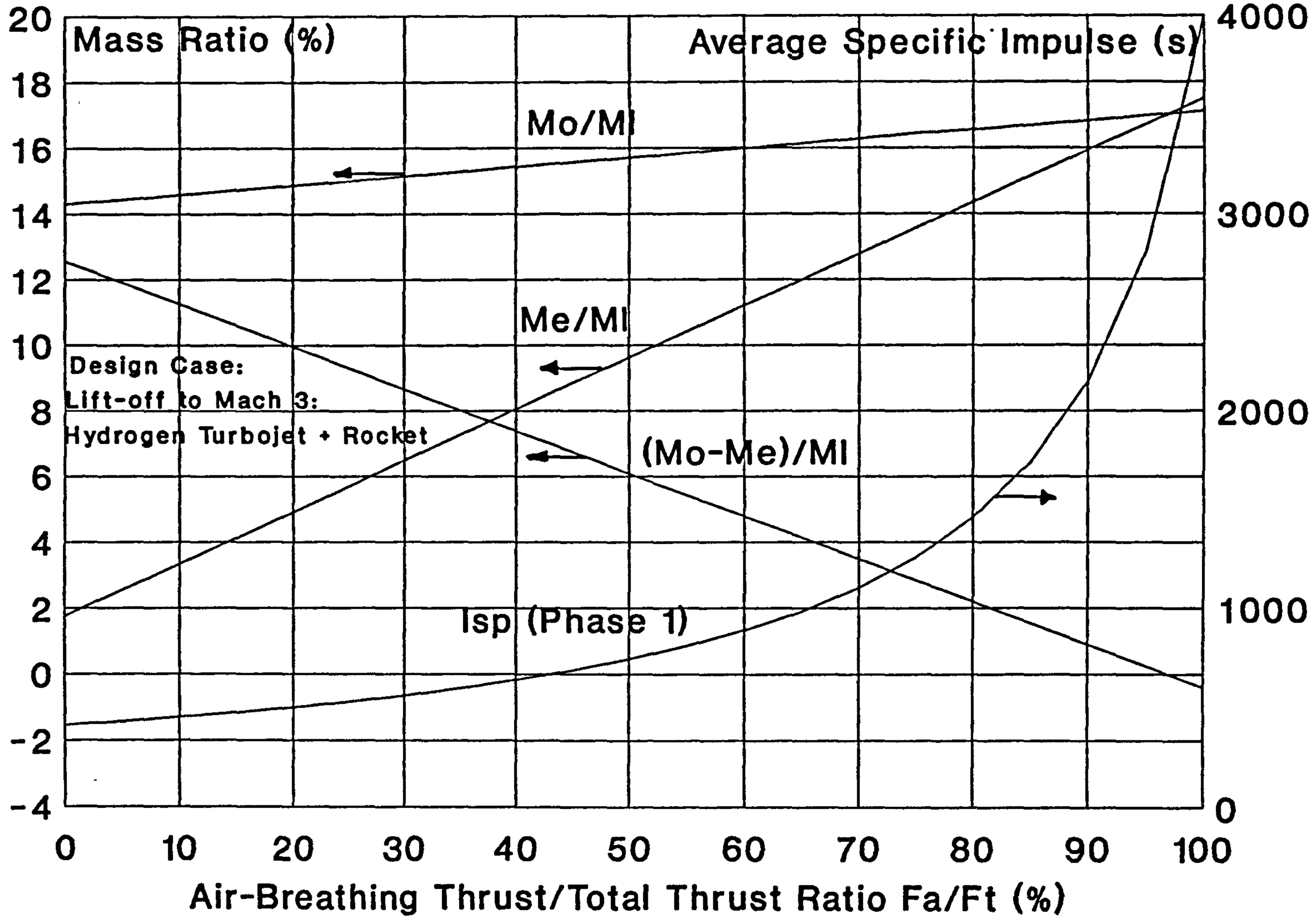

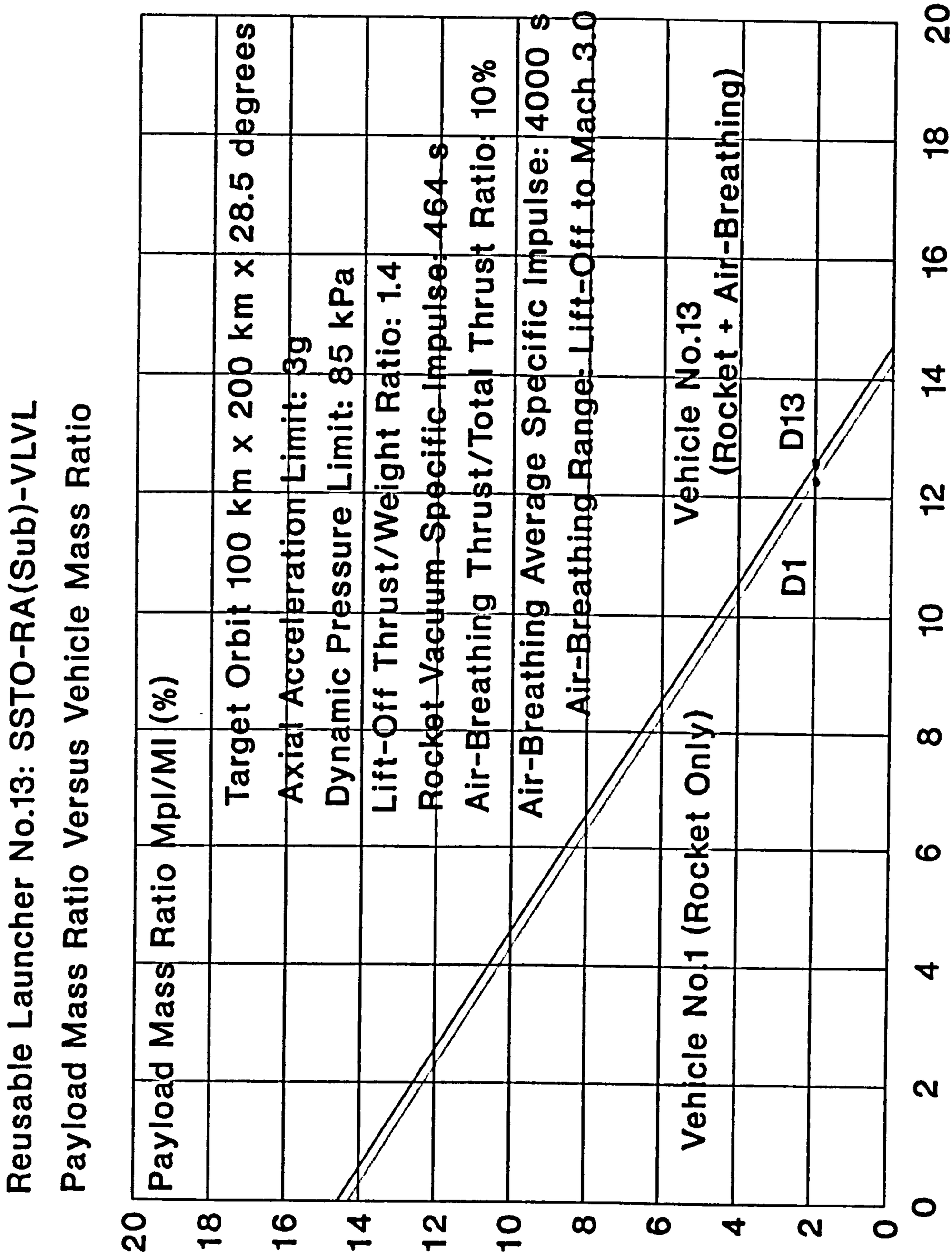
Reusable Launcher No.13: SSTO-RA(Sub)-VLVL
Payload Mass Ratio Versus Vehicle Mass Ratio
Payload Mass Ratio Mpl/Ml (%)
Target Orbit 100 km x 200 km x 28.5 degrees
Axial Acceleration Limit: 3g
Dynamic Pressure Limit: 85 kPa
Lift-Off Thrust/Weight Ratio: 1.4
Rocket Vacuum Specific Impulse: 464 s
Air-Breathing Thrust/Total Thrust Ratio: 10%
Air-Breathing Average Specific Impulse: 4000 s
Air-Breathing Range: Lift-Off to Mach 3.0
Vehicle No.1 (Rocket Only)
Vehicle No.13
(Rocket + Air-Breathing)
D1
D13
Vehicle Mass Ratio Mv/Ml (%)
0
2
4
6
8
10
12
14
16
18
20

FIGURE 5.47

5.18 Comparative Performance of the Candidate Reusable Launchers

In Chapter 5.5 to 5.17, the absolute limits of the payload mass ratios of each of the 13 candidate launchers were determined and where relevant, the performance of each launcher was discussed and compared with that of its most comparable equivalent vehicle. This Chapter now compares the performances of all the launchers to establish their relative performance ranking.

Table 5.1 shows the calculated performance results of all the candidate launchers. It would have been illustrative to show the Payload Mass Ratios versus Vehicle Mass Ratios for all the launchers plotted together using the standard graphical presentation. However, the graphical scale that would have had to be used would have resulted in a too close bunching of the characteristics of many vehicles to be meaningful. Instead, to show more clearly the comparative performance of the candidate launchers, the barchart shown in Figure 5.48 has been drawn. This shows the launchers ranked from left to right in ascending order of the maximum allowable Vehicle Mass Ratios for zero payload and also for our design point Payload Mass Ratio of 2 %.

Examination of Figure 5.48 shows that:

- the SSTO vehicles have smaller and therefore more demanding Vehicle Mass Ratio values than the TSTO vehicles;

- among the SSTO launchers, the air-breathing/rocket-propelled vehicles have more demanding Vehicle Mass Ratio requirements;

- among the TSTO launchers, the air-breathing/rocket-propelled vehicles have larger, and therefore less demanding, Vehicle Mass Ratio Values;

- the performance characteristic for Launcher No.9, the TSTO-RA(Sub)-HLHL (Undercarriage-Launched) Vehicle, has an exceptionally higher Vehicle Mass Ratio value than all the other vehicles.

TABLE 5.1 COMPARATIVE PERFORMANCE OF THE CANDIDATE REUSABLE LAUNCHERS

VEHICLE	DESIGNATION	THIS RESEARCH		REFERENCE DATA		REFERENCE
		PAYLOAD MASS RATIO (%)	VEHICLE MASS RATIO (%)	PAYLOAD MASS RATIO (%)	VEHICLE MASS RATIO (%)	
RL1	SSTO-R-VLVL	2	12.28	3.25	10.	IAF - 86 - 122
RL2	SSTO-R-VLHL	2	11.03	0.96	11.48	IAF - 92 - 0865
RL3	TSTO-R-VLHL	2	17.43	5.00	14.26	IAF - 92 - 0865
RL4	SSTO-RA(Sub)-HLHL(u/c)	2	9.1	-	-	
RL5	SSTO-RA(Sub)-HLHL(Sled)	2	13.0	1.65	14.28	ESA WLC Phase 3
RL6	SSTO-RA(Sub)-ILHL(Ramp)	2	13.0	-	-	
RL7	SSTO-RA(Sup)-HLHL(u/c)	2	18.5	-9.00	27.50	ESA WLC Phase 5
RL8	TSTO-RA(Sub)-HLHL(Air-Launch)	2	12.21	3.40	10.86	IAF - 92 - 0865
RL9	TSTO-RA(Sub)-HLHL(u/c)	2	50	2.06	50.82	ESA WLC Phase 4
RL10	SSTO-R-HLHL(u/c)	2	12	-6.4	18.48	IAF - 92 - 0865
RL11	SSTO-R-HLHL(Sled)	2	11	1.96	11.46	IAF - 92 - 0865
RL12	TSTO-R-HLHL(u/c)	2	24	3.40	21.56	IAF - 92 - 0865
RL13	SSTO-RA(Sub)-VLVL	2	12.56	-	-	

Figure 5.48

Comparative Performance of Candidate Reusable Launchers
Maximum Allowable Vehicle Mass Ratio Values

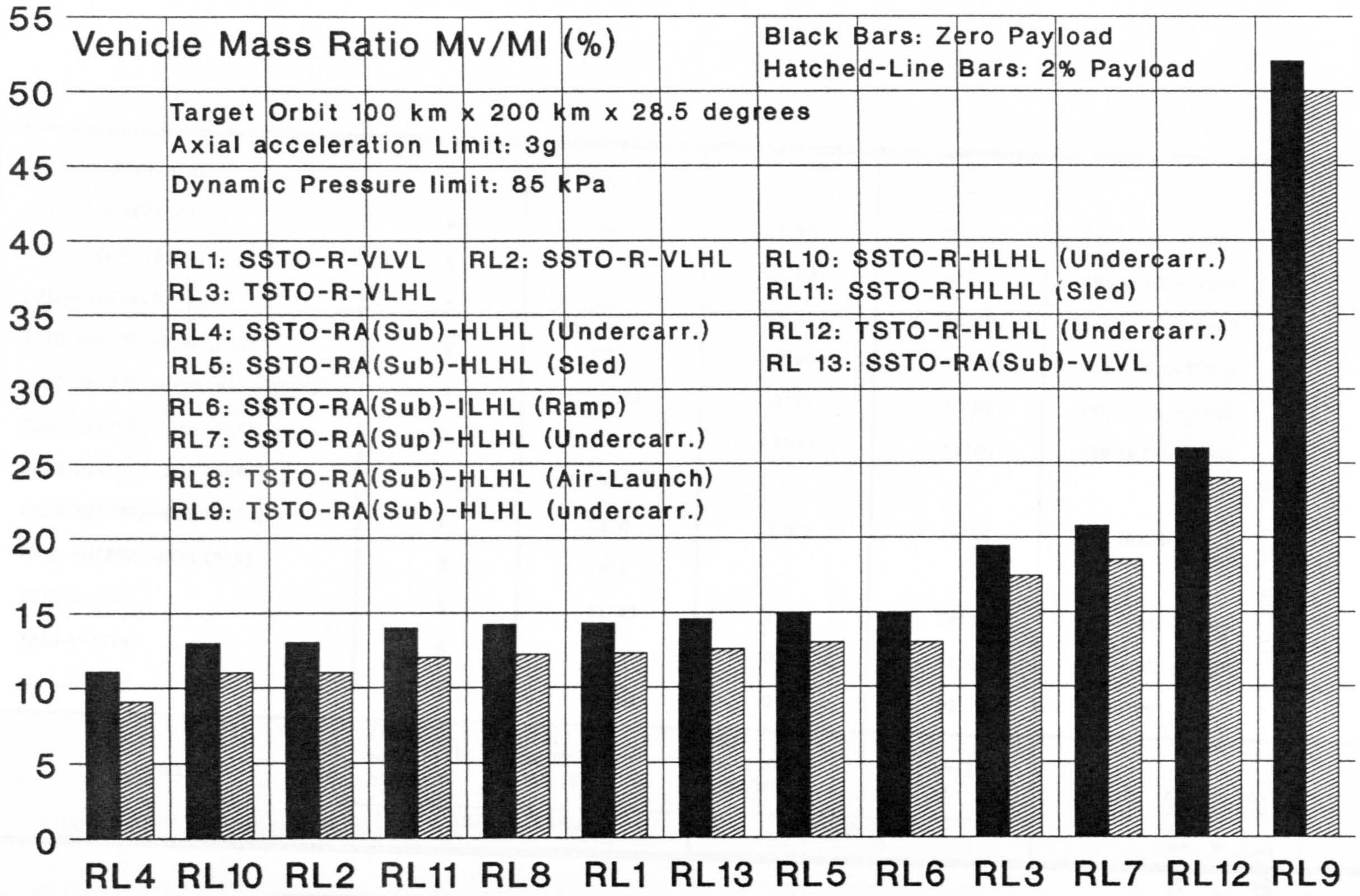

5.19 Comparison of the Calculated Performance Results with those from other System Studies

So far, for each vehicle type, the performance results that have been presented only show the absolute allowable limits of the Vehicle Mass Ratios for any required Payload Mass Ratio. Although these results are already a significant contribution to the understanding of Reusable Launchers, they can give no indication whatsoever on the actually achievable values of the Vehicle Mass Ratio for any required Payload Mass Ratio. These actual values of the Vehicle Mass Ratio must, ideally, be determined from actual vehicle masses, or as the next best option, from detailed engineering designs of the respective vehicles. There are of course, currently, no reusable launchers available from which to derive actual payload and vehicle masses. Consequently, a major effort in this research was expended to review the literature on reusable launchers to try to find sufficiently mature vehicle design studies, from which actual vehicle mass ratios and payload mass ratios could be determined. The author was lucky in this respect, because several literature references were found on some reusable launcher concepts which had been adopted as candidates in this research. A review of these references, followed up by personal contact with the authors, gave assurance that indeed, in all cases, the detailed engineering designs, having been undertaken by large industrial teams, were mature enough to allow the vehicle mass data to be used with confidence in this research, thus yielding realistic estimates of the achievable mass ratios. The candidate vehicles for which reliable designed mass data were available are:

- Reusable Launcher No.1: SSTO-R-VLVL

An excellent study on such a vehicle was performed by the MBB Company in Germany in 1986 and published under Reference 10.

- Reusable Launcher No.2: SSTO-R-VLHL
- Reusable Launcher No.3: TSTO-R-VLHL
- Reusable Launcher No.8: TSTO-RA(Sub)-HLHL (Air-Launched)
- Reusable Launcher No.10: SSTO-R-HLHL (Sled-Launched)
- Reusable Launcher No.11: SSTO-R-HLHL (Undercarriage)
- Reusable Launcher No.12: TSTO-R-HLHL (Undercarriage)

A comprehensive design study on all these rocket-propelled vehicles (including Vehicle No.8, the TSTO air-breathing/rocket-propelled vehicle, which is really a rocket-propelled SSTO) has been performed by the Russian Central Hydrodynamics and Aerodynamics Institute (TsAGI) in 1991 and published in 1992 under Reference 11.

- Reusable Launcher No.5: SSTO-RA(Sub)-HLHL (Sled-Launched)

A detailed study on this vehicle has been performed by European Industry in 1989-90 under the auspices of the ESA Winged Launcher Configuration (WLC) Study and the results were published in 1989 under Reference 12.

- Reusable Launcher No.7: SSTO-RA(Sup)-HLHL (Undercarriage)

A detailed study on this vehicle has been performed by European industry in 1992 under the auspices of the ESA WLC Study Phase 5 and published under Reference 8. However, this study revealed that the analysis of this complex vehicle, employing a four-mode combined cycle engine which includes a scramjet, is so difficult, that much more work on this vehicle is needed before full confidence can be placed in the mass estimates yielded in WLC-5.

- Reusable Launcher No.9: TSTO-RA(Sub)-HLHL (Undercarriage)

A detailed study on this vehicle has been performed by European Industry under the auspices of the ESA WLC Study Phase 4 in 1991 and published under Reference 13. This vehicle has had a major effort applied to its detailed design and there is therefore, very high confidence in the realism of the mass estimates.

The comparative results of this research with those of the referenced system studies has been performed for each vehicle and presented in the standard graphical presentation shown in Figures 5.49 to 5.58.

Examination of each of Figures 5.49 to 5.58 shows a close correlation of the results from this study with those of the respective referenced study. These small differences can be explained by the slightly different target orbits and launch sites for the respective referenced study. These differences are noted on each Figure. This close correlation of the results is very gratifying because it gives confidence in the analysis tools used in this research. However, of much more importance, is the unique data point derived from the reference study of the calculated Payload Mass Ratio and its corresponding Vehicle Mass Ratio. This data point is marked on each Figure by an asterisk. Now, at last, we have a performance result derived from detailed vehicle studies for 10 of our 13 candidate reusable launchers. The missing three vehicles, for which no reliable data was found in the literature are:

- Reusable Launcher No.4: SSTO-RA(Sub)-HLHL (Undercarriage)
Although no reliable performance data was found in the literature, the actual expected performance of this vehicle will be close to the performance characteristic calculated in this research because of the good statistical data available on undercarriage masses and used in this research.

- Reusable Launcher No.6: SSTO-RA(Sub)- ILHL (Ramp-Launched)
This ramp-launched concept for space launchers with a low lift-off acceleration has not been previously considered. The performance characteristic calculated in this research is believed to be realistic, again because of the accurate data that has been used for rocket engine mass estimates.

- Reusable Launcher No.13: SSTO-RA(Sub)-VLVL

The results of the application of air-breathing propulsion to augment the thrust of a vertically-launched rocket-propelled vehicle show that a small gain in the Orbital Mass Ratio is severly negated by the increase in the Engine Mass Ratio. The net result is that the Payload Mass Ratio is substantially reduced. In our reference case, this reduction is 1.58 % compared with that of the rocket-propelled vehicle No.1.

The performance results from this research and those from the referenced studies for each vehicle are now discussed:

- Reusable Launcher No.1: SSTO-R-VLVL

From Figure 5.49, the referenced system study result gives confidence that to achieve our 2 % Payload Mass Ratio, that this vehicle can realistically be designed for a Vehicle Mass Ratio of 11.25 %.

- Reusable Launcher No.2: SSTO-R-VLHL

From Figure 5.50, the referenced system study result indicates that it will not be possible to build this vehicle with the required 10.44 % Vehicle Mass Ratio value to give our design point Payload Mass Ratio value of 2 %. We could however, achieve a 1 % Payload Mass Ratio at a Vehicle Mass Ratio of 10.44 %. This 1 % Payload Mass Ratio is probably too small a value to make it worthwhile to proceed with the development of such a vehicle.

- Reusable Launcher No.3 : TSTO-R-VLHL

From Figure 5.51, the referenced system study result indicates that we can easily achieve our 2 % Payload Mass Ratio value at a very relaxed Vehicle Mass Ratio value of 17.26 %. It must be recalled however, that the Vehicle Mass ratio value for a TSTO vehicle comprises the vehicle mass ratios of both stages. Thus, mass saving measures apply equally to both stages.

- Reusable Launcher No.5: SSTO-RA(Sub)-HLHL (Sled)
From Figure 5.52, the referenced system study result indicates that a Vehicle Mass Ratio of at least 13.93 % is needed to achieve our design point Payload Mass Ratio of 2 %. The referenced study indicates that this might be possible using advanced materials and structural engineering.

- Reusable Launcher No.7: SSTO-RA(Sup)-HLHL (Undercarriage)
From Figure 5.53, the referenced study results indicate that even with a Vehicle Mass Ratio value as high as 27.5 %, that the Payload Mass Ratio is highly negative at -9 %. This vehicle, employing an advanced four-mode combined cycle engine including a scramjet, is supposed to yield an attractive Payload Mass Ratio. The results of this research and those of the referenced study indicate the opposite!. The explanations for this result have already been discussed in Chapter 5.11.3.

- Reusable Launcher No.8: TSTO-RA(Sub)-HLHL (Air-Launched)
From figure 5.54, the referenced study results indicate that our design point Payload Mass Ratio of 2 % can be achieved at a relaxed Vehicle Mass Ratio value of 12.26 %. This air-launched vehicle is therefore an attractive candidate for further study and possible development.

- Reusable Launcher No.9: TSTO-RA(Sub)-HLHL (Undercarriage)
From Figure 5.55, the referenced results indicate that our design point Payload Mass Ratio of 2 % can be achieved at a very high Vehicle Mass Ratio value (for both stages) of 50.88 %. The referenced results show clearly that such a vehicle, using quite conventional subsonic combustion air-breathing propulsion in its First Stage, is inherently a very heavy concept.

- Reusable Launcher No.10: SSTO-R-HLHL (Undercarriage)
From Figure 5.56, the referenced study results indicate that even with a high Vehicle Mass Ratio value of 18.48 %; that this vehicle has a highly negative Payload Mass Ratio of -6.4 %. This poor results derives from the high undercarriage mass and the mass of the propellant required for the take-off run.

- Reusable Launcher No.11: SSTO-R-HLHL (Sled-Launched)
From Figure 5.57, the referenced results indicate that our design point Payload Mass Ratio of 2 % can marginally not be achieved. A reduced Payload Mass Ratio value of 1.96 % appears to be feasible at a Vehicle Mass Ratio value of 11.46 %.

- Reusable Launcher No.12: TSTO-R-HLHL (Undercarriage)
From Figure 5.58 the referenced study results indicate that our design point Payload Mass Ratio of 2 % can be achieved at a Vehicle Mass Ratio Value of 22.96 % (for both stages).

Finally, the results from the referenced system studies have been compared to give a ranking to the candidate vehicles.

Again, although highly desirable, it has not been possible to show the results of all the referenced study results plotted together in the standard graphical presentation, because the graphical scale that would have to be used would result in the close bunching of the characteristics. Instead, to show clearly the performance ranking of the candidate launchers, a barchart of the referenced study results is given in Figure 5.59. This shows the calculated Payload Mass Ratio performance of the vehicles in ascending order from left to right. The barchart also shows clearly for each launcher type, the maximum Vehicle Mass Ratio value that must be achieved in an actual design to obtain the calculated Payload Mass Ratio.

In summary, the results of this research, validated by the referenced study results show that:

- Reusable Launchers 1, 3, 5, 8, 9, 10 and 12 can deliver a positive payload;

- Reusable Launcher 2 has a very marginal capability to deliver a positive payload;

- Reusable Launchers 7 and 11 cannot deliver a positive payload. By deduction from these results, the related Reusable Launcher No 4 (also undercarriage-launched) can also not deliver a positive payload. However, Reusable Launcher No.6, the ramp launched vehicle, can probably deliver a marginal positive payload;

- Reusable Launcher No.13 shows a significant reduced performance potential over its comparable Vehicle No.1 and is therefore assessed to be able to deliver only a small positive payload.

FIGURE 5.49

Comparison Of Results With Those Of Other System Studies
Reusable Launcher No.1: SSTO-R-VLVL
Payload Mass Ratio Versus Vehicle Mass Ratio

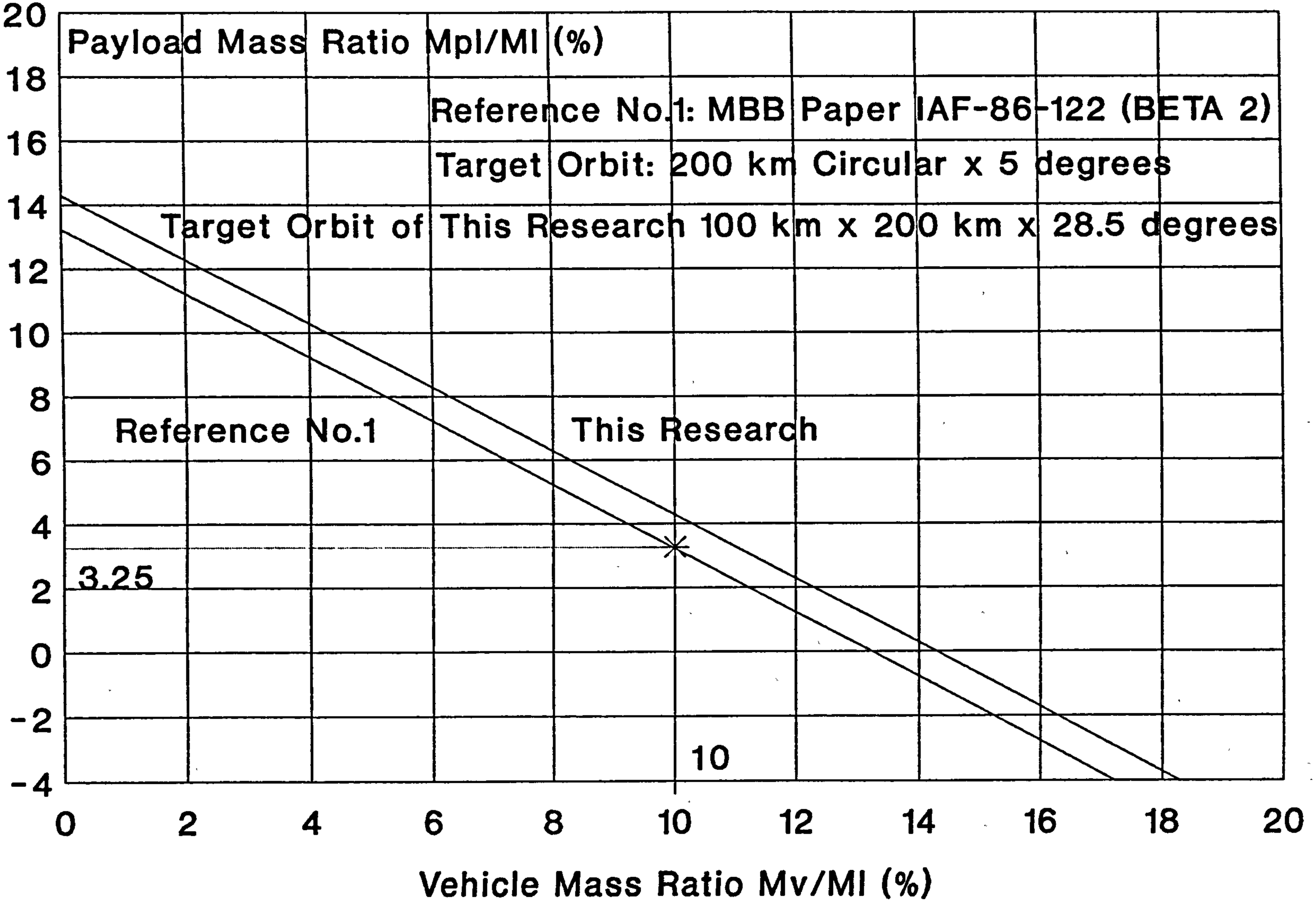

FIGURE 5.50

Comparison Of Results With Those Of Other System Studies

Reusable Launcher No.2: SSTO-R-VLHL

Payload Mass Ratio Versus Vehicle Mass Ratio

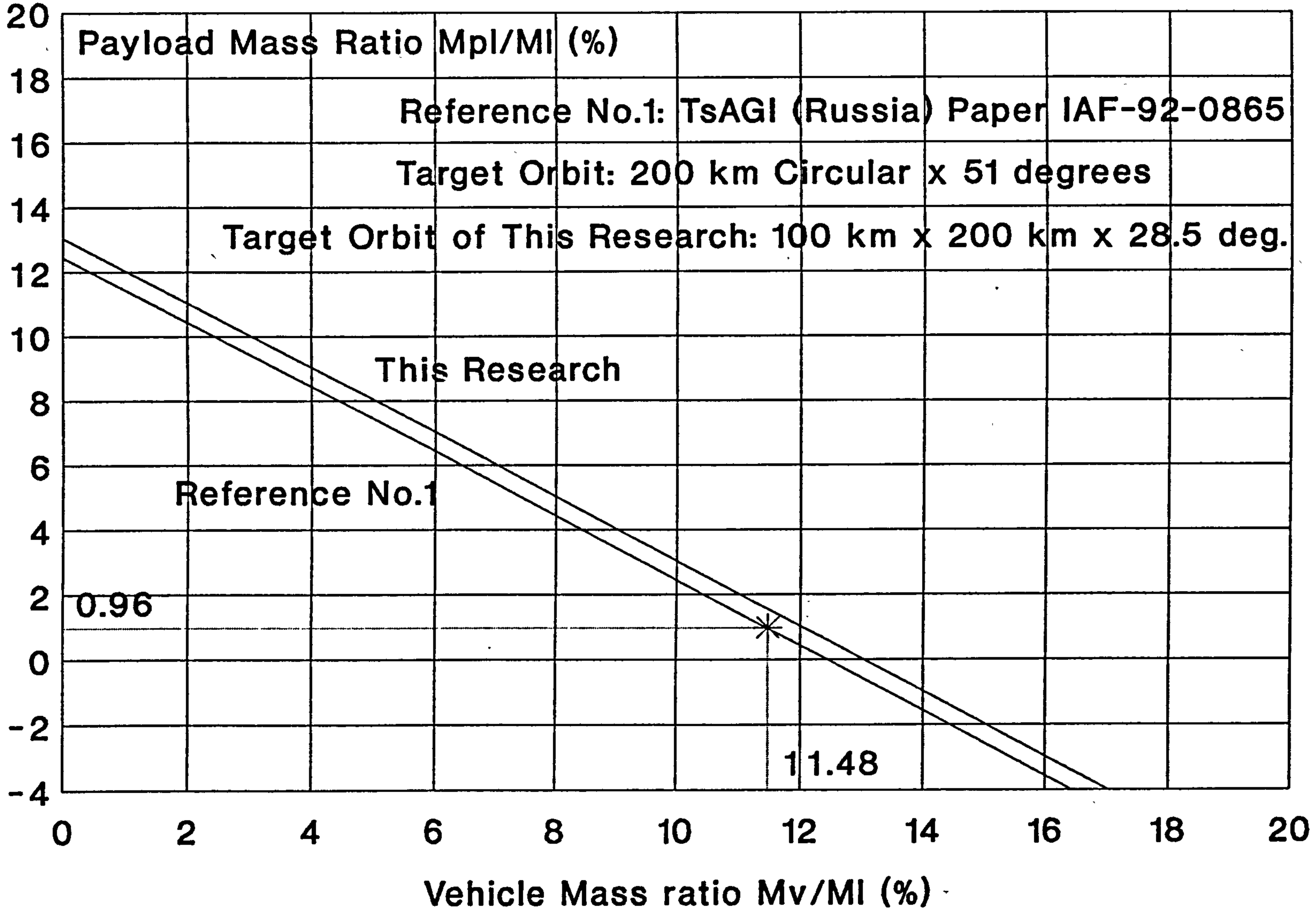

FIGURE 5.51

Comparison Of Results With Those Of Other Studies

Reusable Launcher No.3: TSTO-R-VLHL

Payload Mass Ratio Versus Vehicle Mass Ratio

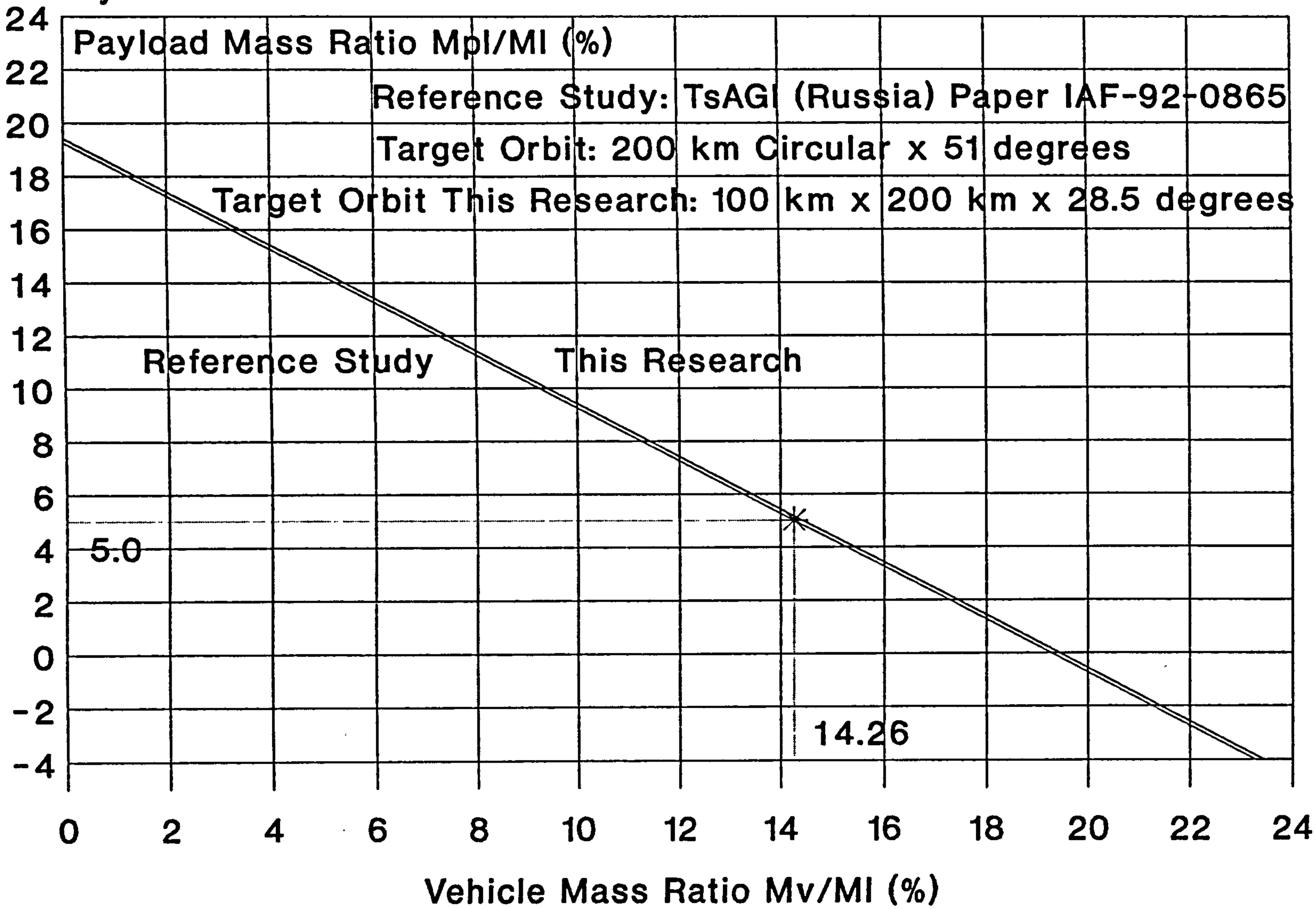

FIGURE 5.52

Comparison Of Results With Those Of Other System Studies
Reusable Launcher No.5: SSTO-RA(Sub)-HLHL(Sled)
Payload Mass Ratio Versus Vehicle Mass Ratio

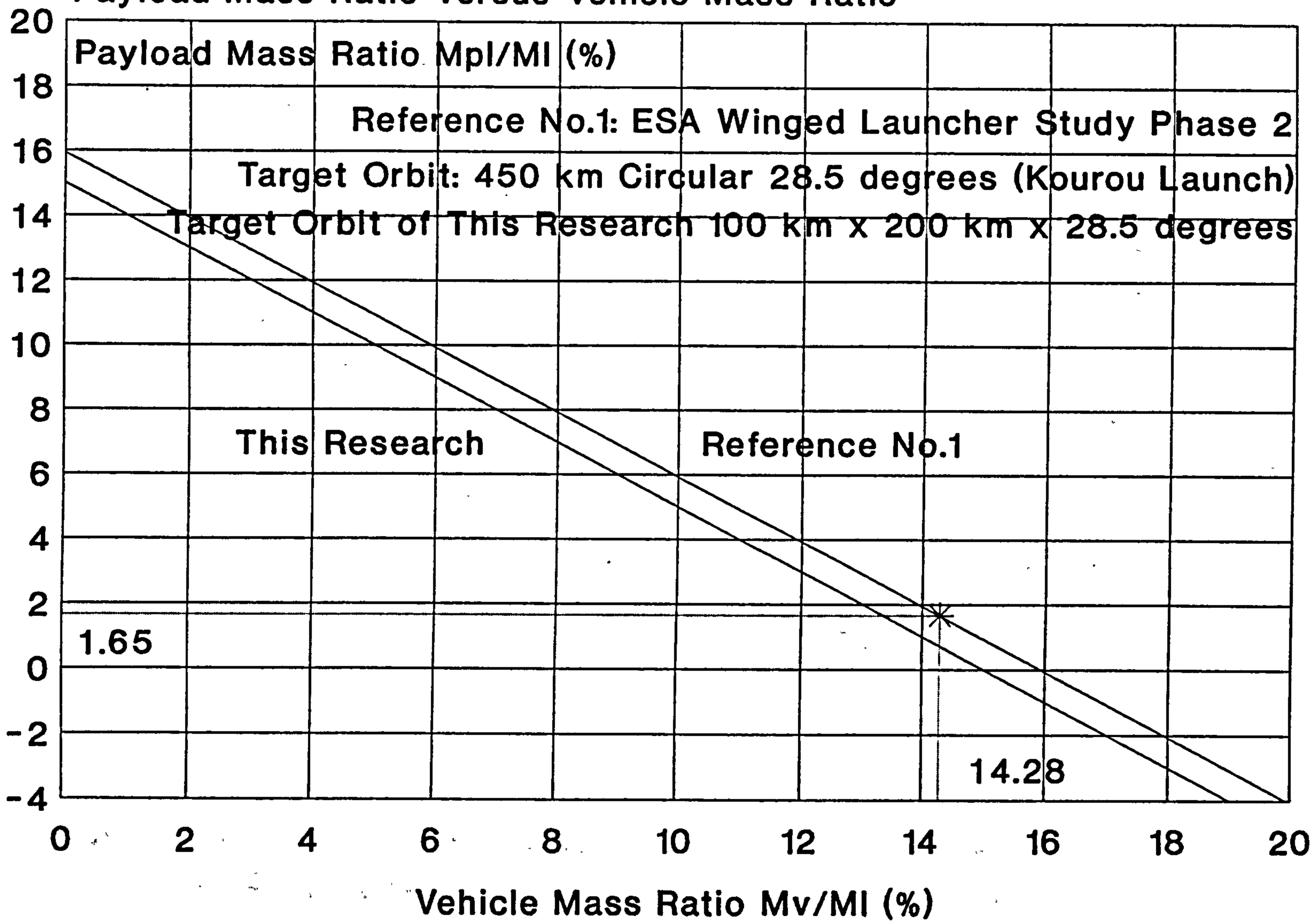

FIGURE 5.53

Comparison Of Results With Those Of Other System Studies
Reusable Launcher No.7: SSTO-RA(Sup)-HLHL (Undercarr.)
Payload Mass Ratio Versus Vehicle Mass Ratio

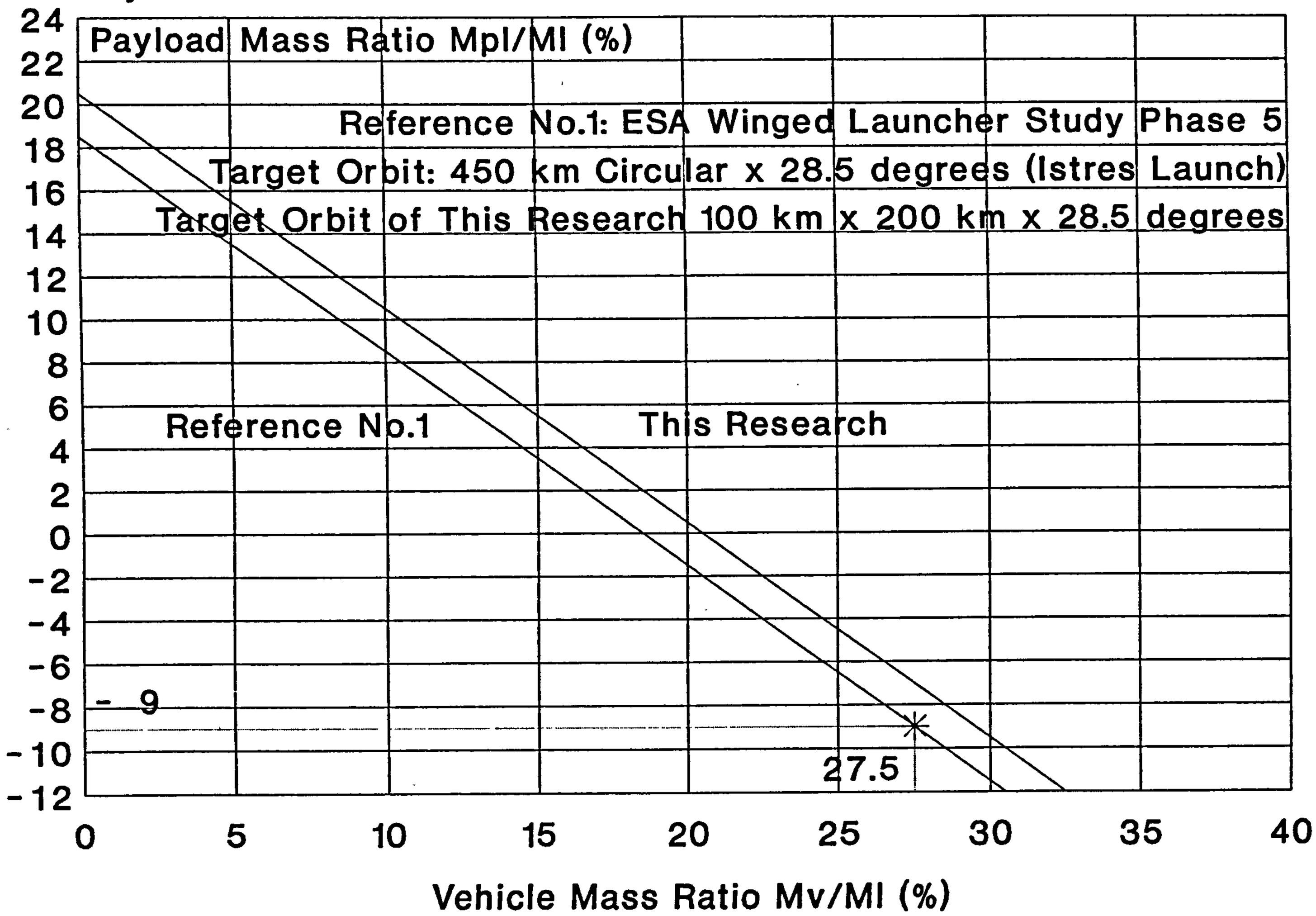

FIGURE 5.54

Comparison Of Results With Those Of Other System Studies
Reusable Launcher No.8: TSTO-RA(Sub)-HLHL(Sub) (Air Launch)
Payload Mass Ratio Versus Vehicle Mass Ratio

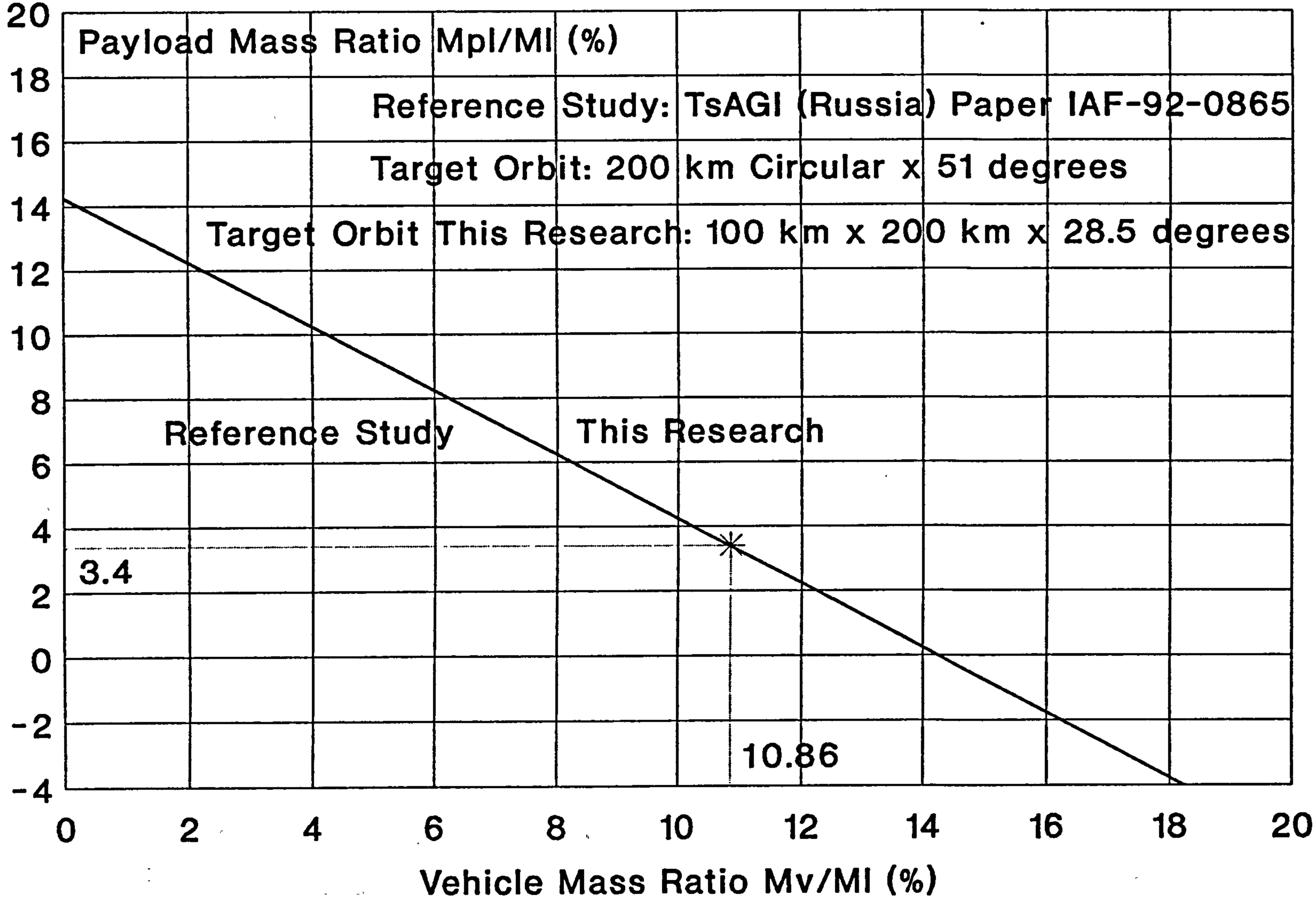

FIGURE 5.55

Comparison Of Results With Those Of Other System Studies
Reusable Launcher No.9: TSTO-RA(Sub)-HLHL(Sup) (Undercarr.)
Payload Mass Ratio Versus Vehicle Mass Ratio

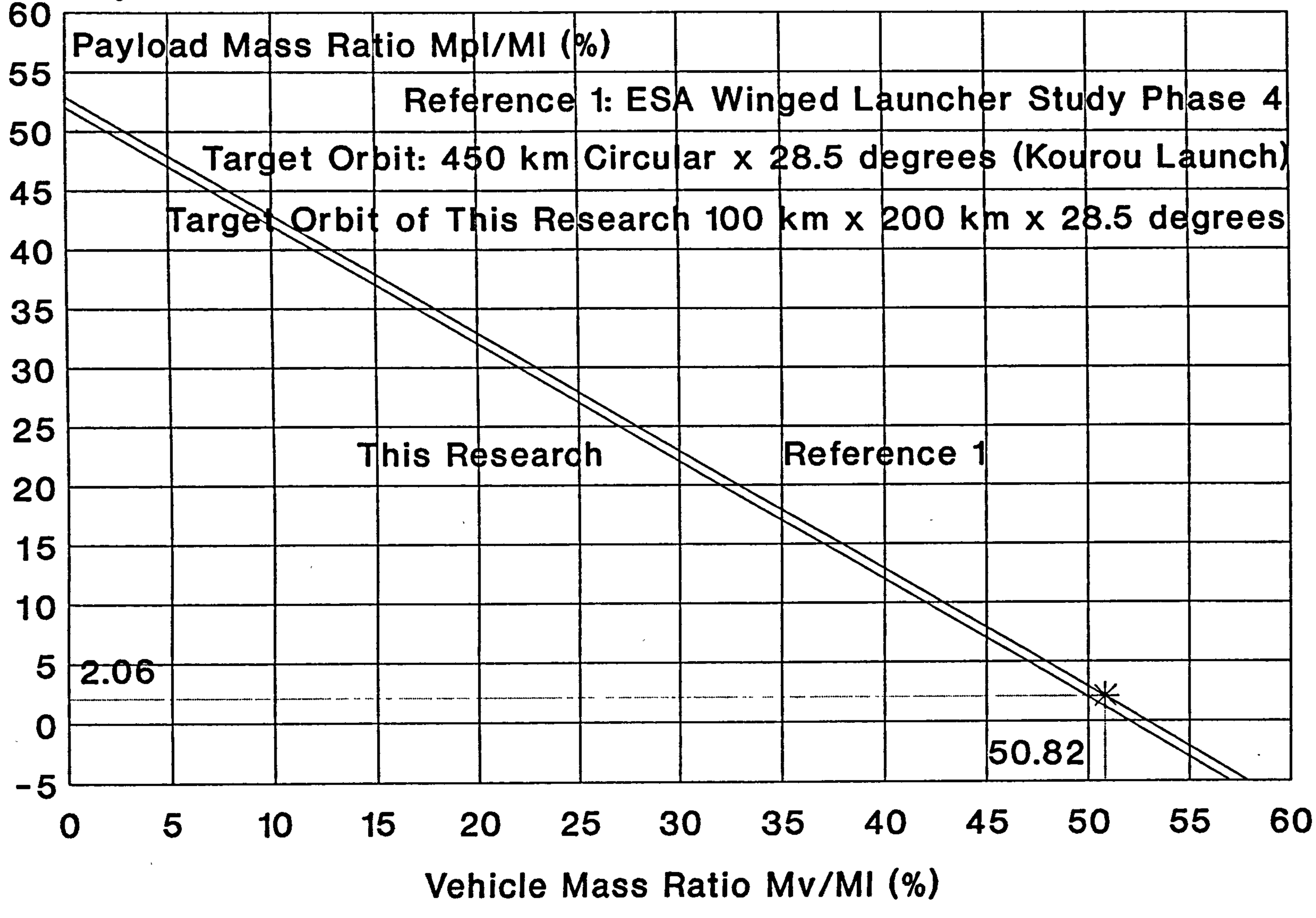

FIGURE 5.56

Comparison Of Results With Those Of Other Studies
Reusable Launcher No.10: SSTO-R-HLHL(Undercarriage)
Payload Mass Ratio Versus Vehicle Mass Ratio

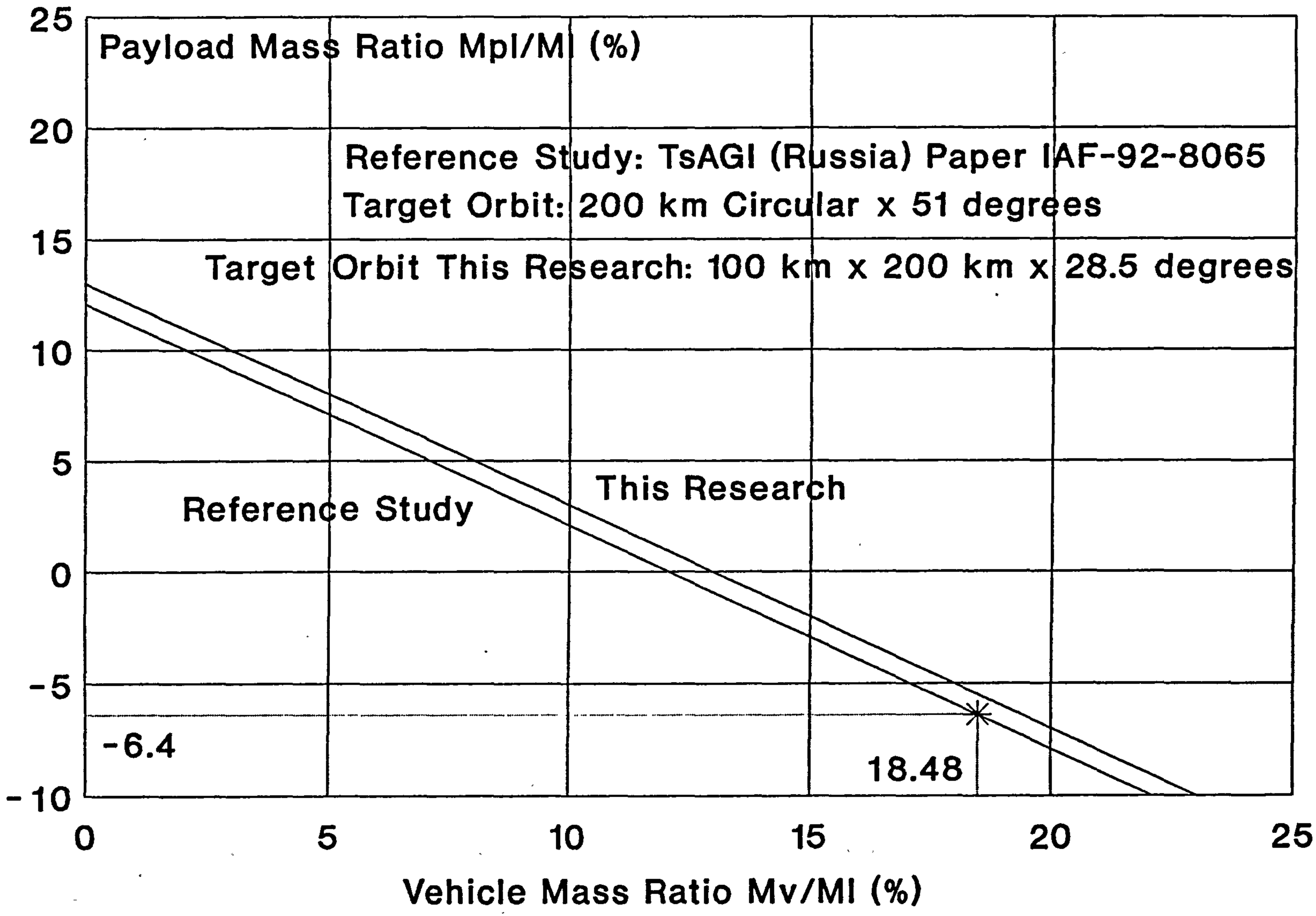

FIGURE 5.57

Comparison Of Results With Those Of Other Studies
Reusable Launcher No.11: SSTO-R-HLHL(Sled Launch)
Payload Mass Ratio Versus Vehicle Mass Ratio

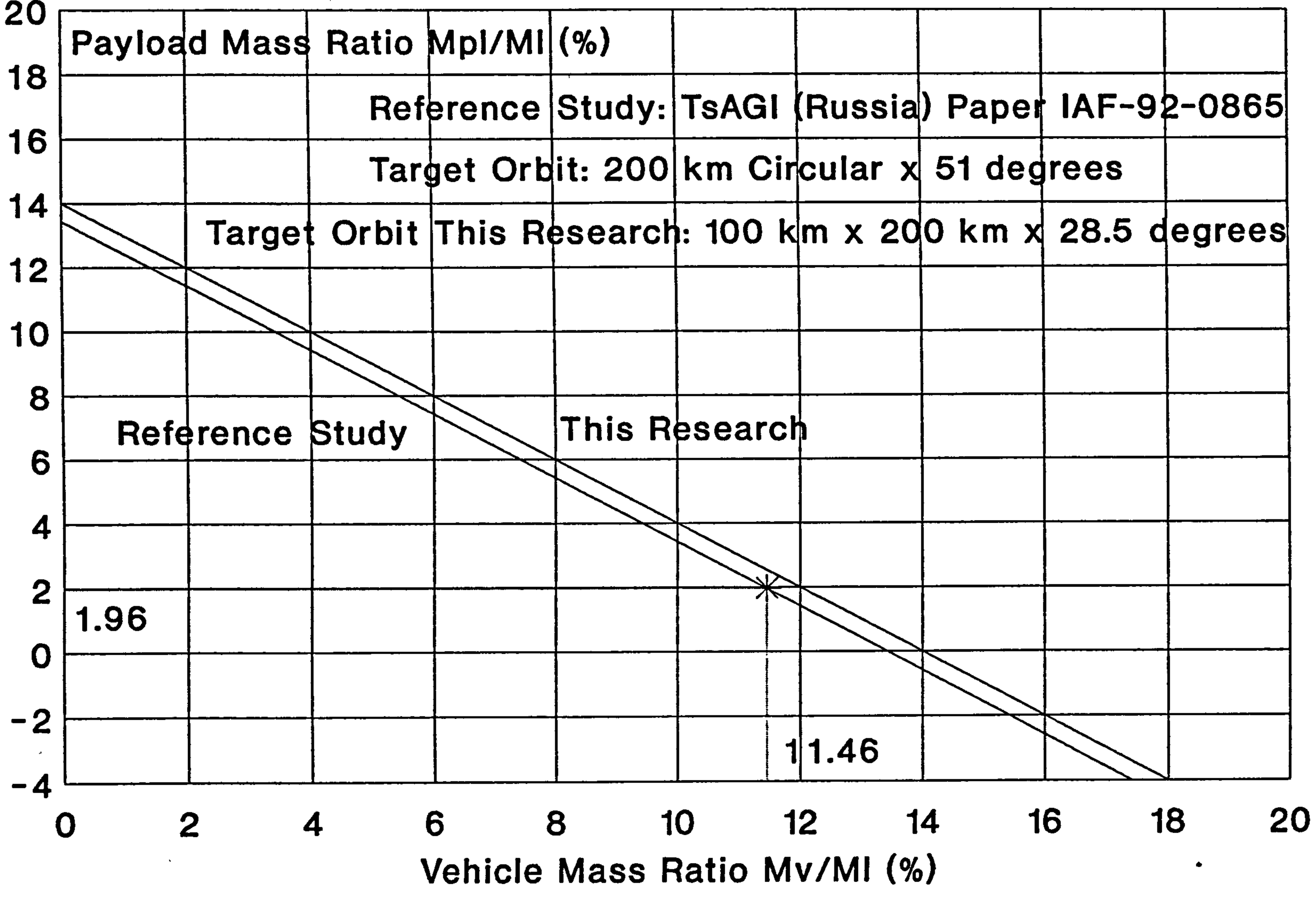

FIGURE 5.58

Comparison Of Results With Those Of Other Studies

Reusable Launcher No.12: TSTO-R-HLHL (Undercarriage)

Payload Mass Ratio Versus Vehicle Mass Ratio

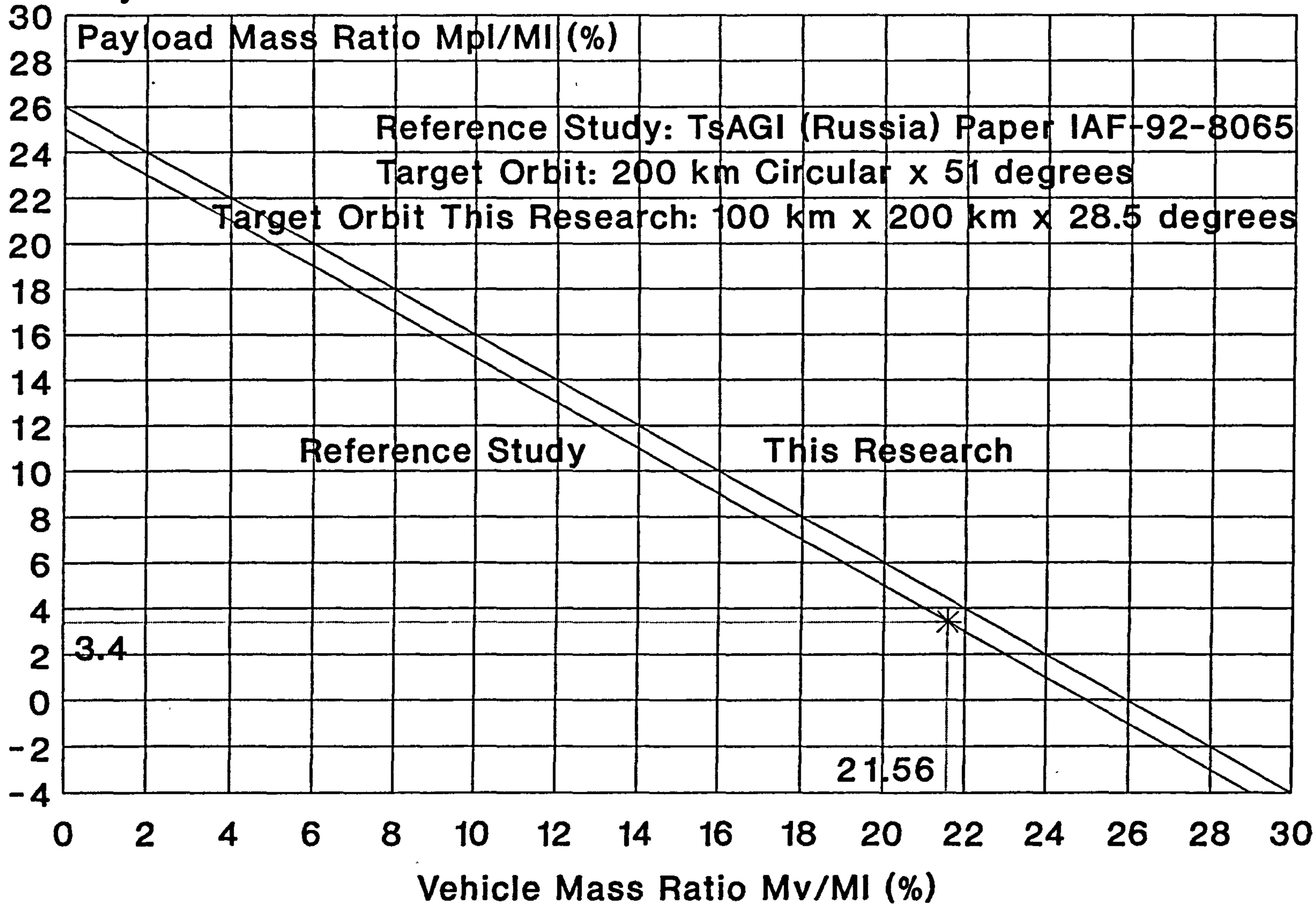

FIGURE 5.59

Comparative Results Of Other System Studies

Calculated Vehicle Mass Ratios and Payload Mass Ratios

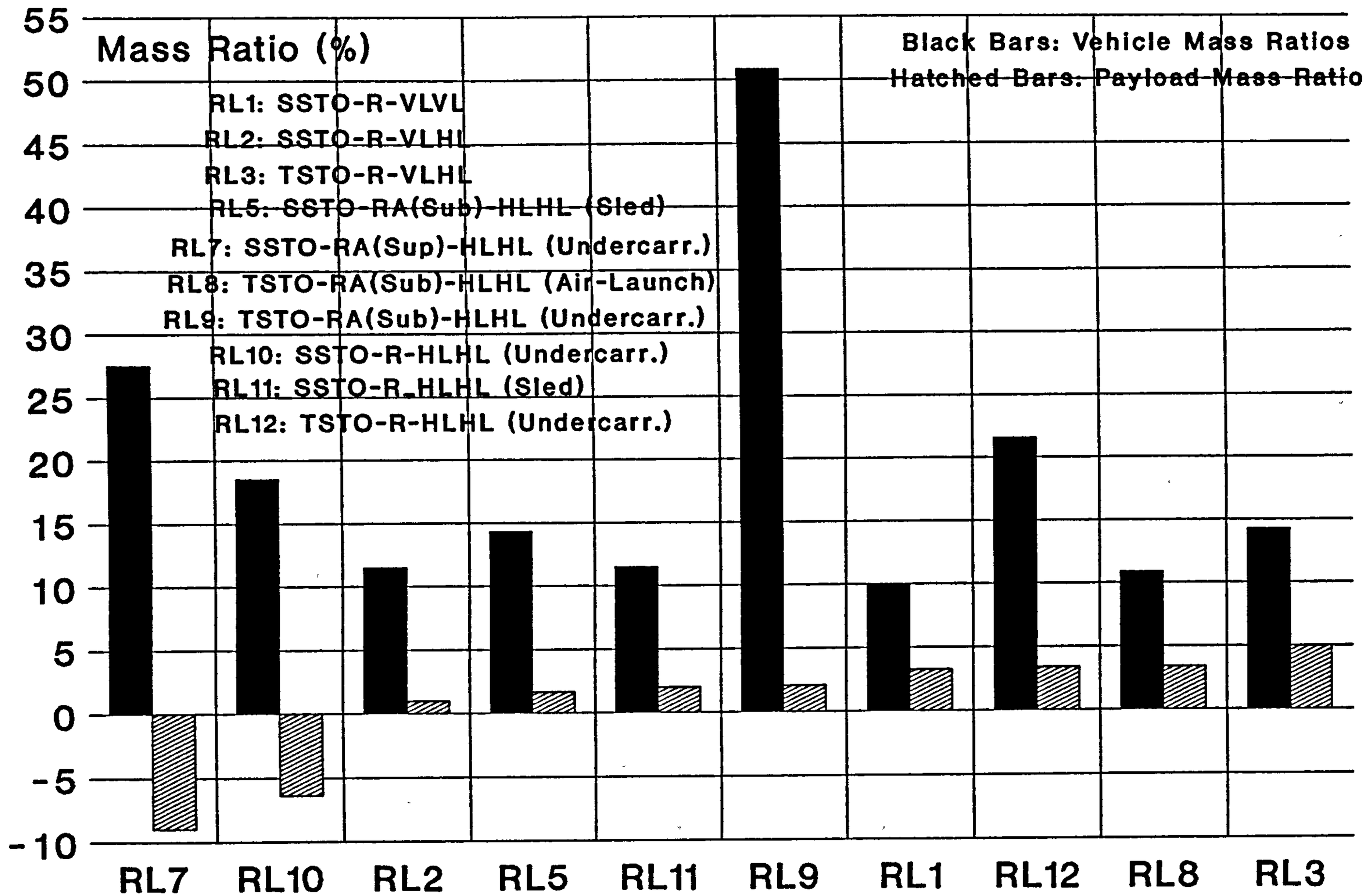

6 TECHNOLOGY ASSESSMENT FOR REUSABLE LAUNCHERS

In Chapter 5, the performance of each of the 13 candidate reusable launchers was calculated to provide answers to the first of the three imperative questions which are central to this research: which reusable launcher concepts can actually deliver a positive payload mass to orbit? This Chapter of the Thesis now addresses the second imperative question: what advanced technologies are needed to enable the practical realisation of each reusable launcher concept and is it feasible to develop these technologies in a reasonable time scale and at affordable costs?

The technologies required for space launchers are:
- propulsion;
- aerodynamics and aerothermodynamics;
- materials, structures and thermal protection;
- trajectories, guidance and control;
- vehicle subsystems.

The collective benefit of advances made in all these technology areas will be necessary to make reusable launchers possible. The status of development, the new technological problems posed by reusability and the potential advancements in each of these technologies have been assessed in this research. The results of this assessment are presented in this Chapter for the most critical of these technologies, in the following order and grouping of the related technologies: rocket propulsion; airbreathing propulsion; materials, structures and thermal protection. The value of this assessment is the identification of emerging technical developments and design approaches that are deemed by the author to be feasible and could enable the successful practical realisation of reusable launchers.

6.1 Rocket Propulsion Systems

Rocket propulsion systems will be required for all reusable launcher concepts. This is obvious for those vehicles which are entirely rocket-propelled. For air-breathing propelled vehicles, rocket-propulsion will be indispensable for propelling the vehicle through the final high altitude ascent phase because the very low air density at altitude is insufficient to support air-breathing propulsion. Furthermore, rocket propulsion will also be indispensable for orbital manoeuvring and the re-entry retro-propulsion of the vehicle. Thus, the continuing development of advanced rocket propulsion systems is a high priority to make reusable launchers possible.

Among the range of developed rocket propulsion technologies, liquid oxygen/hydrogen rocket propulsion systems have emerged to be the highest performing, practically feasible propulsion system for space launchers. Indeed, LOX/LH2 rocket propulsion technology has made possible the development of the world's current partially reusable launchers: NSTS and Energia/Buran. LOX/LH2 rocket propulsion will therefore be indispensable for reusable launchers and further developments of this system is deemed by the author to be a major key to achieving full reusability. It is therefore well worthwhile to explore the potential for the further development of LOX/LH2 rocket propulsion and this has been undertaken in this research.

6.1.1 Current Status of LOX/LH2 Rocket Propulsion

Table 6.1 shows the current status of LOX/LH2 rocket propulsion systems. This data has been compiled from References 1 and 15. It can be seen from Table 6.1 that all the major space nations have mastered this technology. It can also be seen that LOX/LH2 propulsion was first developed for

use in upper stage propulsion of multi-stage expendable launchers and that its use has now been extended to lower stage (booster and core stage) propulsion. Indeed, the trend is towards the complete use of LOX/LH2 propulsion for all the stages of expendable launchers.

The performance characteristics of each engine are also shown in Table 6.1. It can be seen that although the vacuum specific impulse is a function of the mixture ratio, combustion pressure and nozzle area ratio, that the most influencing parameter is the area ratio. Because of the widely varying engine sizes, the thrust/weight ratio is an important comparative performance parameter and these values are also shown in Table 6.1. It can be seen that the thrust/weight ratio is strongly influenced by the engine size as signified by its vacuum thrust level. This result is demonstrated further in Figure 6.1, which shows engine mass versus vacuum thrust. It can be seen that it is possible to define a simple logarithmic relationship between mass and thrust for LOX/LH2 engines, allowing first-order mass estimates to be made for any engine with the same materials technology.

6.1.2 Required Advancements in LOX/LH2 Rocket Propulsion

The required advancements are:
- higher specific impulse;
- higher thrust/weight ratio.

Higher specific impulse will yield a series of cumulative mass reduction effects, beginning with a reduction of the propellant mass as the first step in this chain. This then results in a reduction of the tankage volume and therefore the tankage mass. This then results in a reduction of the launcher size and therefore its dry mass. The launcher size reduction then results in a reduction of the aerodynamic drag

losses, which leads to a further reduction of the propellant mass.

Higher thrust/weight ratio leads directly to a decrease in the engine mass for the same thrust level. This engine mass reduction allows to increase the payload mass for all reusable launchers and is of maximum benefit for rocket-propelled SSTO vehicles, where the total mass reduction allows to increase the payload mass by the same amount.

We can now quantify the payload mass ratio gains that would be achieved by increases in the specific impulse and the thrust/weight ratio:

For example, for Reusable Launcher No.1: SSTO-R-VLVL, the influence of an increase in specific impulse is calculated below:

From Figure 5.3, at a Vehicle Mass Ratio of 10 %:
When I_s = 400 s, M_{pl}/M_l = 1 %
and when I_s = 464 s, M_{pl}/M_l = 4.3 %
Thus ΔI_s = (464 - 400) = 64 s
and $\Delta(M_{pl}/M_l)$ = (4.3 - 1) = 3.3 %
Therefore $\Delta(M_{pl}/M_l)/\Delta I_s$ = 3.3/64 = 0.0516 %/s
Thus, for each second increase in the Specific Impulse, the increase in the Payload Mass Ratio is 0.0516 %

Similarly, for Reusable Launcher No.1, the influence of an increase in the engine thrust/weight ratio is calculated below:

For a lift-off thrust/vehicle weight (F_l/W_l) of 1.4 and a vehicle lift of mass M_l of 350000 kg:
F_l = (1.4 x 350000 x 9.81) = 4806900 N
and for an engine thrust/weight ratio F_l/W_e = 80
$W_e = F_l/80$ = 4806900/80 = 60086 N

and the mass of the engine M_e = 60086/9.81 = 6125 kg
If the engine thrust/weight F_l/W_e can be increased to 100,
then M_e = (6125 x 80/100) = 4900 kg
Then $\Delta(F_l/W_l)$ = (100 - 80) = 20
and ΔM_e = (6125 - 4900) = 1225 kg
Now, the saving in engine mass increases directly the payload mass.
Therefore, $\Delta M_{pl} = \Delta M_e$ = 1225 kg
Therefore, for a Payload Mass Ratio of 2 % and a launcher lift-off mass of 350000 kg:
The new payload mass is (7000 + 1225) = 8225 kg
and the new payload mass ratio M_{pl}/M_l = 8225/350000 = 2.35 %
Therefore, $\Delta(M_{pl}/M_l)$ = (2.35 - 2) = 0.35 %
Thus, $\Delta(M_{pl}/M_l)/\Delta(F_l/W_e)$ = 0.35/20 = 0.0175 %
Thus, for unit increase in the Engine Thrust/Weight ratio, the Payload Mass Ratio increases by 0.0175 %

The combined effect of an increase in the specific impulse and the engine thrust/weight ratio can now be demonstrated for Reusable Launcher No.1, the SSTO-R-VLVL vehicle:

From Figure 5.3, at our design point condition D1, the Vehicle Mass Ratio is 12.3 %, the Vacuum Specific Impulse is 464 s and the Payload Mass Ratio is 2 %
If we can increase the specific impulse by only 1 % from 464 s to 468.64 s and we can simultaneously increase the engine thrust/weight ratio from 80 to 100, the resulting increase in the payload mass ratio is:
$\Delta(M_{pl}/M_l)$ = (0.0516 x 4.64) + (0.0175 x 20) = 0.2394 + 0.35
= 0.5894 %, which is about 0.6 %
This is a significant increase in the payload mass ratio, for what is deemed by the author, to be easily achievable increases in the specific impulse and engine thrust/weight ratio values. How these increases can be achieved are presented in the following Section.

6.1.3 Potential Methods to Improve LOX/LH2 Rocket Propulsion

The potential improvements relating to an increase in the specific impulse and an increase in the engine thrust/weight ratio are addressed separately below.

To increase the specific impulse, the following methods can be employed individually or in combination to maximise the potential increase:

- the use of higher performing thermodynamic cycles;
- the use of higher combustion pressure;
- the optimisation of the mixture ratio at Vehicle level;
- the use of variable mixture ratio, optimised over the ascent trajectory;
- the use of larger nozzle expansion ratios;
- the use of self-adapting, external expansion nozzles.
- the use of the dual fuel engine concept;
- the use of the tripropellant concept.

An analysis of each of these methods for increasing the specific impulse is presented below:

The Use of Higher Performing Thermodynamic Cycles

There are five basic thermodynamic power cycles for rocket engines, from which a large number of combinations can be derived. These basic cycles are classified into two types: open cycles and closed cycles. In the open cycles, the fluid which drives the turbines that power the propellant pumps, is not used in the main combustion chamber but is exhausted through separate nozzles. These open cycles are: the Gas Generator Cycle; the Bleed (or Open Expander Cycle); the Tap-Off Cycle. In the closed cycles, the total propellant mass flow is used in the combustion chamber and exhausted through the propulsive nozzle. These cycles are: the Expander Cycle; the Staged Combustion Cycle. Thermodynamic analysis and engine tests have demonstrated that of these five basic

cycles, the Staged Combustion cycle delivers the highest specific impulse and the Gas Generator cycle delivers the lowest specific impulse. The selection of the best engine cycle must however be based on optimisation at complete vehicle level because maximum specific impulse at engine level does not necessarily imply achieving the highest payload mass ratio or lowest launch cost. In general, the engine complexity, durability, reliability, mass and cost, all increase with the selection of a higher performing engine cycle. The author therefore recommends that, for any future launcher, to select the lowest performing (least complex) cycle which can deliver the required propulsive performance. An excellent analysis of these five basic engine thermodynamic cycles is given in Reference 16.

The Use of Higher Combustion Pressures

For a given thrust level, the use of higher combustion pressures results in a smaller and more compact combustion chamber and nozzle throat area. This permits therefore, to use a larger nozzle expansion ratio within an assigned nozzle length. This in turn, results in an increase in the specific impulse. This increase however, is dependent on the engine cycle used. The influence of combustion pressure on rocket engine performance for different power cycles are described and quantified in Reference 17. A typical result, for the Staged Combustion Cycle, gives a linear specific impulse increase from 465 s to 470 s over the combustion pressure range of 140 bar to 240 bar. This is quite a small gain in specific impulse, being only 1 % However, the main advantage of using higher combusation pressure results from the size reduction of the engine, which yields vehicle configuration advantages.

Optimisation of the Propellant Mixture Ratio

At engine level, thermodynamic analysis shows that the optimum propellant mixture ratio (oxidiser/fuel mass flow ratio) for maximum vacuum specific impulse for LOX/LH2 rocket engines is a value of 6. However, at launch vehicle level, this relatively low mixture ratio value, results in a large and heavy liquid hydrogen tank. This in turn, results in a larger and therefore heavier vehicle. It is postulated that an increase in the mixture ratio could yield a lower propellant mass by the resulting increase in the average density of the propellant (oxygen plus hydrogen). This postulation has been examined in a comprehensive SSTO-R-VLHL launcher study (Reference 18) and has found indeed to be correct and for that particular study, a 3 % reduction in the dry mass of the vehicle was achieved by increasing the mixture ratio from 6 to 6.5, despite a corresponding decrease in the delivered specific impulse.

The Use of Variable Mixture Ratio, Optimised over the Ascent Trajectory

A further refinement in the optimisation of the mixture ratio, is to vary it in an optimal way throughout the ascent trajectory. This implies using a high mixture ratio at lift-off and progressively reducing it as the vehicle ascends. The high value allows to increase the propellant density at lower altitudes and the lower value allows to increase specific impulse. The net result is expected to be a reduction in the dry mass of the vehicle. Such a continuous mixture ratio reduction schedule has not yet been fully studied. The literature does not address this point and the author recommends that such a study is undertaken for each of the entirely rocket-propelled vehicles. However, a variation of the mixture ratio in two discrete steps has been studied in Reference 18. The results show that a very substantial vehicle dry mass reduction of 10 % and a vehicle gross mass reduction of 8.6 % was achieved for the SSTO-R-VLHL vehicle

that was studied. Of course, the use of a continuously variable, and even a two step variable mixture ratio scheme, implies design complexity for the turbopumps, the injectors and the control system of the rocket engine. These practical engineering aspects will have to be addressed before conclusions can be drawn on the feasibility of using variable mixture ratio schemes.

The Use of Larger Nozzle Expansion Ratios

For rocket engines with bell nozzles that have to operate over a large ambient pressure range from sea level to orbital altitudes of 80 to 100 km, the nozzle expansion ratio should ideally be continuously increased with altitude so that optimum expansion to the ambient pressure occurs throughout the ascent. Such an ideal nozzle would then yield the maximum specific impulse over the complete ascent trajectory. Unfortunately, it is apparently not possible to make such a self adapting bell nozzle. Instead, the nozzle expansion ratio must be selected at an optimum value, which is much higher than the required value for sea-level lift-off and is inevitably also much lower than the required value for full expansion at orbital altitude. This optimum value is selected to give the highest value of average specific impulse over the ascent trajectory, whilst being limited by the phenomenon of unsymmetrical flow separation in the nozzle that can occur at lift-off and low altitude flight. This separation occurs due to the severely overexpanded nature of the flow, exacerbated by the unsettled flow conditions in the engine during its start-up phase. Flow separation, if completely symmetrical would not pose a problem and indeed, if it can be guaranteed that the flow would always separate symmetrically, would provide a means to allow the use of much higher nozzle expansion ratios at sea level, despite the thrust loss due to the overexpansion. Unfortunately, imperfections in nozzle shape and surface finish, together with the non uniform flow in the nozzle, always results in an unsymmetrical separation

in overexpanded nozzles. The result of this is an attachment of the separated flow to one side of the nozzle wall, producing a high side-load and heating on the impinged part of the nozzle. This then invariably results in structural failure and break-up of the nozzle. If the nozzle is made strong enough to withstand the side load, the thrust vector deviation can then pose an attitude control problem for the vehicle. A typical value of the optimum area ratio for a large LOX/LH2 engine like the European Vulcain engine for the core stage of the Ariane 5 launcher is a surprisingly small value of 45.

Because nozzle performance is deemed by the author to be one of the key technologies that can enhance rocket engine specific impulse for reusable launchers, the nozzle performance has been investigated in this research and the results are presented below.

Figure 6.2 shows the sea level thrust coefficient and area ratio as functions of the combustion pressure for all nozzle types. It can be seen that the thrust coefficient increases rapidly for combustion pressures up to about 50 bar and then increases very slowly to a maximum at the highest pressure of 250 bar selected for this study.

Figure 6.3 shows the thrust coefficient versus altitude with combustion pressure as a parameter for fully adapted nozzle flow. It can be seen that although the thrust coefficient increases with combustion pressure, that the thrust coefficients for all combustion pressures converge to a single unique value at vacuum conditions.

Figure 6.4 shows the thrust ratio (which is also the specific impulse ratio) versus altitude, with combustion pressure as a parameter, for fully adapted nozzle flow. It can be seen that the thrust ratio decreases with increasing combustion

pressure. This result is intuitively unexpected and is therefore not generally known.

Figure 6.5 shows the thrust ratio as a function of altitude for fully adapted, altitude adapted and sea-level adapted nozzle flows, at a combustion pressure of 250 bars. It can be seen that if it is possible to have a very large area ratio like 830, that significant thrust ratio and specific impulse ratio gains in the order of 10 % can be achieved.

The Use of Self-Adapting, External Expansion Nozzles.

The discussion above on the use of larger area ratio nozzles, revealed the potential of large area ratios to increase specific impulse. Because the conventional bell nozzle is not self-adaptable to the ambient pressure, alternative nozzle types, which do not need mechanical means to adapt their shape, are worth investigating. Such nozzles are: the Expansion-Deflection Nozzle and the Plug Nozzle.

The Expansion-Deflection Nozzle resembles the bell nozzle, but by having a plug at its centre, lets the flow expand outward, with a free flow boundary behind the plug, giving it altitude compensating features.

The Plug or Aerospike Nozzle allows the impinging flow from a rocket chamber throat to expand along the surface of a plug, which acts as an extended expansion surface along the inward side of the flow stream. The outward side of the flow has a free boundary, thus allowing it to adapt to the ambient pressure to provide altitude compensation. Figure 6.6, taken from Reference 19 shows schematically the operation of the Plug Nozzle. The combustion chamber can comprise an annular chamber positioned around the top periphery of the plug and discharging its flow through an annular throat on to the plug surface. Unfortunately, this scheme results in a very small throat annulus gap, which would be difficult to manufacture

and to maintain the small dimensions around the annulus under high temperature and pressure conditions. Furthermore, the small throat size leads to very large heat loads at the throat. To circumvent the throat gap problems, the annulus may be divided into a number, typically 12 to 20, linear combustion chambers, positioned around the plug. The result of this is a more complex flow with three dimensional supersonic flow effects on the plug from the flow discontinuities between the linear modules, resulting in propulsive losses and high heat loads at the mixing areas of the plug. Another, more practical approach, is to position small coaxial rocket engines around the plug and to accept the mixing losses in the interests of mechanical simplicity and cost. Thrust vector control can be achieved by differential throttling of engine modules around the plug. Engine-out failure tolerance is then automatically provided by switching out the opposite engine and throttling-up all engines to compensate the loss of thrust. Alternatively, the mission may be allowed to proceed to a lower energy orbit, without the added complexity of throttling-up the remaining engines.

The higher specific impulse advantage of the plug nozzle is illustrated in Figure 6.7, which has been taken from Reference 20. This shows the specific impulse versus altitude for several current LOX/LH2 rocket engines and the specific impulse of the ideal plug nozzle and that of the multi-engine plug concept as described above. It can be seen by comparing the areas under each specific impulse curve, that the plug engine can deliver a major increase in specific impulse. The author recommends that the potential advantage of the plug nozzle warrants its urgent investigation in an experimental testing programme. This could begin with tests using small scale, cold inert gas flows and leading progressively to full scale reacting gas flows.

The Use of the Dual Fuel Engine Concept

The dual fuel or mixed-mode propulsion concept was suggested in 1971 (Reference 21) as a means to achieve a practical SSTO vehicle. It involves the use of a dense, good performing propellant combination at lift-off, followed by a less dense, but higher performing propellant combination at altitude. This results in vehicle dry mass reductions because of lower tankage and vehicle structural mass. Various propellant combinations have been evaluated for the lower altitude flight phase (hydrocarbon fuels with LOX). For the high altitude flight phase LOX/LH2 is used. Various thermodynamic power cycles and engine operating modes have also been suggested. Among these, the Dual Fuel Dual Expander Engine has emerged as an attractive concept (Reference 22). The engine generates an outer, primary stream produced by a LOX/LH2 staged combustion cycle, and an inner secondary stream produced by a LOX/LHC gas generator cycle. Both streams are operated at lift-off (Mode 1). At altitude, where the highest performance is required, only the outer stream is operated (Mode 2). Apart from the inherently higher specific impulse derived from the LOX/LH2 propellants, an additional increase in performance is then derived because of the larger area ratio of the nozzle which results because the LOX/LH2 flow now fills the complete nozzle.

The Use of the Tripropellant Engine Concept

Whereas dual fuel cycles use two propellant combinations which are burned in separate combustion chambers within the same engine, a tripropellant engine burns a combination of two different fuels and an oxidiser at the same time in the same combustion chamber.

Currently, only one tripropellant engine is known to be under development. This is the Russian RD701, under development by NPO Energomash in its Khimky Plant near Moscow.

In Mode 1, the propellants LOX/LH2/RP1 are burned simultaneously for the lift-off and low altitude flight phase. The mixture ratio is 81.4 % LOX plus 6 % LH2 plus 12.6 % RP1. The thrust from two chambers is 408 tonnes. The Combustion Pressure is 300 bars. The Vacuum Specific Impulse is 416 s. In Mode 2, the propellants are LOX/LH2. The mixture ratio is not known. The thrust from two chambers is 162 tonnes. The Combustion Pressure is 126 bars. The Vacuum specific Impulse is 462 s.

The RD701 engine is apparently being designed for the MAKS partially reusable launcher, which is to be launched from the Antonov 225 aircraft and also for the Interim HOTOL Vehicle of British Aerospace, which is a rocket-propelled reusable launcher, also to be air-launched from the Antonov 225 Heavy-lift cargo aircraft. The status reached is that a complete metallic, full-scale mock-up of the engine was available in March 1992 (Reference 23).

Increase in the engine thrust/weight ratio can be achieved by:

- selection of the engine thermodynamic cycle and design parameters (mixture ratio, combustion pressure, nozzle area ratio), **based on optimisation at complete vehicle level for minimum engine mass;**
- the use of advanced high specific strength (tensile strength/ density ratio) materials for the construction of the engine;
- the designers skill to minimise engine mass.

The impact of the combined effect of these three mass reduction methods is best illustrated by comparing the

thrust/weight ratios of the USA's SSME (1970's technology) and STME (1990's technology) LOX/LH2 engines. From Table 6.1, it can be seen that the thrust/weight ratio projected for the STME engine has been considerably increased to a value of 91 compared to a value of 67.2 for the SSME engine, which is currently the world's most performing and advanced LOX/LH2 engine. This represents a very substantial 35 % increase in the thrust/weight ratio!

Because the author perceives that the major contributor to the reduction in engine mass is the use of advanced materials, the development status and application potential of these materials has been investigated in this research and the results are summarised below.

Of all the mechanical engineering technologies, rocket engines and LOX/LH2 engines in particular, pose the most demanding material requirements. These materials must operate under extreme conditions:
- a temperature range, from 20 K for cryogenic hydrogen to 3500 K for LOX/LH2 combustion products;
- a combustion pressure range, currently about 200 bar, but likely to increase to about 300 bar for future engines;
- the oxidising environment of hot (3500 K) oxygen combustion products;
- the embrittlement environment of hot (3500 K) hydrogen combustion products.

Under these severe conditions, the materials must retain their mechanical properties and the component parts of the engine must retain their dimensional stability. All these requirements will be made much more demanding for reusable engines.

To meet these material requirements, engine components require active cooling schemes using the relatively colder

propellants, in both liquid and gaseous phases, to cool the hot walls of combustion chambers and nozzles. To improve engine performance, at the expense of higher complexity, the recovery of the heat energy in the coolant flow must be used in regenerative cooling schemes.

For the purposes of defining the specific material requirements, LOX/LH2 engines may be split into the following major components:

- gas generators;
- turbopumps;
- thrust chamber;
- nozzle extension;
- engine valves;
- propellant tubes and manifolds;
- engine gimbals and actuators;
- engine control electronics.

Materials for Gas Generators: Gas generators operate with low mixture ratios to provide hydrogen-rich combustion gases at about 1000 k to drive the turbines of the turbopumps. This necessitates the use of nickel alloys which are resistant to hydrogen embrittlement and are easily welded. The currently used material is the nickel-based Super Waspalloy. This material requires no coatings to protect it under the embrittlement conditions at 1000 K. Because of the low mass of gas generators using Super Waspalloy (about 3 % of the total engine mass), the author has concluded that potential mass reductions from the use of more advanced materials would be quite small and therefore not worth pursuing. The continued use of Super Waspalloy is recommended, with the use of cast and/or machined combustion chambers to reduce the number of welds and thus improve the reliability and costs.

Materials for Turbopumps: Current turbopumps employ mostly nickel-based alloys for their construction and their masses in these materials range from about 24 % of the total engine mass in a gas generator cycle (Vulcain) to about 28 % in a staged combustion cycle (SSME). Turbopumps are therefore good candidates for the application of advanced materials to reduce their mass. The highest potential for mass reduction is the replacement of the current Super Waspalloy turbine disks and blades by 'blisks' made from ceramic matrix composites (CMC) materials. A potentially attractive CMC material is carbon-silicon carbide (C-SiC). If feasible, the low density of 2500 kg/m3 would substantially reduce the mass of these components, currently made from Super Waspalloy with a density of 8250 kg/m3.

Materials for Thrust Chambers: The mass of current thrust chambers is about 42 % of the total engine mass. Indeed, the thrust chamber is the heaviest part of the engine, comprising the injector, the combustion chamber and the upper part of the expansion nozzle. The application of advanced materials in thrust chambers could therefore yield substantial mass reductions. Unfortunately however, the author has assessed that because of the extreme demands on material characteristics for thrust chambers, it will be extremely difficult to find lighter materials to replace the current highly developed copper alloys that are used. To illustrate the materials problem for thrust chambers, the requirements are listed below:

- high resistance to hydrogen embrittlement;
- high thermal conductivity to transfer heat from the chamber wall to the cooling fluid, thus allowing adequate cooling of the chamber;
- high creep resistance;
- high ductility to withstand cyclic thermal loads;
- good machinability;
- good weldability;

- good base for electroplating with higher strength nickel.

Major research efforts have been expended in the development of copper alloys to meet these exacting requirements. The best available material that has emerged and is used in the SSME and Vulcain thrust chambers is the North American Rockwell alloy NARLOY (Cu Ag Zr). Research efforts are still engaged to develop improved copper alloys.

Materials for Nozzle Extensions: The mass of the nozzle extension on current LOX/LH2 engines is about 20 % of the engine mass. Nozzle extensions are therefore a good candidate for the application of advanced materials to reduce their mass. The nozzle of the Vulcain engine, being typical of a modern LOX/LH2 engine, is made from spirally wrapped and welded, square section Inconel 600 tubes, allowing the nozzle to be cooled by relatively cool hydrogen gas which is not recovered in a regenerative scheme (dump-cooling). With a density of 8430 kg/m3, such nozzles are very heavy. The SEP company in France, having developed a range of CMC materials, are now engaged in the investigation of their use for radiation cooled rocket nozzle extensions. Such a nozzle made from C-SiC, if feasible, with a density of 2500 kg/m3, would reduce the mass of the nozzle by about 70 %. This would be a very substantial mass reduction, with the additional advantage of higher engine performance because of the saving of the dumped nozzle cooling propellant flow. Thus, in the near term, if only the mass of the nozzle extension could be reduced by 70 %, this would already yield an increase of the engine thrust/weight ratio by 14 %.

Materials for Engine Valves, Propellant Tubes and Manifolds; Engine Gimbals and Actuators: The combined masses of these components are typically about 4 % of the total engine mass. The application of advanced materials would then yield only small mass reductions. Nevertheless, effort should be made to

reduce the masses of these less complex and performance demanding components.

Materials for Engine Control Electronics: The mass of the SSME engine controller is 97 kg. This is a surprisingly large value and reflects the 1970,s technology in electronic components, computers and packaging. A substantial mass reduction to perhaps half this value would be a reasonable design aim for future large engines.

In conclusion, the author is confident that the application of advanced materials in the design of LOX/LH2 engines can yield substantial mass reductions. A design aim can be set to increase the engine thrust/weight ratio to a value of 100 from its current average value of 80, representing a 25 % increase.

TABLE 6.1 CRYOGENIC OXYGEN/HYDROGEN ROCKET ENGINE CHARACTERISTICS

COUNTRY	ENGINE	STATUS	ENGINE CYCLE	THRUST (KN)		SPECIFIC IMPULSE (S)		MIXTURE RATIO (o/f)	COMBUST PRESSURE (bar)	NOZZLE AREA RATIO	DRY MASS (Kg)	VAC. THRUST / WEIGHT	APPLICATION
				VACUUM	SEA LEVEL	VACUUM	SEA LEVEL						
CHINA	YF-73	OPERATIONAL 1984	GAS GEN.	44.1	-	425	-	-	-	40	-	-	LONG MARCH CZ3 THIRD STAGE
	YF-75	OPERATIONAL 1992	GAS GEN.	78.5	-	440	-	-	-	-	-	-	LONG MARCH CZ3A AND CZZE/HO THIRD STAGE
CIS	RD-0120	OPERATIONAL 1987	-	1961	1451	455	-	6.0	222	-	3500	57.1	ENERGIA FIRST STAGE CORE
EUROPE	HM7B	OPERATIONAL 1984	GAS GEN.	62.3	-	444.6	-	5.14	35.5	83.1	155	41	ARIANE 4 THIRD STAGE
	VULCAIN	DEVELOPMENT	GAS GEN.	1075	815	431	-	6.2	105	45	1475	74.3	ARIANE 5 CORE STAGE
JAPAN	LE 5	OPERATIONAL	GAS GEN.	103	-	448	-	5.5	35.8	140	255	41.2	H1 SECOND STAGE
	LE 5A	DEVELOPMENT	HZ BLEED	121.5	-	452	-	5.0	39.5	130	242	51.2	H2 SECOND STAGE
	LE 7	DEVELOPMENT	STAGED COMB.	1078	843	445.6	-	6.0	206	54	1714	64.1	H2 FIRST STAGE
USA	RD10A 3-3A	OPERATIONAL 1984	EXPANDER	73.39	-	444.4	-	5.0	32.2	61	138	54.2	ATLAS-CENTAUR TITAN-CENTAUR
	SSME	OPERATIONAL 1981	STAGED COMB.	2091	1668	452.9	-	6.	204	77.5	3177	67.2	NSTS MAIN ENGINE
	STME	DEVELOPMENT	GAS GEN.	-	2847	-	-	-	-	-	3175	91	NLS CORE AND BOOSTER

Figure 6.1

LOX/LH2 ENGINE MASS VERSUS VACUUM THRUST

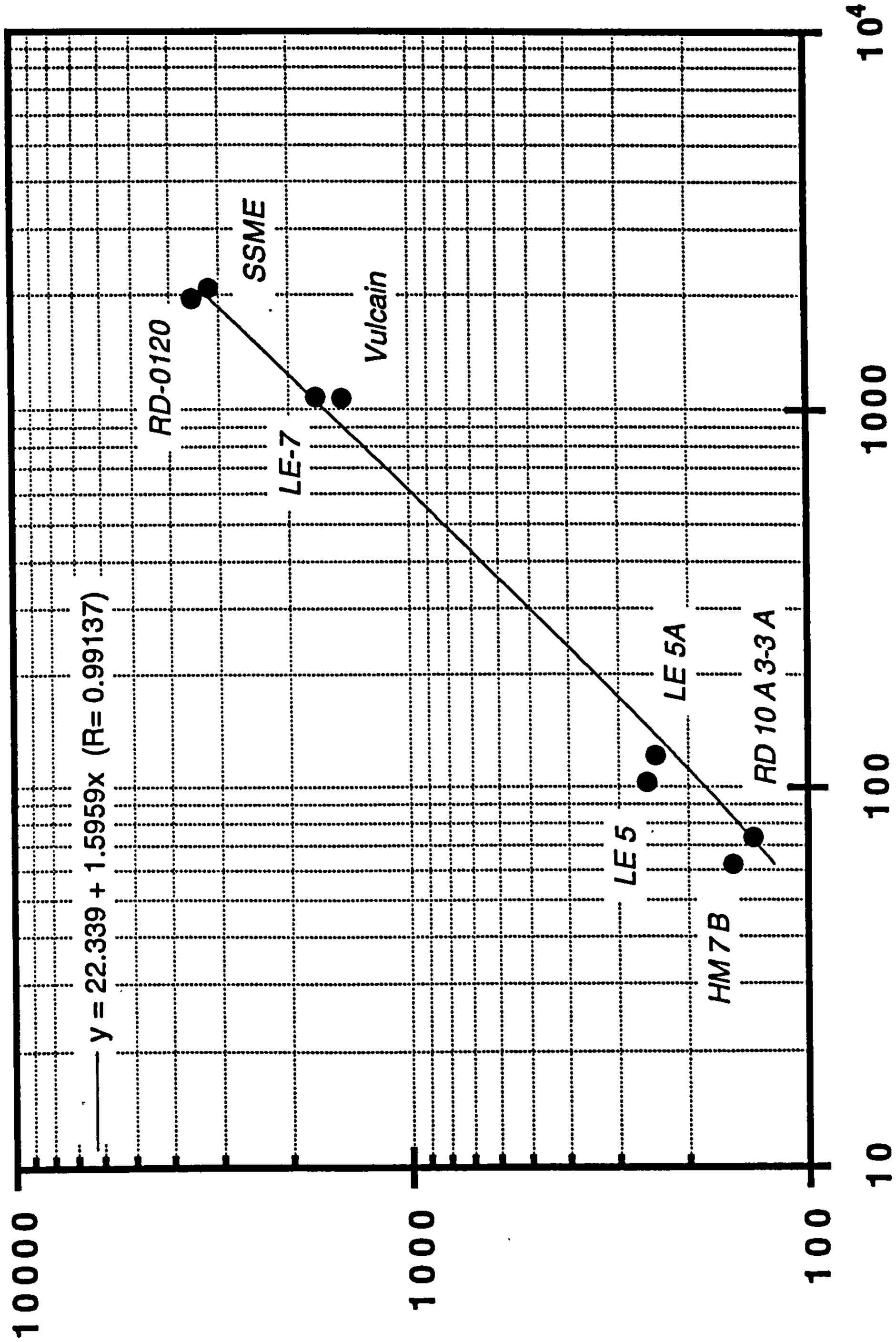

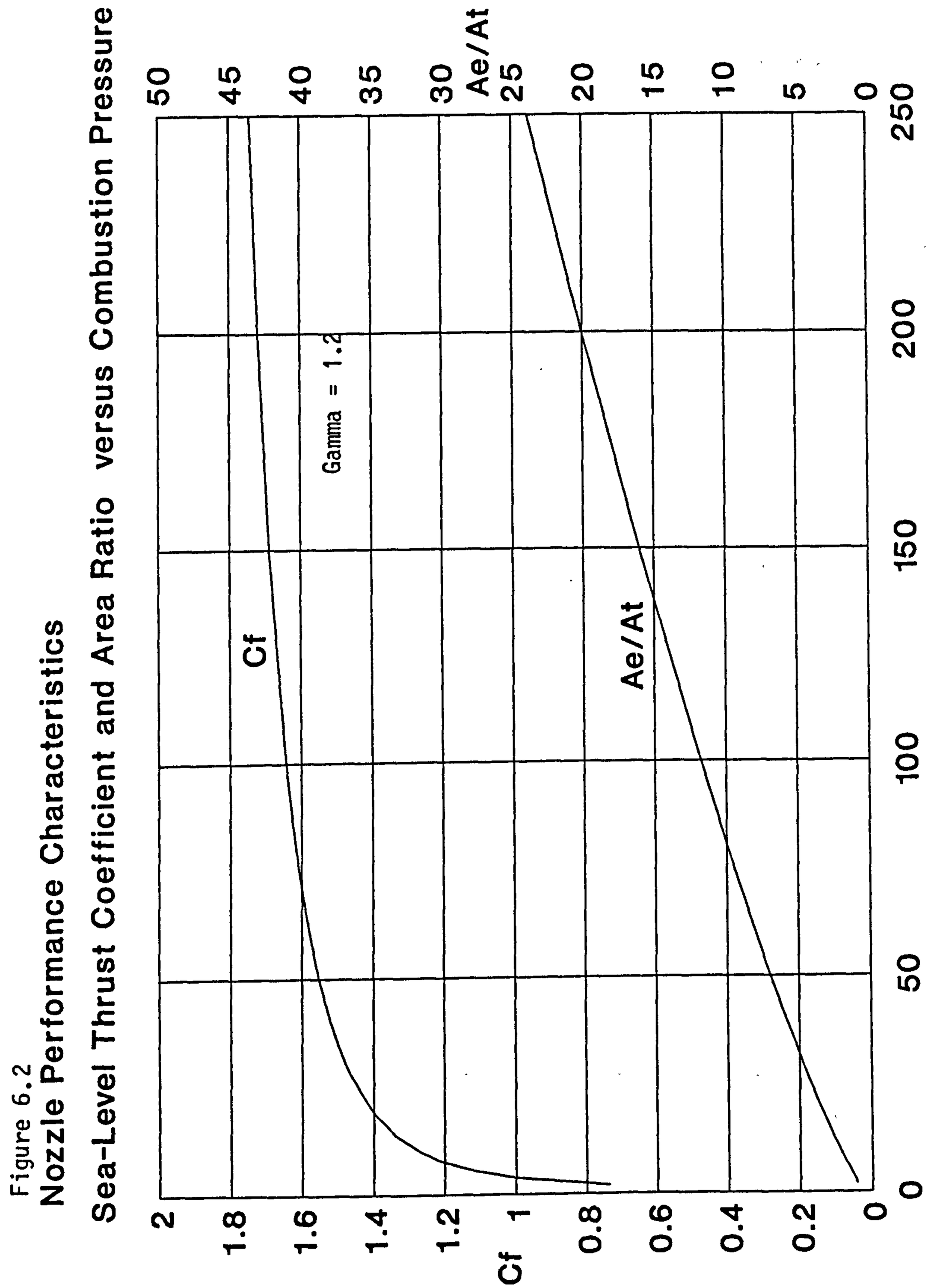
Sea-Level Nozzle Performance Characteristics versus Combustion Pressure
Cf
Ae/At
Gamma = 1.2
Cf
Ae/At
Pc (bar)
0
50
100
150
200
250
0
0.2
0.4
0.6
0.8
1
1.2
1.4
1.6
1.8
2
0
5
10
15
20
25
30
35
40
45
50

Figure 6.2

Figure 6.3 Nozzle Performance Characteristics

Thrust Coefficient versus Altitude (Adapted Flow)

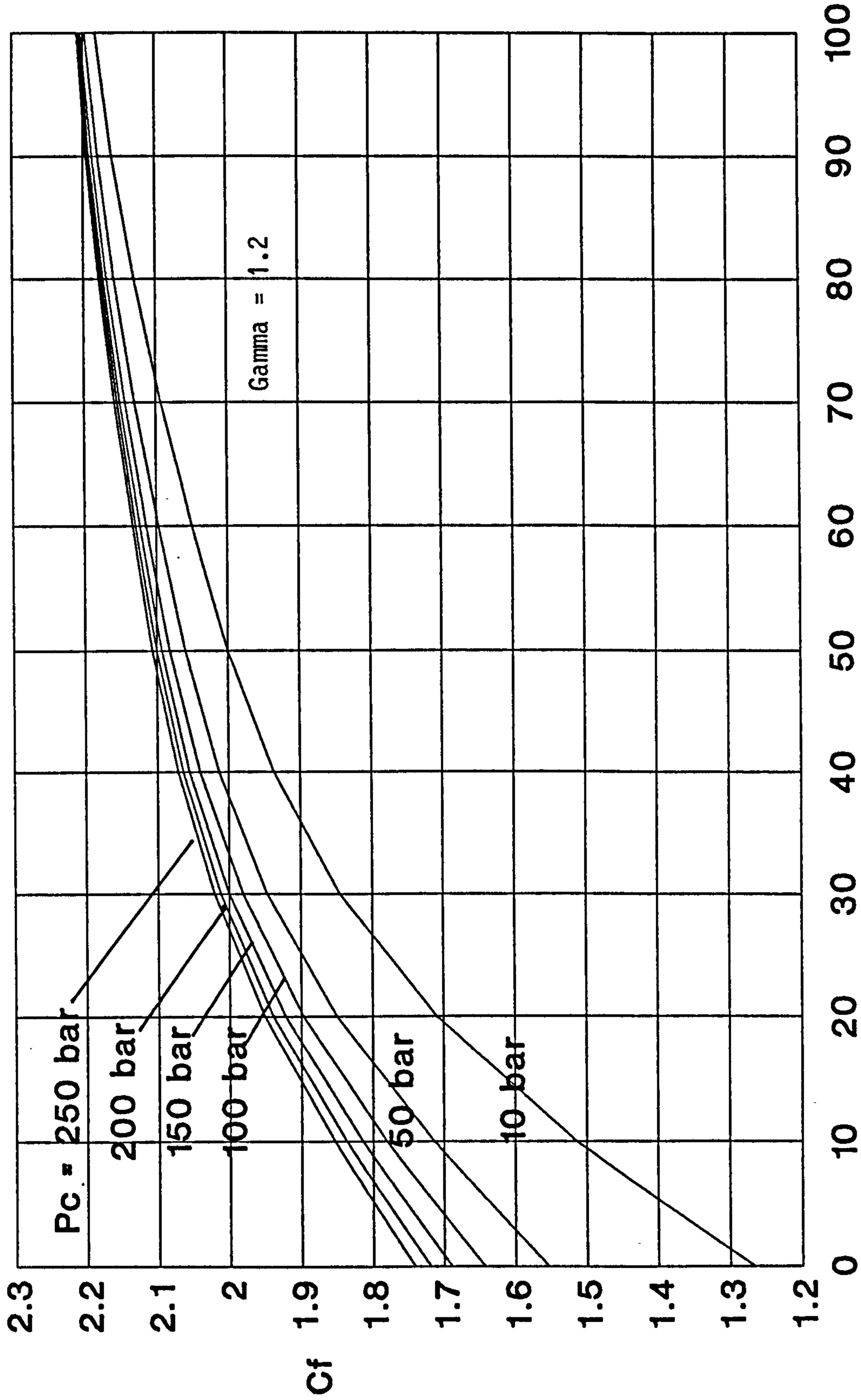

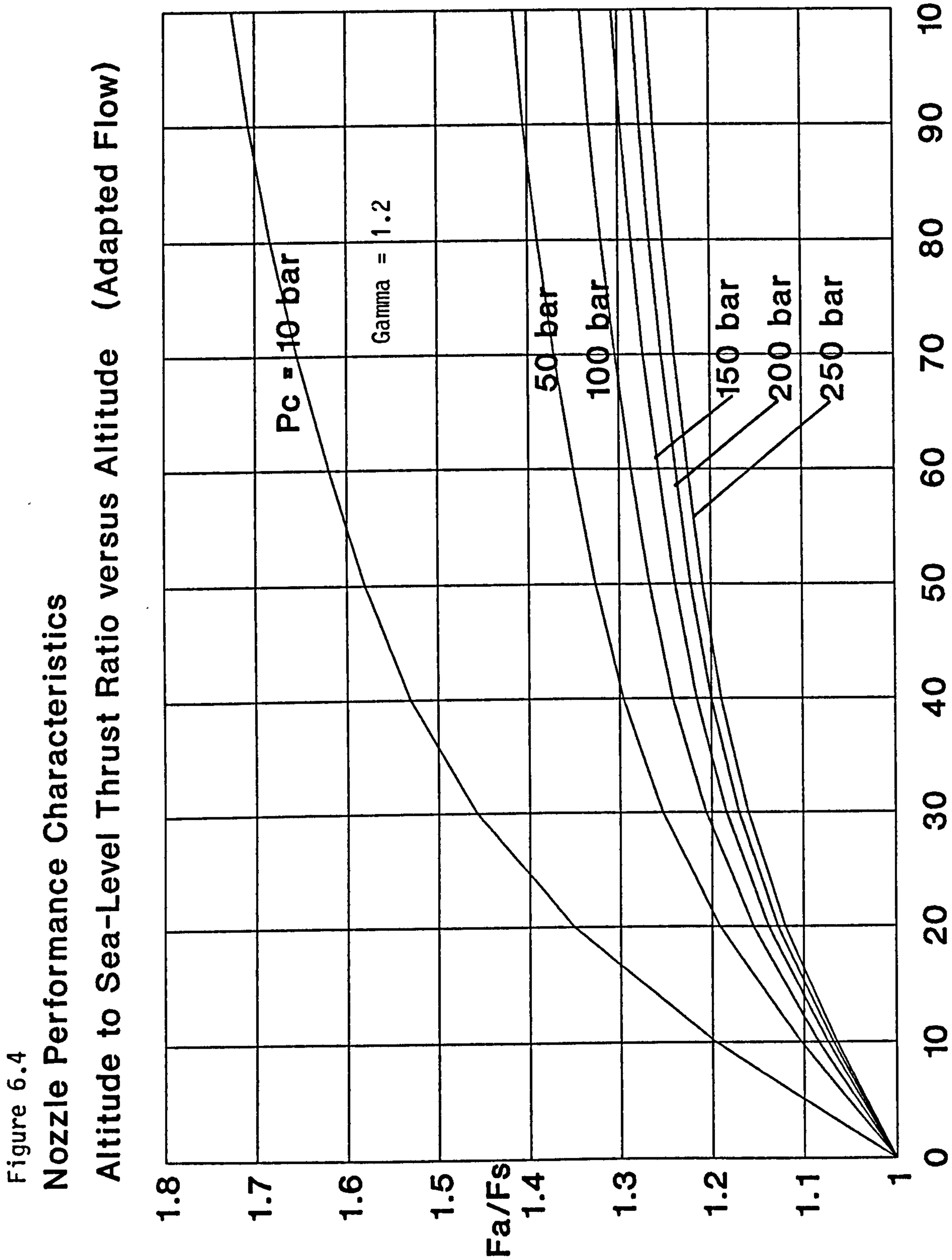

Figure 6.4 Nozzle Performance Characteristics
Altitude to Sea-Level Thrust Ratio versus Altitude (Adapted

Figure 6.5
Nozzle Performance Characteristics:
Full and Partially Adapted Thrust Ratios versus Altitude

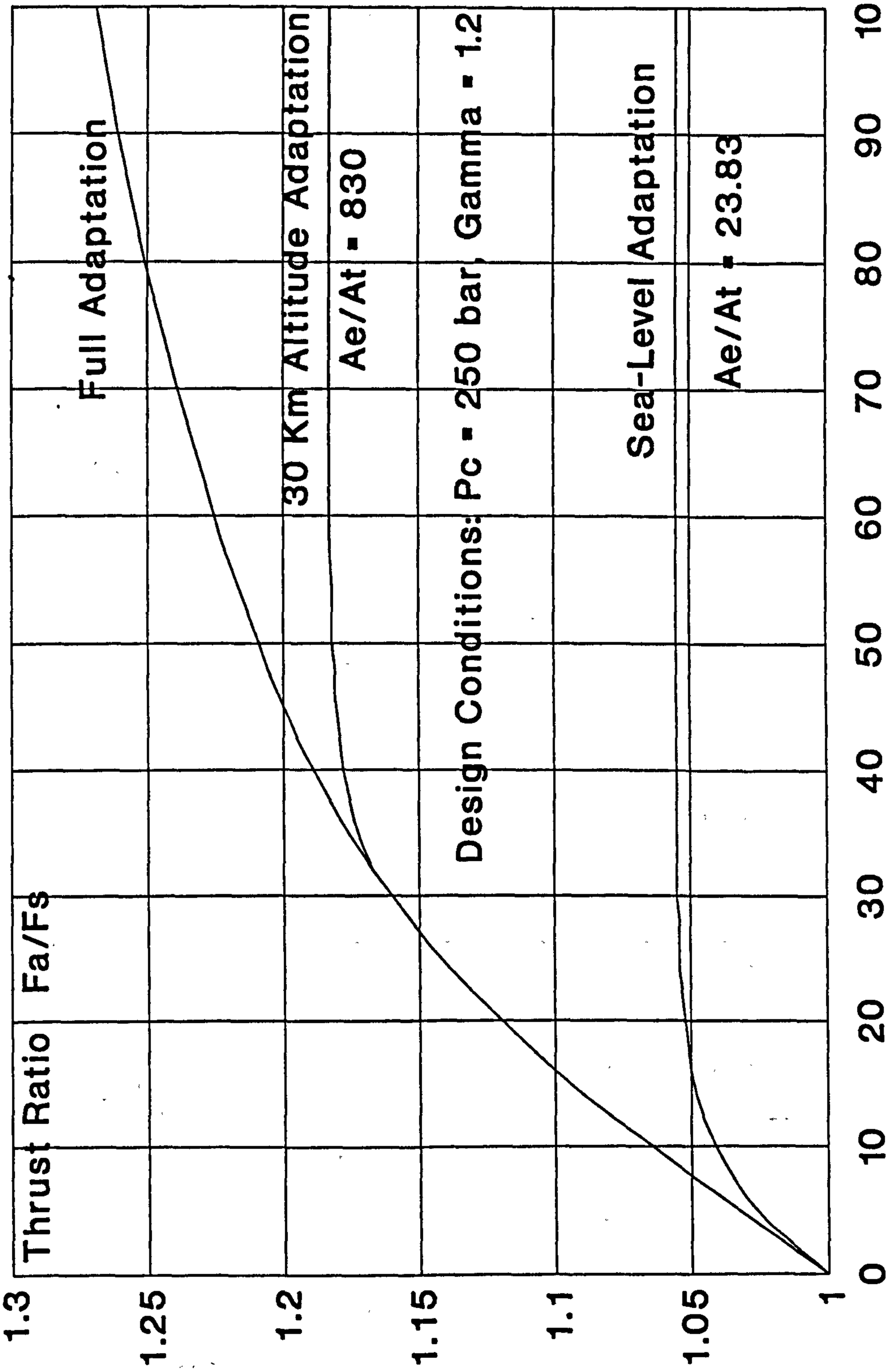

Figure 6.6

Schematic Presentation of the Operation of the Plug nozzle
(Taken from Reference 19)

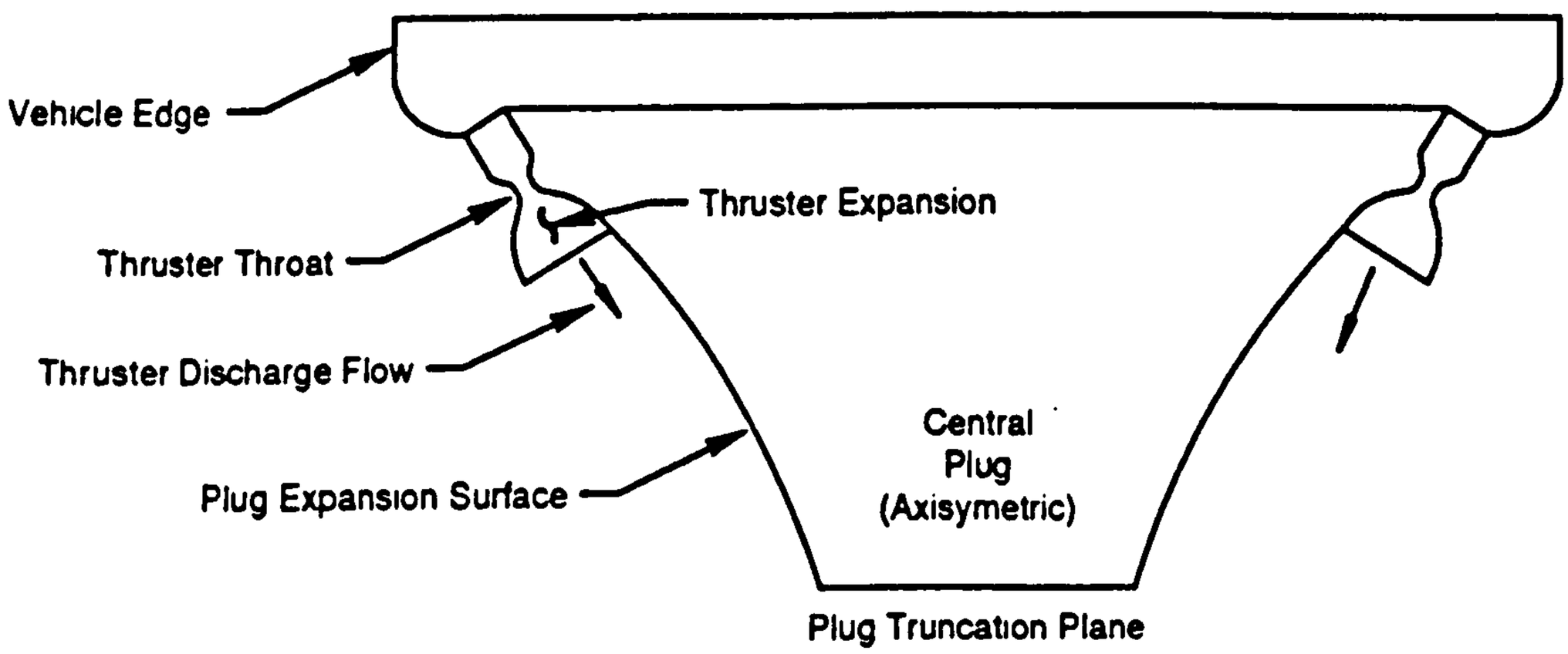

Figure 1. Typical Plug Engine Cross-Section

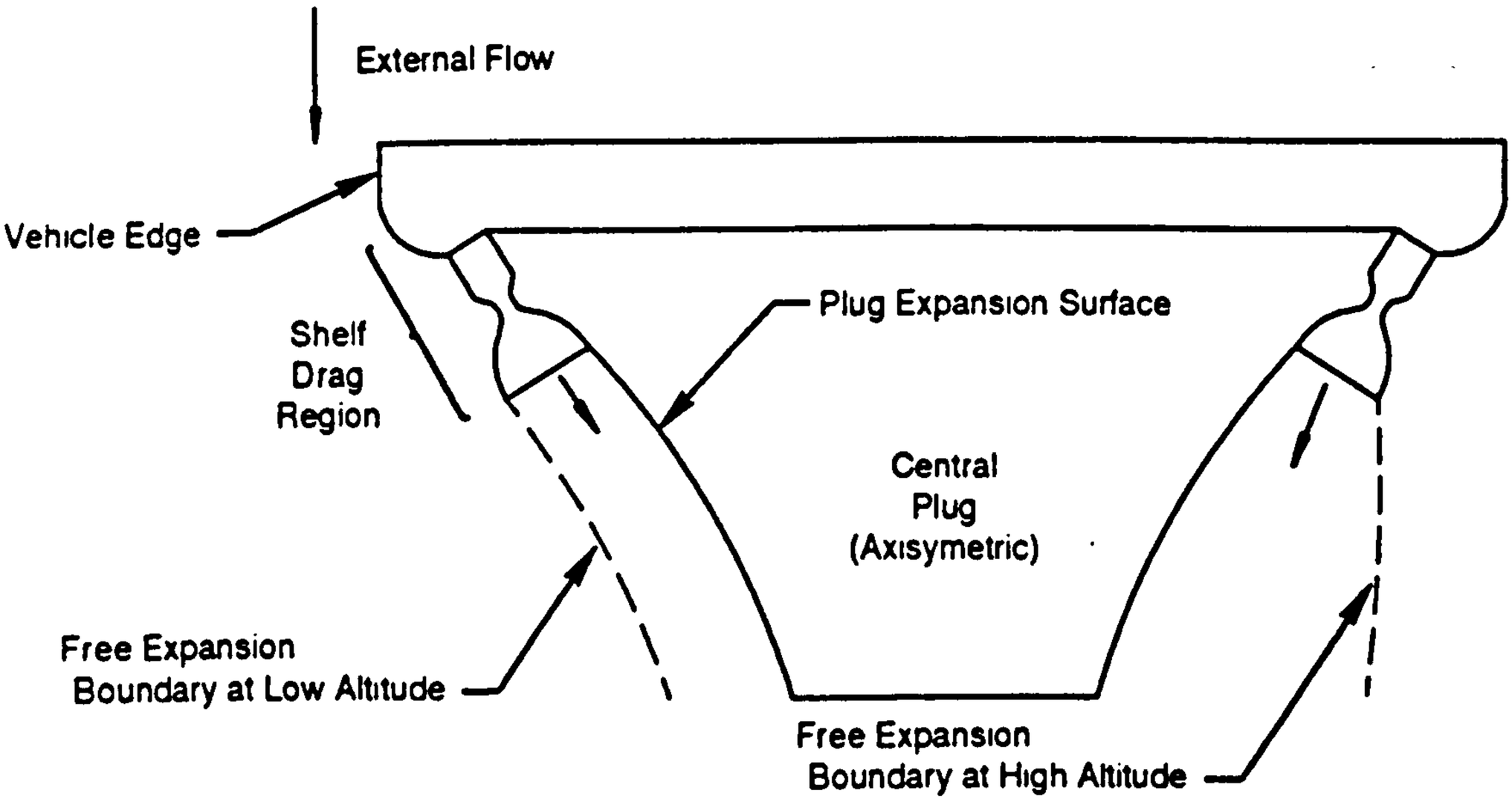

Figure 6.7

Comparison of the Specific Impulse Versus Altitude of LOX/LH2 Rocket Engines with Bell and Plug Nozzles (Taken from Reference 20)

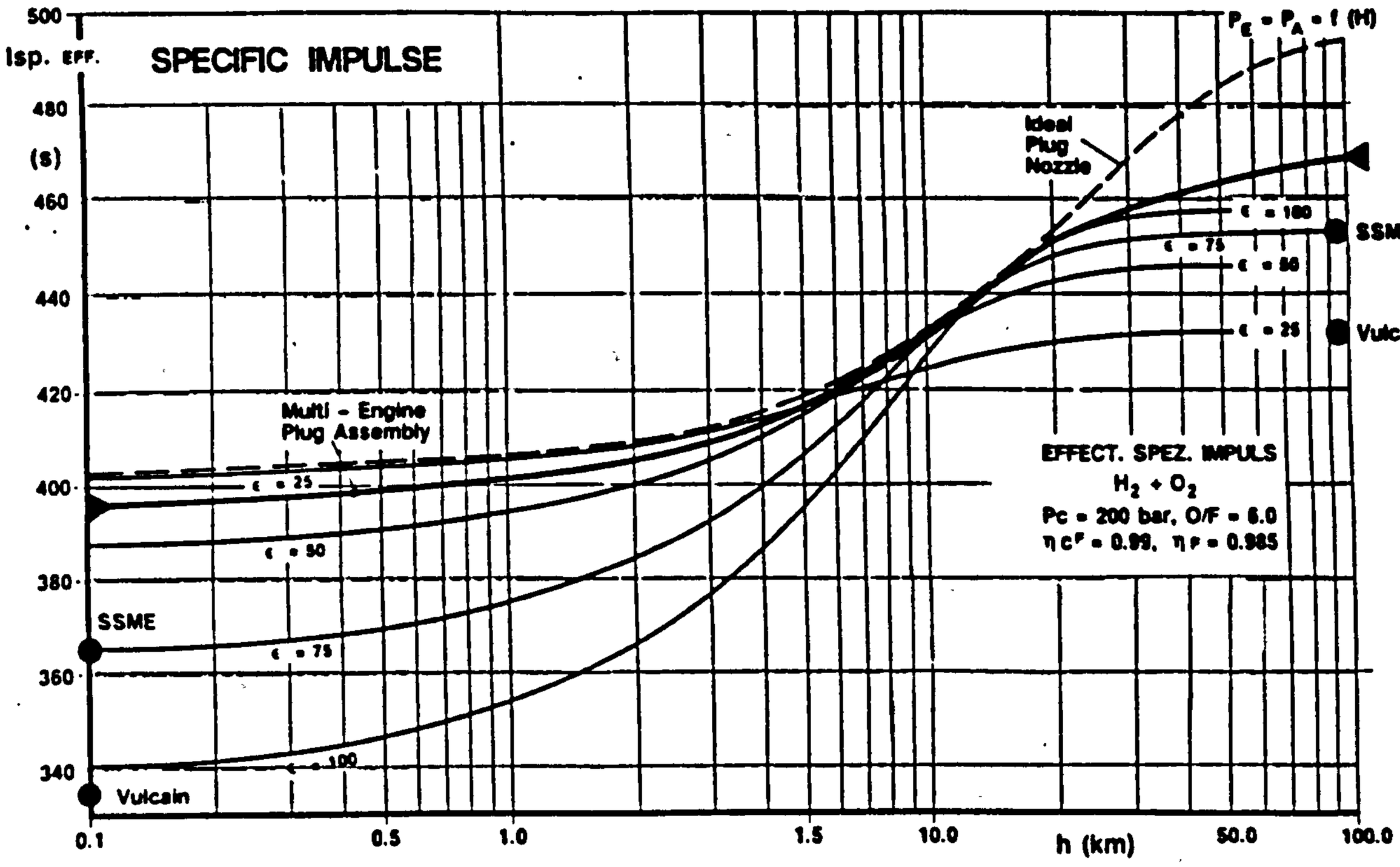

6.2 Air-Breathing Propulsion

6.2.1 Background

At the start of this research in March 1989, the author was well aware of the development status and performance capabilities of rocket propulsion for Earth to Orbit launchers. He felt then, that the status of rocket propulsion was near the limits of its development potential and that further developments were hardly conceivable. Thus, influenced by the large international resurgence of interest in air-breathing propulsion systems for fully reusable launchers, compounded by the apparent performance limits of rocket propulsion, the author was led to believe, that air-breathing propulsion was indeed the way ahead, not only to achieve full launcher reusability, but to achieve it with increased payload mass ratios and with substantial reductions in launch operation costs! At that time, world efforts were underway with the study of revolutionary air-breathing launcher concepts: HOTOL in the United Kingdom; Saenger in Germany; STS 2000 and STAR-H in France; NASP/X30 in the USA; SSTO and TSTO studies in Japan. All this work was being undertaken in an atmosphere of high excitement and with great expectations of success. Indeed, then, it was not doubted or disputed whether air-breathing propulsion could make reusable launchers possible, but rather, the discussion was focused on what type of vehicle and what type of air-breathing propulsion system was the best. Four years have passed and the world has expended much effort to complete their air-breathing vehicle system studies. This research has also been undertaken during this four year period and the author has invested major efforts to follow the air-breathing vehicle studies around the world, whilst undertaking his own independent research. The results of this research on the use of air-breathing propulsion systems for Earth to Orbit launchers are presented here. **These results are focused on the usefulness of air-breathing propulsion as determined from**

its integrated performance at vehicle level. This is a departure from the approach that has been consistently found in the literature, of assessing the performance at engine level only. And, such an assessment makes all the difference!

6.2.2 The Allure of Air-Breathing Propulsion

The accurate performance analysis of Reusable Launcher No.1, the SSTO-R-VLVL vehicle which is propelled by LOX/LH2 rocket engines, shows from Figure 5.3, that even at the highest value of vacuum specific impulse of 464 s, that the propellant mass ratio is a high value of 85.7 %, Thus, with a typical average mixture ratio of 6, the oxygen mass to be carried in the vehicle is a very high value of about 73.5 % of the launch mass. The allure of air-breathing propulsion is then based on the simple assumption that if all or a large percentage of this oxygen mass can be taken from the atmosphere as the vehicle ascends, that substantial reductions in the vehicle size and therefore its dry mass can be achieved and that these mass savings can then be used to increase the payload mass. Furthermore, because the gross (un-installed engine) specific impulse of air-breathing propulsion systems is typically an order of magnitude higher than that of rocket propulsion, that the payload mass ratio of air-breathing vehicles can then be further increased.

A further simple assumption is that because the gravity force on a steeply ascending rocket-propelled vehicle is large and results in a large gravity loss, that the use of aerodynamic lift from a winged vehicle climbing at low flight path angles to compensate the vehicle's weight and thus reduce substantially the gravity loss, results also in a lower vehicle net mass.

Based on these simple assumptions, the promise of air-breathing propulsion has warranted its study across the world

for the propulsion of Earth-to-orbit launchers. This study has also been undertaken in this research and the detailed performance analysis and results of air-breathing propelled vehicles has been presented in Chapter 5. These results have been disappointing. The reasons for this generally poor performance of air-breathing propulsion systems need a clear explanation. This has been undertaken by the author and although the explanations, presented in the next Section, appear to have been easily derived, the reality is that this research work has been necessary to be able to derive the explanations and to present them clearly and succinctly. Thus, the author deems that the following analysis is a significant contribution to the understanding of the limitations on the use of air-breathing propulsion for Earth-to-orbit launchers.

6.2.3 The Reality of Air-Breathing Propulsion

Air-breathing propulsion engines require large volumes of air, even at stoichiometric mixture ratios. To maintain engine inlet ducts and engine inlet diameters to a minimum size, it is then necessary to fly for as long as possible at low altitudes where the air density is higher, to gain speed before having to pull-up to orbital altitude using rocket propulsion. Now, the longer we fly at low altitude and the faster we fly as the vehicle is accelerated, the aerodynamic drag and the resulting velocity losses increase rapidly. Furthermore, the aerodynamic heating of the vehicle increases, necessitating the use of additional thermal protection and/or active cooling schemes, which introduces additional mass and severe complications in the vehicle's design, with its attendant reliability reduction and cost increases. The severity of high speed flight at lower altitudes is demonstrated by the fact that the aerodynamic drag is proportional to the density and the square of the flight velocity and aerodynamic heating is proportional to

the square root of the density and the cube of the flight velocity. Indeed, the use of air-breathing propulsion for Earth-to-Orbit launchers is a paradox, particularly for single stage vehicles: the objective is to propel the vehicle to orbital speed and altitude, where there is no air to breathe, so air-breathing propulsion compels to fly in accelerated flight for as long as possible at low altitudes to accumulate the highest possible velocity!

We can use a specific example from the accurately calculated performance of air-breathing and rocket propelled vehicles from Chapter 5 to illustrate clearly the performance penalties imposed by the use of air-breathing propulsion:

- the performance analysis of Reusable Launcher No.1, the entirely rocket-propelled vertically launched SSTO vehicle, gives a gravity loss of 1200 m/s and a drag loss of only 120 m/s, amounting to a total velocity loss of 1320 m/s, which is 17.66 % of the ideal velocity increment of 7472 m/s (see Chapter 5.5);

- this can be compared with the performance analysis of Reusable Launcher No.7, the air-breathing/rocket propelled horizontally launched SSTO vehicle, employing the most advanced air-breathing combined engine cycle which includes a scramjet, gives a gravity loss of 800 m/s and a drag loss of 2250 m/s, amounting to a total velocity loss of 3050 m/s, which is 41 % of the ideal velocity increment (see Chapter 5.11). Thus, the total losses are nearly three times higher than that of the rocket-propelled vehicle!

So far, we have only addressed the performance penalties arising from the velocity losses imposed by the installed performance of air-breathing propulsion systems. We can now address three other important penalising factors: the mass

and volume of air-breathing propulsion systems and the low density of liquid hydrogen fuel:

- Air-breathing propulsion systems are heavy. They have a thrust/weight ratio in the range 5 to 8, compared to rocket engines with a thrust/weight ratio of about 80 at their current development status. This high mass arises principally from the large dimensions of all air-breathing engines and from the inherently high mass of turbomachine variants. The large dimensions result from the large duct sizes that are needed to swallow the required low density air. This contrasts directly with rocket engines, in which the oxidiser is in the liquid phase and is dense, thus requiring relatively small ducts (tubes) to feed the engine via the turbopumps. Thus, rocket engines are very compact and small. In addition to the large duct sizes that make air-breathing engines inherently heavy, the operation of these engines over their respective altitude and Mach number ranges, necessitates the use of variable air inlets and expansion nozzles. This results in substantial mass increases, principally from the mass of the control actuators and their primary power source (electrical or mechanical power).

Addressing now the mass impact on air-breathing propelled vehicles due to the low density of liquid hydrogen fuel, this can be best illustrated by calculating and comparing the propellant volumes for Reusable Launcher No.1 (the entirely rocket-propelled SSTO vehicle) and that of Reusable Launcher No.7 (the advanced air-breathing and rocket-propelled SSTO vehicle):

For Reusable Launcher No.1, the accurately calculated rocket propellant mass ratio M_{pr}/M_l for the reference mission of Chapter 5 is 0.857

Thus, $M_{pr} = (0.857 \times M_l) = (0.857 \times 350) = 299.95$ tonnes

Now, the rocket propellant comprises both fuel M_{prf} and oxidiser M_{pro}. Thus:

$M_{pr} = M_{prf} + M_{pro}$ (1)

and for a mixture ratio $M_{pro}/M_{prf} = 6$

$M_{prf} = 299.95/7 = 42.85$ tonnes

and $M_{pro} = (299.95 - 42.85) = 257.1$ tonnes

Now, the density of liquid hydrogen fuel is an extremely low value of 71 kg/m3 at normal pressure, whilst the density of liquid oxygen is a very high value of 1141 kg/m3 at normal pressure.

Thus, the volume of the liquid hydrogen V_{prf} is:

$V_{prf} = (42.85 \times 1000) / 71 = 603.52$ m3

and the volume of the liquid oxygen V_{pro} is:

$V_{pro} = (257.1 \times 1000) / 1141 = 225.33$ m3

For Reusable Launcher No.7, for the same reference mission of Chapter 5, the accurately calculated propellant mass ratio M_p/M_l is 0.794

Thus, the total propellant mass M_p is:

$M_p = (0.794 \times 350) = 277.9$ tonnes

Now, the total propellant mass comprises the propellant mass in the air-breathing phase M_{pa} and the propellant mass in the rocket phase M_{pr}. Thus:

$M_p = M_{pa} + M_{pr}$ (2)

and from the accurate analysis of Chapter 5:

$M_{pa} = 141.7$ tonnes and $M_{pr} = 136.2$ tonnes

Now, for the air-breathing phase, the total propellant is fuel. Thus:

$M_{pa} = M_{paf} = 141.7$ tonnes

Now, for the rocket phase, at a mixture ratio M_{pro}/M_{prf} of 6,

$M_{prf} = 136.2/7 = 19.46$ tonnes

and $M_{pro} = (136.2 - 19.46) = 116.74$ tonnes

Therefore, the total fuel mass M_{pf} is:

$M_{pf} = M_{paf} + M_{prf} = (141.7 + 19.46) = 161.16$ tonnes

and the total oxygen mass $M_{po} = M_{pro} = 116.74$ tonnes

Thus, the total liquid hydrogen volume V_{pf} is:

V_{pf} = (161.16 x 1000) / 71 = 2270 m3

and the total liquid oxygen volume V_{po} is:

V_{po} = (116.74 x 1000) / 1141 = 102.3 m3

Now comparing the propellant volumes of Reusable Launchers 1 and 7:

	RL1	RL7
Liquid Hydrogen Volume (m3)	603.52	2270
Liquid Oxygen Volume (m3)	225.33	102.3
Total Propellant Volume (m3)	828.85	2372.3

It can be seen that because of the very large volume of the liquid hydrogen for RL7, that this air-breathing propelled vehicle requires a propellant tankage volume that is 2372.3/828.85 = 2.86 times larger than that of the rocket-propelled vehicle RL1.

This illustrates clearly that LH2-fuelled air-breathing vehicles are inherently large compared to LH2-fuelled rocket propelled vehicles and that the higher specific impulse of air-breathing propulsion systems is eroded again by the additional LH2 tank mass and, much more significantly, by the resulting additional vehicle airframe structure mass. Then, the additional drag losses due to the resulting larger vehicle, lead again to higher LH2 mass and volume!

Noting these results, it is then not surprising that Reusable Launcher No 7, the advanced air-breathing propelled vehicle, was found to have a very poor peformance, resulting in a negative payload!

There is a further limitation of air-breathing propulsion systems that severely penalises their operational convenience, adds costs and gives a further increase in their installed mass. This limitation is that, unlike rocket propulsion, there is no single air-breathing engine type that

can operate over the required Mach range of 0 to 25 and over the required altitude range, typically 0 to 100 km. A series of different air-breathing engines must then be used, either as separate engines, or as a combined-cycle engine. In both cases, rocket propulsion is still needed for propulsion at the higher altitudes and into orbit. This multiplicity of engines leads to complex operational transitions between the different engines or between the different operational modes within a combined cycle engine. The final result is that those engines that have completed their propulsion function, must then be carried as dead mass all the way to orbit for single stage vehicles, or up to the staging point for two stage vehicles.

Finally it is illustrative, using a simple analytical method, to demonstrate the erosion of the high specific impulse of air-breathing propulsion systems when applied to the propulsion of Earth-to-orbit launchers in accelerating, climbing flight:

For both rocket and air-breathing propulsion systems, the average specific impulse I_{sa} for ascent over the trajectory for the unrealistic case of ascent in a gravity-free field and in vacuum is given by:

$$I_{sa} = I_t/M_p \qquad (1)$$

where I_t is the total impulse delivered, M_p is the propellant mass and I_{sa} is the average specific impulse in s.

Now, $I_t = {}_0\int^t F dt$ (2)

and $M_p = g_0 \, {}_0\int^t m_p dt$ (3)

where m_p is the propellant mass flow rate in kg/s

Thus, substituting (2) and (3) into (1):

$$I_{sa} = {}_0\int^t F dt / g_0 \; {}_0\int^t \dot{m}_p dt \qquad (4)$$

This average specific impulse is equivalent to the specific impulse value of an engine under static ground test conditions.

Considering now the realistic case of ascent in the Earth's gravity field and atmosphere, we can now define an 'effective average specific impulse' I_{sae} over the ascent trajectory. Using the nomenclature given in the force diagram of Figure 4.2:

$$I_{sae} = {}_0\int^t (F\cos\alpha_1 - W\sin\gamma - D) / g_0 \; {}_0\int^t \dot{m}_p dt \qquad (5)$$

where α_1 is the thrust angle, γ is the flight path angle, W is the weight of the vehicle and D is the drag force.

It can be seen from (5) that for this realistic ascent case, that the average specific impulse is degraded considerably from that of the unrealistic ascent case given in (4) by the thrust reduction contributions of the thrust angle, the weight component and the aerodynamic drag force. Even if the thrust is along the velocity vector ($\alpha_1 = 0$) and the flight path angle γ is zero, the drag force D then still predominates the degradation of thrust and therefore average specific impulse. Now, as demonstrated earlier in this Chapter, although equation (5) is applicable to both rocket and air-breathing propulsion systems, the very much higher values of drag of the air-breathing propulsion systems compared to rocket propulsion systems, results in a severe degradation of the installed or net thrust and average specific impulse of air-breathing propulsion systems.

To demonstrate the degradation of specific impulse due to aerodynamic drag on air-breathing propelled vehicles,

accurate values of the 'effective average specific impulse' given by Equation (5) have been calculated for Reusable Launcher No.1, the rocket-propelled SSTO vehicle and for Reusable Launcher No.7, the advanced air-breathing/rocket-propelled vehicle, for the standard reference mission of Chapter 5:

- For RL1, the value of I_{sae} is 391.6 s, which is a high value for this rocket-propelled vehicle, which uses rocket engines with a vacuum specific impulse of 464s. The relatively high value of I_{sae} results from the rather low total velocity losses of 17.66 % for this vehicle (comprising 16.05 % gravity loss and 1.61 % drag loss).
- For RL7, the value of I_{sae} is only 482 s. It can be seen that this low value of the effective average specific impulse of the advanced air-breathing vehicle reflects clearly the penalties of the very high total velocity losses of 41 % for this vehicle (comprising 30.1 % drag loss and 10.9 % gravity loss).

6.2.4 Candidate Air-Breathing Propulsion Systems for Earth-to-Orbit Launchers

In this Section of the Thesis, only a very brief summary of candidate air-breathing propulsion systems is presented. This is deliberate because several excellent and comprehensive reviews have been recently published. Four of the most useful publications are given in Reference 24 to 27. In particular, the Introduction to Reference 24 gives an excellent, reasoned and structured overview of the different air-breathing propulsion engines and their domains of application, classified into low speed and high speed propulsion systems. References 25, 26 and 27 give detailed descriptions of the various engine thermodynamic cycles and estimates of their respective performances. Figures 6.8 and 6.9, extracted from Reference 24, have been included here because these Figures are now classical representations of air-breathing engine

performance. Figure 6.8 shows the approximate specific impulse ranges for the classical types of LH2-fuelled air-breathing engines. Figure 6.9 shows the generic form of the specific impulse versus engine thrust/weight ratio and vehicle thrust loading (lift-off thrust/vehicle weight) for air-breathing engines. The Figure shows clearly, that high specific impulse is, unfortunately, synonymous with low engine thrust/weight ratio.

Low speed air breathing propulsion systems are candidates for use in the first stage of two stage vehicles and for the take-off and early flight phase of single stage vehicles. For both applications, one or more engine types may be used sequentially or as combined-cycle engines. These engines are:

- turbojet and turbofan engines, based on the classical, fully developed technology base of current kerosene-fuelled engines, but to be developed further into engines fuelled by liquid hydrogen and capable of operation up to speeds around Mach 3;

- pre-cooled derivatives of turbojet engines, using the high heat capacity of the liquid hydrogen fuel to pre-cool the intake air to yield higher performance;

- hydrogen-fuelled ramjet engines to cover the intermediate speed range from about Mach 2.5 to Mach 6;

- combined-cycle engines which link the turbojet to the ramjet (the turboramjet);

- combined-cycle engines that link the turbojet with the rocket (the turborocket);

- liquified air cycle engines (LACE), which use the high heat capacity of liquid hydrogen to liquify the intake air, which

is then pumped to higher pressures for use in a rocket engine. Derivatives of LACE also include engines that separate the liquified oxygen from the liquified nitrogen. The nitrogen is then used for heat exchange purposes to further increase the specific impulse.

High speed air-breathing engines, for use at speeds in the range Mach 6 to Mach 15 are limited in reality to one basic engine type, which is the supersonic combustion ramjet (scramjet). There are many further combined cycle variations of the scramjet, which link it to lower speed engines. Concepts that are receiving detailed attention are: the dual mode ramjet, which is a ramjet linked to a scramjet; the ramlace engine, which is a LACE combined with a dual mode ramjet.

Within this research, the air-breathing engines that have been studied and their performance data used in the vehicle performance analysis of Chapter 5 have been deliberately chosen because they represent the least complex of the dozens of possible air-breathing engine types that are theoretically possible by combined cycle derivatives. These selected engines are:

- the turbojet for take-off and low speed propulsion of Reusable Launcher No 8, the TSTO-RA(Sub)-HLHL vehicle;

- the turboramjet for propulsion of Reusable Launcher No.4, the SSTO-RA(Sub)-HLHL(Undercarriage) vehicle and for the derivative vehicles, Reusable Launchers 5 and 6, which are the sled and ramp-launched vehicles respectively;

- the combined cycle engine that has been used for Reusable Launcher No.7, the advanced SSTO-RA(Sup)-HLHL vehicle. This combined engine comprises four operating modes: take-off with an ejector rocket, a first transition to a ramjet, a second

transition to a scramjet and a third and final transition to a rocket. As has been demonstrated in Chapter 5, the performance of this vehicle was surprisingly poor and the vehicle was not able to deliver a positive payload. This combined cycle is believed to be that adopted and extensively studied by the USA for its NASP/X30 SSTO demonstrator. It has not been possible to compare the performance of Reusable Launcher No.7 from this research with that of the NASP/X30 because no information on the engine or vehicle performance is available. Some of the detailed performance characteristics of the ejector, ramjet and scramjet modes of the combined-cycle engine for Reusable Launcher No.7 have already been presented in Figures 5.22 to 5.24. This particular combined engine cycle is receiving great attention in the USA, CIS and Europe. A comprehensive publication on the performance of the engine is given in Reference 28. Figure 6.10 has been extracted from Reference 28 to show the converging world consensus on what might be an achievable performance from this engine. However, this reference, like so many others in the field of air-breathing propulsion, unfortunately only address the performance of the engine. The critical matter of the engine thrust/weight ratio is hardly addressed and the cost aspects, in the authors search and close monitoring of air-breathing engine studies, have never been addressed!

Figure 6.8

Approximate Performance of Hydrogen-Fuelled Engines (Reference 24)

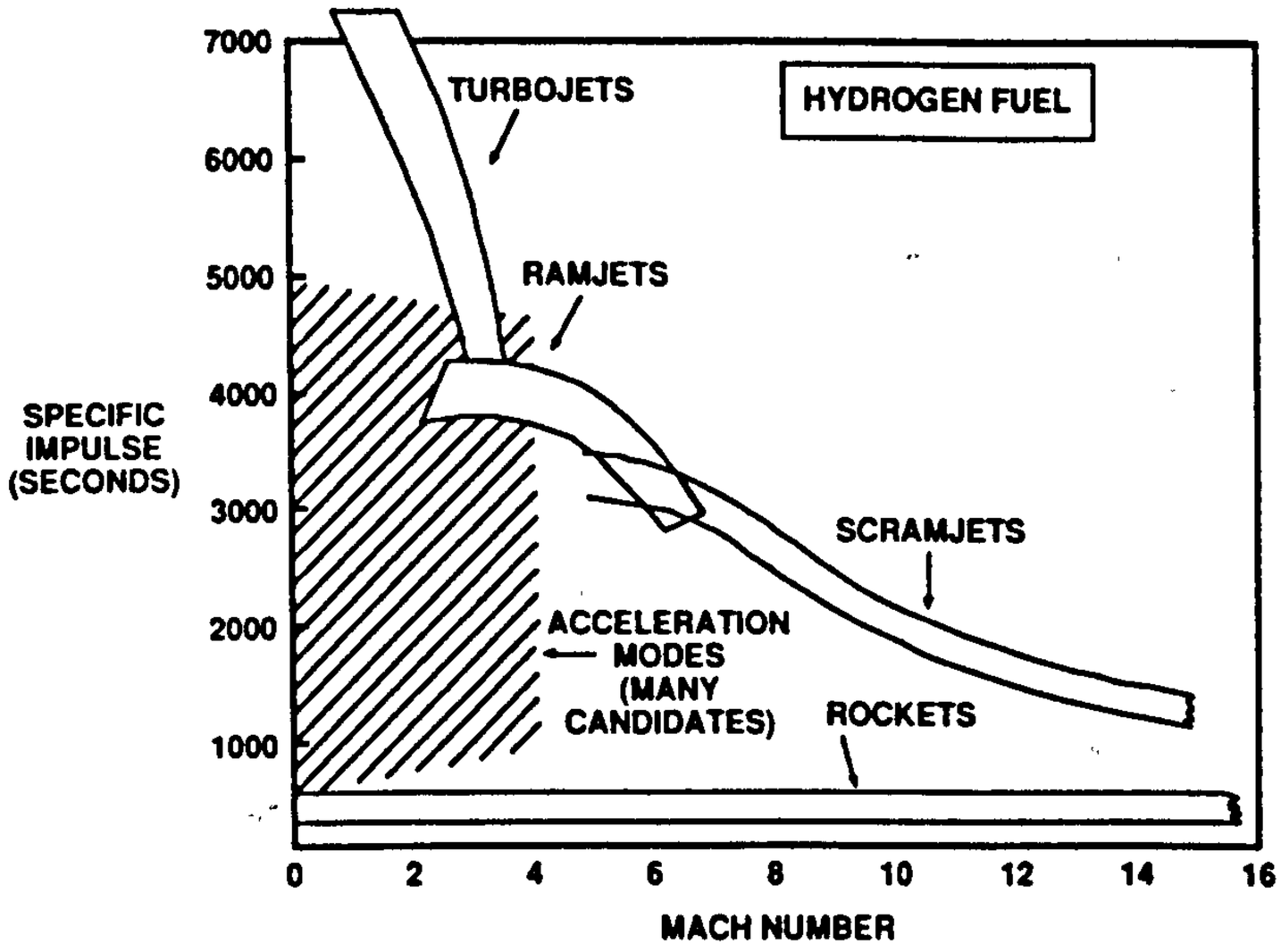

Figure 6.9

Air-Breathing Engine Performance: Specific Impulse Versus Engine Thrust/Weight Ratio and Vehicle Thrust Loading (Reference 24)

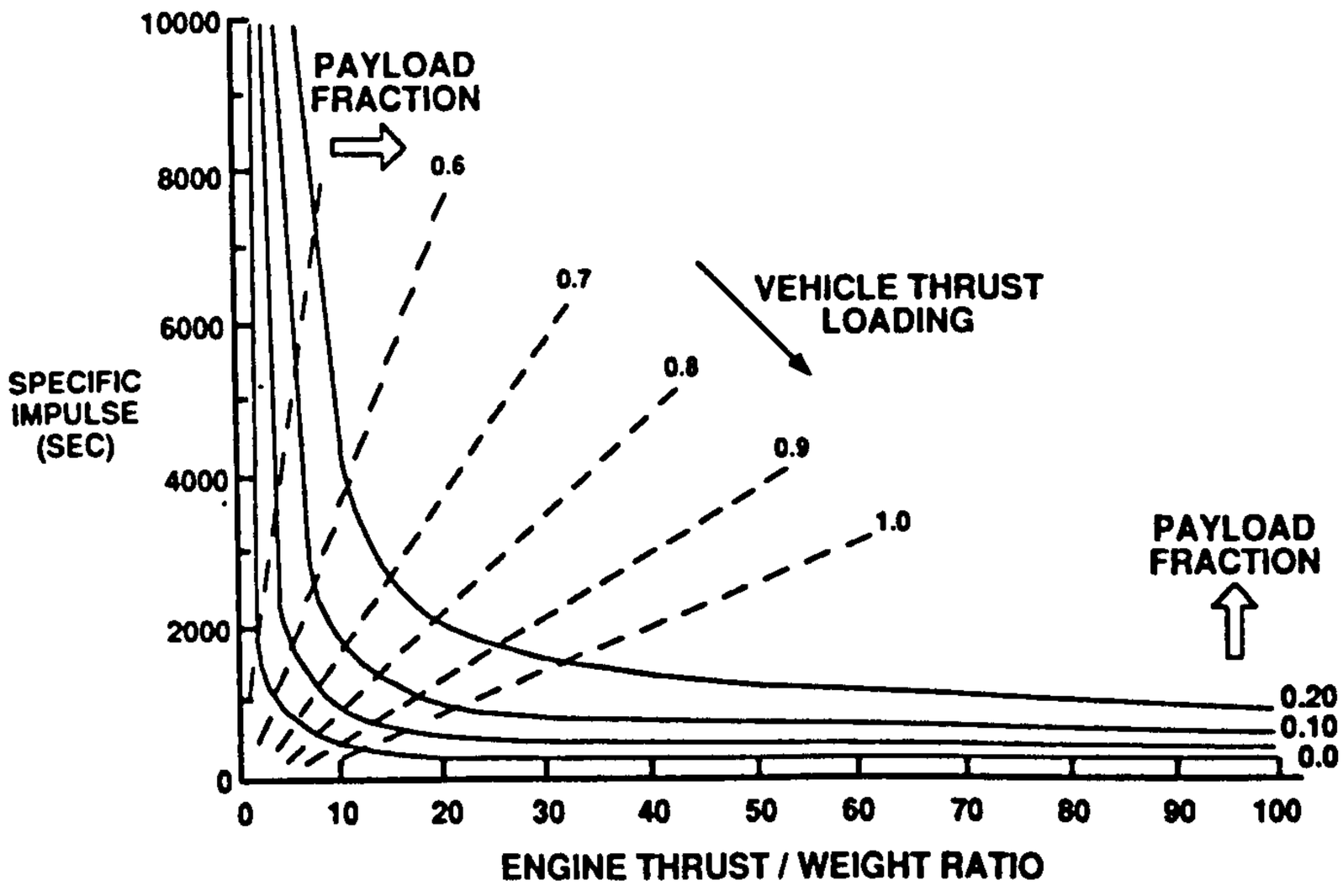

Figure 6.10

Performance of Hydrogen-Fuelled Air-Breathing Engines: Comparative Results from USA, CIS, European and Japanese Studies (Reference 28)

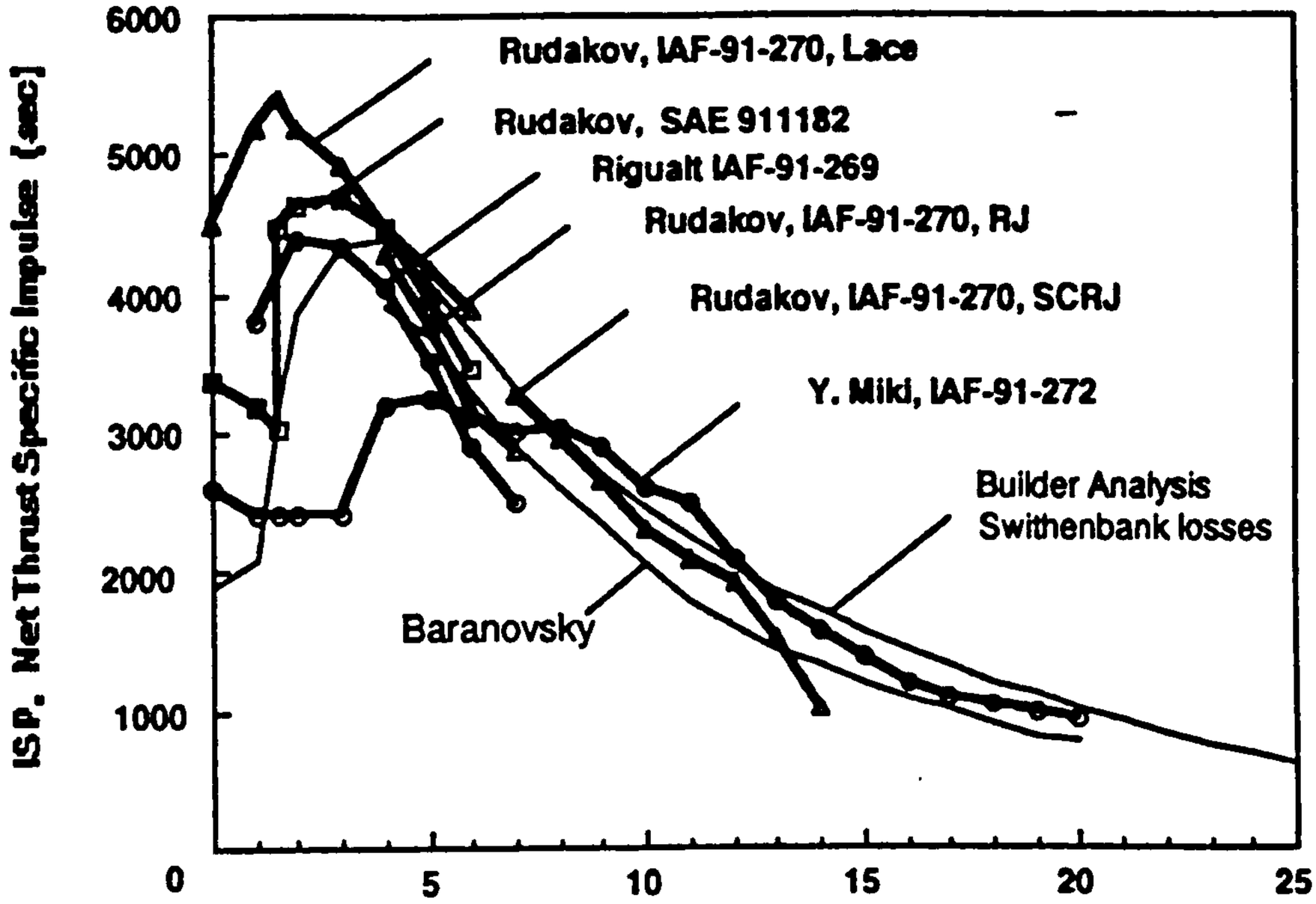

6.3 Materials, Structures and Thermal Protection Systems

More than in any other branch of aeronautics, space launch systems impose the most demanding requirements for light-weight structures, necessitating the development of advanced structural engineering concepts and the use of the highest specific strength materials. Furthermore, it is necessary, again to minimise structural mass, to adopt the lowest possible design safety factors, which then necessitates highly accurate requirements on the reproducibility of material properties and the use of proven manufacturing techniques under the strictest quality control. Without these exacting requirements, the current expendable launchers would not be available. To illustrate the efficiency of current structural engineering for launchers, From Reference 29, the dry mass of the core cryogenic stage for the ESA Ariane 5 launcher, including the attachment structures for the Solid Boosters and the Vehicle Equipment Bay is 15450 kg. The launch mass of this stage, filled with propellant is 153044 kg. Thus, the stage dry mass/launch mass ratio is only 10.1 % Now, this is the achievable mass ratio for an expendable stage of a vertically launched, rocket-propelled vehicle. How then are we to obtain the required low vehicle mass ratios for even the most comparable and least demanding reusable launcher, which is Reusable Launcher No.1: the SSTO-R-VLVL vehicle? For this vehicle, the performance analysis of Chapter 5 shows from Table 5.1, that for a modest payload mass ratio of 2 %, which is the same as that for the expendable Ariane 5 launcher, that the vehicle mass ratio must not exceed 12.28 %. This does not give much margin for the additional mass that will have to be provided for the thermal protection system of the vehicle, to protect it from the re-entry aerodynamic heating environment. The answer to the question on how to achieve lower structural mass, must be by the use of advanced high specific strength materials. For this reason, the development of these advanced materials,

which is currently under way, primarily for the aeronautics industry, is essential for the aerospace industry, to make reusable launchers possible. Indeed, in the USA, NASA is making a major effort to develop advanced materials for the NASP programme (Reference 30). This Reference reports on a 150 Million US Dollar development programme that was initiated in 1988, led by five major USA aerospace companies and employing over 100 additional specialist materials research companies. The results of this programme are already benefitting other USA reusable launcher design and development efforts, notably that of the McDonnell Douglas Delta Clipper SSTO-R-VLHL vehicle concept (Reference 31). In Europe, the Commission of the European Communities (CEC) has taken the initiative to develop advanced materials under its BRITE and EURAM programmes (Reference 32), but primarily to meet the needs of the aeronautics industry. The specific requirements of the European aerospace industry for its future space launchers, has currently only a low interest within the CEC programmes and efforts by ESA are under way to improve this situation.

6.3.1 Materials and Structural Challenges for Reusable Launchers

All reusable launchers will impose major advances in materials and structural engineering concepts. However, the rocket-propelled vertically launched, non-lifting ascent vehicles pose less stringent demands than the air-breathing/rocket-propelled, horizontally launched, lifting ascent vehicles. The reasons for this are:

- the rocket-propelled vertically launched vehicles are close derivatives of the current expendable launchers and, as such, material advances can be addressed in a progressive, evolutionary way. Also, their required vehicle mass ratio values, as determined in Chapter 5, are only slightly more

demanding than those of current expendable launchers. Such vehicles ascend quickly through the atmosphere and have minimum interaction with the atmosphere. For example, the accurate performance results of Reusable Launcher No.1 presented in Chapter 5.5, have shown that the total velocity loss due to aerodynamic drag for this vehicle is only 120 m/s or 1.5 % of the total velocity increment. Thus, the imposed additional loads from aerodynamic heating on the ascent are negligible and the vehicle's thermal design is then determined by the re-entry aerodynamic heating loads. A logical approach to solve this problem is to maintain the use of a cold primary structure for such vehicles, and to provide external thermal protection using a long-life, easily replaceable, ceramic matrix composite (CMC) material, in the form of large, monolithic, formed sections. Such a material could be Silicon Carbide-Silicon Carbide (SiC-SiC) or Carbon-Silicon Carbide (C-SiC).

- in direct contrast to the rocket-propelled vehicles, the most technically demanding advanced air-breathing/rocket propelled vehicle, which is Reusable Launcher No.7, has a major interaction with the atmosphere during its ascent, both for its air-breathing propulsion mode and its external aerodynamics. Chapter 5.11 shows that the aerodynamic drag losses for this vehicle are 2250 m/s, which is 30.1 % of the theoretical total velocity increment. This high loss results from having to fly at high dynamic pressure for a long duration and results in turn, in severe heating of the nose, wing leading edges, control surfaces and air-breathing engine inlet lips. These areas will then require complex, costly and mass-consuming active cooling thermal protection systems. Candidate systems are: heat pipes embedded in hot leading edges; transpiration-cooled (total loss) systems; hydrogen-fuel cooled regenerative systems. Indeed, the problem of aerodynamic heating on the ascent trajectory of such vehicles when propelled by air-breathing propulsion to high speeds in

the range Mach 15 to 18, can exceed significantly, the re-entry aerodynamic heating. This is demonstrated in Figure 6.11, taken from Reference 33.

Additionally, irrespective of the type of reusable launcher, a severe materials challenge is posed by having to design a vehicle, with some of its parts exposed to cryogenic hydrogen temperatures of 20 K, whilst other parts are exposed to aerodynamic heating-induced temperatures up to 2000 K. Furthermore, the materials in contact with hydrogen have to withstand its embrittlement environment, whilst materials in contact with hot, dissociated oxygen due to aerodynamic heating, have to withstand the oxidation environment. Compounding the oxidation problem, are the high heat loads that can occur due to laminar to turbulent transition in the boundary layer at hypersonic speeds and the additional heat loads due to catalytic reactions of decomposed air products with the impinged thermal protection and hot-structure materials.

6.3.2 Advanced Materials under Development and their Potential Use for Reusable Launchers

The subject of advanced materials is receiving major attention in Europe and the USA and there are many excellent and thorough references in the literature concerning their characteristics, domains of application and development status. (References 30, 34, 35, 36 and 37). Therefore, only a short presentation of these materials is given below.

Materials are categorised into:

- isotropic and homogeneous materials which are the classical metals and metallic alloys and new metallic alloys;
- anisotropic and non-homogeneous materials which comprise the growing range of composite materials.

To highlight the whole range of advanced materials under development, Figure 6.12, taken from Reference 37, presents a family tree of advanced material groups. It can be seen that the major groups of advanced materials are:

- polymeric composites;
- advanced metals;
- metal matrix composites (MMC)
- high temperature composite systems, which are further subdivided into carbon, glass, glass/ceramic and ceramic composites (CMC).

Figure 6.13, also taken from Reference 37, shows the further classification of advanced metallic and ceramic materials with temperature. It can be seen that a severe oxidation barrier occurs at a temperature of about 1250 C and that operation at higher temperatures will necessitate elaborate oxidation resistant coatings for the carbon-carbon composites or the use of exotic refractory metals, which are both heavy and expensive due to their low natural abundance.

Figure 6.14, also taken from Reference 37, shows the specific strength versus temperature characteristic for advanced materials. This shows the unique characteristic of carbon-carbon composites: the high specific strength, which increases with temperature up to 1700 C and its suitability for operation up to a very high temperature of 2200 C. Indeed, this material, protected by a SiC coating is already in use on the nose cone and wing leading edges of the NSTS Orbiter vehicle.

Despite this wide range of emerging advanced materials, their application domains have not been studied in depth for future reusable launchers. General usage classifications, based on an assessment of the material properties have been made, but the feasibility of developing the required manufacturing processes have not yet been demonstrated. This is identified

by the author as an urgent activity to be undertaken by the launcher community. Thus, at this time, we can only conclude that the emerging range of advanced materials offer major potential mass reductions for future launchers, but that a major effort is needed in the development and proving of manufacturing processes.

Figure 6.11

Comparison Between Ascent and Reentry Stagnation Point Aerodynamic Heating for an Aerospace Plane, and the Reentry Stagnation Point Heating of the NSTS Orbiter (Reference 33)

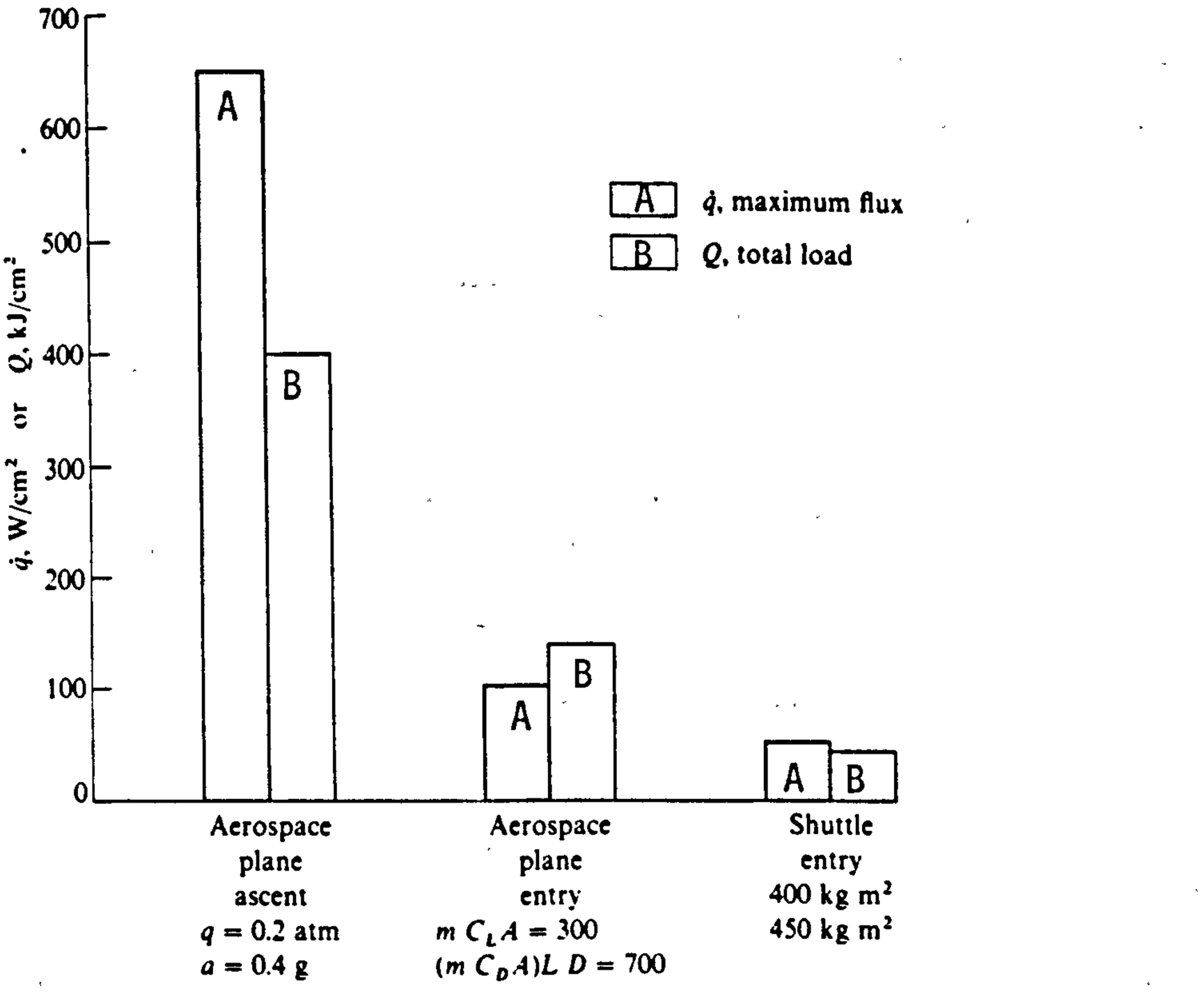

Figure 6.12

Family Tree of Advanced Materials (Reference 37)

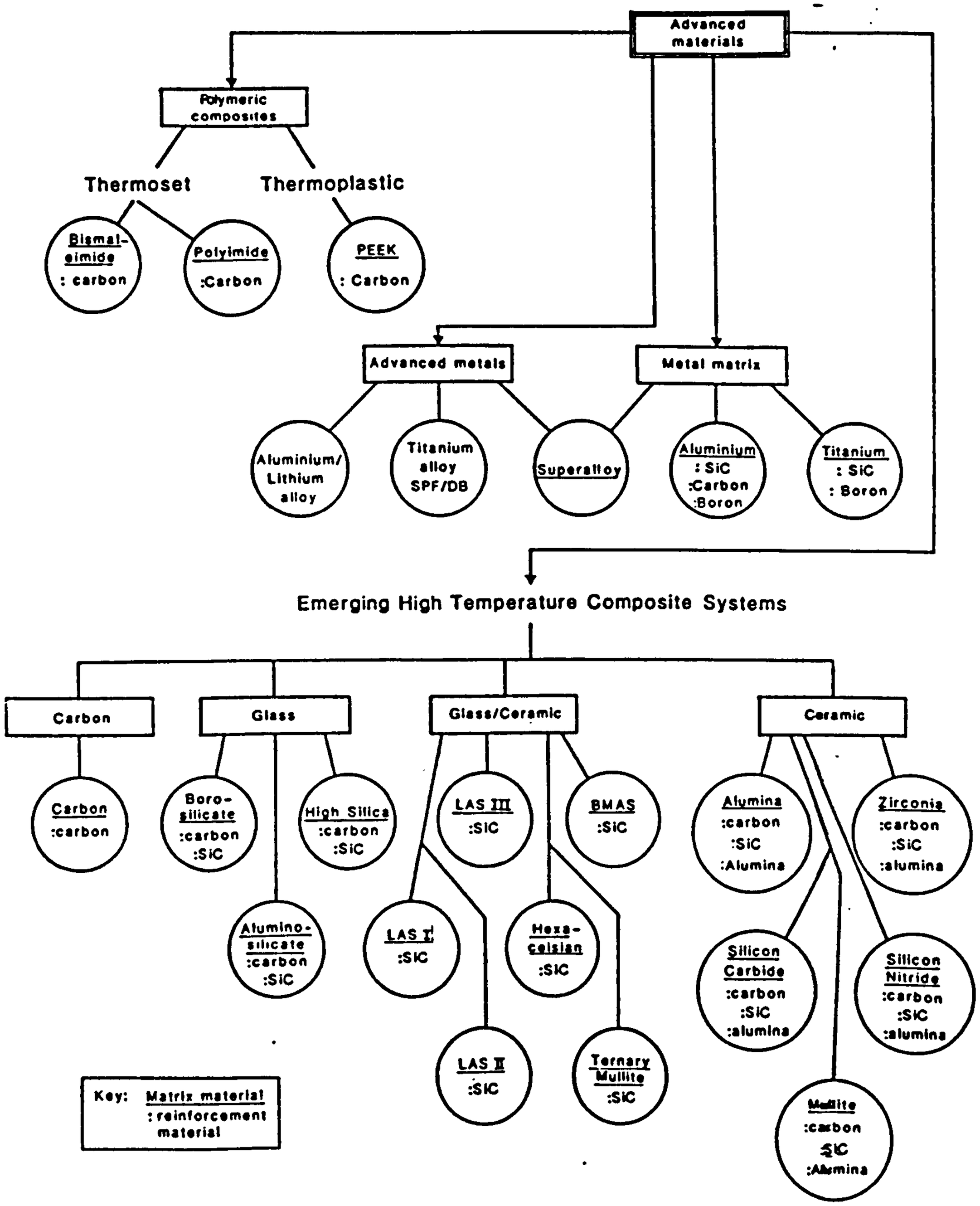

Figure 6.13

Classification of Advanced Metallic and Ceramic Materials with Temperature (Reference 37)

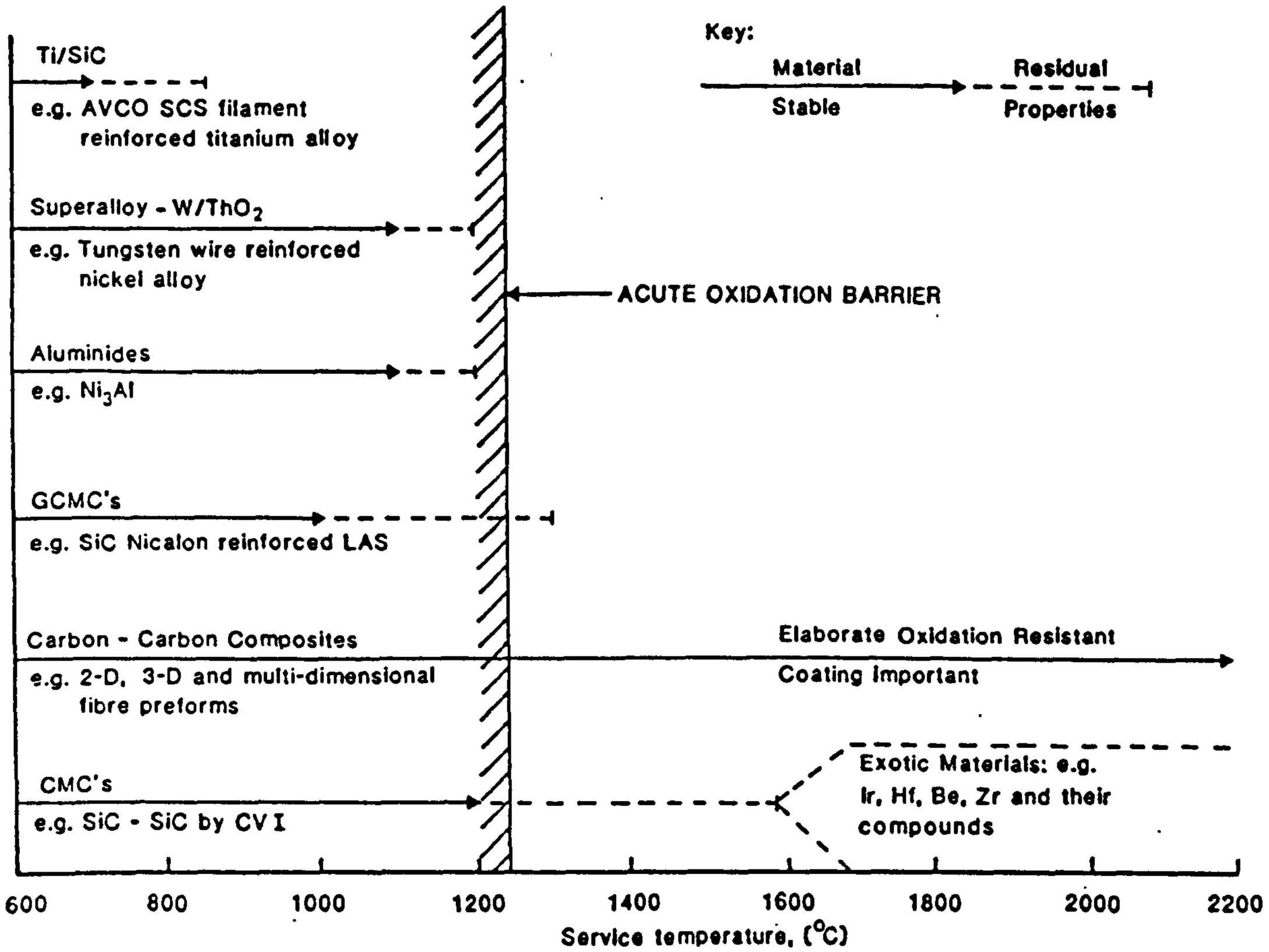

Figure 6.14

Specific Strength of Advanced Materials Versus Temperature (Reference 37)

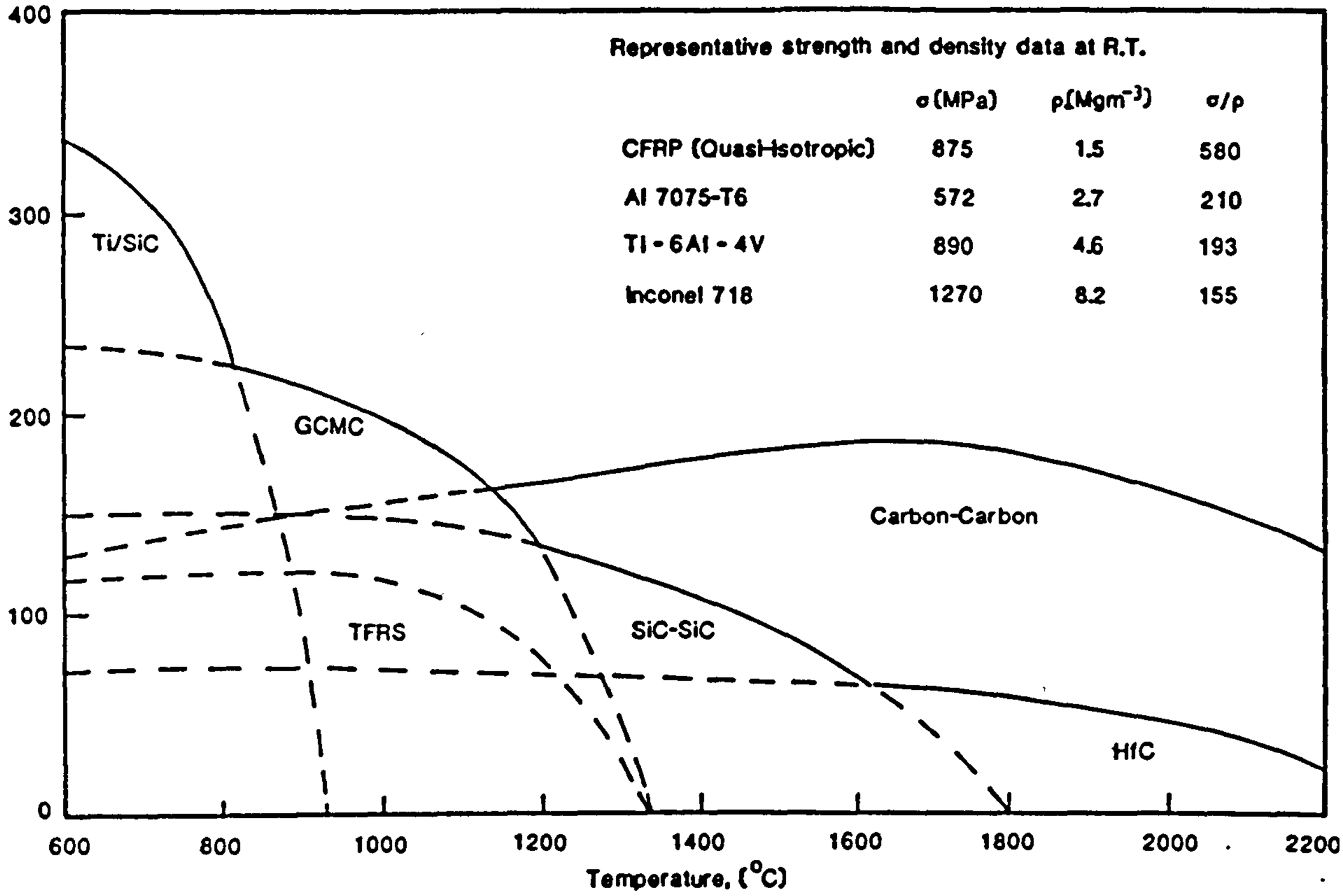

7 COST ANALYSIS OF REUSABLE LAUNCHERS

From the Performance Analysis of Reusable Launchers, presented in Chapter 5, those launchers that could deliver a positive payload to orbit were identified and the surprising result emerged that some of the launchers employing advanced technology could not meet this fundamental, but imperative requirement. Then, in Chapter 6, Technology Assessment for Reusable Launchers, the feasibility of developing the required technologies was assessed and the conclusion was drawn that it was indeed feasible to develop the required technologies for those vehicles that could deliver a positive payload. Now, so far so good, but the crucial subject of the costs of these reusable launchers must be assessed, to establish firstly, if they are lower than the costs of the current expendable launchers, and secondly, to compare the differences in the costs of the various vehicles.

This Chapter presents the cost analysis of the 13 candidate reusable launchers. Firstly, the selection of a standard cost analysis model is addressed. Secondly, the cost analysis methodology is described. Thirdly, a standard life cycle operational model for the service utilisation of the launchers is defined, for which the total life cycle costs of each vehicle concept are derived. Fourthly and finally, the costs of the vehicles are compared.

7.1 Standard Cost Analysis Model

Rather than trying to develop a cost analysis model from scratch, the author decided to adopt the most appropriate available cost model. A survey revealed, not surprisingly, that because cost analysis for advanced high technology projects is a very difficult subject, that there were very few cost models available. The model which was found to be the most appropriate, was the TRANSCOST model (Reference 14),

which has been progressively developed over the last thirty years by Dr.Dietrich E.Koelle of DASA Aerospace (formerly MBB) in Germany. TRANCOST has been adopted as the standard cost model within the ESA Winged Launcher Configuration Studies and has also been used to establish the costs of the German Saenger Reusable Launcher. The model is receiving international recognition and acceptance in the space transportation community, through the standardisation efforts of the International Astronautical Federation (IAF).

7.2 Description of the TRANSCOST Model

TRANSCOST has been conceived as a tool for modern space transportation system engineering, which aims to select the best vehicle based on maximum performance to cost ratio as the selection criterion. The specific features of the model, are best quoted directly using the words of its author in Reference 14:

" The TRANSCOST model:
- is designed for the initial conceptual design phase of all propulsive space transportation system elements and engines;
- is a system model that does not try to go further into subsystems (except the engines proper) since this is not considered appropriate or feasible for the initial vehicle design phase;
- is a 'transparent model' with graphical display of the reference data points (instead of a classified computer data base);
- is based on a comprehensive 30 year (1961 to 1990) database from US and European space vehicle and engine projects;
- has been conceived such that it can be used not only for the design of conventional vehicles but also for advanced space transportation system concepts;
- uses the 'Man Year' (MY) as a costing unit in order to have an internationally valid reference, independent from annual

changes due to inflation and other factors (including currency conversion rate fluctuations);
- has a costing accuracy of +- 20 %, which is considered to be not only the maximum that is feasible for such a model but also sufficient for an initial vehicle design effort."

The basis of the TRANSCOST model is the use of 'Cost Estimation Relationships' (CER). These CER's are cost equations established for each vehicle type and engine type based on statistical cost versus mass data from actual vehicle and subsystem developments, procurement and operations. Thus, the vehicle or subsystem mass is the basic parameter on which costs are calculated. These costs are then factored by coefficients which account for the significant cost influencing parameters. An example of a CER is given below and the influencing parameters are explained:

The CER for an advanced liquid propellant rocket engine is:

$C_e = 152(M_e)^{0.635} f_1 f_2 f_3$

f_1 is the 'Development Standard Factor'.
f_1 is in the range 1.3 to 1.1 for a first generation system with advanced technology.
f_1 is in the range 1.0 to 0.8 for a new design, but with existing components and/or subsystems similar to existing systems;
f_1 is in the range 0.7 to 0.4 for variation of an existing design, with minor modifications or size.

f_2 is the 'Technical Quality Factor', which is an element-specific correction factor, related to technical features and lies in the range 0.8 to 1.5

f_3 is the 'Team Experience Factor'.
f_3 is in the range 1.5 to 1.2 for a new team endeavour with no relevant direct company experience;

f_3 is in the range 1.1 to 0.9 for a team with some related company experience;
f_3 is in the range 0.8 to 0.6 for extensive team experience with similar designs/products.

7.3 Cost Analysis Methodology

The ultimate aim of this cost analysis is the derivation of the total vehicle life cycle costs and its major cost elements. These are:

1) The Development Cost
2) The Procurement Cost
3) The Operation Cost

The development cost has again been broken down into:
- vehicle cost (without engines);
- engine cost.

The Development Cost includes: design, development, manufacture of test articles and test demonstrators, ground facilities and flight testing.

The Procurement Cost is the cost of production, acceptance testing and delivery to the customer of the flight vehicle;

The Operation Cost includes: the use of the launch range and facilities; the actual pre-flight vehicle preparation, mission control of each flight and the post flight activities including maintenance and refurbishment; the management and administrative overheads, the insurance costs per flight. The Operation costs per flight and for the total life cycle duration have been calculated.

7.4 Standard Life Cycle Operational Model

A standard life cycle operational model was derived, from which the costs could be calculated. This model, which is deemed by the author to be a realistic scenario, is similar

to that adopted for the NSTS partially reusable launcher system, is given in Table 7.1 below:

Table 7.1: Reusable Launcher Operational Model

1) Operational Mission:	Payload delivery to LEO
2) Mission Type:	Automatic, no crew transported
3) Utilisation Period in Years:	20
4) Maximum Launches per Year:	12
5) Number of Vehicles in Fleet:	3
6) Total flights in Utilisation Period:	240
7) Design Number of Flights per Vehicle:	100
8) Design Number of flights per Engine:	50
9) Design Number of flights for Thermal Protection:	20
10) Insurance Cost per Flight:	20 % of Launch Cost

7.5 Cost Analysis Results

Firstly, to be able to assign valid values to the 'f' coefficients of the CER's for each reusable launcher type, it was necessary to understand clearly the characteristics and complexity level of each launcher. The results of this activity are shown in Table 7.2. It can be seen from Table 7.2 that, resulting from the basic characteristics of each vehicle (winged, air-breathing, undercarriage etc.), that ratings have been assigned on a scale of 10 for the complexity of the three critical vehicle subsystems: Structure, Thermal Protection; Guidance and Control.

Secondly, based on the complexity of each vehicle, the CER's and coefficients for each launcher were derived. These values are shown in Table 7.3.

Thirdly, because the vehicle and element masses are the basic parameter on which the costs are based, a mass breakdown of each launcher into 'Vehicle (without engines)' and 'Engines'

was made. To determine the engine masses, it is of course necessary to know the engine thrust at lift-off (or take-off) and the engine thrust/weight ratio. The results of the mass breakdown are shown in Table 7.4 and are derived from the results of the Performance Analysis of each vehicle as presented in Chapter 5.

Finally, the costs for each launcher were calculated, broken down into: development; procurement; operation cost per flight; operation cost for the total utilisation programme; total life cycle costs for each launcher. The results are shown in Table 7.5. in units of Man Years and 1992 US Dollars. It should be noted, that although Vehicles 4, 7 and 10, as found from the Performance Analysis, cannot deliver a positive payload to orbit, their costs have nevertheless also been calculated and shown in Table 7.5. for completeness, and also to see how much it would cost to build these useless vehicles!.

To be able to compare easily the costs of each launcher, the results of Table 7.5 have been plotted in ascending order of the costs, in the following bar charts:

- Figure 7.1 shows the comparative Development Costs;
- Figure 7.2 shows the comparative Procurement Costs;
- Figure 7.3 shows the comparative Operating Costs Per Flight;
- Figure 7.4 shows the comparative Life Cycle Costs.

Again, in these bar charts, the costs of those vehicles with negative payloads are also shown.

7.6 Discussion of the Cost Analysis Results

Firstly, the comparative results are discussed. Secondly, the individual cost estimates are discussed. Finally, the individual cost estimates are compared with the actual costs of the Ariane 44L Launcher.

Examination of Figure 7.4 and Table 7.4 shows that the life cycle costs range from 80821 MY for the cheapest launcher which is RL No.1 (SSTO-R-VLVL), to 955583 MY for the most expensive one which is RL No.7, (SSTO-RA(Sup)-HLHL (Undercarriage). This is nearly 12 times more!. The very high cost of RL No.7, which is the most advanced launcher among the candidates is particularly poignant, because this vehicle is one of the three vehicles which has a negative payload, and has, in fact, the largest negative payload of 9 % as calculated in the Performance Analysis!. If we therefore neglect RL No.7, the next most expensive vehicle is No.9, (TSTO-RA(Sub)-HLHL (Undercarriage)). The life cycle cost difference between RL No.1 and RL No.9 is now a factor of nearly 8, which is still surprisingly large.

Examining now the significance of the individual launcher cost estimates, we need only to discuss the costs of the cheapest launcher as an example. The cheapest launcher is No.1 the SSTO-R-VLVL vehicle, which, not by coincidence, is also the least technically demanding one, which has a total life cycle cost of 15558 Million US Dollars. Assuming firstly, that if this vehicle is developed entirely as a commercial venture, the amortised cost per launch, neglecting inflation over the 20 year life, is then 15558/240 flights, which is 64.8 Million US Dollars. Assuming, secondly, that any future launcher development is financed by governments (which has been the case for the current commercial launchers), then only the procurement and operation costs need to be recovered. In this case, Launcher No.1 would have a life cycle cost of 6196 Million US Dollars, giving an amortised cost per launch of 6196/240 flights, which is 25.8 Million US Dollars.

Finally, we can compare the amortised costs per launch with that of the actual launch cost of the European Ariane 44L

expendable, multi-stage, rocket-propelled launcher. The cost per launch for an Ariane 44L is 110 Million US Dollars. Insurance costs are currently at 20 % of the launch cost. Thus, the total insured cost per launch of Ariane 44L is (1.2 x 110), which is 132 Million US Dollars. We can see therefore, that if our simplest and cheapest Reusable Launcher No.1 were developed, that in the case of an entirely commercial development, that the launch cost reduction would be (132 - 64.8), which is 67.2 Million US dollars. This is a virtual halving of the current costs per launch!. In the case where the development was funded and written-off by ESA, as has been the case for the development of all the Ariane Launchers to date, the cost reduction per launch would be even more dramatic, being (132 - 25.8), which is 106.2 Million US Dollars per launch or 106.2/132, which is a staggering reduction of 80 %!. In this example, the payload mass delivery performance of both the Ariane 44L vehicle and our RL No.1, are compatible and therefore comparable, being 9600 kg into a 200 km, circular, Low Earth Orbit. This means that RL No.1 would have to have a Payload Mass Ratio of 9600/350000, which is 2.74 %, which is probably achievable, for a launch mass of 350 tonnes, which is a reasonably small vehicle. The equivalent values for Ariane 44L are: Payload Mass Ratio of 2 %; Launch Mass of 470 tonnes!.

Even if we intentionally limited the payload mass ratio of RL No.1 to 2 % to ease the technological requirements, the resulting vehicle launch mass would now be 480 tonnes, which is about the same launch mass as that of Ariane 44L.

TABLE 7.2 REUSABLE LAUNCHER CHARACTERISTICS AND COMPLEXITY

VEHICLE NUMBER	DESIGNATION	STAGE	AIRFRAME	PROPULSION	LANDING GEAR	COMPLEXITY LEVEL 0 = EASY 10 = VERY DIFFICULT		
						STRUCTURE	THERMAL PROTECTION	GUIDANCE AND CONTROL
RL1	SSTO-R-VLVL	1	BALLISTIC	ROCKET	SUPPORT LEGS	3	3	5
RL2	SSTO-R-VLHL	1	WINGED	ROCKET	UNDERCARRIAGE	6	5	5
RL3	TSTO-R-VLHL	1 2	WINGED WINGED	ROCKET ROCKET	UNDERCARRIAGE UNDERCARRIAGE	6 6	5 5	5 5
RL4	SSTO-RA (Sub) - HLHL (u/c)	1	WINGED	ROCKET RAMJET	UNDERCARRIAGE	6	5	6
RL5	SSTO-RA (Sub) - HLHL (Sled)	1	WINGED	ROCKET RAMJET	UNDERCARRIAGE	6	5	6
RL6	SSTO-RA (Sub) - ILHL (Ramp)	1	WINGED	ROCKET RAMJET	UNDERCARRIAGE	6	5	6
RL7	SSTO-RA (Sup) - HLHL (u/c)	1	WINGED	AIR EJECTOR RAMJET SCRAMJET ROCKET	UNDERCARRIAGE	8	10	8
RL8	TSTO-RA (Sub) - HLHL (air)	1 2	WINGED WINGED	TURBOJET ROCKET	UNDERCARRIAGE UNDERCARRIAGE	1 8	0 5	0 6
RL9	TSTO-RA (Sub) - HLHL (u/c)	1 2	WINGED WINGED	TURBOJET RAMJET ROCKET	UNDERCARRIAGE UNDERCARRIAGE	6 6	5 5	6 5
RL10	SSTO-R-HLHL (u/c)	1	WINGED	ROCKET	UNDERCARRIAGE	6	5	6
RL11	SSTO-R-HLHL (Sled)	1	WINGED	ROCKET	UNDERCARRIAGE	6	5	6
RL12	TSTO-R-HLHL (u/c)	1 2	WINGED WINGED	ROCKET ROCKET	UNDERCARRIAGE UNDERCARRIAGE	6 6	5 5	6 6
RL13	SSTO-RA (Sub) - VLVL	1	BALLASTIC	ROCKET TURBOJET	SUPPORT LEGS	4	3	5

TABLE 7.3 REUSABLE LAUNCHER DEVELOPMENT COST ESTIMATION RELATIONSHIPS (CER)

VEHICLE	DESIGNATION	VEHICLE (without engines)				ENGINES			
		CER	f1	f2	f3	CER	f1	f2	f3
RL1	SSTO-R-VLVL	$Cv = 1000\ M_v^{0.335}$ f1 f2 f3	1.0	1.0	1.0	Rockets: $Ce = 152\ Me^{0.635}$ f1 f2 f3	0.8	0.8	0.8
RL2	SSTO-R-VLHL	$Cv = 1000\ M_v^{0.335}$ f1 f2 f3	1.2	1.2	1.2	Rockets: $Ce = 152\ Me^{0.635}$ f1 f2 f3	0.8	0.8	0.8
RL3	TSTO-R-VLHL	$Cv = 1000\ M_v^{0.335}$ f1 f2 f3	1.2	1.2	1.3	Rockets: $Ce = 152\ Me^{0.635}$ f1 f2 f3	0.8	0.8	0.8
RL4	SSTO-RA(Sub)-HLHL (u/c)	$Cv = 1880\ M_v^{0.335}$ f1 f2 f3	1.3	1.3	1.3	Combined Rocket & Air-Breathing $Ce = 300\ Me^{0.635}$ f1 f2 f3	1.3	1.3	1.3
RL5	SSTO-RA(Sub)-HLHL (Sled)	$Cv = 1880\ M_v^{0.335}$ f1 f2 f3	1.3	1.3	1.3	Combined Rocket & Air-Breathing $Ce = 300\ Me^{0.635}$ f1 f2 f3	1.3	1.3	1.3
RL6	SSTO-RA(Sub)-ILHL (Ramp)	$Cv = 1880\ M_v^{0.335}$ f1 f2 f3	1.3	1.3	1.3	Combined Rocket & Air-Breathing $Ce = 300\ Me^{0.635}$ f1 f2 f3	1.3	1.3	1.3
RL7	SSTO-RA(Sup)-HLHL (u/c)	$Cv = 1880\ M_v^{0.335}$ f1 f2 f3	1.5	1.5	1.5	Combined Cycle 4 Mode Engine $Ce = 500\ Me^{0.635}$ f1 f2 f3	1.5	1.5	1.5
RL8	TSTO-RA(Sub)-HLHL (Air Launch)	$Cv = 1880\ M_v^{0.335}$ f1 f2 f3	1.2	1.2	1.2	Rockets & Turbojets $Ce = 152\ Me^{0.635}$ f1 f2 f3	0.8	0.8	0.8
RL9	TSTO-RA(Sub)-HLHL (u/c)	$Cv = 1122\ M_v^{0.335}$ f1 f2 f3	1.3	1.3	1.3	Turboramjets & Rockets $Ce = 200\ Me^{0.635}$ f1 f2 f3	1.3	1.3	1.3
RL10	SSTO-R-HLHL (u/c)	$Cv = 1880\ M_v^{0.335}$ f1 f2 f3	1.2	1.2	1.2	Rockets: $Ce = 152\ Me^{0.635}$ f1 f2 f3	0.8	0.8	0.8
RL11	SSTO-R-HLHL (Sled)	$Cv = 1880\ M_v^{0.335}$ f1 f2 f3	1.2	1.2	1.2	Rockets: $Ce = 152\ Me^{0.635}$ f1 f2 f3	0.8	0.8	0.8
RL12	TSTO-R-HLHL (u/c)	$Cv = 1122\ M_v^{0.335}$ f1 f2 f3	1.2	1.2	1.2	Rockets: $Ce = 152\ Me^{0.635}$ f1 f2 f3	0.8	0.8	0.8
RL13	SSTO-RA(Sub) - VLVL	$Cv = 1000\ M_v^{0.335}$ f1 f2 f3	1.1	1.1	1.1	Rockets & Small Turbojet $Ce = 160\ Me^{0.635}$ f1 f2 f3	0.8	0.8	0.8

Cv = Vehicle (without Engines) Development Cost (Man Years)
Ce = Engines Development Cost (Man Years)
f1 = Development Standard Factor
f2 = Technical Quality Factor
f3 = Team Experience Factor

TABLE 7.4 REUSABLE LAUNCHER MASS BREAKDOWN AND LIFT-OFF THRUST LEVELS

VEHICLE	DESIGNATION	STAGES	LAUNCH MASS (TONNES)	ORBITAL MASS (TONNES)	PAYLOAD MASS (TONNES)	VEHICLE NET MASS (TONNES)	AIRFRAME MASS (TONNES)	ENGINE MASS (TONNES)	LIFT-OFF THRUST (KN)
RL1	SSTO-R-VLVL	1	350	43	11.38	35.00	30.19	4.81	4807
RL2	SSTO-R-VLHL	1	350	43.54	3.36	40.18	35.37	4.81	4807
RL3	TSTO-R-VLHL	2	350	67.41	17.50	49.91	43.10	6.81	4807
RL4	SSTO-RA(Sub)-HLHL(u/c)	1	350	38.85	0	38.85	35.42	3.43	2060
RL5	SSTO-RA-(Sub)-HLHL(Sled)	1	350	55.76	5.78	50.00	46.57	3.43	2060
RL6	SSTO-RA(Sub)-ILHL(Ramp)	1	350	55.76	5.78	50.00	46.57	3.43	2060
RL7	SSTO-RA(Sup)-HLHL (u/c)	1	350	64.75	0	64.75	59.75	5.00	2060
RL8	TSTO-RA(Sub)-HLHL (Air-Launch)	2	350	49.91	11.90	38.00	33.19	4.81	4807
RL9	TSTO-RA(Sub)-HLHL (u/c)	2	350	185	7.21	177.9	159.30	18.60	2060
RL10	SSTO-R-HLHL (u/c)	1	350	42.28	0	42.28	40.56	1.72	2060
RL11	SSTO-R-HLHL (Sled)	1	350	46.97	6.86	40.11	38.39	1.72	2060
RL12	TSTO-R-HLHL (u/c)	2	350	87.50	11.90	75.46	72.72	2.72	2060
RL13	SSTO-RA (Sub)-VLVL	1	350	44.10	4.55	39.55	34.34	5.21	4807

TABLE 7.5 REUSABLE LAUNCHER COST BREAKDOWN

VEHICLE	DESIGNATION	DEVELOPMENT COST		PROCUREMENT COST		OPERATION COST - PER FLIGHT - 240 FLIGHTS		TOTAL LIFE CYCLE COST (20 YEARS, 3 VEHICLES, 240 FLIGHTS)	
		MAN YEAR	MILLION US DOLLARS	MAN YEAR	MILLION US DOLLARS	MAN YEAR	MILLION US DOLLARS	MAN YEAR	MILLION US DOLLARS
RL1	SSTO-R-VLVL	48634	9362	14427	2777	74 17760	14.245 3418.8	80821	15558
RL2	SSTO-R-VLHL	74675	14375	15138	2914	75 18000	14.438 3465.0	107813	20754
RL3	TSTO-R-VLHL	82815	15942	30000	5775	91 21840	17.518 4204.2	134655	25921
* RL4	SSTO-RA (Sub) - HLHL (u/c)	253875	48871	142762	27481	102 24480	19.635 4712.4	421117	81065
RL5	SSTO-RA (Sub) - HLHL (Sled)	267129	51422	169411	32612	103 24720	19.827 4758.6	561260	108042
RL6	SSTO-RA (Sub) - ILHL (Ramp)	280485	53993	169411	32612	103 24720	19.827 4758.6	474616	91363
* RL7	SSTO-RA (Sup) - HLHL (u/c)	629423	121164	300000	57750	109 26160	20.983 5035.8	955583	183950
RL8	TSTO-RA (Sub) - HLHL (Air-Launch)	123182	23712	132477	25502	91 21840	17.518 4204.2	277499	53419
RL9	TSTO-RA (Sub) - HLHL (u/c)	328374	63212	280000	53900	97 23280	18.673 4481.4	631654	121593
* RL10	SSTO-R-HLHL (u/c)	122433	23568	148430	28573	74 17760	14.245 3418.8	288623	55560
RL11	SSTO-R-HLHL (Sled)	120360	23619	143186	27563	74 17760	14.245 3418.8	281306	54151
RL12	TSTO-R-HLHL (u/c)	94115	18117	219814	42314	78 18720	15.015 3603.6	332649	64035
RL13	SSTO-RA (Sub) - VLVL	62797	12088	17441	3357	74 17760	14.245 3418.8	90096	17344

* Vehicles with Negative Payload

1992 Conversion Rate 1 MY = 192500 USD

FIGURE 7.1

Comparative Costs of Candidate Reusable Launchers

Comparison of Development Costs

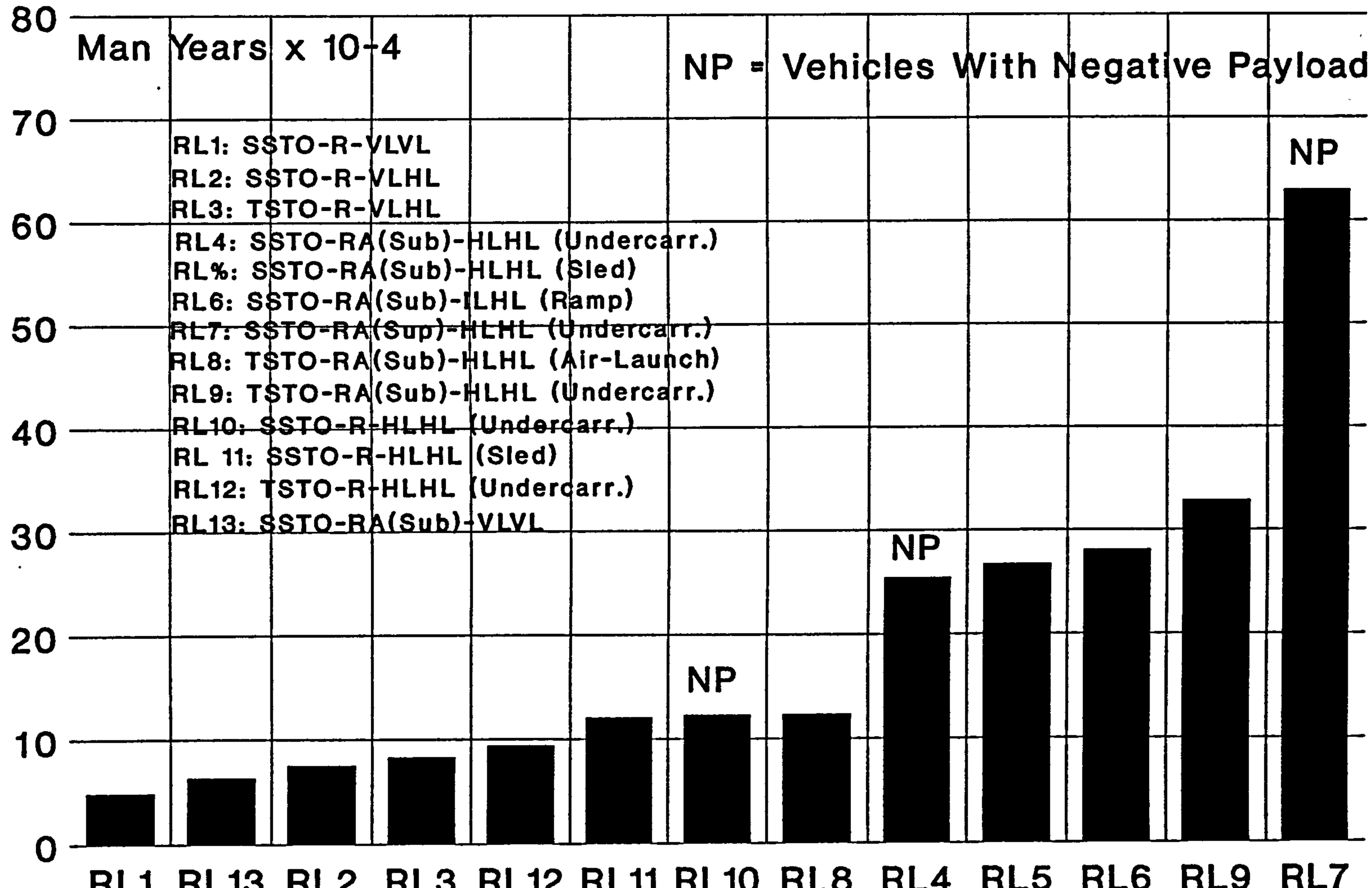

FIGURE 7.2

Comparative Costs of Candidate Reusable Launchers

Comparative Fleet Procurement Costs (3 Vehicles)

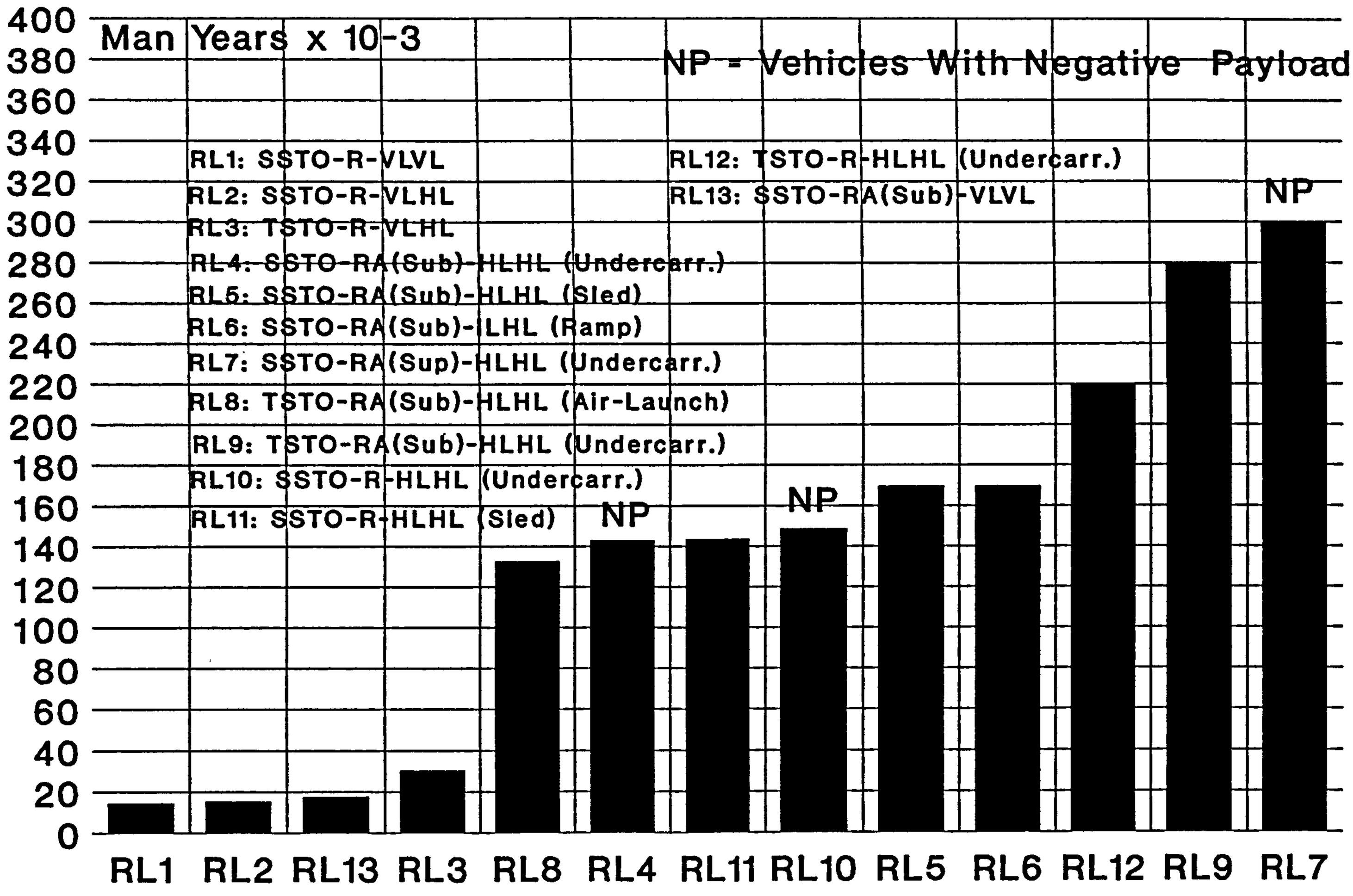

FIGURE 7.3

Comparative Costs of Candidate Reusable Launchers

Comparison of Operating Costs Per Flight

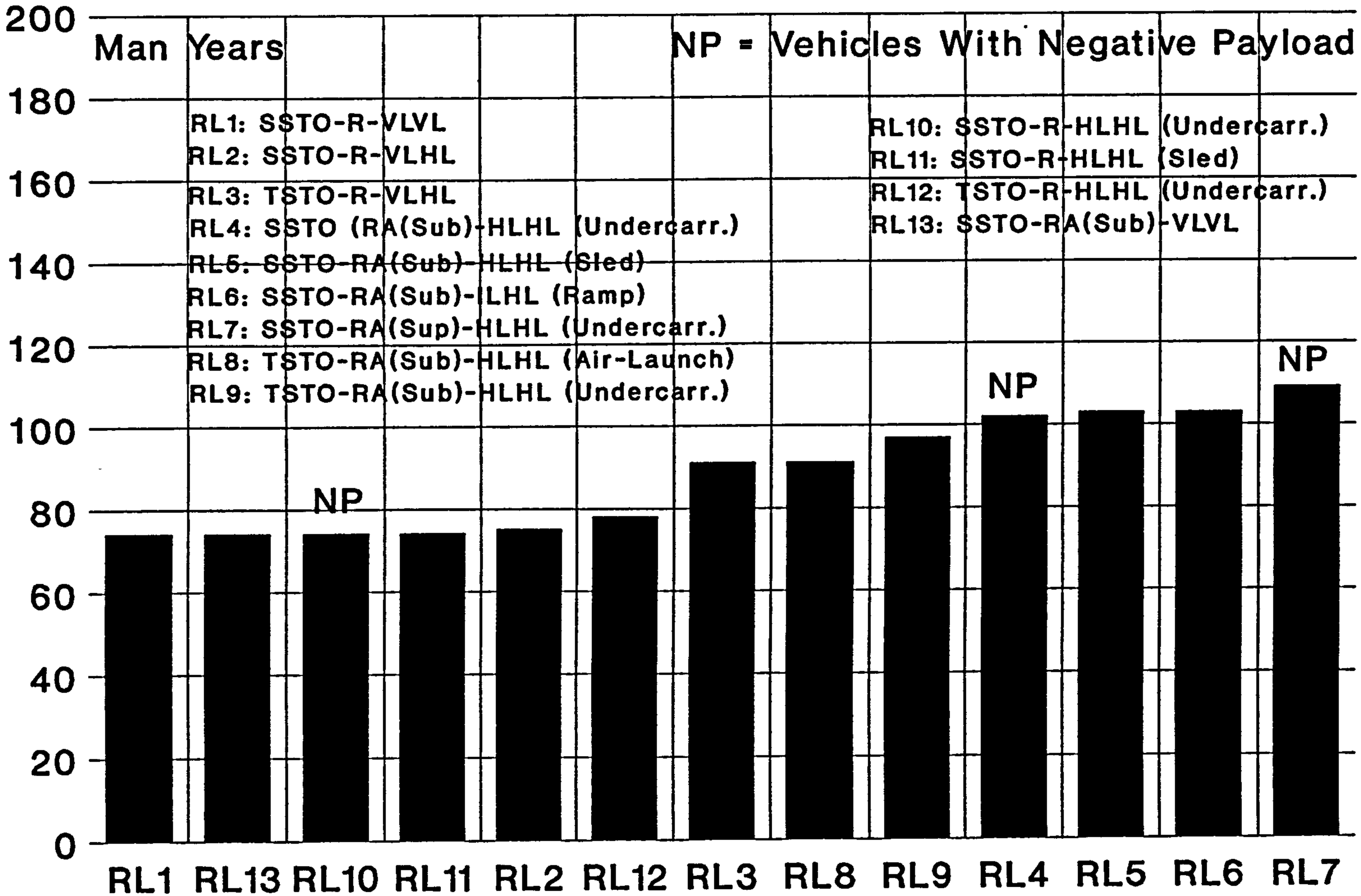

FIGURE 7.4

Comparative Costs of Candidate Reusable Launchers

Comparison of Total Life Cycle Costs

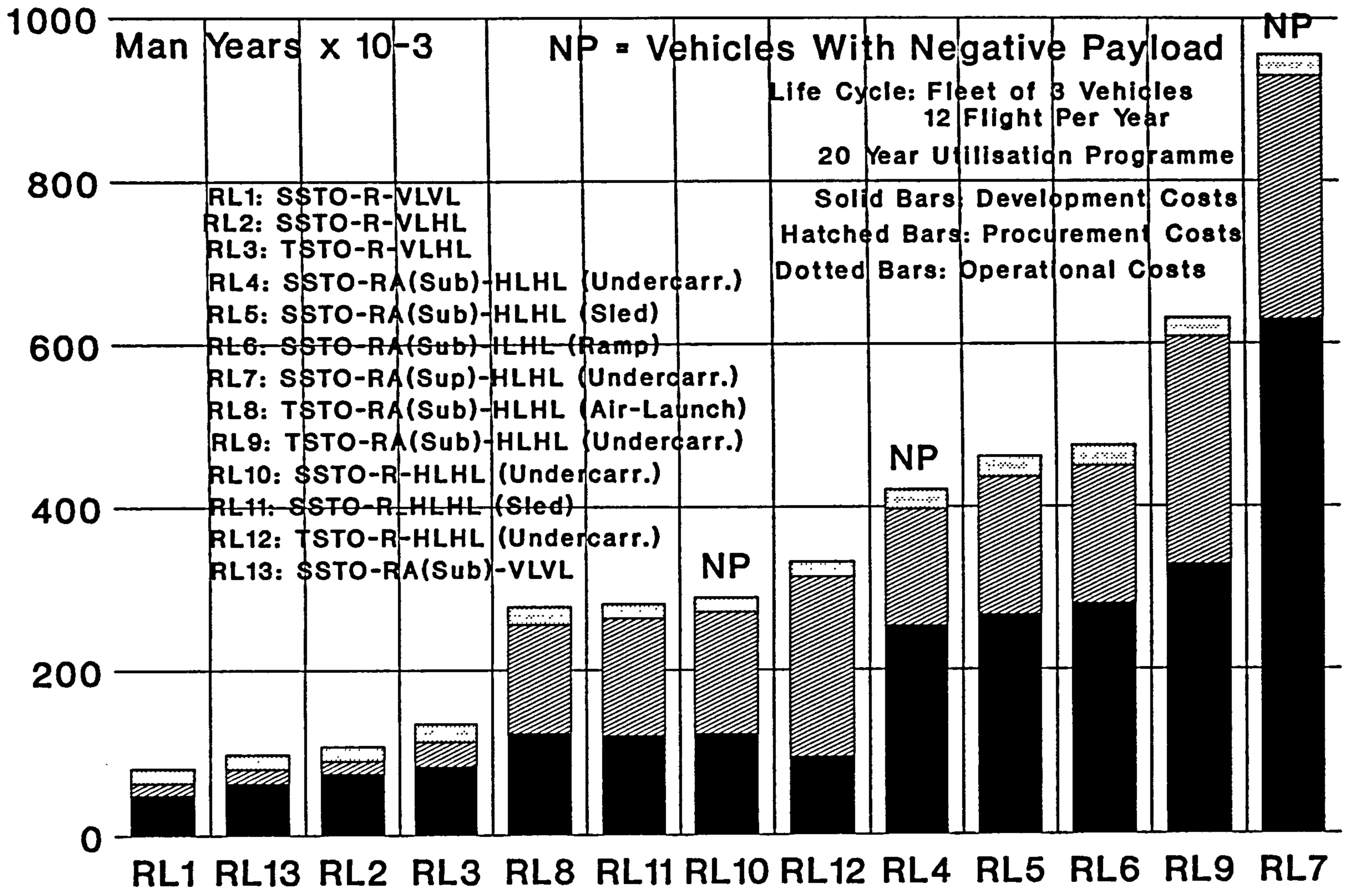

8 COMPARISON OF THE CANDIDATE REUSABLE LAUNCHERS

The Performance, Technical Feasibility and Operational Cost analyses that have been presented in Chapters 5, 6 and 7 respectively, now allow an overall comparison of the candidate reusable launchers to be made. This work is presented in this Chapter. Firstly, the comparison criteria are defined and described. Secondly, the comparison of the launchers on individual criteria is performed. Thirdly and finally, the overall comparison of the launchers is made and the results are discussed.

8.1 Comparison Criteria

The comparison criteria for this overall analysis of the 13 reusable launcher concepts have been divided into Primary and Secondary Criteria.

8.1.1 Primary Comparison Criteria

The Primary Criteria are the three fundamental but imperative requirements that were defined in the Objectives of the Research, described in Chapter 1.2. These are:

1) **Adequate performance to deliver a positive payload mass to orbit.** A value of 2 % Payload Mass Ratio has been selected as the acceptance criterion because this is the achievable value of the current expendable launchers. The probable, achievable values that have been used for each of the candidate reusable launchers are those that have been derived in Chapter 5: Calculated Performance of Reusable Launchers.

2) **Feasibility to develop successfully the required technologies.** These technologies are the classical ones for space launchers:

- propulsion;
- aerodynamics and aerothermodynamics;
- materials, structures and thermal protection;
- guidance, control and trajectories;
- vehicle subsystems (auxiliary propulsion, electrical power, hydraulic and pneumatic power, telemetry and telecommand);

The feasibility to develop each of these technologies has been assessed for each of the candidate launchers. This has been based on a qualitative assessment, using experience, engineering judgement and knowledge gained from the extensive literature survey, to assign a mark between 0 and 10 to signify the degree of difficulty to develop the required technology. A mark of 0 signifies that the required technology is fully developed and is in operational use. A mark of 10 signifies that it will be very difficult, probably infeasible, to develop the required technology. The acceptance criterion that has been adopted is a total average mark of less than 5, which signifies that the developments will be challenging, moderately difficult, but feasible.

3) **Operational costs that are substantially lower than those of the current expendable launchers.** The acceptance criterion that has been adopted is an operational cost that is less than 50 % of that of the Ariane 44L launcher, which has been selected as a reference case because of its relevance for a future European Reusable Launch System.

8.1.2 Secondary Comparison Criteria

The Secondary Comparison Criteria are those inherent vehicle characteristics that give operational ease and convenience. These are:

1) Versatility:

This is defined as the quality that allows a reusable launcher to be readily launched from different geographical launch sites and also to land at different launch sites. Furthermore, this quality extends to the ability to access different target orbits from each launch site. The target orbits considered are those that have been derived in Chapter 3.2: Space Transportation Needs in the 21st Century. These are:

- A LEO Payload Delivery Orbit: This is typically, a circular orbit of 200 km altitude with an inclination equal to the latitude of the launch site;

- A Space Station Servicing Orbit: This is typically a circular orbit at a Space Station altitude of 450 km, inclined at 28.5 degrees;

- A Polar Orbit for Earth Observation: This is typically a circular orbit between 500 and 800 km altitude and with an inclination of about 97 degrees.

It can be readily seen that vehicles with air-breathing propulsion are inherently able to be used on missions which include long cruise phases because of the high specific impulse of air-breathing propulsion. As another example of versatility, winged vehicles have inherently good down and cross range capabilities during their gliding re-entry. They can therefore be launched from one site and land at another.

2) Resiliency:

This is defined as the quality that enables the launcher to fulfil its mission despite failures in primary systems like the propulsion, guidance and control, electrical and

mechanical power systems. For example, a resilient launcher will be able to complete its mission after a failure in flight of one of its engines.

3) Inherent Reliability:

This quality derives from the inherent nature of the launcher. For example, SSTO vehicles are inherently more reliable than TSTO vehicles because:

- there are no stage separation manoeuvres to perform, which are always critical;

- failures can only occur in one stage only;

4) Operational Convenience:

Again, this derives from the inherent nature of the launcher. For example, vertically launched vehicles pose greater difficulties and necessitate more complex facilities and operations to integrate their payloads compared to horizontally-launched vehicles, which have a convenient payload bay, accessible from the top of the vehicle. Another example is the manoeuvrability for ground movements offered by vehicles which have their own undercarriage.

8.2 Comparison of the Performance of the Candidate Reusable Launchers

Table 8.1 shows the Performance Comparison. The Payload Mass Ratios calculated in Chapter 5 are shown for each launcher. This allows the adopted acceptance criterion of a 2 % Payload Mass Ratio value to be applied. It can be seen that, based on this criterion, that only 5 of the 13 launcher concepts are accepted. These vehicles are:

- RL1: SSTO-R-VLVL

- RL3: TSTO-R-VLHL
- RL8: TSTO-RA(Sub)-HLHL (Air-Launched)
- RL9: TSTO-RA(Sub)-HLHL (Undercarriage-Launched)
- RL12: TSTO-R-HLHL (Undercarriage-Launched)

Examination of these accepted vehicles shows that:

- three of the vehicles are entirely rocket-propelled (RL1, RL3, RL12)
- RL8 is in reality an air-launched rocket-propelled SSTO.

Thus, we can say that 4 of the five vehicles are essentially rocket-propelled launchers. The fifth vehicle is RL9, which is an air-breathing launcher, but it only uses subsonic combustion (turboramjet) air-breathing propulsion in its First Stage.

8.3 Comparison of the Technical Feasibility of the Candidate Reusable Launchers

The results of this comparison are shown in Table 8.2. Qualitative marks have been assigned for each technology for each launcher on a scale of 0 to 10. The total average mark for each launcher is also shown. This allows the acceptance criterion of a mark of less than 5 to be applied. The results show that only 7 of the 13 launchers pass this criterion. These are:

- RL1: SSTO-R-VLVL
- RL2: SSTO-R-VLHL
- RL3: TSTO-R-VLHL
- RL8: TSTO-RA(Sub)-HLHL (Air-Launched)
- RL10: SSTO-R-HLHL (Undercarriage-Launched)
- RL12: TSTO-R-HLHL (Undercarriage-Launched)
- RL13: SSTO-RA(Sub)-VLVL

Examination of these accepted vehicles shows that 6 of the 7 vehicles are rocket-propelled and that the remaining one, RL8, the air-launched TSTO, comprises a conventional aircraft as its First Stage and an entirely rocket-propelled vehicle as its Second Stage. This result is of course not surprising because rocket-propulsion systems are fully developed.

8.4 Comparison of the Operational Costs of the Candidate Reusable Launchers

The results of this comparison are shown in Table 8.3. The amortised operational cost per launch of each launcher is shown, based on the Utilisation Model adopted in Chapter 7: a fleet of 3 Vehicles, a 20 year operational period; a total of 240 flights; a maximum of 12 flights per year. This cost excludes the development cost of the launcher. This has been done to be able to compare the costs with that of Ariane 44L, for which the development costs are also not included. The results show that only 4 of the 13 launchers can meet the acceptance criterion of less than 50 % of the operational cost per launch of Ariane 44L. These vehicles are;

- RL1: SSTO-R-VLVL
- RL2: SSTO-R-VLHL
- RL3: TSTO-R-VLHL
- RL13: SSTO-RA(Sub)-VLVL

Examination of these accepted vehicles shows that, again, they are all rocket-propelled vehicles, including RL13, which only uses a simple turbojet air-breathing engine to augment the lift-off rocket thrust.

Table 8.3 also shows the amortised costs per kilogram of payload delivered to low Earth orbit. Again, it can be seen that on this criterion, that 7 of the 13 vehicles have costs per kilogram payload which are less than the Ariane 44L value

of 26190 USD/kg. These vehicles, listed in ascending order of costs are: RL1, RL3, RL13, RL2, RL8, RL12, RL11. Here again, all these vehicles are essentially rocket-propelled launchers.

8.5 Overall Comparison of the Candidate Reusable Launchers

The individual results of the comparisons of the performance, technical feasibility and operational costs, shown in Tables 8.1, 8.2 and 8.3 respectively, have been collated and shown in Table 8.4. The acceptance criterion adopted here for this overall comparison is that only those vehicles which have passed all three individual acceptance criteria are acceptable. The results show that only 2 of the 13 vehicles are acceptable. These are:

- RL1: SSTO-R-VLVL
- RL3: TSTO-R-VLHL

Examination of these accepted vehicles shows, again, that they are both rocket-propelled vehicles. This result is of course not surprising, because these vehicles are the simplest ones and could be developed from the well established knowledge and experience base of the current expendable launchers. These two vehicles have also been ranked in order of preference. The best vehicle is RL1, the SSTO-R-VLVL. The second best vehicle is RL3, the TSTO-R-VLHL. This ranking has been derived from an overall assessment of the Secondary Evaluation Criteria: Versatility; Resiliency; Inherent Reliability; Operational Convenience.

TABLE 8.1 COMPARISON OF THE PERFORMANCE OF THE CANDIDATE REUSABLE LAUNCHERS

VEHICLE	DESIGNATION	PAYLOAD MASS RATIO (%)	ACCEPTANCE CRITERION 2% PAYLOAD MASS RATIO	
			PASS	FAIL
RL1	SSTO-R-VLVL	3.25	√	
RL2	SSTO-R-VLHL	0.96		X
RL3	TSTO-R-VLHL	5.00	√	
RL4	SSTO-RA(Sub)-HLHL (u/c)	- 3		X
RL5	SSTO-RA(Sub)-HLHL (Sled)	1.65		X
RL6	SSTO-RA(Sub)-ILHL(Ramp)	1.65		X
RL7	SSTO-RA(Sup)-HLHL(u/c)	- 9.00		X
RL8	TSTO-RA(Sub)-HLHL(Air-Launch)	3.40	√	
RL9	TSTO-RA(Sub)-HLHL(u/c)	2.06	√	
RL10	SSTO-R-HLHL(u/c)	- 6.40		X
RL11	SSTO-R-HLHL(Sled)	1.96		X
RL12	TSTO-R-HLHL(u/c)	3.40	√	
RL13	SSTO-RA(Sub)-VLVL	1.67		X

TABLE 8.2 COMPARISON OF THE TECHNICAL FEASIBILITY OF THE CANDIDATE REUSABLE LAUNCHERS

VEHICLE	DESIGNATION	TECHNICAL DISCIPLINE MARKS: 0 = CURRENT TECHNOLOGY 10 = VERY ADVANCED					TOTAL AVERAGE	ACCEPTANCE CRITERION TOTAL AVERAGE ≤ 5	
		PROPULSION	AEROTHERMO DYNAMICS	MATERIALS STRUCTURES THERMAL PROTECTION	GUIDANCE AND CONTROL	VEHICLE SUBSYSTEMS	TOTAL AVERAGE	PASS	FAIL
RL1	SSTO-R-VLVL	3	4	6	4	4	4.2	✓	
RL2	SSTO-R-VLHL	3	4	7	5	5	4.8	✓	
RL3	TSTO-R-VLHL	3	4	5	5	5	4.4	✓	
RL4	SSTO-RA(Sub)-HLHL(u/c)	6	6	6	5	5	5.6		X
RL5	SSTO-RA(Sub)-HLHL(Sled)	6	6	6	5	8	6.2		X
RL6	SSTO-RA(Sub)ILHL(Ramp)	6	6	6	5	6	5.8		X
RL7	SSTO-RA(Sup)-HLHL(u/c)	10	10	10	6	8	8.8		X
RL8	TSTO-RA(Sub)-HLHL(Air Launch)	3	5	7	5	5	5.0	✓	
RL9	TSTO-RA(SUb)-HLHL(u/c)	6	6	5	6	5	5.6		X
RL10	SSTO-R-HLHL(u/c)	3	4	8	5	5	5.0	✓	
RL11	SSTO-R-HLHL(Sled)	3	4	8	5	7	5.4		X
RL12	TSTO-R-HLHL(u/c)	3	5	6	5	5	4.8	✓	
RL13	SSTO-RA(Sub)-VLVL	4	4	6	5	5	4.8	✓	

TABLE 8.3 COMPARISON OF THE OPERATIONAL COSTS OF THE CANDIDATE REUSABLE LAUNCHERS

VEHICLE	DESIGNATION	* AMORTISED COST PER KILOGRAM DELIVERED TO LOW EARTH ORBIT 1992 USD/kg.	* AMORTISED COST PER LAUNCH (BASED ON 240 FLIGHTS IN 20 YEARS)	PERCENTAGE OF ARIANE 44L LAUNCH COST (132 MUSD)	ACCEPTANCE CRITERION ≤ 50% OF ARIANE 44L LAUNCH COST	
					PASS	FAIL
RL1	SSTO-R-VLVL	2268	25.8	19.5	✓	
RL2	SSTO-R-VLHL	7917	26.6	20.2	✓	
RL3	TSTO-R-VLHL	2377	41.6	31.5	✓	
# RL4	SSTO-RA(Sub)-HLHL(u/c)	-	134.1	101.6		X
RL5	SSTO-RA(Sub)-HLHL(Sled)	40848	235.9	178.7		X
RL6	SSTO-RA(Sub)-HLHL(Ramp)	42390	244.8	185.5		X
# RL7	SSTO-RA(Sup)-HLHL(u/c)	_	261.6	198.2		X
RL8	TSTO-RA(Sub)-HLHL(Air-Launched)	10403	123.8	93.4		X
RL9	TSTO-RA(Sub)-HLHL(u/c)	33745	243.3	184.3		X
# RL10	SSTO-R-HLHL(u/c)	-	133.3	100.1		X
RL11	SSTO-R-HLHL(Sled)	18542	127.2	96.4		X
RL12	TSTO-R-HLHL(u/c)	16075	191.3	144.9		X
RL13	SSTO-RA(Sub)-VLVL	3747	21.9	16.6	✓	

* EXCLUDING DEVELOPMENT COSTS
\# VEHICLES WITH NEGATIVE PAYLOAD
ARIANE 44L SPECIFIC LAUNCH COST = 26190 USD/kg

TABLE 8.4 OVERALL COMPARISON OF THE CANDIDATE REUSABLE LAUNCHERS

VEHICLE	DESIGNATION	COMPARATIVE CRITERION			ACCEPTANCE STATUS (3V)		RANKING OF ACCEPTABLE VEHICLES (1 IS BEST)
		PERFORMANCE (≥ 2% PAYLOAD MASS)	TECHNICAL FEASIBILITY (< 50%)	OPERATION COST PER LAUNCH (≤ 50%) ARIANE 44L	PASS	FAIL	
RL1	SSTO-R-VLVL	√	√	√	√		1
RL2	SSTO-R-VLHL	X	√	√		X	
RL3	TSTO-R-VLHL	√	√	√	√		2
RL4	SSTO-RA(Sub)-HLHL (u/c)	X	X	X		X	
RL5	SSTO-RA(Sub)-HLHL(Sled)	X	X	X		X	
RL6	SSTO-RA(Sub)-ILHL(Ramp)	X	X	X		X	
RL7	SSTO-RA(Sup)-HLHL(u/c)	X	X	X		X	
RL8	TSTO-RA(Sub)-HLHL(Air Launched)	√	√	X		X	
RL9	TSTO-RA(Sub)-HLHL(u/c)	√	X	X		X	
RL10	SSTO-R-HLHL(u/c)	X	√	X		X	
RL11	SSTO-R-HLHL(Sled)	X	X	X		X	
RL12	TSTO-R-HLHL(u/c)	√	√	X		X	
RL13	SSTO-RA(Sub)-VLVL	X	√	√		X	

9 CONCLUSIONS

The conclusions of this research on Reusable Launchers are presented under three categories:

- **General Conclusions**, relating to the overall research;
- **Specific Conclusions**, relating to the research results;
- **Contributions of the Research**, relating to the specific advancement of knowledge in Reusable Launchers.

9.1 General Conclusions

1) The author feels that the motivating objectives of the research have been achieved satisfactorily. The achievements are:

- a fundamental, comparative system study at vehicle system level has been performed for 13 of the most plausible reusable launcher concepts. The analysis has been made using a consistent set of design tools and analysis methodology for a standard reference mission, thus allowing the results to be compared on a fair basis.

2) The results of this study are deemed by the author to provide a proper technical basis for selecting appropriate reusable launcher concepts to meet any specified set of future reusable launcher requirements;

3) The detailed analysis of each candidate launcher has determined its performance capabilities, technical feasibility and operational costs;

4) The comparative analysis of the 13 candidate launchers has provided clear results on the three fundamental, but imperative requirements:

- the reusable launcher concepts that can deliver a positive payload mass to orbit have been identified;
- the reusable launcher concepts that are deemed to be technically feasible have been identified;
- the reusable launcher concepts that have a substantially lower operational cost than the current expendable launchers have been identified.

9.2 Specific Conclusions

1) Only 2 of the 13 candidate reusable launcher concepts were found in this research to meet all the acceptance requirements of adequate performance, technical feasibility and operational costs. These vehicles, ranked in the order of their preference are: RL1, the SSTO-R-VLVL vehicle; RL3, the TSTO-R-VLHL vehicle.

2) The two feasible vehicles are both rocket-propelled launchers:

- RL1, the SSTO-R-VLVL is the most fundamental vehicle of the 13 candidates. It represents the simplest conceivable concept in terms of its configuration (single stage), its propulsion mode (entirely rocket-propelled), its ascent and landing modes (vertical). It derives its technical inheritance from the highly developed expendable rocket launcher, thus posing the absolute minimum in technical risk.

- RL3, the TSTO, rocket propelled, vertical launch and horizontal landing vehicle is attractive because it also has all the simple features and technology inheritance of RL1 for each of its two stages. The substantially increased orbital mass derived from its staging concept is used partly to accommodate the increased vehicle mass that is required for its horizontal landing mode. But

despite this, its payload mass ratio is increased substantially to 5 % compared with the already high value of 3.25 % for RL1.

3) The research results show that, as expected, the more complex the vehicle, the higher are its amortised operational costs. An important contribution however, has been the quantifying of these costs, which show, that for most of the candidate vehicles, which include all the air-breathing concepts, that they are up to twice as expensive as the current expendable launchers!. The exceptions to this finding are the two vehicles RL1 and RL3, which meet all the acceptance criteria. For these vehicles, the operation costs were found to be about 20 % that of Ariane 44L, the reference vehicle adopted for this comparison.

4) The substantial reduction in operating costs per launch for the two acceptable vehicles RL1 and RL3, make it well worthwhile to invest in further feasibility studies and then to a possible development of one of these launcher types: RL1 being the preferred concept.

5) The results of this research have convinced the author that the concept which has the highest potential for practical realisation into a technically feasible and cost effective reusable launcher is the simplest conceivable concept: the single-stage-to-orbit, rocket-propelled, vertical launch and vertical landing vehicle.

9.3 Contributions of this Research to the Advancement of Knowledge in Reusable Launchers

Apart from the deep system knowledge that the author has personally gained from this research in reusable launchers, the author feels that he has made the following contributions to the advancement of knowledge in this field:

- contributing the first comprehensive comparative analysis of a wide range of reusable launcher concepts, showing clearly, for the first time, the performance capability boundaries of each concept when compared under identical analysis conditions. Specifically, the required maximum allowable Vehicle Mass Ratio for each launcher has been identified for any desired value of Payload Mass Ratio.

- devising a simple but valuable analysis methodology for the derivation of the performance boundaries for any vehicle type, **before engaging in major efforts of detailed analysis.** This allows to avoid wasted efforts and expenditure in the detailed analysis of useless vehicle concepts. This is deemed to be a significant practical contribution.

- Identifying clearly the reasons for the **poor practical performance of air-breathing propulsion systems for Earth-to-orbit launchers,** which results from their installed operational characteristics:
  - the high gross specific impulse is eroded by high installed drag losses of the engines, compounded by the higher vehicle drag losses which result from having to fly along high dynamic pressure trajectories;
  - the thrust/weight ratio of air-breathing engines is too low, negating the effect of the high gross specific impulse.
  - the low density of liquid hydrogen fuel results in very large vehicles with penalties on structural mass, aerodynamic drag and vehicle control.
  - the complexity of air-breathing engines results in high costs.

10 REFERENCES

Reference 1: International Reference Guide to Space Launch Systems 1991 Edition, Steven J.Isakowitz, AIAA, USA

Reference 2: Paper AIAA-91-5089: Spaceflight in the Aero-Space Plane Era, R.Hannigan and D.Webb

Reference 3: NLR Aero Code, NLR Amsterdam, TR 80124 and TR 89165

Reference 4: Supersonic Hypersonic Arbitrary Body Program, BAe, Sowerby Research Centre, Bristol, England

Reference 5: US 1976 International Standard Atmosphere, NOAA/S/T76 1562, NOAA, Washington

Reference 6: Jacchia Atmospheric Model: SAO Special Report No.313, May 1970

Reference 7: ESA Winged Launcher Configuration Study Phases 1 and 2, Final Report, MBB Report No.URV- 182 (89)

Reference 8: ESA Winged Launcher Configuration Study Phase 5, Final Report DASA-TN-RTL11-WLC 13 (93)

Reference 9: ESA Winged Launcher Configuration Study Phase 4, Final Report, MBB Report ESA7379/87.MBB 100

Reference 10: Paper IAF-86-122: The Single-Stage Reusable Ballistic Launcher Concept for Economic Cargo Transportation, D.E.Koelle and W.Kleinau, MBB, Ottobrunn, FRG.

Reference 11: Paper IAF-92-0865: Comparative Analysis of Various Concepts for Reusable Aerospace Systems, L.M.Shkadov et al, Central Aerohydrodynamics Institute (TsAGI), Moscow, Russia

Reference 12: Paper IAF-89-216: An Investigation of Future European Winged Launcher Concepts, H.K.H.Grallert (MBB), S.G.Furniss (BAe), F.A.Hewitt (Rolls-Royce)

Reference 13: Paper IAF-91-199: Progress in ESA Winged Launcher Configuration Studies, H.K.H.Grallert/MBB and W.Berry/ESTEC

Reference 14: TRANSCOST: Statistical-Analytical Model for Cost Estimation and Economic Optimisation of Space Transportation Systems, 1991 Edition, D.E.Koelle, MBB-Report No.URV-185(91)

Reference 15: Interavia Spaceflight Directory, 1991-1992

Reference 16: Modern Engineering for Design of Liquid Propellant Rocket Engines, by D.K.Huzel and D.H.Huang; Volume 147, Progress in Aeronautics and Astronautics, AIAA, 1992

Reference 17: Rocket Engine Propulsion Power Cycles, by A.Martinez, Threshold, 1991

Reference 18: Paper AIAA-92-3504, Propulsion system Requirements for Reusable Single-Stage-to-Orbit Rocket Vehicles, Douglas O.Stanley, Walter E. Engelund, Roger Lepsch, NASA Langley Research Center, Hampton, VA, USA

Reference 19: Paper IAF-92-0647, Plug Engine Systems for Future Launch Vehicle Applications, H.Immich, D.E.Koelle, MBB Deutsche Aerospace, Munich, Germany and R.C.Parsley, United Technologies Corporation, Pratt and Whitney, West Palm Beach, Florida, USA

Reference 20: Personal Communication from Dr.H.Immich, MBB Deutsche Aerospace, Munich, Germany

Reference 21: Mixed-Mode Propulsion for the Space Shuttle, R.Salkeld, Astronautics and Aeronautics, Volume 9 No.8, August 1971, Pages 52-58

Reference 22: Paper IAF-89-224, Space Transportation Propulsion Application- A Development Challenge, R.Beichel, C.J.O'Brien and J.P.Taylor

Reference 23: Russian Liquid Rocket Bureau Designing Three Fuel Engine, D.Hughes, Aviation Week and Space Technology, March 30, 1992, Page 23

Reference 24: High Speed Flight Propulsion Systems, Edited by S.N.B. Murthy and E.T.Curran, Progress in Astronautics and Aeronautics, Volume 137, AIAA, 1991

Reference 25: Evaluation of Advanced Air Breathing Propulsion Concepts, Final Report, Volume 3, ESA Contract 6822/86/F/HEW(SC), Rolls Royce and MBB/ERNO Space Systems, July 1987

Reference 26: Evaluation of the Advanced Airbreathing Propulsion Concepts, Final Report, ESA Contract 6823/86/HEW(SC), SNECMA/SEP/Fiat Aviazione/SNIA BPD, 1987

Reference 27: Performance of Earth-to-Orbit Transports Breathing Air, PhD Thesis, Graham Edward Dorrington, King's College, Cambridge University, December 1988

Reference 28: Paper IAF-92-0858 Space Transportation Systems Requirements Derived from the Propulsion Performance Reported in the Hypersonic and Combined Cycle Propulsion Session at the 1991 IAF Congress, Paul A.Czysz, St Louis University, Illinois, USA

Reference 29: Updated Performance of Ariane 5 for GTO and Escape Missions, M.A.S. Working Paper 316, by E.Gonzlez-Laguna, ESA/ESOC, August 1991

Reference 30: Materials for Hypersonic Engines, Terence M.F.Ronald, NASP Joint Program Office, Paper 36 in AGARD-CP-479, Issued December 1990, Hypersonic Combined Cycle Propulsion

Reference 31: Paper IAF-92-0854, Single Stage Rocket Technology, W.A.Gaubatz, P.L.Klevatt, J.A.Cooper, McDonnell Douglas Space Systems Company, Huntington Beach, Cal., USA

Reference 32: BRITE/EURAM Programme, Second Edition 1992, Commission of the European Communities, Brussels, Catalogue No. CD-NA-14042-EN-6, ISBN 92-826-3350-0

Reference 33: Hypersonic and High Temperature Gas Dynamics, John D.Anderson Jr, McGraw Hill Book Company. Book ISBN 0-07-001671-2, 1989, Chapter 6

Reference 34: Material Technology Challenges in Space Transportation, D.G.Desnoyer, SEP France, Proceedings of the 2nd European Aerospace Conference on Progress in Space Transportation, ESA SP-293, August 1989, Pages 429 to 438

Reference 35: New Materials and Structural Concepts for Space Transportation Systems, H W Bergman, W Bunk and G Gruninger, DLR, Brunswick, Germany, Proceedings of the 2nd European Aerospace Conference on Progress in Space Transportation, ESA SP-293, August 1989, Pages 439 to 448

Reference 36: Aerodynamic and Structural Design Challenges of a Reusable Single Stage to Orbit Air-Breathing Launch Vehicle, B.R.A.Burns, BAE, Preston, UK, Proceedings of the 2nd European Aerospace Conference on Progress in Space Transportation, ESA SP-293, August 1989, Pages 255 to 260

Reference 37: Composites Design Handbook for Space Structure Applications, Annex: Advanced Metallic and Ceramic Materials, ESA PSS-03-1101, BNF-Fulmer, Document R1176/D17/March 1992

Reference 38: Optimal Trajectories in Atmospheric Flight, Nguyen X Vinh, Elsevier Scientific Publishing Company, 1981, Chapter 3: Equations of Motion